A SURFACE AND COLLOID CHEMICAL STUDY OF THE INTERACTION OF PROTEINS WITH POLYSTYRENE LATEX (PSL)

By

ANDREW DANDY OLAL

B.Sc., Makerere University, Kampala, Uganda, 1978
M.Sc., University of Bristol, Bristol, U.K., 1981

A THESIS SUBMITTED IN PARTIAL FULFILLMENT OF

THE REQUIREMENTS FOR THE DEGREE OF

DOCTOR OF PHILOSOPHY

in

THE FACULTY OF GRADUATE STUDIES

(Chemistry Department)

We accept this thesis as conforming

to the required standard

THE UNIVERSITY OF BRITISH COLUMBIA

May 1990

In presenting this thesis in partial fulfilment of the requirements for an advanced degree at the University of British Columbia, I agree that the Library shall make it freely available for reference and study. I further agree that permission for extensive copying of this thesis for scholarly purposes may be granted by the head of my department or by his or her representatives. It is understood that copying or publication of this thesis for financial gain shall not be allowed without my written permission.

Department of CHEMISTRY

The University of British Columbia
Vancouver, Canada

Date 26th September, 1990

ABSTRACT

In this thesis various physicochemical factors which determine the characteristics of latex agglutination immunoassays are examined. A model of antibodies reacting with antigen (bovine serum albumin; BSA) adsorbed to the surface of polystyrene latex (PSL) beads was examined.

The adsorption studies of BSA to PSL showed that the mass of BSA adsorbed at saturation depends on the type of polystyrene latex. Latexes with highly hydrophobic surfaces adsorbed more BSA molecules than those with lower hydrphobicity. Desorption studies showed that latexes that maximize adsorption lost the lowest fraction of their bound BSA molecules following extensive buffer wash. Partial desorption of BSA from PSL was achieved by the addition of detergent, whereas the addition of more BSA molecules or other macromolecules such as PEG or IgG did not displace the adsorbed BSA molecules. Examination of the material removed from the surface of the latexes by SDS-PAGE analysis showed that the composition of the adsorbed layer was enriched in the higher molecular weight oligomers of BSA, relative to their concentrations in the stock solution. A model in which adsorbed protein is assumed to undergo a polymerization reaction provides a general explanation of the observed results. Studies of polyclonal antibody (anti-BSA IgG) binding to antigen-coated PSL showed that the surface concentration of bound antibody depends on the surface concentration of antigen on the latex particles and on the availability of PSL surface area not occupied by antigen.

Analysis of shear induced aggregation results show that for low surface coverage of latex particles by protein antigen in stable suspension, relatively low concentrations of specific antibodies are required to cause agglutination. Increasing surface density of antigen requires significantly higher concentrations of specific antibodies to produce agglutination. For a given surface coverage of antigen, results show that increasing the shear rate decreases the antibody concentration necessary to produce a given degree of agglutination.

A remarkable structure formation and long range ordering exhibited by flocs of latex coagulating in salt under intermediate shear rates was observed. This structure formation was not observed during antibody-induced agglutination under shear.

Table of Contents

List of Tables

LIST OF FIGURES

Figure Page

Figure Page

Acknowledgements

I am deeply grateful to Dr. D. E. Brooks for the guidance, continuous support and encouragement that he provided me throughout the course of this work.

I would also like to thank J. Sibley for his invaluable assistance in the maintenance of all those equipment that went kaput each time I used them, and also for constructing the shear aggregometer that I used for my kinetic experiments.

Finally, I would like to thank everybody in the lab for their understanding and assistance. I am especially grateful to C. Ramey for his patience in explaining things to me and for his help with PC communications.

To Margaret and Atim

CHAPTER ONE

GENERAL INTRODUCTION

1.1 Introduction

Dispersions of polystyrene latex (PSL) particles sensitized with antibodies (Ab) or antigens (Ag) are widely used in slide agglutination tests for qualitative as well as semi-quantitative analysis of Ab and Ag from biological fluids **[1-3]**. In these analysis, latex particles are first sensitized (i.e. rendered sensitive to the action of specific antibody or antigen) with either Ab or Ag. The sensitization involves immobilization of the reactants (Ab or Ag) on the surface of the latex particles either by physical adsorption or by covalent coupling, making them also antigenic **[4]**. Addition of a sample containing the homologous Ab or Ag to the dispersions causes Ag-Ab linkages to occur between the surfaces of the particles. Because of the relatively large size of the latex particles (diameter range 0.1 to 1 μm), the reaction causes the formation of visible precipitates (or aggregates) of the latex.

The most familiar example of latex-based immunoassay technique is the pregnancy slide test **[5]**. The pregnancy test is a test for the presence of human chorionic gonadotropin (hCG), the hormone produced in normal pregnancy. In this assay, a preparation of latex particles, to which has been attached the antibody to human chorionic gonadotropin (hCG), is mixed with a drop of urine. Using a clean plastic rod, the latex suspension and urine sample are thoroughly mixed until a uniform distribution of the latex particles is achieved. The slide is then gently tilted back and forth, as the reaction proceeds for a given length of time. This "rocking" imparts fluid motion to the system which

increases the number of collisions resulting in agglutination (i.e. the formation of large and visible aggregates as a result of interaction between Ag-coated particles with specific Ab) in about two to ten minutes. In a variation, the hCG is linked to the latex particles. An aliquot of urine is mixed with the antibody (anti-hCG) reagent, to allow any hCG in the urine to react. Then the antigen (hCG) is immediately added. If there is no hCG in the sample, the antibody reacts with the antigen, and agglutination occurs, indicating a negative result. If there is small amount of hCG in the urine, the antibody binds to the hCG and is unavailable to react with the Ag-latex particles, so no agglutination occurs.

The use of latex particles in analysis of Ab and Ag in biological fluids has increased rapidly over the last few years **[6,7]**. However, latex immunoassays do not as yet provide a definitive diagnosis. This is probably because most of the latex diagnostic tests, at present, are developed on an empirical basis due to the fact that there are numerous imprecisely understood physicochemical factors that influence the outcome of latex agglutination tests. These include: protein adsorbing properties to latex particles; the stability of latex particles prior to, during and after protein coating procedure; solution conditions such as pH, buffers, electrolyte and protein concentrations; and the latex particle size, density and surface characteristics. In addition, out of necessity, the antigen and antibody preparations used in these tests are often impure and contain a wide variety of materials not involved in the antigen-antibody reaction of interest. All these factors make it difficult to fully describe and outline the mechanism involved in such complex mixtures and has meant that relatively little published research

outlining the mechanisms involved in such systems is available. In this thesis, an attempt has been made, using a model antigen (bovine serum albumin (BSA)) and polyclonal anti-BSA antibody, to provide some basic information regarding the behaviour of protein adsorption to latex particles and the reactions that such systems undergo when antigens and antibodies are present.

1.2 Polymer Latex Particles

1.2 (a) *Description and Classification*

Latex particles are spherical polymer particles, often referred to as microspheres, synthesized from a variety of monomers by emulsion polymerization. They possess different properties depending on the specific monomers used [8]. These particles are dispersed, usually in aqueous media, but also commonly in non-aqueous media to form suspensions. Most latex suspensions are colloidal in nature, meaning that the dimensions of the particles in the dispersion medium range from 1nm to 1000nm. Polymer latexes can be classified as homopolymers or heteropolymers.

Homopolymer latexes are formed by the polymerization of a single species of monomer, for example polystyrene latex (PSL) derived from the styrene monomer and polyvinyl toluene (PVT) latex made from vinyl toluene. Heteropolymer latexes are produced by copolymerization of two or more different species of monomer, for example styrene-butadiene copolymer. The polymerization of a mixture of two or more monomers gives a copolymer with properties intermediate between those of the

corresponding homopolymers. The properties of copolymers depend not only on the overall composition of the polymer molecules, but also on the compositional distribution of monomer molecules in the polymer chains and the distribution of polymer molecular weights. Copolymerization is often used to produce latex particles with differing physical properties such as density, solubility and optical characteristics **[9]**.

1.2 (b) *Preparation*

The four basic ingredients in an emulsion polymerization process are the monomer (e.g. styrene), a surface active agent such as sodium dodecyl sulfate; a free-radical initiator such as potassium persulphate ($K_2S_2O_8$) or hydrogen peroxide (H_2O_2), and water **[10]**.

The surface active agents are normally amphiphatic long chain fatty acid salts with a hydrophilic "head" and a hydrophobic "tail". When such surface active agents are placed in high enough concentration in water, they form micelles consisting of 50 to 100 molecules oriented with their hydrophobic tails inwards and their hydrophilic heads in contact with the water, thus creating an interior environment of hydrocarbon. These micelles are formed once the monomeric concentration of the solute molecules reaches a critical value, the critical micelle concentration (CMC); the aggregates exist in equilibrium with free solute molecules in the aqueous phase.

Micelles tend to be composed of the same number of surface active molecules and are therefore uniform in diameter. Addition of more surface active molecules simply leads to the formation of more micelles of the same size.

When a monomer such as styrene is added to the micelles in water, some of it migrates to the central hydrophobic phase of the micelles, thereby swelling them, and some remains in the aqueous phase as droplets.

The most commonly used initiator is persulphate, which produces sulfate free radicals:

$$K_2S_2O_8 \longrightarrow 2K^+ + 2^{\cdot}OSO_3^-$$

These free radicals react with the double bond in the styrene monomer (M) producing monomeric free radicals which react with other styrene monomer side chains to form oligomeric radicals:

$$^{\cdot}OSO_3^- + M \longrightarrow {}^{\cdot}M\text{—}OSO_3^-$$

$$^{\cdot}M\text{—}OSO_3^- + nM \longrightarrow {}^{\cdot}M\,(M)_n\text{—}OSO_3^-$$

Thus, a chain reaction is initiated and linear polymerization occurs. The polymerization will proceed until the supply of monomeric styrene is exhausted or until the growing oligomeric radicals react with one another to terminate the polymerization.

The linear chain terminates with sulfate groups at both ends of the chain:

$$^{\cdot}M\,(M)_n\text{—}OSO_3^- + {}^{\cdot}M\,(M)_n\text{—}OSO_3^- \longrightarrow {}^-O_3SO\,(M)_{m+n}OSO_3^-$$

There are two basic hypotheses for the mechanism of emulsion polymerization; the monomer-swollen emulsifier micelles hypotheses was postulated by Harkins **[11]**, and quantified by Smith and Ewart **[12]**. In

this model, which is mainly applicable to monomers which are sparingly soluble in water such as styrene and butadiene, nucleation is thought to be initiated by free radicals which diffuse through the aqueous phase and penetrate both the monomer-swollen micelles and the droplets. Since the concentration of the micelles far exceeds that of the droplets, polymerization takes place almost exclusively in the micelle interior. The nucleation stage ends when all of the micelles have been transformed into polymer particles.

The continuous aqueous phase mechanism is the second emulsion polymerization hypothesis, proposed by Priest *et al* **[13]** and developed further by Stannett *et al* **[14]** and Fitch *et al* **[15]**. It is applicable to monomers such as vinyl acetate and vinyl chloride which are more soluble in water. The mechanism of nucleation in the aqueous phase is thought to be through the initiation of a free radical in the aqueous phase, followed by addition of monomer molecules until the oligomeric radical exceeds its solubility and precipitates from the solution. The precipitated oligomeric radical either nucleates a particle or flocculates with a particle already nucleated depending on whether its surface area exceeds a critical value. The function of the surface active agent here is simply to stabilize the suspensions that are formed.

Kotera *et al* and Goodwin *at el***[16]**, have developed methods for making surfactant-free polystyrene latexes. Surfactant-free latexes offer clear advantages over those made in the presence of surfactants in that the removal of adsorbed surfactant is a lengthy and tedious process; and the presence of any residual surfactants in latex preparation can cause reduction in protein adsorption onto latex surfaces. The principle involved in surfactant-free latex preparation is the same as that of

general emulsion polymerization in that the monomer is polymerized in an aqueous phase through initiation by a free radical. The solubility of styrene in water is low and so the bulk of the monomer in the reaction vessel forms a separate phase. Rapid stirring is required to give rapid transfer of monomer to the water in order to maintain a monomer-saturated aqueous phase. Initiation occurs in the aqueous phase, followed immediately by a small amount of propagation until a critical nucleus size is reached. At this point the rapidly growing hydrocarbon chain collapses into a coil and precipitates. The nuclei have insufficient electrical charge to make them colloidally stable and so coagulation occurs. During coagulation the solvated sulfate end-groups remain at the polymer-water interface and so the surface charge density rapidly increases until colloidal stability is achieved. The coagulation stage is critical both for the control of the degree of monodispersity and the final particle size.

Three types of emulsion polymerization processes are often used in the preparation of polymer latexes **[17]**; batch polymerization, semi-continuous and continuous polymerization.

For batch polymerization, all ingredients are added at the same time at the beginning of the reaction and heated with stirring at the polymerization temperature. Decomposition of initiator forms the free radicals, which initiate the polymerization and nucleate the particles. Nucleation initially proceeds concurrently with particle growth; ultimately only particle growth occurs. Batch polymerization is difficult to control except by cooling and variation of recipe to alter the number of particles.

Semi-continuous or semi-batch polymerization occurs when monomer is

added to the reactor in increments. Nucleation in semi-continuous polymerization is achieved in two ways: either a small portion of the monomer is charged initially and polymerized in batch to prepare a seed latex *in situ* or the monomer is added continuously as the polymerization is started, making nucleation proceed concurrently with particle growth until it stops and only particle growth occurs. The different modes and rate of monomer addition give different results since they control the rate of polymerization and, if two monomer types are present, the copolymer composition distribution. Semi-continuous emulsion polymerization is used to make particles with a variation in composition from center to surface, by adding different monomer compositions in sequence. These are known as structured or multi-phase latexes; latexes with a well-defined concentration composition gradient are called core-shell latexes. The use of finely divided magnetite has resulted in the preparation of magnetized polymer latexes (core-shell latexes with magnetite as core) **[18]**.

In continuous polymerization all ingredients are added continuously to one part of the reactor system and partially or completely converted latex is removed continuously from another part. The rate of polymerization is controlled by the rate of monomer addition, but nucleation occurs throughout the reaction so the number of particles varies continuously and the particle size distribution is more difficult to control.

All three processes consist of nucleation and particle growth stages which may occur sequentially or concurrently. The nucleation stage is not always reproducible and this causes batch variation in number and particle size of successive polymerizations using the same recipe. The

particle growth stage, however, is reproducible and can be easily followed. In all three processes seeded emulsion polymerization may be used to control the number of particles and the particle size distribution, thus obviating the unreproducible particle nucleation stage.

Advances in emulsion polymerization like the modeling of batch, semi-continuous and continuous polymerization and copolymerization processes and the use of functional monomers such as acrylic acid, sodium styrene sulphonate or acrylamide and polymeric emulsifiers tailored to specific applications have enabled the production of latex particles with excellent colloidal stability and surface characteristics that are more suitable for the many different applications than those made with conventional emulsifiers.

1.2 (c) *General Uses*

Polymer particles have been extensively used in a wide variety of applications **[1-4,19-28]**. They have been used as additives to various materials: styrene-butadiene copolymer latexes are used as additives for paper coatings, carpet backing, non-woven fabrics, reinforcement of concrete; polyvinyl acetate and vinyl acetate copolymer latexes are used as additives in adhesives, paints and other coatings; polychloroprene latexes are used as additives for synthetic rubber and generally as rheological modifiers; inverse polyacrylamide latexes (water-soluble polymers) are used as additives for flocculation, sludge treatment and oil recovery.

Small quantities of monodispersed polymer latexes are used as size

calibration standards for light scattering instruments, electron and optical microscopes and various particle counting devices such coulter counters, and for the determination of pore sizes.

Because of their perfect spherical shape, extremely uniform size distribution, and well-characterized surfaces, polymer latexes are widely used as model colloids to test theories in colloid, surface and rheological sciences.

Recently a significant number of additional applications of polymer latexes in the biomedical field have emerged. These applications exploit advances in polymer chemistry and the new developments in biotechnology. Some of these applications are fully realized now whereas others are still at the early developmental stages.

Magnetic monosized polymer latexes with appropriate monoclonal antibodies are used to remove T cells from bone marrow that is to be used for transplantation across histocompatibility barriers **[25]**. Removal of the T-cells prevents graft-versus-host disease, which is presumably caused by minor differences in histocompatibility complexes. The same method can also be used to remove tumor cells from human bone marrow cell suspensions that are used in autologous bone marrow transplantation.

Polymer latex microspheres loaded with chemotherapeutic agents and targeted selectively to the tumor site using monoclonal antibodies are potentially an excellent drug delivery system since targeting and controlled release of drug can both be achieved by this method **[26,27]**. Although a number of polymer latexes have been studied extensively for applications to drug delivery systems, their use has been limited because of the rigid demands on the properties of the microspheres; in order to be accepted for use they must be biocompatible, biodegradable, non-toxic

and allow the entrapment and release of drugs at controllable rates, and at the same time have appropriate size to penetrate blood capillaries.

As mentioned in the introduction, protein-coated polymer latexes have been extensively used in diagnostic immunoassays as solid supports. Latex particles between 0.1μm and 1.5μm in diameter are used mainly as carriers for Ag-Ab reactions in latex agglutination tests **[1-4]**. The particles are coated with soluble antigens and used as reagents for testing the presence of antibodies or antigens in a given fluid sample. Since each antibody molecule has two binding sites when the test sample containing the appropriate antibody is added to the antigen-coated latex particle suspension, a precipitate forms as a result of the interaction between the antigen and the antibody. Dissolved antigen competes with bound Ag for Ab so if the response to a known Ab concentration is known its modification by the presence of soluble Ag can be calibrated to allow estimation of the Ag concentration in the test fluid. This process is examined in some detail in this thesis.

Particles with sizes from 1.5μm to 100μm or larger, are used in immunoassays in which labels such as gamma and beta emitting isotopes, free radicals, enzymes and coenzymes, or fluorescent, bioluminescent, or chemiluminescent molecules are employed **[3]**. The label is used only as a tracer and does not usually interfere with the Ag-Ab interaction.

Porous and non-porous styrene-divinylbenzene latex particles in the size-range 10-1000μm have been traditionally used in a number of chromatographic systems. The particles can be used as such or modified to give ion exchange resins. More recently, strongly hydrophilic porous particles made from highly hydrophilic vinyl compounds in water and oil emulsions have found wide use in fast protein liquid chromatography

(FPLC) [28]. These particles are of uniform size with very highly hydrophilic surfaces and are produced in the form of strong cation and anion exchangers with poly-buffer exchanger capacity for chromatofocusing. The FPLC systems have found wide applications in separation and analysis of biological materials and the polymer particles used with them have proven to be superior to other natural polymers like dextran and agarose.

Other applications of latex particles in the biomedical field include their use as flow cytometry standards, latex based DNA/RNA hybridization assays, *in vivo* imaging applications such as the use of radioidonated microspheres to determine the site of internal bleeding, and phagocytosis research to identify blood cells or to insert chemicals into cell interiors [6].

1.3 Properties of Polymer Latexes

1.3 (a) *Surface Functional Groups*

Most polymer latex particles have an inherent surface functional group such as sulfate ($-OSO_3H$), carboxyl (-COOH), hydroxyl (-OH), or amide ($-CONH_2$) which is introduced during polymerization using an appropriate choice of initiator: sulfate groups can be introduced by using potassium persulphate as initiator, and carboxyl groups by using cyanopentanoic acid as initiator. Functional groups can also be added to the particle surface after polymerization by surface chemical modification.. Several functional groups, in varying proportions, can be

added to the latex particle surface giving a latex with carboxyl, sulfate, and hydroxyl surface functional groups. Typical latex surface functional groups are shown in Figure 1.

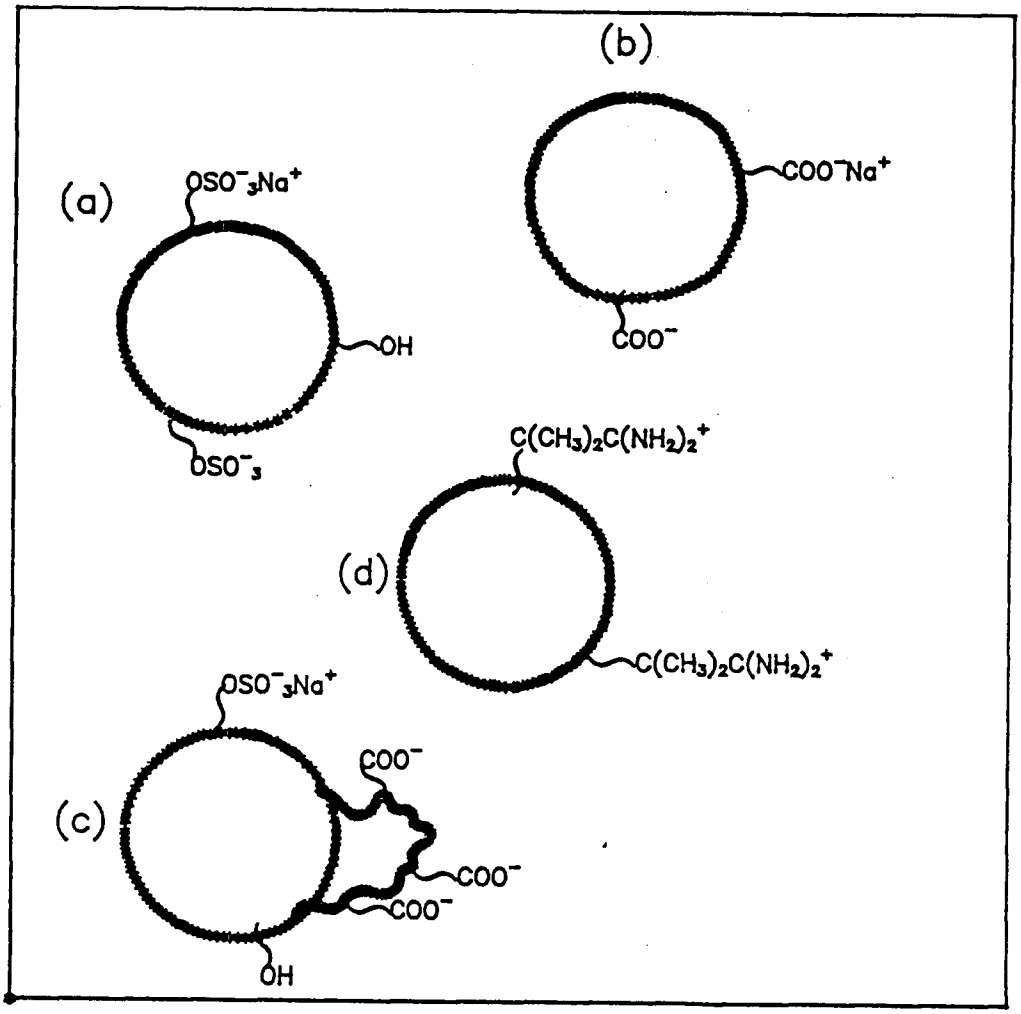

Figure 1. Surface functional groups of typical latex particles.

(a) Sulfate latex
(b) Carboxyl latex
(c) Carboxyl Modified latex
(d) Amidine (+) latex

The ionisation of these surface functional groups in solution results in a net charge at the particle surface. The surface charge density ranges from about one charge group per every 100 $Å^2$ of the particle surface down to about one charge group for every 3000 $Å^2$ depending on the type of charge group and the conditions used in the preparation of the latex particles. Latex particles with low surface charge density are predominantly hydrophobic in character and those with high surface charge density are predominantly hydrophilic. Many latex types, however, can have intermediate surface characteristics.

The surface charge density is important as an indication of the number of the active chemical functional groups that might be available for surface reaction, as an indication of the ratio of hydrophobic to hydrophilic areas of the particle surface, and as a guide to the latex stability.

The stability of the polymer latex suspensions arises mainly from the ionisation of the chemical groups at the particle surface or by adsorption of surface active agents from solution **[29]**. A net charge develops at the particle surface, and this affects the distribution of ions in the surrounding interface region, resulting in an increased concentration of counter ions (ions of charge opposite to that on the particle surface) close to the surface and an outer diffuse region away from the surface where the ions distribution is determined by a balance of electrostatic forces and random thermal motion. This distribution or arrangement of ions around the particle in such a manner is known as the electrical double layer and is formed around each particle in the dispersion **[30]**. This is schematically represented in Figure 2.

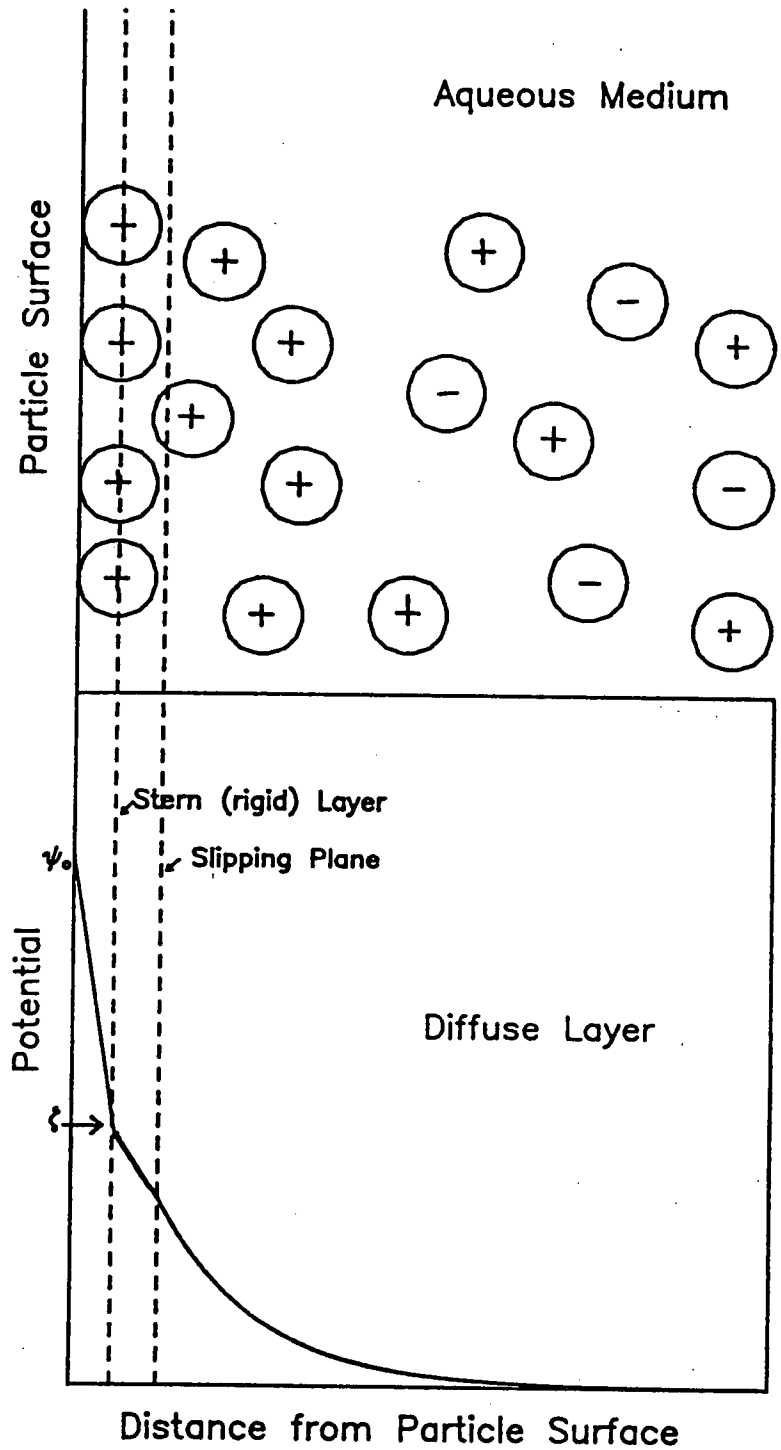

Figure 2. The electrical double layer in the interfacial region close to a charged particle surface and the potentials in the interface region. (Adapted from Lyklema, J. [29]).

The latex particle surface charge can be determined by direct conductiometric titration to detect the equivalence point, in a similar way to conductiometric acid-base titration. For the latex particles, however, all the charged groups must be converted to the acid form, and any adsorbed surface material which is not an integral part of the latex surface, must be removed prior to titration **[10]**. This is usually accomplished by one of the following methods: dialysis of the latex particles in distilled water, repeated wash by centrifugation/decanting procedure, or more efficiently by treating the latex dispersion with a mixed-bed ion-exchange resin. The conductiometric titration method determines all the charge groups within the peripheral zone of the latex particle and as such may not give an accurate indication of the number or distribution of peripheral surface groups which determine the latex interaction with its environment. It is therefore often used in combination with other techniques such as electrophoresis to provide a more complete characterization of the surface charge of the particle.

In electrophoresis the surface charge of the latex is calculated from the particle velocity resulting when an electric field is applied to a suspension of the particles. The particles migrate towards the electrode of opposite charge at constant velocity and the electrophoretic mobility (particle velocity per unit of applied electric field) is a measure of the surface charge of the particles. An individual particle and its most closely associated ions (Stern layer, **[31]**) move through the solution as a unit, and the potential at the boundary of this layer, that is, at the hydrodynamic surface of shear between the particle and its ion atmosphere is known as the zeta potential, ζ (see Figure 2.). The zeta potential is accepted as a measure of the particle surface potential, but

it is lower than the potential generated at the particle surface by the charged (ionized) functional groups. Nevertheless, it is the relevant electrical potential when discussing particle stability. It also determines the local ionic concentration close to the electrophoretic surface of a particle which will differ from the concentration of ions in the bulk suspending medium. Since the H^+ and OH^- ion distributions are affected by the local potential, the pH near the surface, pH_s, will differ from the bulk value as measured by a conventional pH meter. Thus, for a negatively charged latex particle pH_s will be lower than the bulk value since the hydrogen ions concentration will be higher near the negatively charged surface. For a positively charged latex, the surface pH will be higher than the bulk value. Hartley and Roe [32] showed that there is a difference of one unit of pH between the bulk medium and the latex surface for every 59mV of a zeta potential.

In terms of the adsorption of ionic species, the zeta potential is a useful indicator of the ease of access of the ionic species to the surface of the latex particles.

1.3 (b) *Particle Size*

As indicated earlier, polymer latexes can be prepared with sizes that cover a wide range of diameters, from about 0.02μm to 100μm, depending on a variety of factors during the polymerization process. These include the availability of monomer and free radical initiators during polymerization, and the temperature of the reaction.

The particle sizes of latexes can be determined by a variety of methods including transmission electron microscopy [33], light scattering [34], electrophoresis [35], hydrodynamic chromatography [36], electronic particle size analysis [37], and centrifugation [38]. Transmission electron microscopy is frequently used for particle size determination because the whole of the particle size range can be measured by this method. However, light scattering is also a popular method because of the simplicity of the technique.

Usually batch preparations with a coefficient of variation on the diameter of less than 10 per cent are termed "monodisperse" and those with a higher coefficient of variation are considered as "polydisperse".

The physicochemical behavior of polymer latexes is dependent on their particle size and state of dispersion. Characteristics such as stability and viscosity of latex suspensions are greatly influenced by their size and monodispersity. In general, latex particles with diameters larger than approximately 0.6μm tend to sediment under the action of gravity on prolonged standing. Such latex particles can be redispersed readily by gentle agitation. Surface active agents such as sodium dodecyl sulfate (SDS) are often used at low concentrations (<0.1%) to assist in the redispersion of latexes if the surfactant can be tolerated later in the use of the particles.

Some of the applications of the latex particles mentioned earlier depend primarily on the uniformity and size range of the particles. The use of latex particles as standards to calibrate equipment like particle counters, electron and optical microscopes and the various light scattering instruments depend specifically on the uniform size of the particles and on the ability to measure them accurately. Particles with

known diameters are used to check openings in filters, pores and blood vessels [39]. Larger particles (>3μm) are used in various chromatographic columns. The importance of uniformity in particle size here is to control the pressure drop necessary to get flow through the packed bed. Uniform spheres give packing with more porosity (void space) and larger pore diameter than non-uniform spheres. The use of uniform latex spheres minimizes the pressure drop and leads to better flow.

1.3 (c) *Colloidal Stability*

Colloidal dispersions are two-phase systems, the dispersed phase in the present case being a solid (polystyrene latex) and the dispersion medium a liquid, water. If the dispersed phase is highly compatible with the dispersion medium, the colloidal system is described as hydrophilic or lyophilic. When the two phases are incompatible, the system is described as hydrophobic or lyophobic.

The concept of stability in colloid science is generally understood to mean kinetic stability, i.e., stability imposed by a potential energy barrier larger than the average kinetic energy of the particles and acting to reduce contact between the suspended particles. The average translational energy of colloidal particles undergoing Brownian motion is of the order of (3/2)kT per particle, where k is Boltzmann's constant, and T is the absolute temperature. Thus, provided the potential energy barrier is sufficiently high, compared with kT, the dispersion is said to be colloidally stable. If the ratio of the potential energy barrier to kT is reduced to less than 2, then colloidal instability ensues.

Polymer latex particles dispersed in a continuous medium are in constant Brownian motion. They experience interaction forces of various types, the magnitudes of which strongly depend on the inter-particle distances. Four types of forces between colloidal particles have been distinguished: London-van der Waals attraction, electrical double-layer repulsion, steric effects due to adsorbed or grafted polymers, and short-range structural forces associated with structural differences between the interfacial region of fluid in the vicinity of a particle compared with the bulk liquid **[40]**. The overall colloidal stability of the dispersion is therefore determined by the combination of the various type of interaction forces.

London-van der Waals forces originate from the fluctuations in the charge distribution in one molecule polarizing a second molecule and vice versa. The London free energy of attraction between a pair of atoms or molecules, ΔG_A, is very short range, varying inversely with the sixth power of the separation distance **[41]**:

$$\Delta G_A = - \frac{(3/4)h\nu_0\alpha_0^2}{H^6}. \qquad (1.1)$$

where α_0 is the atomic polarisability, h is Planck's constant, ν_0 is the dispersion frequency and H is the distance of separation of the atoms.

For an assembly of atoms or molecules London forces are, to a first approximation, additive and the total attractive energy between the assembly of particles can be computed by summing the attractions between all interparticle pairs. For example, a colloidal dispersion containing

say, 10^3 particles would have the attractive interaction magnified by a factor of 5×10^5, as a result of additivity **[42]**.

The theory of the stability of colloidal dispersions distinguishes between lyophobic dispersions, in which the dispersed particles are not significantly solvated, and lyophilic dispersions, in which layers of solvent molecules cover the surface of the particles and help stabilize them against aggregation.

The theory of the stability of lyophilic dispersions is still not well understood. However, it is well known that this system can be aggregated by partial removal of the solvent layer either by addition of relatively large amounts of ions that hydrate readily, or by the addition of a second solvent with high affinity for the dispersion medium.

For hydrophobic dispersions, such as PSL in water, the insignificance of the solvent layer means that the stability of the system is largely determined by the interaction between the particles during the course of their collision. When charged latex particles dispersed in aqueous medium approach each other, electrostatic interactions between the individual ionic double layers surrounding the particles lead to mutual repulsion. This repulsive force is dependent on the charge on the particle (and hence on the electric potential at its surface) and on both the type of electrolyte and its concentration in the medium of dispersion. A balance between the electrical properties of the particles and the London-van der Waals attractive forces determines the suspension stability. This is the basis of the theoretical model of classical colloid stability as put forward by Derjaguin and Landau **[43]** and independently by Verwey and Overbeek **[44]** who described the interaction in energetic terms and combined the repulsive potential

energy of the particles due to their electrical double layer interactions and the attractive potential energy due to the London-van der Waals forces to give the total potential energy of interaction for a pair of hydrophobic particles. When attraction dominates, the particles adhere and the dispersion aggregates and becomes unstable. When repulsion dominates, the system remains in a stable, dispersed state. This theory is commonly known as the DLVO theory, in recognition of its originators. A summary of the principles involved in this theory, with no detailed derivations, is given below.

Electrical Double Layer

In an aqueous medium, most colloidal particles acquire an electrical charge on the surface which gives rise to a surface electrostatic potential , ψ_0, which is assumed to be at the effective slipping plane between the particle (and associated fluid) and the bulk fluid. The total free energy of electrostatic repulsion arising from interaction between individual double layers of two particles, ΔG_R near each other, is best represented as **[44]**:

$$\Delta G_R = 4\pi\varepsilon_s\varepsilon_0\psi_0^2 a^2 \frac{\exp(-\kappa(H-2a))}{H} \quad \ldots\ldots(1.2)$$

where ε_s is the dielectric permittivity of the medium; ε_0 is the permittivity of free space; a is the radius of particle; H is the distance between the centers of the particles; and κ is the reciprocal

Debye-Hückel electrical double layer thickness.

If the ionic double layer is thin, i.e. $\kappa a \gg 1$, then the alternative Derjaguin approximation provides the appropriate free energy of interaction for particles with constant ψ_0 **[45]**:

$$\Delta G_R = 4\pi\varepsilon_s\varepsilon_0\psi_0^2 \ln \{1 + \exp(-\kappa(H-2a))\} \quad \ldots\ldots(1.3)$$

The Debye-Hückel electrical double layer thickness is given by:

$$\frac{1}{\kappa} = \left[\frac{1000\varepsilon kT}{8\pi e^2 N_A I} \right]^{1/2} \quad \ldots\ldots(1.4)$$

where k is Boltzmann's constant; e is the electron charge; T is the absolute temperature; N_A is Avogadro's number; and I is the ionic strength of the solution = $1/2 \sum_i z_i^2 C_i$; z_i is the valency of the i^{th} ionic species; and C_i is the molar concentration of the i^{th} ionic species. When the thickness of the double layer $1/\kappa$ is large , the free energy of repulsion decreases very slowly with separation distance whereas the opposite is the case with small double layer thickness. This thickness in turn is controlled by the type and concentration of electrolyte in the system, i.e. by the ionic strength. Thus, at low ionic strengths the electrostatic repulsion provides a long range term, whereas at high ionic strengths the repulsion energy term decays very rapidly with distance.

van der Waals Attractive Potential

The total free energy of interaction, ΔG_A, between two spherical particles of equal radius, at small separations (H-$2a$), was derived originally by Hamaker **[46]** in the form:

$$\Delta G_A = - \frac{Aa}{12H} \qquad (1.5)$$

where A is the composite Hamaker constant for particles in the medium, given by

$$A = (A_{11}^{1/2} - A_{22}^{1/2})^2 \qquad (1.6)$$

with A_{11} = the Hamaker constant of the particles and A_{22} that of the medium.

The Hamaker (microscopic) approach to the calculation of the attractive energy between particles assumes additivity of interatomic dipole-induced dipole interactions and deals with a dispersion frequency characteristic of the material for calculating the interaction constant. This approach has been shown to be unsatisfactory **[47]**, as there are contributions to the interaction constant from all the frequencies, and, in addition, allowance for the presence of a medium is unsatisfactory. Some of these problems associated with the Hamaker (microscopic) theory

are overcome by the continuum theory of Lifshitz **[48]**, in which expressions are derived for the interaction between two bodies separated by a medium, including contributions from all interaction frequencies. This results in a more accurate calculation of the van der Waals attractive forces. However, to apply the Lifshitz theory, one has to use experimental data on bulk samples and the necessary data are often not available for many materials.

The electromagnetic waves which are responsible for the London attraction between particles propagate at the speed of light between the particles. Thus, for a widely separated pair of particles, a time lag or a phase difference develops between the vibrations at the two locations. This time lag or retardation increases as the separation becomes comparable to the wavelength of the propagating field. Consequently the dispersion forces will decrease more rapidly than predicted by the Hamaker equation (1.5).

Total Free-Energy of Interaction (DLVO Theory)

Usually the zeta potential (ζ) of the particle, i.e., the potential at the hydrodynamic shear plane of the particle, is equated with the surface potential of the particle, ψ_o. For the situation in which only electrostatic and van der Waals interactions are predominant, the total free energy of interaction between two particles, ΔG_T, is given by the DLVO theory as **[41]**:

$$\Delta G_T = \Delta G_A + \Delta G_R \quad \text{.....(1.7)}$$

The total free energy curves for ΔG_T, ΔG_A, and ΔG_R between two particles are illustrated in Figure 3. The sharp increase of repulsion energy at very close approach is due to repulsion between the electron clouds of atoms of the particles and is referred to as the Born repulsive energy. In general, the energy-distance curve can show three main features: a primary minimum, M_1, at close contact, a maximum P , and a shallow secondary minimum at long distance of separation, M_2. The introduction of a distance of closest approach is important with regard to the shape of the total interaction energy-distance curve. A deep primary minimum is obtained only if the particles come into contact. But direct contact is unlikely since the distance of closest approach is determined by adsorbed layers of counter ions (in the Stern layer) and/or adsorbed solvent molecules.

The higher the value of P , the more kinetically stable the suspension. According to the DLVO theory, an energy barrier of about 15 kT is sufficient to produce a highly dispersed system. In practice, however, there is a spread of potential energies and coagulation can occur at this energy barrier level, so a value of P in excess of 25kT is taken as a criteria for stability. The theory also indicates that the magnitude of the energy barrier depends on the dimensions of the particles and their surface potential. With large particles, the net potential energy may develop a secondary minimum at an appreciable distance of separation. For latex particles, calculations show that the influence of the size of particles on the energy barrier is such that for particles with radii $\approx$ 200 nm or greater, a secondary minimum of sufficient depth for flocculation is formed.

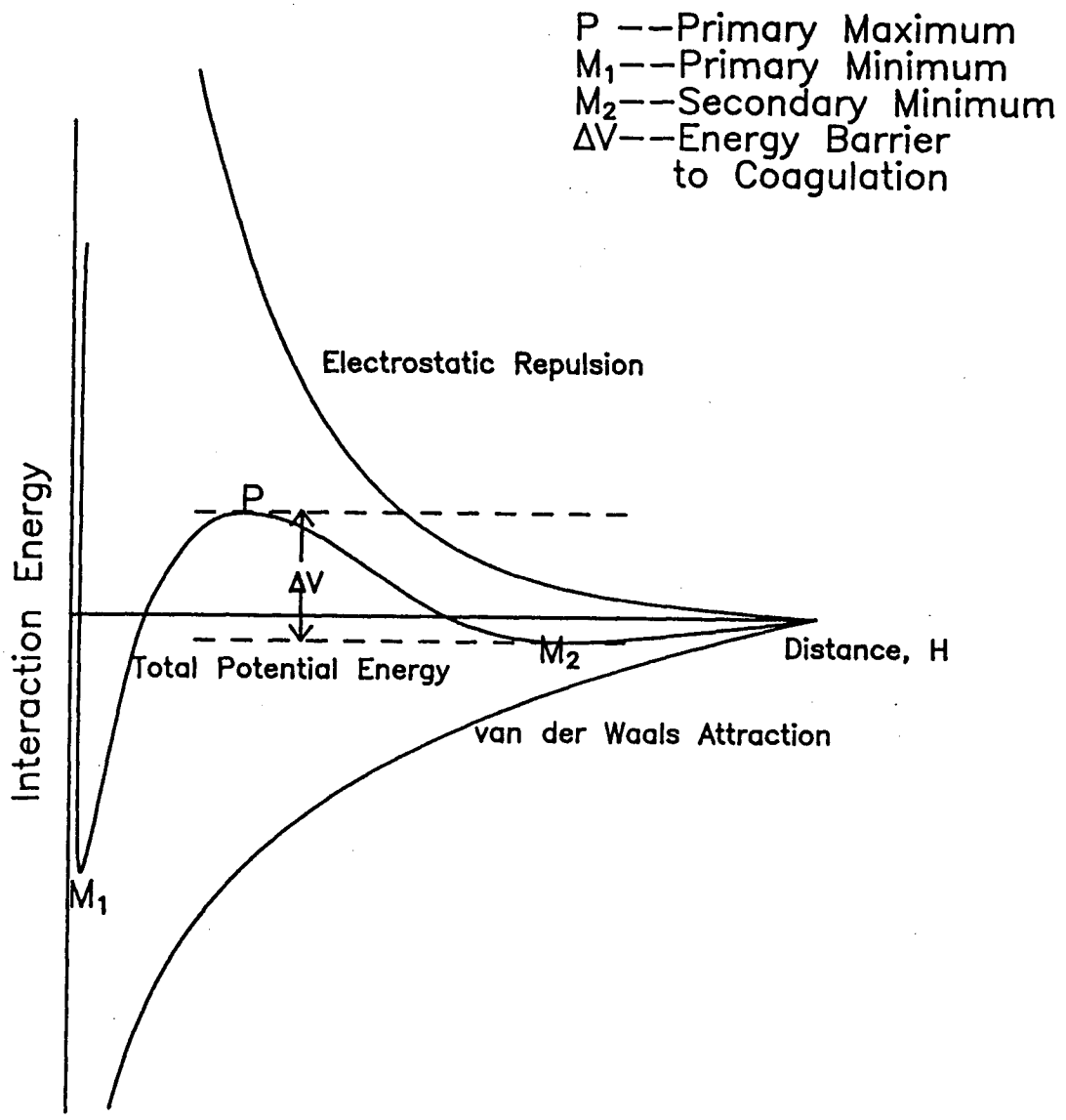

Figure 3. Typical form of the total-interaction free energy between electrostatically stabilized polystyrene latex particles with separation distance H. (Adapted from Everett, [53]).

Therefore in practice, primary minimum coagulation and secondary minimum coagulation can occur simultaneously under certain conditions. The characteristics of the aggregates formed in the secondary minimum are quite different from those formed in the primary minimum. Primary minimum aggregates are compact and usually extremely difficult to redisperse, whereas the aggregates formed in secondary minimum are weak and can easily be disrupted by hydrodynamic shear forces.

Although the DLVO theory forms the basis of classical colloid stability theory, more recently various other interactions between colloidal particles have been identified. These include the steric forces which are long-range repulsion arising from polymers adsorbed and/or anchored to the interacting surfaces; and structural forces, which are strong repulsive forces that arise as a result of changes in the solvent structure in the vicinity of the colloidal particle surface or interface.

Steric Forces

Additional repulsive interactions can occur when the particles bear adsorbed layers of surfactants or macromolecules. An adsorbed layer thickness, δ, may be defined in terms of the configuration of the adsorbed surfactant or macromolecule in analogy, for instance, to the radius of gyration of a free polymer molecule **[140]**. When two particles with adsorbed layers approach each other to a separation distance that is less than twice the adsorbed-layer thickness ($H<2\delta$), interference may occur. Under certain conditions this interference may lead to repulsion for the following possible reasons **[49]**:

(i) The mixing of adsorbed layers may lead to repulsion. This is because the solvent chemical potential in the overlap region is lower than that in the bulk solution and as a result, diffusion of solvent molecules occurs from the bulk solution to the overlap region, leading to repulsion.

(ii) As the adsorbed layers approach each other, the volume available for the adsorbed chains becomes restricted. The loss of configurational entropy of the chains as a result of such an approach leads to repulsion. This effect is often referred to as the volume-restriction effect.

(iii) The van der Waals attractive force between the particles in dispersion varies with distance of separation as a power law (i.e $\propto r^{-6}$). Thus the effect of increasing adsorbed-layer thickness is to effectively reduce the attractive van der Waals forces **[51]**.

Various models have been developed for steric interaction forces and expressions have been derived for the contribution of steric interaction to the total repulsive energy of interaction between two particles. For example, Napper, **[50]** has given the following approximate expression for the steric interaction between two spheres with adsorbed polymer layers:

$$V_R^S = \frac{2\pi a k T V_2^2 \Gamma_2^2}{V_1} (1/2 - \chi) S_{mix} + 2\pi a k T \Gamma_2 S_{el} \quad .....(1.8)$$

where V_1 is the solvent molecular volume, V_2 is the polymer molecular volume, Γ_2 is the adsorbed amount of polymer per unit area, χ is the Flory polymer/solvent interaction parameter, and S_{mix} and S_{el} are the geometric functions that depend on the form of the segment concentration

profile $\rho(z)$, in the adsorbed layer normal to the interface. The need to establish the variation of the concentration profile, $\rho(z)$ with separation distance of the particle and the many assumptions made in the derivation of the equation limits the applicability of this expression in practical systems.

In general, the presence of polymer either on the surface of colloidal particles or free in solution can lead to other types of interactions between the particles. For example, high molecular weight polymers present in low concentration can cause bridging flocculation by attaching to several particles at the same time **[52]**. An excess of non-adsorbed polymer in a colloidal dispersion can also cause depletion flocculation in which polymer molecules are excluded from the space between particles as they approach each other, reducing the concentration of polymer between the particles below that in the bulk solution. The osmotic pressure difference between the gap and the bulk solution results in an interparticle attraction.

Agglutination of Antigen-coated PSL

When the mechanism producing particle aggregation arises from specific interparticle bridging by ligands or macromolecules, as in the case of an antigen-antibody interaction, the process of aggregation is termed "agglutination." The forces involved in agglutination reactions include the short range van der Waals attractive forces, repulsive electrostatic force, steric repulsion, and the specific antigen-antibody interactions. The short-range van der Waals attractive forces are, to a first approximation, independent of pH and ionic strength. The

electrostatic repulsive force is controlled by the pH and ionic strength of the system, its magnitude being dependent upon the charge of the particle which in turn is dependent upon the charge of the coating protein. The antigen-antibody interaction force can involve electrostatic, hydrogen bonding, hydrophobic, and van der Waals forces but is primarily dependent on the spatial complementary configuration of the reactive binding site on the antibody and the determinants on the antigen molecule.

Total Free-Energy of Interaction (General Equation)

It is clear from the brief consideration above that the total free interaction energy between two colloidal particles can be influenced to a varying degree by several contributions. Thus, the most general equation for the total free energy difference between particles can be obtained by adding all the contributions **[41]**:

$$\Delta G_T = \Delta G_A(\text{van der Waals}) + \Delta G_R(\text{short range}) + \Delta G_R(\text{electrostatic}) + \Delta G_R(\text{steric}) + \Delta G\ (\text{other effects}) \quad ...(1.9)$$

However, in practice it is not necessary to consider all these contributions simultaneously, except in certain special cases.

Relative Stability

The measure used to determine the relative stabilities of different polymer latexes that are stabilized by electrostatic interaction is called the critical coagulation concentration (the c.c.c. value). Coagulation of charge stabilized latexes occurs at a well-defined electrolyte concentration that is strongly dependent on the valence of the added counterion. It has been established that the critical coagulation concentration varies inversely as the sixth power of the counterion valency; this is known as the Schultze-Hardy rule **[53]**.

Similar expressions are used to describe flocculation of colloidal particles induced by the presence of polymer either on the surface of the particles or simply present in solution. For example, the term "critical flocculation concentration" (c.f.c.) is used to describe the critical particle volume fraction for the onset of flocculation in the presence of polymer, and "critical flocculation temperature" (c.f.T) to describe the observation that for a given particle volume fraction, a critical flocculation temperature is reached, beyond which the onset of weak (reversible) flocculation is observed.

1.3 (d) *Fluid Motion and Colloid Stability*

Coagulation caused solely by Brownian motion of the particles is usually referred to as "perikinetic coagulation" and that caused solely by a velocity gradient is called "orthokinetic coagulation". Any

coagulation caused by external forces is treated as a special case of orthokinetic coagulation, since the movement of particles relative to the liquid also creates velocity gradients.

In terms of the attractive and repulsive forces that are operative during coagulation, "rapid coagulation" occurs when there are no surface repulsive forces between the particles, that is when every collision leads to aggregation; and "slow coagulation" occurs when only a fraction of the collisions result in aggregation, that is when there exists a significant surface repulsion force causing a barrier to coagulation.

The theoretical analysis of coagulation kinetics was first outlined by Smoluchowski **[54]**, who considered the case where double layer interaction between the particles was absent, so that the rate of coagulation is fully governed by Brownian motion (perikinetic coagulation). For monodispersed colloidal particles, Smoluchowski showed that the rate of diffusion-controlled coagulation is proportional to the collision radius of the particles, the diffusion coefficient, and the square of the concentration of the particles:

$$\frac{-dn}{dt} = 4\pi D_i R_i n^2 = k_i n^2 \qquad \text{.....(1.10)}$$

where

D_i = diffusion constant of a spherical particle of radius a_i

= $kT/6\pi\eta a_i$ (Einstein Equation)

η is viscosity of the continuous phase, k is Boltzmann's constant, and T is absolute temperature. R_i = collision radius (= $2a_i$ for homodisperse

particles), n = number of particles per cm^3, and $k_i = 4\pi D_i R_i$, is the rate constant for diffusion-controlled coagulation. Since coagulation is a continuous process, particles of different radii are involved in the coagulation even if the original system is homodispersed. That is, the values of diffusion constant, the collision radius, and the rate constant should strictly be: $k_{ij} = 4\pi D_{ij} R_{ij}$, $R_{ij} = a_i + a_j$, and $D_{ij} = D_i + D_j$. However in theory it is assumed that $a_i = a_j$ to simplify the rate expressions. Equation 1.10 only applies to rapid coagulation that occurs by Brownian diffusion and bulk fluid motion is of no consequence, and where there are no energy barriers present to interfere with the coagulation process.

At another extreme, Smoluchowski also considered coagulation caused solely by bulk flow of fluid in a laminar shear field giving a constant velocity gradient (shear-induced or orthokinetic coagulation). In this case Smoluchowski considered a stationary reference particle in a constant velocity gradient and assumed that the uniform shear field is unperturbed by the presence of the particles, and, therefore, the path followed by a particle is rectilinear. He also assumed that only binary collisions occurred, each resulting in a new aggregate composed of two interacting particles. Using similar assumptions and simplification as for the case of Brownian coagulation, i.e. uncharged spherical particles interacting through van der Waals attractions, Smoluchowski obtained the following equation for coagulation under uniform shear field:

$$\frac{-dn}{dt} = \frac{4G\phi n}{\pi} \quad \text{.....(1.11)}$$

where G is the velocity gradient, and ϕ is the volume fraction of particles. Equation 1.11 is strictly applicable for coagulation caused solely by a uniform shear field. However, in practice it is difficult to obtain a uniform shear field as constant velocity gradients are difficult to achieve. A close experimental form of a uniform shear field occurs in the annular gap between coaxial rotating cylinders (couette apparatus).

More recently, the effects of interparticle forces on shear-induced aggregation have been treated theoretically. Using improved hydrodynamic results for binary interactions between spheres presented by Batchelor and Green **[55]**, Curtis and Hocking **[56]**, van der Ven and Mason **[57]**, and Zeichner and Schowalter **[58]** have developed a trajectory analysis approach for the determination of shear stability which incorporates hydrodynamic forces as well as London-van der Waals attractive forces and electrostatic repulsive forces as described by the DLVO theory. These analyses indicate that the presence of fluid between the particles as they approach one another reduces the likelihood of a collision and so reduces the coagulation rate. Van der Ven and Mason have calculated that in the absence of any repulsive forces between particles this hydrodynamic effect caused a reduction in coagulation rate which was proportional to the shear rate to the 0.18 power. When combined with the explicit first order coagulation rate dependence on shear rate, this gives rise to a coagulation rate which is proportional to the 0.82 power of the shear rate.

Slow Coagulation

The coagulation analyses presented above consider two extreme cases where coagulation occurs rapidly either by Brownian collision only or by shear collision only. The frequency with which the reference particle is bombarded by the other particles is given by **[59]**:

$$J_B^o = 4\pi D_{ij} R_{ij} n \quad \text{(for Brownian collision)}$$

$$\text{and} \qquad J_S^o = 4/3\ n\ R_{ij}^3\ G \quad \text{(for shear collision)}$$

Coagulation can also occur with slower rates of collisions as when there is an energy barrier in the form of double layer repulsion between the particles, or , put another way, the coagulation occurs in the secondary minimum, the primary maximum being assumed to be so large that it is insurmountable.

In this case, the departure of coagulation rates from the extreme cases (rapid) can be expressed as a stability ratio:

$$W = J^o / J \qquad \text{.....(1.12)}$$

where J^o can be a Brownian or a shear-induced collision frequency limit. This idea was introduced by Fuchs **[60]** who considered the case of coagulation where particle interactions are important and found that the total collision rate is lowered by an amount W. He obtained the

following expression for W:

$$W = 2a \int_{2a}^{\infty} \frac{\exp (V/kT)}{H^2} \, dr \quad \ldots\ldots\ldots\ldots\ldots (1.13)$$

where V is the potential energy of interaction and kT is the thermal energy. W can also be defined simply as the ratio of the rate constant of the fast coagulation to that of the slow coagulation:

$$W = k_f / k_s \quad \ldots\ldots\ldots\ldots\ldots\ldots\ldots\ldots\ldots (1.14)$$

where k_f the rate constant of fast coagulation, where there is no energy barrier, and k_s is the rate constant of slow coagulation where there is an energy barrier due to interparticle repulsive forces.

A plot of log W versus log C (C = concentration of electrolyte) can be used in practice to distinguish between slow and fast coagulation **[61]**. Above a critical coagulation concentration, that is in the region of rapid coagulation, W = 1 and so log W = 0. Below the CCC value, it is observed that log W increases linearly with decrease in log C.

1.4 Interaction of Proteins with Polymer Surfaces

1.4 (a) *General Considerations*

The ongoing interest in (bio)polymer adsorption to particles is largely due to its importance in technical applications such as the control of stability, flocculation and rheological properties of colloidal dispersions **[23]**. The role of polymer adsorption in tertiary oil recovery and the regulation and control of lubricant properties, where surface treatment by polymer is used to adjust wetting are further examples of technical applications **[62]**. The adsorption of biopolymers in membranes, cell walls and in natural and artificial blood vessels leads to important phenomena in biology, pharmacology and medicine **[63]**. In different types of chromatography, biopolymer adsorption is a key factor in controlling the fractionation of uncharged and charged macromolecules by gel permeation, affinity, and hydrophobic chromatography.

Polymer and biopolymer adsorption studies are also of special interest from a purely theoretical and experimental viewpoint in that they give insight into structural, thermodynamic and dynamic properties of macromolecules in solution and at interfaces. This in turn contributes to our understanding of biochemical processes such as blood coagulation and cell adhesion to artificial surfaces.

Understanding of the properties of colloidal systems dispersed in solutions containing molecular species such as proteins must be based on a thorough knowledge of the interaction between the colloidal particles

and the protein molecules in solution and of the structure of the resulting interface between the colloidal particle and the protein molecule. The protein molecule adsorbs onto the particle surface due to forces such as the London-van der Waals interaction force, hydrophobic interactions, hydrogen bonding , and ionic interactions.

Many authors, using a wide variety of different techniques, have reported on the adsorption of proteins at the solid/liquid interface **[64-75]**. Hence, many of the general aspects of protein adsorption to a solid surface are well documented: the amount of adsorbed protein is known as a function of protein concentration in solution, and as a function of adsorption conditions for solids surfaces with different characteristics **[76-79]**. Other parameters such as the competitive adsorption behavior of proteins, the conformation of the protein at the solid surface as a function of total surface area available for adsorption, the adsorbed layer thickness and structure, and the consequence of such conformational changes and layer thickness on the interaction forces between the surfaces are less well documented **[66]**. This is partly because of the many variables which affect the adsorption of proteins onto solid surfaces.

Protein adsorption can be affected by the nature of the protein including its size, charge, structure, purity, and concentration; the nature of the solid surface such as hydrophobic/hydrophilic ratio, uniformity and surface energetics, and by experimental conditions such as the buffer, pH, ionic strength, and equilibration (flow or static) conditions **[66]**. Consequently, different results have been observed for protein adsorption at seemingly similar conditions and, likewise, various interpretations have been proposed to explain similar trends in protein

adsorption. For example, plateau values are often found to be not far from those of the close-packed monolayer of native molecules in a side-on or end-on orientation **[70]**. On the other hand, multilayer adsorption has also been noted **[80-85]**. The increase in adsorption towards the isoelectric point of the protein is explained by Norde *et al* **[86]** as being due to structural changes of the albumin molecule. They conclude that the adsorption behavior of albumin is determined mainly by the structural changes of the albumin molecule. Roe, **[86]**, on the other hand, explains similar increase in adsorption of BSA onto polyoxymethylene surface as arising mostly from reduced electric charge on BSA molecule and not from any change in its shape. He concludes that the predominant factor governing the adsorption of BSA on the polyoxymethylene surface is the electrostatic repulsion between the adsorbing BSA molecules. With regard to protein adsorption to polymer latexes, the factors that control the interaction seem to be the hydrophobic/hydrophilic balance on the surface of the latex, electrostatic interactions, and solution conditions **[87]**. For most proteins, hydrophobic interactions between the hydrophobic amino acid side chains of the protein and the uncharged regions of the polymer latexes seem to be responsible for adsorption. Several authors have noted that the affinity between a given protein and an adsorbent increases with the hydrophobicity of the surfaces **[88-100]**. Hence, for a given protein, adsorption increases with the hydrophobicity of the polymer latex surface **[100]**. The hydrophobic/hydrophilic ratio is determined by the number of functional groups on the latex surface, since the bulk polymer is hydrophobic. Too many functional groups on the latex surface can interfere with physical or chemical binding of proteins.

Since latexes have various hydrophobic to hydrophilic ratios, adsorption of proteins onto the surface of latex particles differ from one particle to another. For latex particles that are highly hydrophobic (<5 charges per 1000Å of surface), protein adsorption shows characteristics that are often independent of the sign of the net charge on both the protein and the polymer latex as, for instance, the pH changes. For ideal adsorption, latex particles should have sufficient hydrophobic surface area for protein adsorption. Hydrophobic interactions lead to protein molecules being strongly adsorbed to the latex surface; proteins desorb more easily from hydrophilic surfaces **[101]**.

Electrostatic interactions may also strongly influence the patterns of protein adsorption onto polymer latex surfaces **[76,88,90-93]**. The electrostatic effects, however, seem to be only superimposed upon the stronger hydrophobic effects. This is indicated by the fact that all proteins studied to date adsorb strongly to polymer latexes, regardless of the sign of charge on the latex and by the fact that positively charged polymer latexes show enhanced adsorption of negatively charged proteins, presumably through electrostatic attraction **[71]**. It is not clear, however, if the electrostatic interaction simply acts to increase the local concentration of the protein near the latex particle surface or if it is directly involved in ionic bonding. At high surface coverage, electrostatic repulsion between the polymer latex and protein bearing the same charge signs may hinder further adsorption.

Solution conditions such as the pH and ionic strength strongly affect saturation adsorption of proteins to polymer latexes. For example, it has been shown that protein adsorption is a strong function of pH, with a maximum in the amount adsorbed at pH values near the isoelectric point of

the protein [102]. This is explained in terms of the effect which the charge of the protein molecule has on its configuration and in terms of the repulsion between the adsorbed protein molecules. The lower amount adsorbed at pH values away from the isoelectric point of the protein is attributed mainly to structural rearrangements of the protein molecules. In many cases protein adsorption to polymer latexes is found to increase with ionic strength of the equilibrium buffer. This is thought to be due to the reduction in the protein-surface electrostatic interactions, protein-protein repulsion and protein conformational changes. On the other hand, other results show much less dependence of protein adsorption on pH and ionic strength [80], and, with regard to solution conditions, no general rules seem applicable.

There are many other factors that are involved in the interaction between protein molecules and the polymer latexes, but most of them are either not yet well documented enough to clarify the nature of the interaction, or are difficult to determine by most available experimental techniques. For example, considerable effort is now being devoted to the understanding of the structural and conformational details of adsorbed proteins at the solid/liquid interfaces. Information from such studies will be useful with regards to the orientation or conformation and biological activity (e.g. enzyme activity) of the adsorbed proteins. Surface energetic properties of the adsorbing surfaces is another factor that perhaps deserves more consideration in protein adsorption studies [103-105]. Baszkin [100] concluded that the ratio of the polar and dispersion components of the work of adhesion (W_A^p/W_A^d) determines the degree of affinity of the protein for the adsorbent and that maximum affinity occurs when (W_A^p/W_A^d) approaches unity. Andrade [101] and

Ruckenstein *et al* **[102]** concluded that neither the total surface free energy of the solid nor the fractional contributions of the solid's component surface free energy should be considered indicators of its ability to adsorb protein. Rather, the interfacial energy between the solid and water is a more natural parameter which should be related to protein adsorption. The larger the latter the greater the adsorption. On this basis a surface energetic criterion for biocompatibility of surfaces was suggested **[102]**.

Another aspect of protein adsorption to polymer surfaces that is incompletely understood is the competitive adsorption behaviour of proteins **[106]**. Much of the work done in this area has been focused on: (a) the understanding of the behaviour protein adsorption, as it occurs from relatively complex solutions of protein mixtures, to implanted biomaterials **[107]**; (b) a desire to understand the sequence of events leading to clot and thrombus formation on solid surfaces in contact with blood **[108]**; and (c) protein chromatography **[109-111]**. Horbett and Brash **[106]** list some of the important properties of proteins that influence competitive adsorption as follows: molecular size and electrical charge of the protein, hydrophobicity-hydrophilicity and chemical functional groups on the surface of the protein, conformational stability, interlayer (i.e. protein-protein) interactions in the adsorbed layers; and the surface characteristics of the adsorbent. An important result that is reported in a number of competitive protein adsorption studies is that initially, the effect of concentration on diffusion dominates and so the protein with the highest bulk concentration is adsorbed first. Later, as the concentration of higher affinity trace proteins near the surface increases they are adsorbed and the first adsorbed protein is

displaced. This mechanism is the basis of sequential adsorption in multi-protein systems **[112]**.

The effect of fluid shear on the adsorption of proteins has been studied by a number of authors **[113-116]**. Brash *et al* **[108]** utilized polyethylene and glass surfaces in the form of tubing segments and found that as much as 75% of adsorption is complete within a few minutes and equilibrium is attained within about one hour. Their results show that exchange of proteins between surface and solution occurs and that this exchange varies with the nature of the surface (i.e greater for hydrophilic than for hydrophobic), and depends upon such factors as protein concentration and flow rates. Rudee *et al* **[114]** designed a flow cell to which a thin film of test material (e.g. polystyrene) could be mounted on its surface. In the flow cell, the test material is exposed to flowing protein solutions under well characterized conditions. Following exposure of the test surface in the flow cell, the surfaces were examined in an electron microscope. Their results show differences in the morphology of the adsorbed individual protein molecules and protein films formed, on the type of surface to which the proteins are adsorbed, and the flow conditions under which the protein solutions contact the materials. However, the mechanism leading to the formation of the network of adsorbed proteins is not understood.

Robertson *et al* **[115]** studied the initial adsorption, desorption, and exchange kinetics of BSA on six polymer surfaces with widely varying surface properties and functionalities using total internal reflection fluorescence and found that the initial adsorption of BSA on surfaces such as polydimethylsiloxane (PDMS) is diffusion limited up to wall shear rates of 4000 s^{-1}, whereas adsorption of BSA on polystyrene sulphonate

(PSS) is diffusion limited at shear rates below approximately 70 s^{-1} but becomes kinetically controlled at higher shear rates. They also found that BSA adsorption on polymethyl methacrylate (PMMA) is kinetically controlled, and polyethylene oxide (PEO) surfaces show no adsorption of BSA under the conditions studied. Nakamura *et al* **[116]** examined BSA adsorption onto porous polymer resins by a pulse injection method and showed that the amount of BSA bound irreversibly to the resins is independent of the protein concentration and the flow rate studied.

Usually the adsorbed mass per unit area, Γ, is determined as a function of the equilibrium protein concentration in solution, C_p, and an adsorption isotherm (Γ vs. C_p) is constructed. For flexible, highly solvated polymers, high-affinity isotherms are almost always obtained. A typical high-affinity isotherm is given in Figure 4a. At low polymer concentration, virtually all the polymer is adsorbed until the surface is fully covered; the initial part of the isotherm merges with the ordinate axis. With higher polymer concentration, a continuously increasing value of Γ is usually found. This is explained by structural rearrangements in the adsorbed molecules, involving a decreasing number of attached segments per molecule. Near saturation Γ reaches a few mg/m^2 of the adsorbent surface **[71]**.

Pure, single globular proteins (compact molecules), in many cases develop well-defined plateau values with a finite initial slope as shown in Figure 4b **[71]**. The plateau values are often reached at dilute or semi-dilute protein concentrations in solution, depending somewhat on the conditions (adsorbent surface charge (σ_o), pH, temperature, and salt concentration) and correspond to a close-packed monolayer of native

proteins in a side-on or end-on orientations.

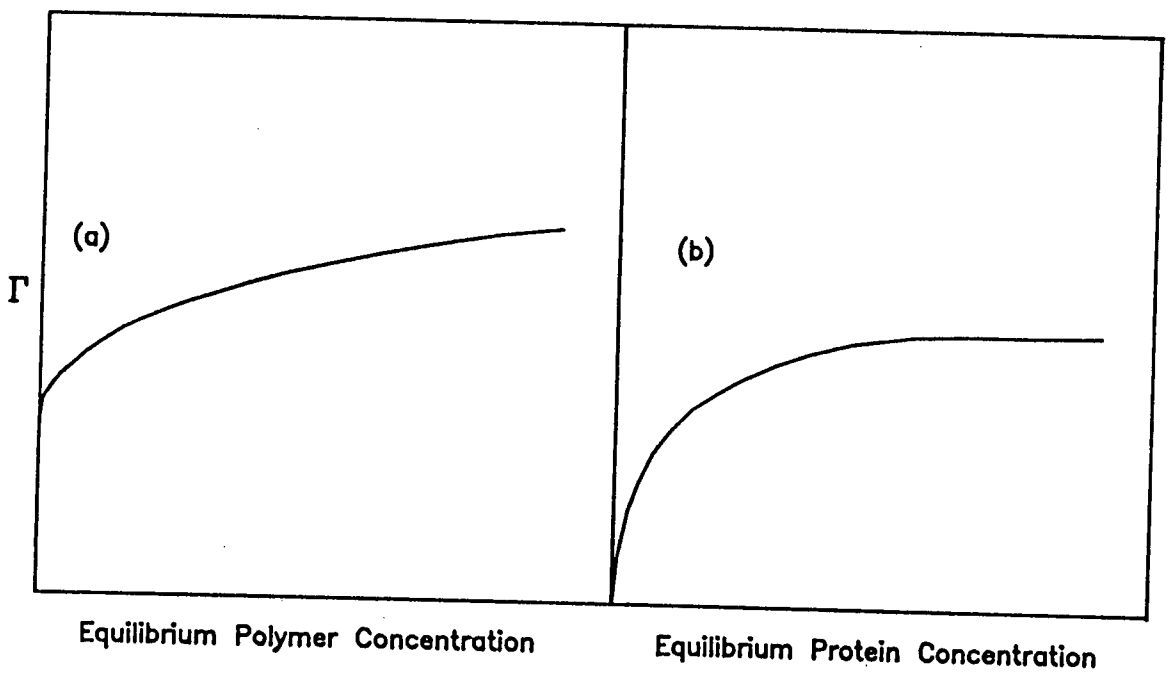

Figure 4. Typical adsorption isotherms for (a) flexible, highly solvated polymers and (b) globular proteins (compact molecules). (Adapted from Norde, W. **[71]**).

1.4 (b) *Theoretical Considerations*

Analyses of polymer adsorption have ranged from very simple applications of models derived for small molecules, to detailed statistical mechanical treatments of the conformational changes that usually accompany polymer adsorption **[117-125]**. Biopolymers such as globular proteins do not have the flexibility nor the simplicity of synthetic polymers. They display a complex 3-dimensional structure with a multiplicity of intramolecular interactions, surface functional groups, and conformational dynamics **[126]**. In principle the synthetic polymer statistical method could be extended to the adsorption of proteins, but there are serious limitations that have not been resolved to date. A major limitation is the use of the mean-field approximation to compute the lateral interaction between segments, which does little justice to the characteristically high specificity of proteins. On the other hand, relevant advances are being made and the extension of the theory to polyelectrolytes (polypeptides) has accounted, at least semi-quantitatively, for the effects of pH and ionic strength on adsorption of these types of polymer **[127]**.

One other aspect of polymer and protein adsorption that has not been widely considered in both theoretical treatments and experimental analysis of adsorption isotherms is the polydispersity effect. Many (bio)polymers used in experimental studies are either polydisperse, by nature of their synthesis, or form oligomers in solution **[128]**. Usually adsorption isotherms are interpreted assuming the adsorbed species is a single (monomeric) (bio)polymer solute. There is an increasing amount of

experimental and theoretical evidence **[129,130]** that shows that larger polymeric molecules, in a mixture, adsorb preferentially over smaller ones. Other studies show the existence of weakly and tightly bound proteins **[131]**. The physical reason for preferential adsorption of larger polymeric molecules is based on the idea that protein adsorption occurs via multiple contact points with the solid surface; and that higher affinity molecules bind preferentially. Thus, more bonds per molecule are formed for larger molecules than for smaller molecules. Indeed, the model proposed by Cohen Stuart *et al* **[130]**, in which the polydispersity of the polymer is taken into account, shows that many discrepancies between polymer adsorption theory and experiment (e.g. the rounded shape of isotherms, the dependence of the adsorbance on adsorbent concentration, and the lack of desorption upon dilution) can be attributed to polydispersity effects. The simple theory developed in Cohen Stuart *et al* **[130]** predicts that the dependence of the amount adsorbed on the surface area to solution volume ratio, which is due to polydispersity, can be eliminated if adsorption is plotted as a function of polymer concentration, (C_p), times the ratio of solution volume to adsorbent area (V/S). That is, for the adsorption of polydispersed polymers the relevant independent variable is not the equilibrium solution concentration, (C_p), but the non-adsorbed amount per unit area : $\Gamma^* = C_p / (S/V)$. The prediction of this theory **[130]** is that the dependence on (S/V) due to polydispersity ought to collapse to a single curve if plotted as described above.

1.4(c) *Immunoglobulin G Structure*

Protein molecules present in blood serum or body fluids of an animal that combine with specific antigens are called antibodies. Proteins with antibody activity are referred to as immunoglobulins (Ig). Most immunoglobulins are Y-shaped. Each such immunoglobulin molecule consists of four polypeptide chains, consisting of two light, L (M_r 22000 to 24000 and two heavy, H, carbohydrate-containing chains (M_r 50000 to 73000), as shown in Figure 5 **[132]**. There are five known classes of immunoglobulins, IgA, IgD, IgE, IgG and IgM, based on the primary structures of their respective heavy chains.

The heavy chains are linked to each other by one or more disulfide bonds (two shown here for IgG); and the lights chains are linked to the heavy chains by disulfide bonds. Each chain is made up of a series of homology units of approximately 110 amino acids held together in a loop, or domain. The overall structure is also stabilized by strong non-covalent bonds. Studies show that the two H chains are composed of variable V_H, C_H1, C_H2 and C_H3 domains and the two light L chains of V_L and C_L domains. Cleavage of the IgG molecules at the hinge generates two identical Fab fragments, each containing one intact light chain disulphide-bonded to a fragment of the heavy chain containing the V_H and C_H1 domains **[133]**. Each Fab fragment contains one antigen-combining site. The remaining portion of the IgG molecule consists of a dimer of C_H2 and C_H3, called the Fc portion. The Fc portion is homogeneous and contains no antigen-binding activity. The variable regions of the H- and L-chains are located at the *N*-terminal of the amino acid sequence of the homology units.

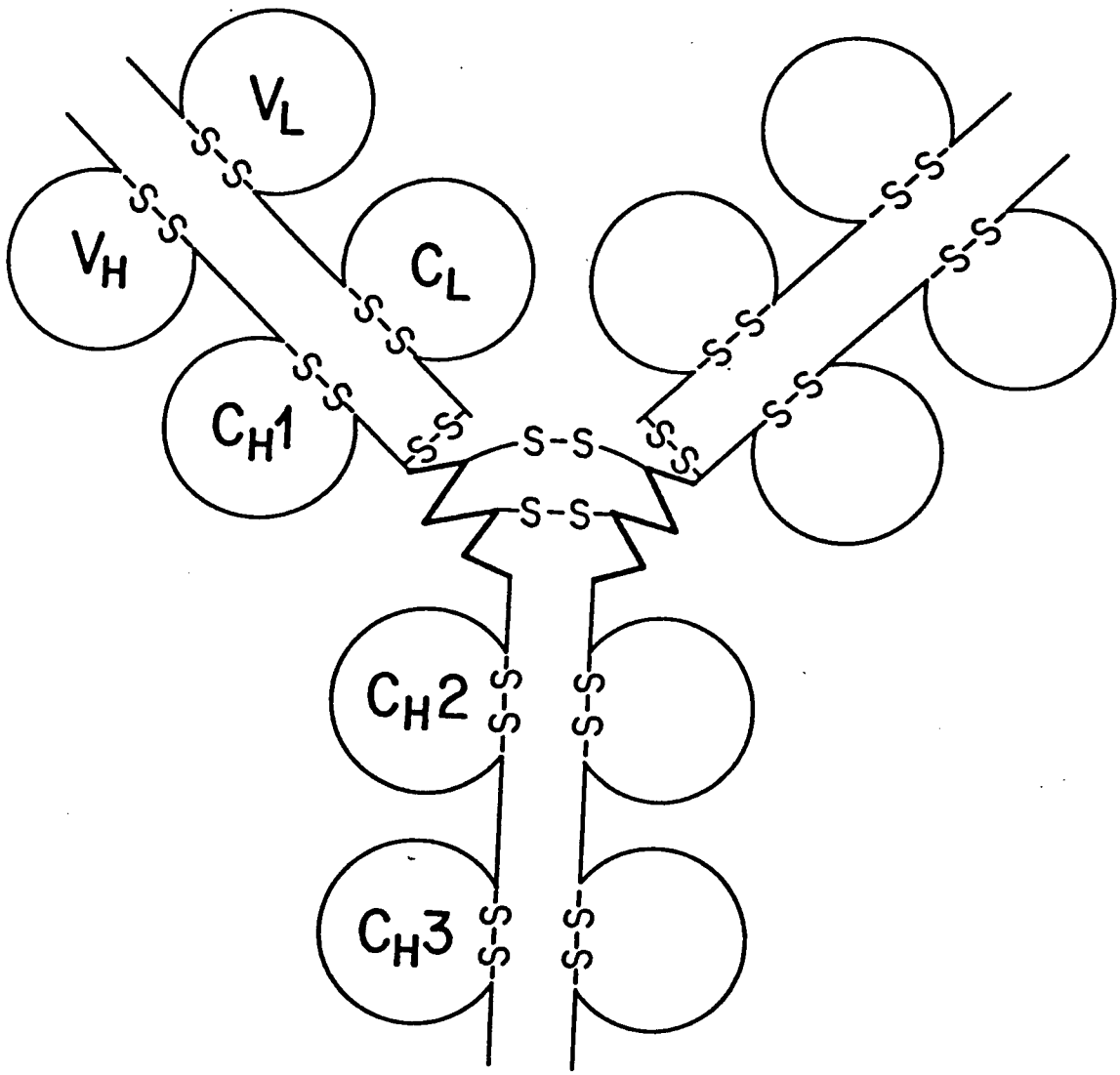

Figure 5. Schematic representation of Immunoglobulin G (IgG) molecule. The two heavy chains are composed of V_H, C_H1, and C_H2 and C_H3 and the two light chains of V_L and C_L domains. (Adapted from [132]).

The sequence within the variable regions are extremely variable at some locations, called the hypervariable regions, but conserved at other locations. The V_H and the V_L domains fold in such a way that the hypervariable regions are brought together to form an antigen-combining site.

1.4(d) *Binding of Antibody to Antigen-Coated Polystyrene Latex (PSL)*

The binding of a specific antibody to an antigen-coated latex suspension can cause the antigen-coated particles to adhere and form clumps. This process, commonly known as agglutination is similar to precipitation, but the latex particles used in agglutination are larger and are in suspension rather than in solution. The formation of clumps results from cross-linking of antigen-coated particles by antibodies from solution. Thus multivalent antibodies (e.g. IgG with a valency 2 or IgM with a valency of 10) can induce agglutination, whereas monovalent antibodies (e.g. Fab fragment) with only a single binding site cannot cause cross-linking of antigen-coated particles by this mechanism.

The process of agglutination can be conceptually divided into two steps. In the first step, the binding of free antibody in solution to the antigen-coated particles leads to a partition of antibody molecules into those that are free in solution, not bound to any antigenic molecules, and those that are bound to one or more antigens on the particles. The second step is the formation of cross-links (bridges) between antigen-coated particles. This second step is somewhat similar to a polymerization reaction in which the antigen-coated particles constitute the monomeric units and the linking of one antigen-coated

particle with another by specific antibodies leads to the formation of a network of particles connected by antibodies.

It is to be expected that antibody binding to the antigen-coated latex particles would be affected by such factors as the surface area of the latex particle and its total concentration, the antibody binding constant (or affinity) and its concentration in solution, and the total antigen concentration which is determined by the density of antigen coverage on the surface of a particle and the total particle concentration. However, there has been very little work done on the details of such reactions, with respect to antigen-coated latex particles. Considerable work, which is relevant to latex immunoreactions *in vitro*, has been done on (a) the binding of antibodies to antigens on cell surfaces **[134-141]**; (b) the mechanism of receptor-carrier liposome based immunoassays **[142]**; and (c) studies involving multiple reactive site polymers based on distribution functions describing the probability of polymers having a certain number of sites unreacted **[143,144]**. These theoretical studies have included kinetic as well as equilibrium analyses of monovalent, bivalent, and multivalent ligands interacting with monovalent or bivalent receptors. The binding of ligands to receptors that are cell-bound or otherwise fixed, as on a latex bead, is more difficult to understand theoretically. The results of these theoretical analyses indicate that when receptors are clustered in space, as when they are confined to cell surfaces, their rates and equilibrium constants can be quite different from those observed when they are uniformly distributed in solution. This is because their binding and rate constants are dependent on many physical properties of the system such as the binding site density on the cell surface; diffusion coefficient

differences; concentration, size and shape of the reactants; and orientational requirements for reaction.

1.5 Research Approach

The background outlined above gives a brief description of polymer latexes, some of their applications and uses; their physicochemical properties with emphasis on their colloidal properties and surface chemistry, and a summary of the major qualitative features of their interactions with proteins. The aim of this project is to carry out a systematic study of the interaction of Ag and Ab with well-characterized polystyrene latexes in an attempt to rationalize the surface and colloid chemistry involved in the interactions.

The general approach taken is first to examine the adsorption of a protein Ag (bovine serum albumin) onto polystyrene latexes with different surface characteristics and establish the dominance of such adsorption in determining the colloidal stability of the resultant protein-coated polystyrene latexes. Purified antibodies to the adsorbed protein are prepared and the equilibrium binding of the purified antibody to the antigen-coated polystyrene latex is studied in order to obtain an estimate of the average number of antibodies bound per antigen-coated particle and the variation of this average number with concentration of antigen on the latex surface. To study the kinetics of flocculation (agglutination) of these colloidal dispersions (protein-coated polystyrene latexes) under various shear rate conditions, a couette

shearing device is used in which suspension turbidity can be continuously monitored as a measure of aggregation. The results provide a contribution to the understanding of the mechanism of interactions of proteins with polystyrene latexes and the determinants and kinetics of reversible and irreversible flocculation of Ags and Ag/Ab coated latexes..

For this work surfactant-free polystyrene latex beads with different surface functional groups were chosen (Interfacial Dynamics Inc., Portland, OR). Bovine serum albumin (BSA) Fraction V (Miles Lab.) was used as the antigen, and purified polyclonal rabbit anti-BSA, prepared in this laboratory by immunizing rabbits with BSA Fraction V were used. The antigen (BSA) was adsorbed onto the various polystyrene latex beads, and the degree of surface coverage assayed by measurement of the adsorption isotherms with radioidonated BSA. BSA desorption from the polystyrene surfaces was examined by washing the latex beads with buffer of the same composition and pH as the adsorbing solution. In order to examine to some degree the composition of the adsorbed layers, the latex was washed in a solution of surface active buffer (sodium dodecyl sulfate, SDS-buffer) and the released protein run on SDS electrophoresis gels

The colloidal stability of the various polystyrene latexes coated with BSA at different surface coverage was determined by measuring their rate of flocculation as a function of NaCl concentration using a concentric cylinder constant shear couette device that was designed and built in our laboratory in such a way that it fit the cell compartment of an HP 8450 UV/VIS Spectrophotometer. Using this apparatus, the agglutination of BSA-coated latex particles by rabbit anti-BSA antibody was studied under different shear rates.

CHAPTER TWO

BSA ADSORPTION TO POLYSTYRENE LATEXES

2.1 Introduction

2.1 (a) *Experimental Considerations*

One usually requires measurements of the adsorbed amount, the bound fraction and the layer thickness to characterize an adsorbed polymer fully. This information could be obtained from the concentration profile through the adsorbed layer if it were available but unfortunately the number of experimental systems where this profile can be measured is at present somewhat limited. The most commonly used method to study polymer adsorption is to measure the amount adsorbed per unit area of adsorbent, for which there are two basic approaches: one can detect either the depletion of polymer from the solution or the accumulation of adsorbate on the substrate.

The first of these methods is usually preferred and a wide range of analytical techniques is available for the measurement of the concentration of free polymer in solution. Given the surface area of the substrate, the adsorbed amount per unit area may be calculated. Assuming constant molecular volume it is possible to make generalizations regarding the thickness of the adsorbed layer based on amount adsorbed per unit area at saturation. However, arguments based on such measurements can often be ambiguous as there is no *a priori* information on the conformational state of the polymer in the adsorbed layer, and because the specific surface area "seen" by the polymer is not always precisely known.

The fraction of adsorbed polymer segments, p, can be measured by infrared (IR), nuclear magnetic resonance (NMR), electron spin resonance (ESR) spectrometry and by microcalorimetry **[145-149]**. Using infrared, the IR-bands (vibration or torsion) of functional groups of polymers like carbonyl-, phenyl-, and pyridine can be measured quantitatively in carbon tetrachloride (CCl_4) or chloroform ($CHCl_3$). Upon adsorption, the IR-bands of the adsorbed segments are shifted to lower wave numbers. The NMR technique relies on the difference in mobility of the segments in the layer directly adjacent to the substrate, compared to the mobility of free loops and tails in solution. For ESR, a suitable spin label that can be incorporated in the polymer chain is required. The labels attached to loops and tails are expected to be more mobile than those on the adsorbed part of the polymer, resulting in differences in spectral line width of the labels.

The thickness of an adsorbed polymer layer can be obtained by a variety of techniques including ellipsometry, capillary flow, photon correlation spectroscopy (PCS) and small-angle neutron scattering (SANS). In ellipsometric measurements **[150]**, the change in the state of polarization of light upon reflection from a surface is measured. From the phase shift and amplitude of the reflected beam with respect to the incident beam, the thickness and refractive index of the adsorbate can be calculated. The ellipsometric system requires a flat optically reflecting surface. In both the capillary flow and PCS **[151]** methods a hydrodynamic model is required to interpret the results. In capillary measurements, the hydrodynamic thickness is deduced from the reduction in flow rate of the fluid in a capillary tube when there is polymer adsorbed. The reduction in flow rate is due to a decrease in the radius of the capillary tube. SANS **[152]**, gives a direct estimate of the second

moment of the volume fraction profile, which is independent of a model for the adsorbed layer.

Most of these experimental methods have only been introduced recently and are in developmental stages. In most cases, they are restricted to specified conditions and are not universally applicable. In addition, the spectroscopic techniques used in protein adsorption studies may give information only on localized areas of the protein which is then assumed to apply to the whole protein molecule.

2.1 (b) *Structural Features of Albumin*

The protein antigen used in this work, bovine serum albumin (BSA), is a single polypeptide chain of approximately 580 amino acids; the exact number of amino acids depends on the type of albumin. Earlier models based on physicochemical properties of the protein suggest two general structures for the molecule **[153,154]**. Both models assume that at neutral pH levels the molecule forms a compact globule. Foster *at el* **[153]** suggest that the globule is made of four compact sub-units connected by short lengths of polypeptide chain and on lowering the pH the sub-units move away from one another but still retain their local structure. Franglen *et al* **[154]** suggest that the globule consists of a highly organized core covered by a less organized coating of polypeptide chain and on lowering the pH the molecule expands through unwinding of this coating but the core still retains a high degree of organization.

Later models based on amino acid sequencing **[155]** suggest that the albumin molecule is composed of nine double loops linked together by short chains of amino acids **[156]**. The folding of the nine double loops into the three dimensional structure is dependent on non-covalent bonds.

Based on observable differences in the physicochemical and structural properties of the molecule under various conditions, the number of "subunits" has been reduced to three **[157,158]** and these have been designated as structural and functional domains **[159]**. This has been confirmed recently by crystallographic investigation of the three-dimensional structure of human serum albumin **[160]**, in which the electron density maps reveal the structure of albumin as a predominantly α-helical globular protein, which agrees with a variety of other studies **[161]** that depict albumin to be an oblate ellipsoid with semi-axes of 140 Å by 40 Å.

The entire structure is maintained by 17 disulfide bonds. Each domain, consisting of approximately 190 amino acid residues, is an independent folding unit with a large double loop, a short connecting segment, a small double loop, a long connecting segment (hinge), another large double loop, and a connecting segment to the next domain. Although considerable homology in general structure can be seen between domains, the amino acid sequence and function of each domain are considerably different. The majority of the similarity between all three domains centers on the disulfide bonds **[162]**.

The albumin molecule has its most stable state at pH 6-7 and temperatures just below $5^{o}C$. The bonds which maintain the domains in their three-dimensional structure can be disrupted reversibly by lowering the pH to 3.4-3.6 **[162-164]**. The albumin molecule undergoes reversible expansion under these condition as indicated by changes in its physicochemical properties: the sedimentation constant and the diffusion constant decrease, and the intrinsic viscosity and number of interchangeable hydrogen atoms increases **[162-164]**. Foster **[163]** proposed that in this reversible pH-induced transformation, the molecule

isomerises first from a normal form (N), to an F form (for faster migration) which is somewhat expanded. Later **[163]**, it was established that in this N-F transformation, the molecule loses about 10 percent of the native three-dimensional structure, as measured by its content of α-helix determined by the optical rotation technique. Elevating the pH range from neutrality to about 9 unfolds the protein molecule to a more open structure; this loss in structure is also reversible and is called the N-B transformation. The N-B transition is accompanied by a reduction in the measured α-helix content of as little as 3 percent **[166]**.

The albumin molecule also undergoes temperature-dependent reversible transitions between molecular states which are not well-defined. With respect to temperature, the molecule has its most stable structure at a temperature just below 5^0 C and undergoes transitions above this temperature. At 37^0 C and pH 7.5, there is 20 percent less helical structure than at 5^0 C **[164]**. Above 50^0 C albumin starts to denature irreversibly, before the entire three-dimensional structure is lost. The pH- and temperature-dependent reversible transitions are independent of each other, which indicates that different parts (loops or domains) of the albumin molecule are involved in the unfolding **[164]**.

When the albumin molecule unfolds from the N to the B state the molecule is more easily irreversibly denatured than in the N-state. The heat-induced loosening (unfolding) of the albumin structure also renders the molecule less rigid against irreversible transformations.

It is observed that a specific type of denaturation, due to intramolecular SS-interchange, runs slowly at pH 7 but increases to a maximum value at around pH 8.5 **[167]**; it is also observed that the rate of irreversible heat denaturation and denaturation due to storage change from a minimal to a maximal level in the same pH interval **[165,168]**.

2.1 (c) *Albumin Heterogeneity*

Isolated BSA, especially samples that have been lyophilised, heat-treated, or stored in solution, almost always contain oligomerrs. The formation of the oligomers is thought to occur during preparation and storage of the protein. The proportion of the oligomer depends on a number of parameters such as the nature of the starting plasma, fractionation procedure, addition of stabilizers, concentration of the solution, storage conditions and length of storage **[169-174]**.

Freshly isolated serum albumin monomer consists of approximately 70 percent mercaptalbumin (containing one sulphydryl group per mole of albumin) and 30 percent non-mercaptalbumin (where the sulphydryl group is blocked through mixed disulfide formation with cystine and, to a lesser extent, glutathione **[175]**). The sulphydryl groups are the most reactive of any amino acid side chain and ionize at slightly alkaline pH, giving the reactive anion ($-S^-$). Disulfide exchange reaction between the anion ($-S^-$) of one BSA molecule and a disulfide bond (-S-S-) of another molecule leads to the formation of a dimer molecule with four disulfide bonds **[143]**:

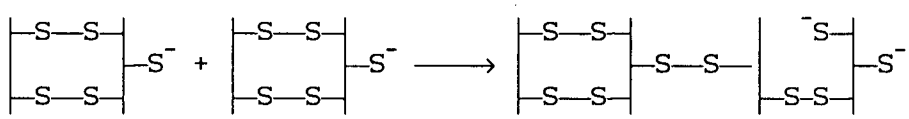

The dimer can then react further to form higher polymeric BSA molecules. This is the basis of the formation of dimers and higher polymeric species of BSA during prolonged storage of the protein. Whether this occurs or not depends on the accessibility of the disulfide

bonds and the free sulphydryl group of the BSA molecule. Protein disulfides are generally stabilized by the protein conformation, so that favorable unfolding of the BSA molecule would have to occur in order for its disulfide bonds to be exposed. Similarly, the free sulphydryl group of the BSA molecule is thought to be attached to the relatively compact N-terminal portion of the BSA molecule that is apparently folded inward to gain protection from oxidation. However, disulfide interchange has been encountered unexpectedly by many workers **[143]**.

That the albumin molecule is able to unfold in several more or less independent steps is not surprising since the net energy which keeps a protein in its three dimensional structure is quite small, at least according to the few cases in which it has been experimentally determined **[176]**. For example, the free energy accompanying the unfolding of ribonuclease and lysozyme from their native structure to a restricted random coil (without breaking any S-S bridges) amounts to only 3 and 4 J g^{-1} **[176]**.

For albumin, the unfolding takes place in several more or less independent steps, and for this reason it has not been possible to determine the free energy of complete denaturation. Hydrogen exchange studies, done at 25^{0}C and pH 6.5, **[164]** give a rough indication of the free energy which holds the albumin molecule together; it is found that less than 25 kJ mol^{-1} is sufficient to open the molecular structure enough to let the surrounding water molecules enter and come into contact with about 60 percent of the peptide bonds of the molecule. Increasing the pH from 6.5 to 7.6 makes the albumin molecule become more unstable, and 70 percent of the peptide bonds are in contact with water.

The nature of the dimer and polymer that usually occur in serum albumin samples is not clear. Hartley *et al* **[177]** found that about half

the dimers in albumin could be split into monomer on treatment with mercaptoethanol. The other half of the dimers that are not split by mercaptoethanol seemed to be relatively stable. What holds them together is not known. Treatment of these dimers with detergent solutions and their stability in mercaptoethanol solutions at low and high pH show that hydrophobic and electrostatic bonding are probably of limited importance for keeping the dimers together. It is suggested that both kinds of dimer (reducible and non-reducible) are kept together by disulfide bonds but that in one of them the disulfide bond is situated in the interior of the molecule and not accessible for reaction with mercaptoethanol in the native state of the molecule **[178]**.

In this work passive adsorption measurements of iodine-125 labeled BSA to polystyrene latexes bearing different surface functional groups were made with the aim of using these BSA-coated latexes as a model in fundamental studies of reactivity of polymer-borne biological molecules.

Our approach to protein adsorption studies was, three-fold:

(*i*). To determine, as accurately as possible, the amount of protein adsorbed by the various types of latexes under different solution conditions using radiolabeled protein.

(*ii*). To determine how much protein is retained on the latex particle surfaces after extensive rinsing with equilibrium buffer; i.e. the reversibility of the adsorption.

(*iii*). To determine the molecular weight distribution of the adsorbed protein.

2.2 BSA Adsorption Procedure

2.2 (a) *Introduction*

Of the several methods available to assay protein concentration and perform protein adsorption studies, we chose to use radiolabeling. This was for two main reasons: it is an accurate method for determining protein concentration over a wide range, and it has the sensitivity to be used to determine the amount of adsorbed protein either directly or by measuring depletion from solution after equilibration with particulates.

In the depletion method, the disappearance of the protein from solution is equated with the amount adsorbed by the substrate, provided that the substrate does not absorb the protein and corrections are made for the inevitable adsorption onto the surface of the tube or vessel containing the adsorption mixture. Usually this method works best when the uptake corresponds to at least a 10 percent change in the protein solution concentration; enough surface area is required for such a change to occur. The other method, of directly counting the labeled protein associated with the substrate surface, involves distinguishing between the adsorbed labeled protein and the labelled protein in solution in the interstitial fluid surrounding the substrate pellet.

It is also important to ensure that the bond between the label and the protein molecule is stable under adsorption conditions and that the labeling method or the label itself does not change the adsorption properties of the protein. The labeled protein is characterized by either chromatographic or electrophoretic methods to ascertain that its behaviour resembles that of the nonlabeled protein. ^{125}I was chosen as the radiolabel and the labeling procedure is described in detail below.

2.2 (b) *Materials*

Iodination

Ion-exchange resin (Dowex SBR 8% cross-linked, 20-50 mesh) was obtained from Sigma. Iodo-beads (immobilized chloramine T molecules on non-porous polystyrene beads (1/8 inch diameter)) were from Pierce Chemical Company. $Na^{125}I$ in dilute sodium hydroxide solution, with typical specific activity of 12-15 mCi per gram, was purchased from Amersham. Bovine Serum Albumin (BSA), Fraction V, Lot # 388 was from Miles Labs. Trichloroacetic acid (TCA), Lot # E5X was from Eastman Kodak Company. An LKB 1282 Compugamma Universal Gamma Counter was used. Sodium azide was from Fisher Scientific Company and sodium chloride was from BDH Chemicals. Mono and dibasic sodium phosphate were from Sigma. Phosphate buffer (0.01M, pH = 7.20), was prepared by adding a solution of 0.2M NaH_2PO_4 (72ml) to 0.2M Na_2HPO_4(28ml) and diluting with distilled water to 2 liters.

Polystyrene

Polystyrene latexes synthesized without surfactants, with different surface functional groups, were monodisperse samples obtained from Interfacial Dynamics Corporation (IDC), Portland, OR. Some of the properties of the polystyrene latexes that were used in the adsorption studies are summarized in Table I. The reciprocal of the surface charge

density represents the average area surrounding each titratable charge group. Comparison of this area per charge group with theoretical area per charge group (e.g. 20-25 $Å^2/SO_4$ or 20 $Å^2$/COOH) gives a rough guide of the percentage of the particle surfaces that are occupied with ionic groups and that which is available for adsorption of molecules like proteins. This is included in Table I and it can be seen that the sulfate latex has about 9% of its surface occupied by the SO_4^- groups, while the carboxyl, carboxyl modified and amidine (+) have 6%, 40-50%, and 17% respectively. Thus, 91% of the sulfate latex and 94%, 50-60% and 84% of the carboxyl, carboxyl modified and amidine (+) latex surfaces are available for the adsorption of protein molecules assuming only the hydrophobic area is active. Particles with lower surface charge densities, for example the sulfate latex with surface charge density of 6.70 $\mu C\ cm^{-2}$, and the carboxyl latex with 2.88 $\mu C\ cm^{-2}$, have more area on their surfaces for adsorption of other molecules than do latex particles with higher surface charge densities. The carboxyl modified latex beads have hydrophilic groups on their surface which add stability to the particle and additionally contain a significant amount of surface attached water-soluble polymer.

The concentrations of latex suspensions used in adsorption studies were determined by diluting the stock suspensions received from the suppliers gravimetrically and drying in an oven at 60-80^{0}C for 24 hours. The stock latex suspensions for adsorption experiments were prepared by centrifuging a weighed amount of the supplier's suspension with 0.01M phosphate buffer, pH 7.2, (4000 $\times$ g for 30-60 min, depending on latex type), and resuspending in the same buffer.

Electrophoresis

SDS(Sodium dodecyl sulfate), Acrylamide, BIS(*N,N*-methlene-bis-acrylamide, TEMED (*N*, *N*, *N'*, *N'*-tetramethylethylnediamine) and ammonium persulphate, were Electrophoresis Purity Reagents from Bio-Rad. Coomassie Blue G-250, was from Kodak, Lot #B9H and Pyronin Y was from Baker Chemical Co., Lot # 923344. Tris-HCl was from Sigma. Methanol, glacial acetic acid and perchloric acid were from BDH. All chemicals were of analytical grade. The electrophoresis procedure followed is given in detail in Appendix 1.

Table I

Characteristics of Polystyrene latexes used in adsorption and agglutination studies

Latex type:	Sulfate	Carboxyl	CML	Amidine
Diameter: (nm)	1073±5.04%	984±5.1%	865±5.3%	489±6.9%
Specific Surface area: ($cm^2 g^{-1}$)$\times 10^3$	53.0	57.8	65.8	116.3
Surface Charge density ($\mu C\ cm^{-2}$)	6.70	2.88	30.7	12.2
Area per charge group ($Å^2$/group)	239	557	52	131
% of Surface occupied with ionic groups	9	6	40-50	17
% of surface that is hydrophobic	91	94	50-60	83

2.2 (c) *Methods*

2.2 (c) (*i*) *Radiolabeling of BSA*

The iodination procedure followed was that developed by Markwell **[179,180]**. Prior to iodination , Dowex SBR anion exchange resin, 8% cross-linked was soaked in water for 10 minutes. A large batch (240 ml) was suspended in 6M NaCl, and washed in a Buchner funnel with decreasing concentrations of sodium chloride. The final suspension was washed and suspended in a 0.15M NaCl containing 0.02% NaN_3 and stored at 4^0C. When required, 6-8ml of the ion-exchange resin was placed in a disposable column, washed thoroughly with phosphate buffer (0.01M, pH 7.20) followed by a 0.1% (w/w) solution of BSA. The ion-exchange resin suspension was then washed thoroughly with phosphate buffer again to remove excess protein.

On the day of iodination, two or three Iodo-beads were washed twice in phosphate buffer (0.01M, pH 7.20) using approximately 1ml/bead in a small beaker, then blotted dry on filter paper. One hundred micrograms of protein in 0.5ml of phosphate buffer was added to an incubation tube along with 5 to 10μl of ^{125}I solution (1-2μCi). The iodination reaction was initiated by the addition of two to three Iodo-beads and allowed to proceed in the capped tube and stirred for 15 minutes at room temperature in an iodinating fume-hood.

The iodinated protein was then transferred to the ion-exchange column with a Pasteure pipette, leaving the Iodo-beads in the reaction tube. For maximal recovery the beads were washed twice with 1.0ml of phosphate buffer and the wash added to the ion-exchange column. Appropriate fractions (10, 15 or 20 drops) containing the iodinated

protein were then collected from the ion-exchange column, eluting with an equal bed-volume amount using phosphate buffer. Aliquots (5μl) of each fraction were collected, transferred into a counting tube and made up to counting volume (2ml) with ice-cold phosphate buffer, containing a 0.2mg/ml albumin and 0.5mol carrier iodide ($Na^{127}I$), for measurement of the total radioactivity present in the sample. After this count, an equal volume (2ml) of 20% (w/v) of TCA was added to the counting tube and mixed well. This is partly to ensure the presence of enough protein for the formation of sedimentable aggregates on precipitation and partly to reduce adsorptive losses of radioactivity on the tube surface.

The suspension was then centrifuged for 10 minutes at 1500 X g while still cold. Two milliliters of the supernatant were transferred to a second tube and both samples were counted for gamma activity. The fraction of radiolabel bound to protein was estimated from the sample activities as: % label bound = (P-S)/P × 100, and % label free = 100-% bound, where P is the total initial count in solution and S is the supernatant count.

It was found that after the separation of radio-labeled protein from the free label through the ion-exchange column, 5-10% of the label was still present free in the labeled protein samples. Further removal of the free label was necessary; this was done using a Centriprep-10 concentrator device made by Amicon. The device is a disposible ultrafiltration tube with a filtrate collector and a membrane cutoff of 10,000 MW. The iodinated-protein samples were collected into the Amicon device and washed through the filter three or four times with buffer, using a centrifuge (3000 × g for 15min). The final filtrate was diluted with fresh phosphate buffer to the desired activity.

2.2 (c) (*ii*) *Adsorption*

The stock latex suspensions for adsorption experiments were prepared by washing a weighed amount of the supplier's suspension with the phosphate buffer. A maximum of four concentrations of latex solution were then determined gravimetrically by drying in an oven at 60-80^{o}C for 24 hours.

The stock protein preparation for adsorption studies was made by mixing 1-5 percent radioactive protein with a solution of nonradioactive protein prepared by dissolving a weighed amount of crystalline BSA in the appropriate phosphate buffer. The concentration of the stock protein mixture was determined from its absorbance and extinction coefficient of BSA at 278nm (i.e., Absorbance Unit of 0.667 for BSA at 278nm = 1 mg/ml). The specific activity of the stock protein concentration was determined by measuring the radioactivity counts of a weighed sample. A Mettler balance with an uncertainty of ±0.0001g was used for all weights.

Adsorption isotherms were determined in three different ways. First, the protein concentration and the surface area of the latexes were varied at constant total volume in order to measure the binding isotherms at different surface areas of the latex. Second, the total protein solution volume in each set of samples was varied while the total surface area of the latex was kept constant. Finally the total surface area of the latex was varied, but the amount of protein and the total volume in each sample was kept constant.

A typical adsorption experiment was carried out as follows: the appropriate amount of stock latex, BSA, and buffer were weighed into a polystyrene tube (Evergreen, 4.5ml). The weighed suspensions were mixed gently and allowed to equilibrate under gentle horizontal shaking, using

a Khan shaker (Eberbach) , for six to eight hours at room temperature. After incubation of the latex particles with the protein, the samples were centrifuged for 60-90 minutes at 12000 X g using a Sorval centrifuge in order to separate the adsorbed protein on the latex surface from the equilibrium protein in solution. Three aliquots ($\cong$ 200μl) of the clear supernatant were removed from each sample tube, weighed and gamma counted. Adsorption isotherms were calculated from the difference in the supernatant and the initial concentration of BSA according to the following expression:

$$\Gamma = \frac{C \times V}{a_s \times m} \quad \ldots\ldots\ldots\ldots\ldots\ldots\ldots\ldots\ldots\ldots \quad (2.1)$$

where Γ = amount adsorbed per unit area (mg cm^{-2})

$C = C_i - C_e$

C_i = initial concentration of BSA ($mg/g_{soln.}$)

C_e = equilibrium concentration of BSA ($mg/g_{soln.}$)

V = amount of fluid in suspension (g)

a_s = specific surface area of latex (cm^2/g)

m = mass of latex added (g)

The initial concentration of BSA in each sample was determined from the amount of BSA solution added and the specific radioactivity of stock BSA. The equilibrium concentration of BSA was determined from the average of the activity of three samples removed from the supernatant and the specific activity of the stock BSA. The mass of latex in each sample was determined from the average of mass fractions of the stock latex suspension obtained gravimetrically. The specific surface area of the latex was calculated from the expression:

$$a_s = \frac{6 \times 10^4}{d\rho} \quad \text{.....(2.2)}$$

where d is the particle diameter in cm, and ρ is the density in g cm^{-3}. An example of these calculations is given in Appendix 2a.

2.2 (c) *(iii)* *Wash Analysis*

In order to determine the molecular weight distribution of the adsorbed protein by electrophoresis analysis and to determine the reversibility of the adsorption of BSA onto the various latex surfaces under different solution conditions, a wash analysis was performed. The samples used in electrophoresis analyses were initially washed with 2ml of 0.01M phosphate buffer, pH 7.2 three or four times using a centrifuge, followed by three 200µl portions of Fairbanks electrophoresis sample reagent containing 2% sodium dodecyl sulfate (SDS). The samples used in reversibility studies were initially washed with 4ml 0.01M phosphate buffer, pH 7.2 under the same conditions as the adsorption measurements, equilibrating each wash for 6-8 hr. The successive wash cycles with pure buffer, nonlabeled BSA, anti-BSA IgG, 2% polyethylene glycol (PEG) solution, and 2% SDS were performed in the same manner, each for 6-8 hr.

2.3. Results and Discussion

2.3 (a). *Adsorption Isotherms for BSA to the Four Latex Types:*

The adsorption isotherms reported below are the results of single isotherm measurements in which three aliquots (≈ 200μl) of the clear supernatant solution were removed from each sample tube. Estimates of the uncertainty in the measured concentration of BSA in each of the three supernatant aliquots, the initial concentration of BSA and the total surface area of latex used in each experiment, formed the basis of the error analysis as outlined in Appendix 2a and given in tabulated results. A separate set of experiments in which the adsorption of BSA to sulfate latex was repeated in order to give an indication of the reproducibility of the adsorption data is given in Appendix 2b.

(i). Variation of Surface Area of the PSL

Figure 6 shows the adsorption isotherms for BSA adsorbing from 0.01M phosphate buffer, pH 7.2 at room temperature to the four latexes described in Table I. In each case three different surface areas of latex were used.

Generally, all the isotherms show the typical "Langmuir" shape reported in many previous studies **[64-72]**. With the exception of the CML isotherms, there is an initial steep rise in the amount adsorbed with increasing BSA concentration to a semi-plateau value that is dependent on the total surface area of the PS latex available for adsorption.

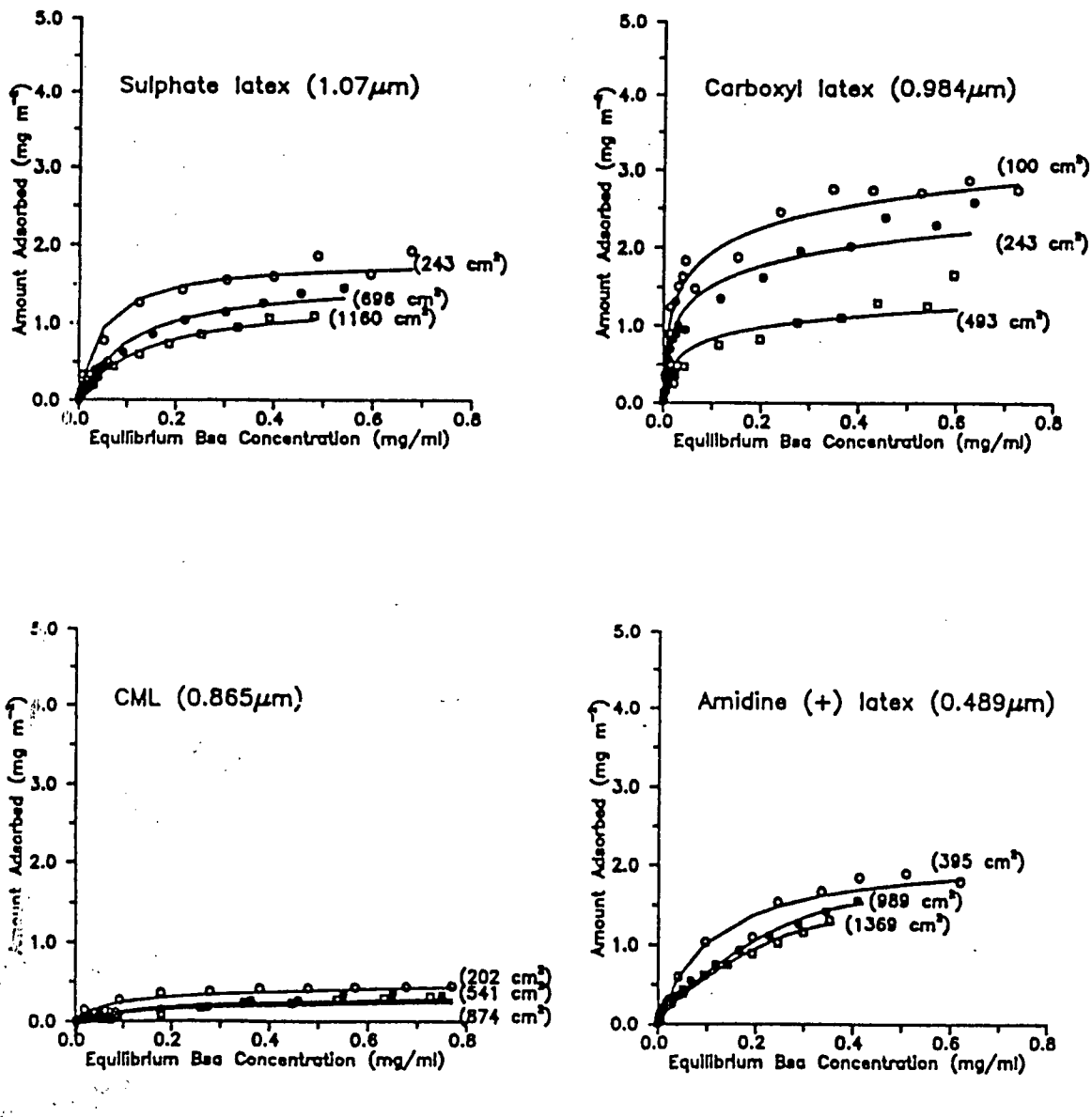

Figure 6. Adsorption isotherms for BSA to the latexes indicated at room temperature from 0.01M phosphate buffer, pH 7.20. The total surface areas of latex used in each experiment are as indicated.

Norde and Lyklema [76] carried out extensive studies on the adsorption of human serum albumin (HSA) to various polystyrene latexes. Since the composition of HSA and that of BSA are very similar [181], a comparison, with respect to general trends in adsorption isotherms, is made here with their results.

Their studies show that the adsorption of HSA on polystyrene latexes develops plateau values at sufficiently high equilibrium concentrations. They considered that different parts of the isotherm reflect interactions that may lead to different modes of adsorption. For example, they suggest that at low coverage of the PSL surface, the shape of the isotherm is initially determined by protein-polystyrene interactions. At high coverage, lateral interactions between adsorbed protein molecules may also play a role in the adsorption process.

Although the adsorption isotherms appear to be Langmurian in nature, the fundamental postulates of the Langmuir isotherms are not fulfilled in most cases in protein adsorption studies [70,71,76,91,92,99]. Protein adsorption on solid surfaces is, generally, found to be virtually irreversible to dilution over times of many hours [69,71,101,113]. This is thought to occur because proteins interact with the PSL surface at many points of the protein molecule, all of which must be released simultaneously for spontaneous desorption to occur. Surface-induced conformation changes may take place upon adsorption and lateral interaction may also occur at high concentrations of adsorbed proteins. Thus, protein adsorption isotherms on solid surfaces cannot be evaluated according to the Langmuir method to extract equilibrium thermodynamic binding constants.

Norde and Lyklema also find inflection points or kinks in their adsorption isotherms for HSA at intermediate coverage and suggest that

reorientation or conformational alteration of the adsorbed HSA molecules is accountable for this. They rule out the possibility of multilayer adsorption on the basis that the adsorption is completely irreversible towards dilution. The present results do not indicate the existence of any inflection points. The isotherms show a rounded shape up to equilibrium concentrations of about 1 mg/ml, for all the latexes.

Saturation values or plateau values were estimated from the adsorption data and their values are listed in Table II. With the exception of the carboxyl modified latex (CML), all the plateau values are within the range of 1 to 5 mg m^{-2} observed by several other investigators using BSA and polystyrene latex **[64-72,76]**.

Taking the BSA molecule to be a oblate ellipsoid with major and minor semi-axes a and b respectively, the side-on cross-sectional area of the molecule is given by πab. Monolayer adsorption for a side-on packing arrangement can be estimated using the cross-sectional area and the relative molar mass of BSA, to a good approximation by,

$$\Gamma = \frac{M_r}{\pi abN},$$

where N = Avogadro's number, M_r = relative molar mass of BSA (66000) and for BSA 2a = 140 Å and 2b = 40 Å **[161]**. This leads to a value of 2-2.5 mg m^{-2} depending on the value of the dimension and molecular weight of the BSA molecule used. Thus, there seems to be no evidence of multilayer adsorption in our experimental results, based on the estimated monolayer plateau values.

Table II

Adsorption maxima of BSA adsorption isotherms in Figure 6, as estimated from the isotherms.

Variation of Surface area:				
	Sulfate	Carboxyl	CML	Amidine
	(mg m^{-2})	(mg m^{-2})	(mg m^{-2})	(mg m^{-2})
1*	1.81±0.12	2.77±0.07	0.44±0.01	1.86±0.04
2*	1.37±0.08	2.42±0.12	0.34±0.01	1.42±0.12
3*	1.03±0.07	1.40±0.18	0.29±0.02	1.17±0.12

NB: 1*, 2*, & 3* correspond to the surface areas of the latexes given in Figure 6 from lowest to highest.

All our adsorption studies were performed at pH 7.2, which is well above the isoelectric point of BSA, approximately pH 5.2. The sulfate, carboxyl and carboxyl-modified latexes are all negatively charged and the BSA molecule is also negatively charged at this pH. If protein-surface electrostatic interactions were dominant, adsorption to these negatively charged latexes would be expected to be minimal because of repulsion. If, on the other hand, protein-surface electrostatic interactions are absent or minimal, then the adsorption of negatively charged BSA to the negatively charged latexes would probably be controlled by hydrophobic interactions. For the positively charged amidine latex, both protein-surface electrostatic and hydrophobic interactions may influence the adsorption of the negatively charged BSA.

Norde and Lyklema observed an increase in plateau adsorption value (Γ_{max}) of HSA with increasing negative charge of the PSL surface at pH values greater than the isoelectric point of HSA. They attribute this to the uneven distribution of charge in the protein molecules, causing different degrees of tilting of the molecule at surfaces having different charge densities. However, they also indicate that the difference in the hydrophobicity of the latexes may equally well be responsible for this observation **[76]**.

It can be seen from Figure 6 that there is a dependence of the amount of BSA adsorbed per unit area on the latex surface area in all cases. As the equilibrium BSA concentration increases, the dependence on latex surface area becomes obvious for all the latexes except the CML which shows only a moderate dependence of surface concentration on surface area. The adsorbed amount decreases, at constant equilibrium BSA concentration, when (at constant BSA solution volume) the total PSL surface area available for adsorption increases. This unexpected result

was observed, to a varying degree, in all of our experimental studies of the adsorption of BSA to PS latexes.

As discussed earlier, BSA can form oligomers in solution. The preferential adsorption of these dimeric and/or oligomeric species may have a great influence on the total amount of protein adsorbed. As will be seen, it seems likely that the latex area dependence is due to the presence of BSA oligomers in solution which adsorb more strongly than monomeric BSA, based on our analysis of the adsorbed BSA molecules (see Electrophoresis Analysis section below) and the fact that this effect has been observed previously in both synthetic polymer adsorption and BSA adsorption in other systems.

Vander Linden and van Leemput **[182]**, using gel permeation chromatography reported experimental evidence for the preferential adsorption of high molecular weight polystyrene to silica surfaces. Zsom **[183]** studied the adsorption of several BSA samples containing different amounts of dimeric and/or polymeric species onto polystyrene latexes by high-performance liquid chromatography (HPLC), and demonstrated that BSA dimers and/or polymers adsorb preferentially to BSA monomer. Lensen, H.G.W. *et al*, **[184]** used high-performance liquid chromatography to follow the adsorption of HSA onto polystyrene and observed a strong preferential adsorption of HSA dimer over monomer. Cohen Stuart *et. al.* **[130]** give a quantitative analysis of these effects and show that for a mixture of two components with different molecular weights, full preference in adsorption is attained if the molecular weights differ by more than a factor of two.

It seems likely the above behaviour is responsible for the area dependence observed. Higher molecular weight fractions show a higher affinity for the surface since there are more groups per molecule

available to interact with the surface. A consequence of this preferential adsorption is that the distribution of the molecular weights between the adsorbent surface and the solution is dependent on the total adsorbent surface area and the solution volume of the system. For example, when a low total surface area is available predominantly the fraction of the polymer with very high molecular weights and therefore high affinity will bind to the surface, resulting in large adsorption values. On the other hand, if a larger area is available, smaller, lower affinity species will occur on the surface, and the amount per unit area and the average molecular weight of the adsorbate will be smaller.

Accordingly, we have used the analysis of Cohen Stuart *et al* **[130]** for the data shown in Figure 6. If their treatment applies, it is predicted that if the data is plotted as Γ , the amount adsorbed per unit area, versus Γ^* = C/(S/V), the nonadsorbed amount per unit area, the area dependence should collapse onto a single curve. The plots are shown in Figure 7.

Generally most of the data fall on the same curve, implying that Γ is a function of Γ^* only and not just C, the equilibrium BSA concentration. The prediction is borne out sufficiently well to give some confidence in the explanation given above.

Figure 8 further illustrates this dependence of the surface concentration of BSA on latex surface area in all cases. In these experiments, the amounts of BSA adsorbed per unit area were determined at an initial concentration of 0.50 mg/ml BSA for different surface areas of each latex, keeping the total volume in each sample constant. A correction for the mass of latex in suspension was made in the calculation of the amount of BSA adsorbed per unit area.

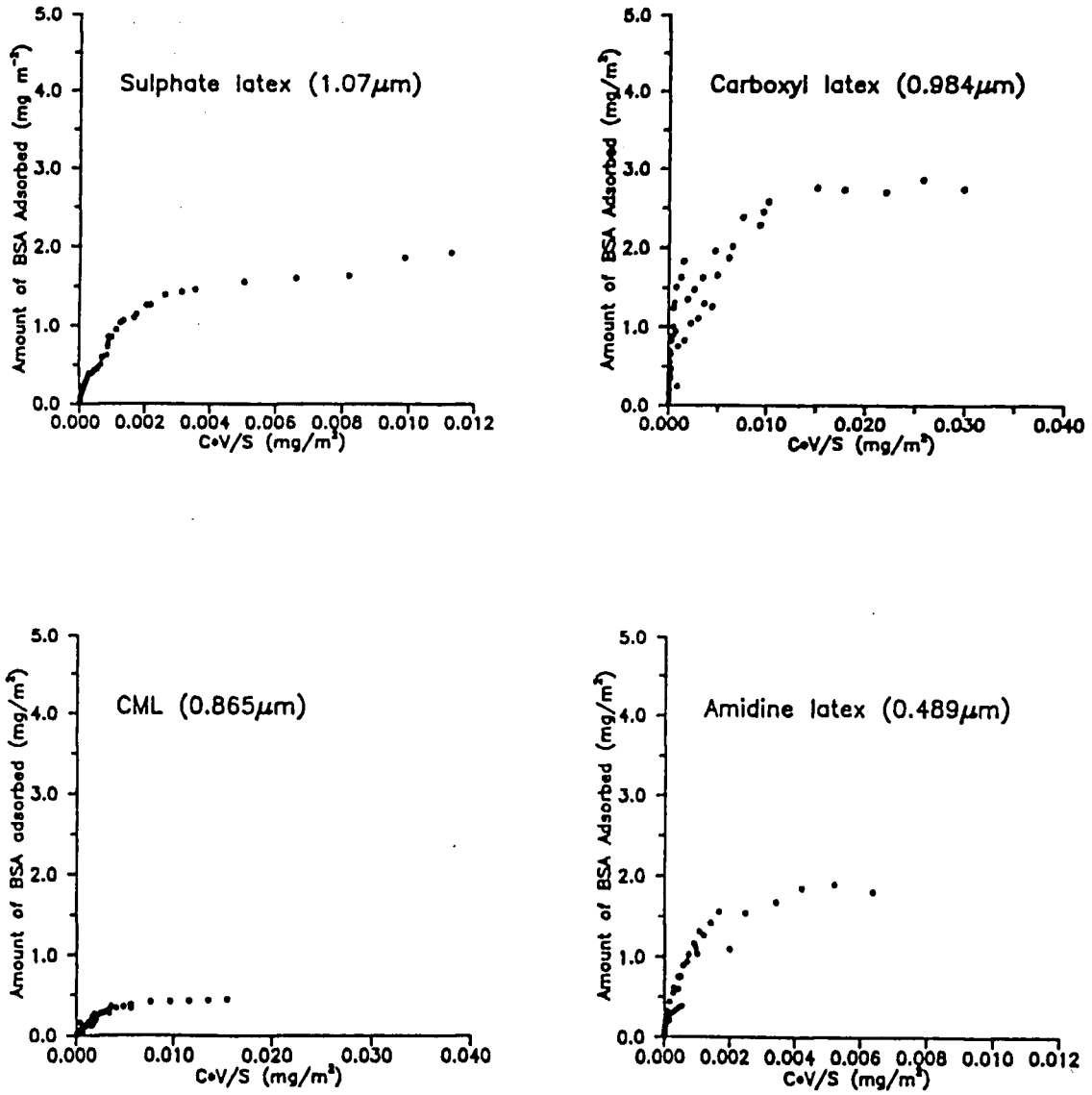

Figure 7. The adsorption data of Figure 6 plotted as a function of the amount of non-adsorbed BSA per unit area in solution, $\Gamma^* = (C \times V/S)$, where C is the equilibrium BSA concentration, V is the volume of supernatant in equilibrium with the latex and S is the total surface area of latex in equilibrium with BSA solution.

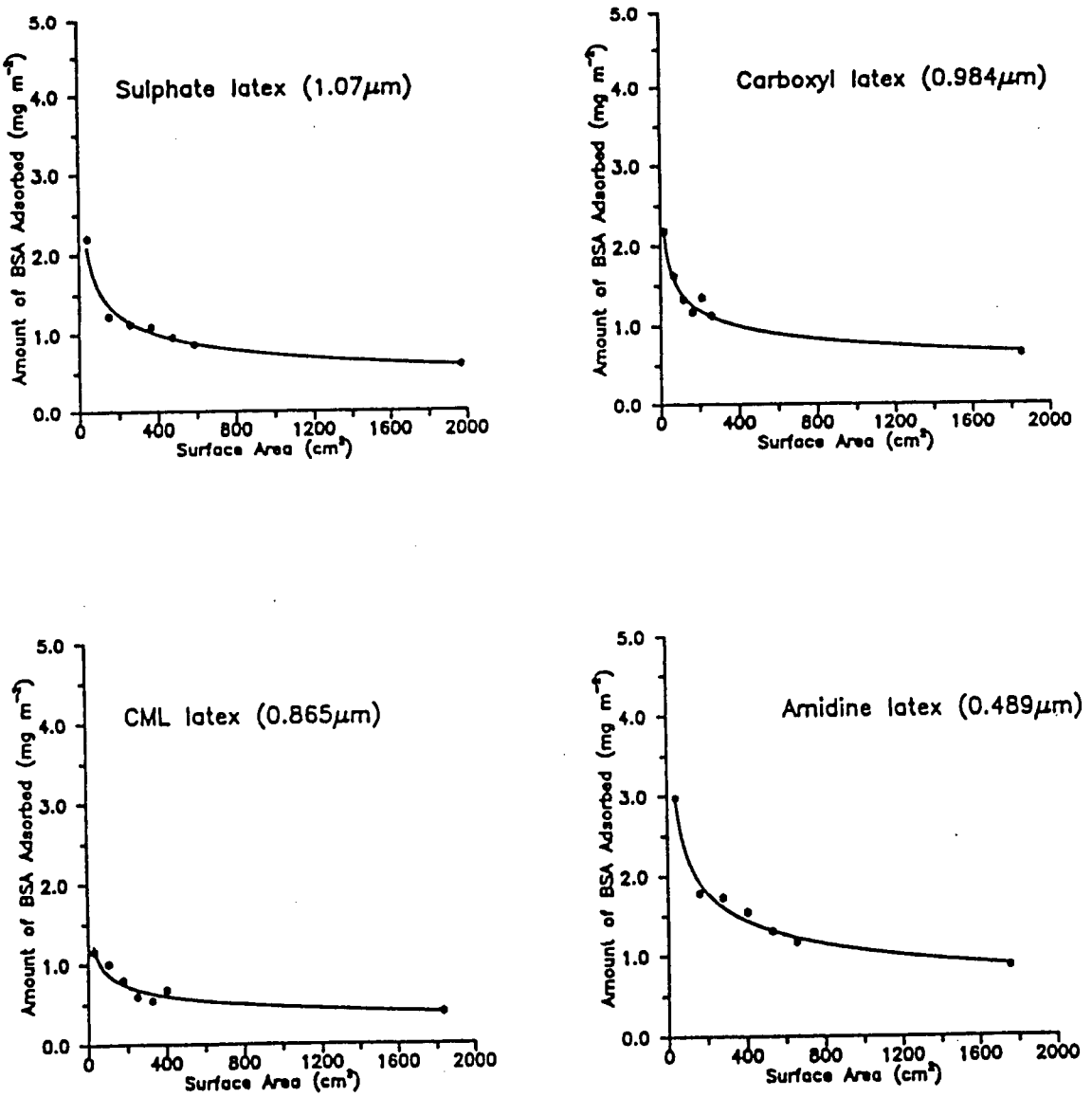

Figure 8. Amount of BSA adsorbed as a function of latex surface area at room temperature from 0.01M phosphate buffer, pH 7.20. Initial [BSA] = 0.50 mg/ml.

The decrease in the amount of BSA adsorbed per unit area is not due to depletion of the protein as a result of latex surface area increase; rather the area dependence shown in these figure is due to the range of affinities of the BSA components in solution and on their concentrations. The rise in the amount of BSA adsorbed per unit area at low surface areas of the latexes, is consistent with the results in Figure 6. If only a single protein species were present one would expect, for a particular latex type, to get the same amount of BSA adsorbed per unit area at all latex concentrations.

(ii). Variation of Total Volume of BSA solution at constant Surface Area of PSL.

In these experiments, the total protein solution volume in each set of samples was varied while the total surface area of the latex was kept constant. In this case the influence of the total aqueous phase volume at identical equilibrium BSA concentration on the distribution of the protein between surface and solution is sought.

These experiments were done for each of the four latex type, and the results are given in Figure 9. As can be seen from the isotherms and the plateau values of the isotherms given in Table III, the observed dependence of the surface concentration on the ratio of surface area to the total volume of the aqueous phase is also seen here. At constant equilibrium concentration, C, a variation in the surface area to volume (S/V) ratio amounts to a change in Γ^* (= C $\times$ V/S), the nonadsorbed amount which, in turn, alters the amount adsorbed per unit area. Thus it is seen that the amount adsorbed increases as the total volume of the

aqueous phase increases.

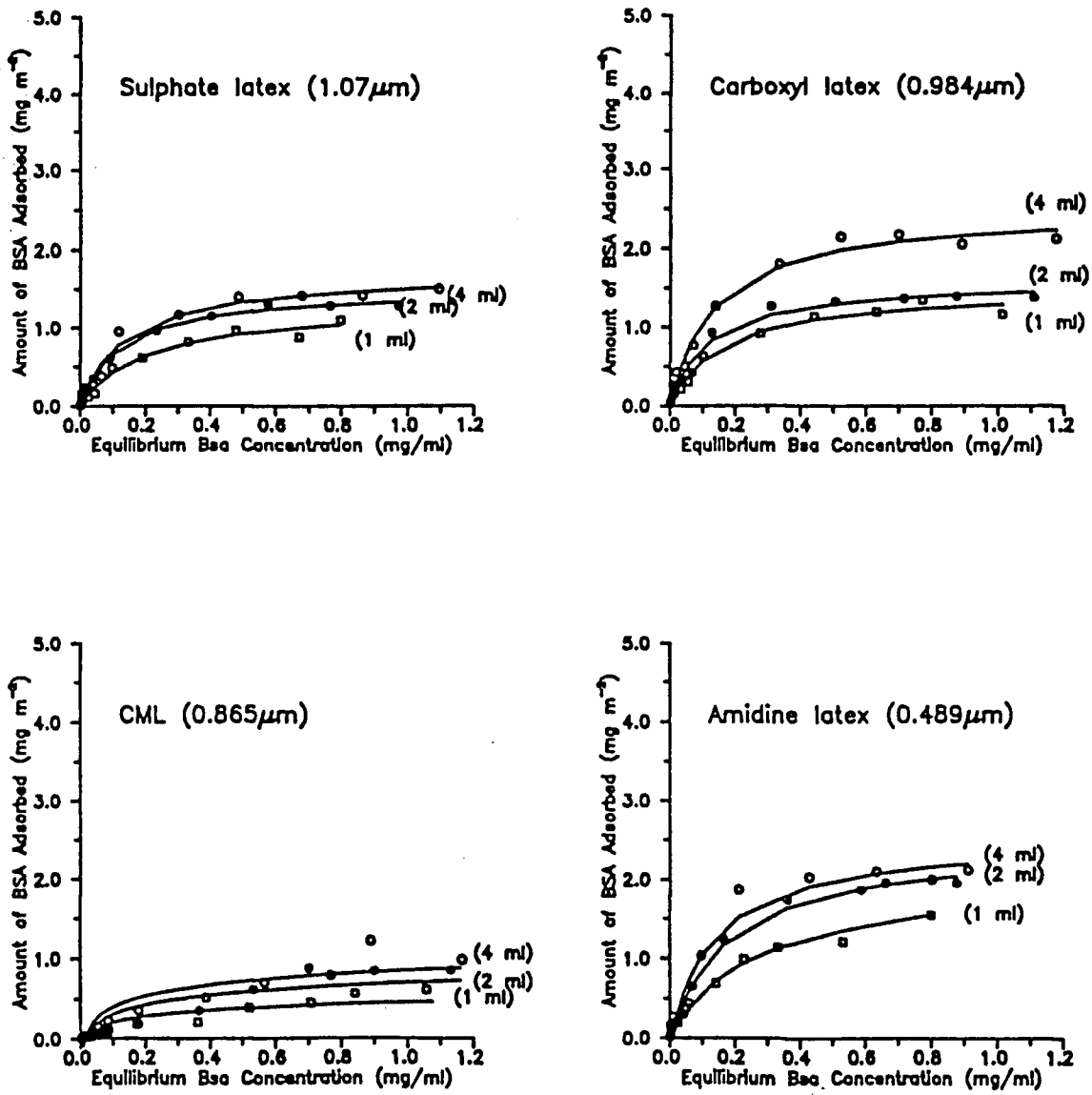

Figure 9. Adsorption isotherms for BSA to the latexes indicated at room temperature from 0.01M phosphate buffer, pH 7.20. The total volume of BSA solution used in each experiment are indicated. The total surface area of the latex used in each isotherm were as follows: Sulfate (361.4), Carboxyl (160.1), CML (247.9) & Amidine (+) (403.6) cm^2.

Table III

Adsorption maxima of BSA adsorption isotherms in Figure 9, as estimated from the isotherms.

Variation of Total Volume				
	Sulfate	Carboxyl	CML	Amidine
1ml	0.98±0.05	1.24±0.04	0.54±0.07	1.35±0.17
2ml.	1.29±0.04	1.42±0.03	0.86±0.01	1.95±0.07
4ml.	1.47±0.04	2.16±0.06	1.00±0.18	2.15±0.05

Figure 10 presents the replot of data of Figure 9 as surface concentration against the non-adsorbed amount of BSA per unit area, instead of the equilibrium solution concentration, as suggested by Cohen Stuart *et al* **[130]**. Again it illustrates the general prediction of their polydispersity theory.

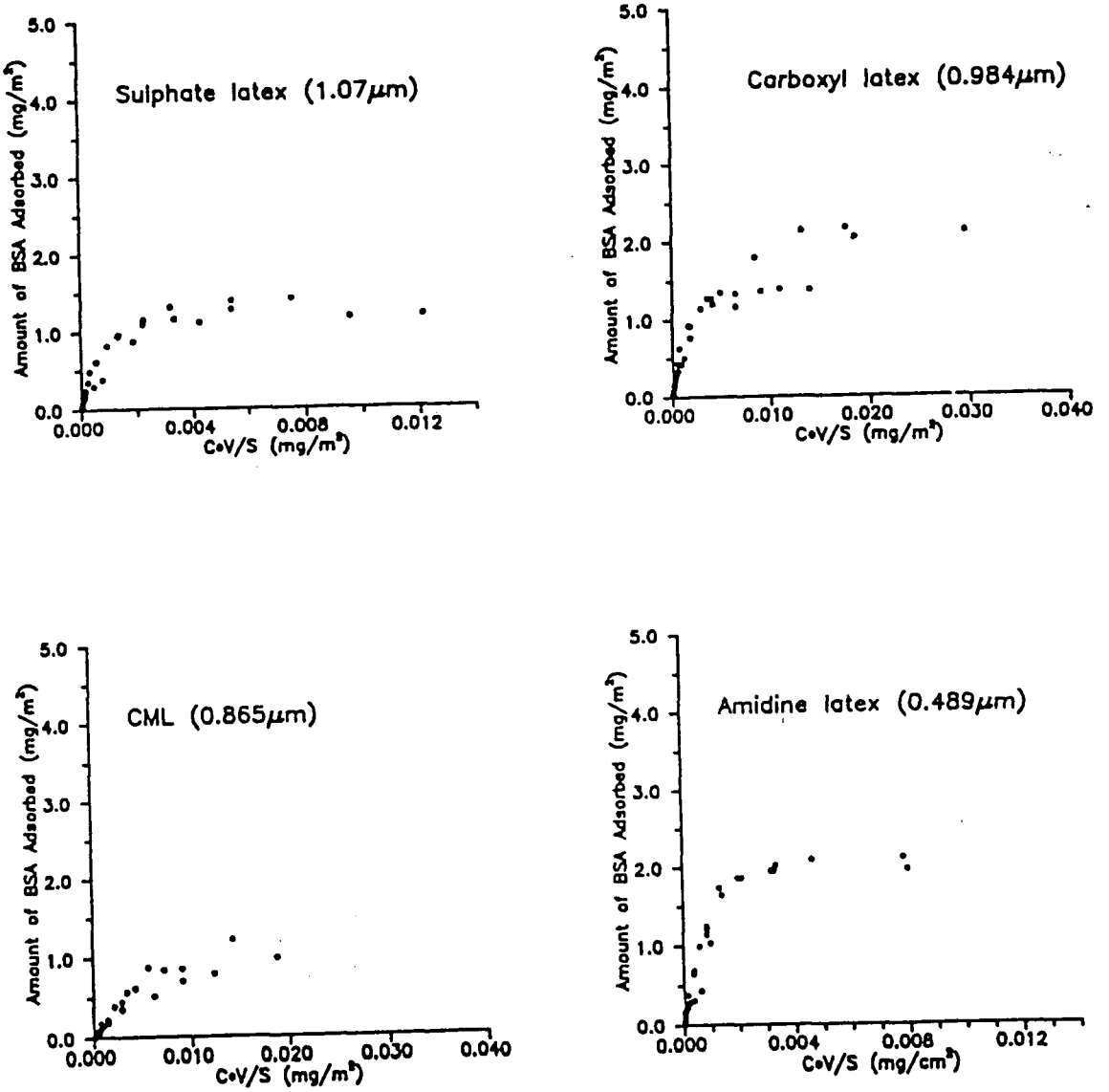

Figure 10. The adsorption data of Figure 9 plotted as a function of the amount of non-adsorbed BSA per unit area in the solution, $\Gamma^* = (C \times V/S)$, where C is the equilibrium BSA concentration, V is the volume of supernatant in equilibrium with latex and S is the total surface area of latex in equilibrium with BSA solution.

2.3. (b). *Comparison of Amount of BSA Adsorbed per Unit Area for the Four Latex Types at Constant Surface Area of Latex*

The difference in the amount adsorbed per unit area for the different latex types can be deduced from the isotherms in Figure 8, in which the amount of BSA adsorbed per unit area is plotted as a function of surface area of latex. The amounts of BSA adsorbed per unit area as the surface area tends to zero is probably a good estimate of the maximum amount of BSA (saturation values) adsorbed by the latex particles. These values are estimated to be 2.98 mg m^{-2} of BSA for the amidine (+) latex, 2.30 mg m^{-2} for the carboxyl latex, 2.20 mg m^{-2} for the sulfate latex, and 1.15 mg m^{-2} for the carboxyl-modified latex. Thus the estimated values from Figure 8 indicate that the greatest adsorption of BSA is for the amidine (+) latex followed by carboxyl, sulfate and carboxyl modified latex (CML). Further support of this trend is illustrated by the summary of adsorption data (Table IV) obtained for similar surface areas of the different polystyrene latexes. Two different equilibrium concentrations of BSA were used in these experiments which were performed at relatively high surface areas of the latexes. The results indicate a similar trend as the estimated values from Figure 8.

Since the adsorption experiments were all performed above the isoelectric point of BSA, a critical factor in this trend of amount adsorbed per unit area seems to be the area of hydrophobic sites available on the surface of the latex particle. As an indication of the ratio of hydrophobic to hydrophilic areas of the particle surface, the cross-sectional area of a typical charged group, e.g. $-OSO_3^-$, is compared with the surface charge density of the charge groups on the latex particle.

Table IV

Comparison of the amount of BSA adsorbed per unit area for four PS latex types at roughly "constant" surface area.

Latex type	Added in Solution		Adsorbed from Solution	
	PS	BSA	%	Total
	cm^2	mg ml^{-1}		mg m^{-2}
			Average	Average
Sulfate	1,967	0.698 0.696	30.6	0.323±0.006
		2.070 2.069	18.5	0.591±0.071
Carboxyl	1,850	0.691 0.690	30.5	0.342±0.006
		2.042 2.061	18.4	0.625±0.038
CML	1,834	0.690 0.702	15.4	0.175±0.002
		2.056 2.057	11.3	0.385±0.020
Amidine (+)	1,756	0.685 0.694	35.5	0.423±0.011
		2.033 2.050	24.3	0.868±0.061

Assuming the cross-sectional area of a charged group to be about 0.20-0.25nm^2 (20-25Å^2) **[4]**, the percentage of the latex particle surface that is hydrophobic and available for physical adsorption is approximately 91% for the sulfate latex, 94% for the carboxyl latex , 50-60% for CML, and 83% for the amidine (+) latex (see Table I). For the three negatively charged latexes (sulfate, carboxyl, and CML), the amount of BSA adsorbed per unit area at the same equilibrium BSA concentrations is related to the area per unit charge group of each latex, i.e., the adsorption increases in the same order as the hydrophobicity. Thus the CML with the lowest hydrophobic to hydrophilic ratio adsorbs the least amount of BSA and the carboxyl the highest. The sulfate latex with hydrophobicity close to that of carboxyl latex, adsorbs similar quantities of BSA. The strong binding of BSA to the positively charged amidine latex, even though the latex has an intermediate hydrophobicity in comparison with the three negative latexes is probably due to the additional effects of electrostatic interactions, expected between the negative BSA molecules and the positively charged amidine latex surface. Thus, although hydrophobicity seems to be a major factor in physical adsorption of proteins to polystyrene latexes, other effects such as electrostatic interactions are often superimposed upon hydrophobic effects.

2.3 (c) *Wash Analysis of BSA Adsorbed onto PS Latexes*:

(i) Buffer Wash

In order to further examine the characteristics of the adsorption of BSA on the latexes and obtain an estimate of how much BSA is retained on the latex surface following exposure to phosphate buffer, a wash analysis

of the adsorbed BSA was done on selected samples from the adsorption experiments.

After spinning down the latex and removing aliquots for counting, the rest of the supernatant was decanted and kept for SDS-PAGE gel electrophoresis analysis. The remaining compact latex pellet was resuspended in pure buffer up to the starting volume and centrifuged again. This centrifugation and washing procedure was repeated until a negligible change in the total count of the latex pellet was obtained. The final count was taken as an estimate of the amount of protein retained on the latex surface after extensive wash. Table V gives the desorption data for the BSA adsorption described in Table IV.

Table V

Amount of BSA retained on the PS latex pellet (experiment reported in Table IV) after extensive wash with equilibrium buffer.

Latex type	Amount bound (before wash)	Amount bound (after wash)	Difference	
	(mg m^{-2})	(mg m^{-2})	(mg m^{-2})	%
Sulfate	0.323	0.269	0.054	16.7
	0.591	0.435	0.156	26.4
Carboxyl	0.342	0.287	0.055	16.1
	0.625	0.472	0.153	24.5
CML	0.175	0.119	0.056	32.0
	0.385	0.202	0.183	47.5
Amidine (+)	0.423	0.380	0.043	10.2
	0.868	0.680	0.188	21.7

As can be seen from Table V, for adsorption at low equilibrium BSA concentration there is a difference of between 10 and 17 percent in the amount of BSA adsorbed per unit area before and after wash with equilibrium buffer for the low surface charge latexes, i.e. carboxyl,

sulfate, and amidine; a larger difference of 22 to 26 percent is observed for adsorption at high equilibrium BSA concentration for these latexes. For the high surface charge CML the difference at low equilibrium BSA concentration is about 32 percent, and much higher, 47.5 percent, at high equilibrium BSA concentration.

For the negatively charged latexes, the trend in desorption also seems to be related to the area per charge group of the latexes. It can be seen that the desorption decreases as the hydrophobicity of the latexes increases. Carboxyl latex with the highest hydrophobicity loses the lowest fraction of bound BSA following extensive buffer wash and the CML, with the least hydrophobicity loses the largest fraction of its adsorbed layer upon adsorption.

This difference in the amount of BSA that is removed by washing from the low surface charge latexes (carboxyl and sulfate) and the high surface charge latex (CML) is probably due to the nature of the interaction between the surfaces and the BSA molecules. The high surface charge latex has a polyectrolyte-type surface and is therefore more hydrophilic; polar interactions between this type of latex and the protein molecule probably have a large influence on the adsorption process. It might be expected that water could compete with these interactions and that repulsive electrostatic interactions would if anything enhance protein release. The removal of the protein from the hydrophilic surface by extensive rinsing is therefore easier than removal from a hydrophobic surface.

When electrostatic attraction is superimposed upon the hydrophobic interactions of BSA molecules with the latex surface as in the case of the positively charged amidine latex, the amount of BSA desorbed following extensive buffer wash is minimal. It can be seen from Table V

that the latex with the highest BSA surface concentration (amidine latex) at equilibrium loses the lowest fraction of its bound protein compared to all the other latexes, although it has an intermediate hydrophobicity in comparison with the negatively charged latexes (carboxyl and sulfate latexes). Conversely, the system with the highest hydrophilicity and negative charge (CML) and the lowest amount of bound BSA at equilibrium releases the largest fraction of its adsorbed layer upon extensive buffer wash. The low desorption from the amidine surface seems also to suggest that the electrostatic interaction between the negatively charged protein and the positively charged latex may involve ionic bonds, since if the electrostatic interactions enhanced adsorption were due simply to increasing the local concentration of the protein molecules near the latex surface, one might expect a greater amount of desorption to occur following extensive buffer wash.

(ii). Comparison of Buffer Wash with SDS, BSA, PEG and IgG Washes

It is well known that an adsorbed layer of polymer on a solid surface, when placed in a solution with a finite bulk polymer concentration, can exchange some molecules with the solution. For example, the displacement of a polymer species in the adsorbed state may be achieved by another polymeric species of larger size **[185]**. For polydisperse samples of synthetic polymers, preferential adsorption of large molecules over small ones occurs, however, extreme preferential adsorption is usually not observed **[129,186]**. Brash *et al* **[113]** found that when proteins of identical mass are adsorbed to various solids, adsorption appears to be irreversible with respect to dilution.

The literature on the reversibility and exchange of adsorbed protein was reviewed in Chapter One Section 1.4 (a). An indication of whether BSA molecules in the adsorbed layer were removable by dilution or exchanged with molecules in solution was obtained by experiments in which radioactively labeled BSA was adsorbed onto the PSL surfaces at saturation values and the amounts of radioactively labeled BSA retained on the PSL after extensive wash cycles with solutions of sodium dodecyl sulfate (2% SDS), unlabeled BSA, rabbit anti-BSA IgG, and 2% polyethylene glycol (6000) were measured.

Figure 11 gives the relative amount of BSA retained on the PSL after successive wash cycles, each step being for between 6 and 8 hours. It can be seen that for all the latexes there is very little desorption of BSA when pure buffer, nonlabeled BSA, anti-BSA IgG or 2% PEG solution is used for washing. There appears to be very little or no exchange between adsorbed BSA molecules and the bulk solution molecules under these conditions, even for the higher molecular weight IgG molecules. The wash analysis measurements were performed under the same conditions as the adsorption experiments, in which the equilibrium state was assumed to be established after $\cong$ 6-8 hours. No kinetic studies were performed, the aim being to use time courses applicable to latex agglutination systems. Since desorption even in the presence of polymeric molecules in solution is a slow process **[185]** and is not diffusion controlled, we cannot draw any conclusions about reversibility and/or irreversibility of adsorbed proteins at the solid/liquid interface over longer time periods. However, on a time of hours to a few days little exchange or desorption occurs.

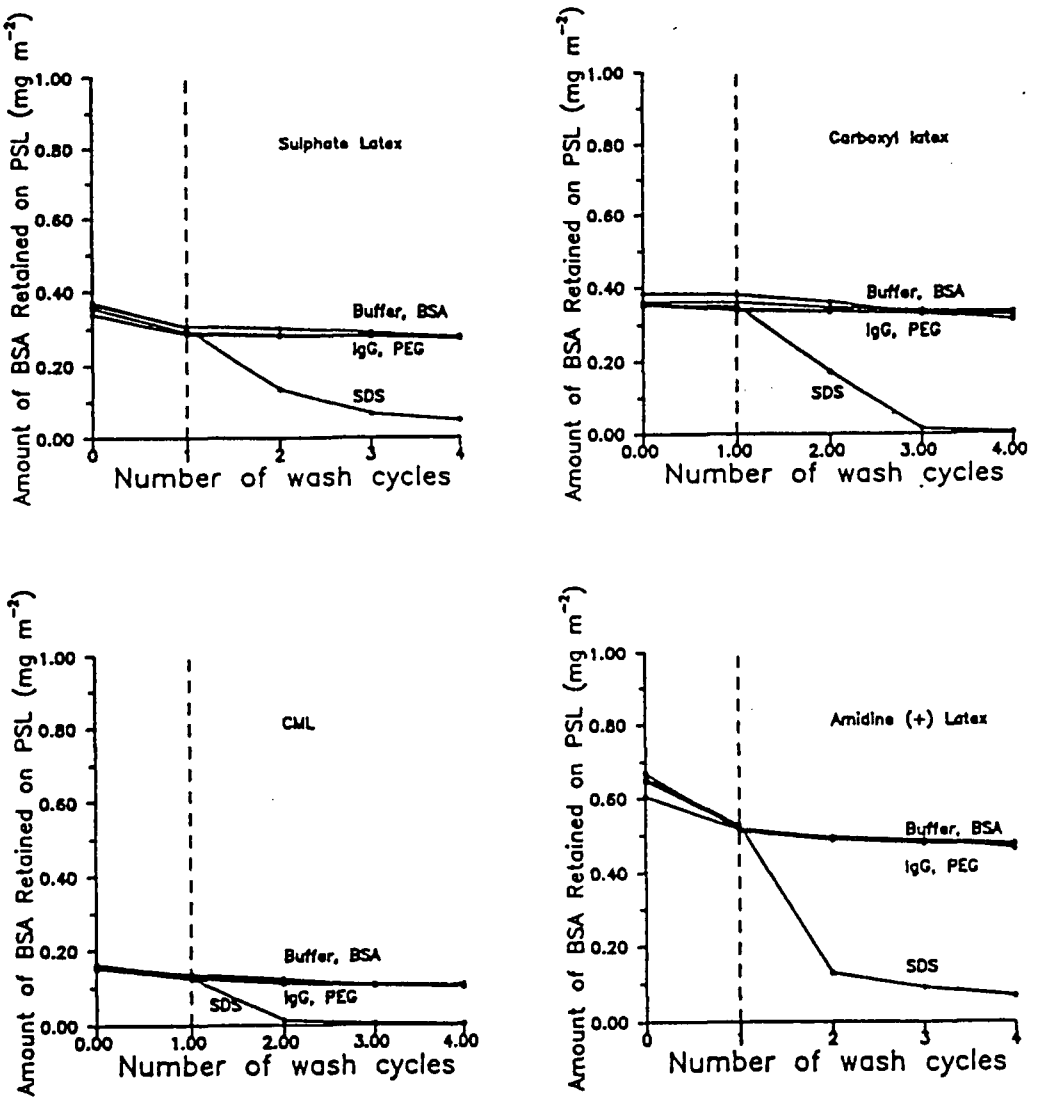

Figure 11. Amount of BSA retained on PSL after washing first with equilibrium buffer, followed by repeated wash cycles with 0.01M phosphate buffer pH 7.20, 2% SDS, nonlabeled BSA (at the concentration with which the surfaces were equilibrated, 1.87 mg/ml), anti-BSA IgG 0.094 mg/ml, and 2% PEG (6000) in 0.01M phosphate buffer, pH 7.2.

Solutions of SDS, however, solubilise and displace adsorbed BSA from the various latex surfaces to a much greater extent. This is clearly indicated by the amount of BSA retained on all the PSL surfaces in Figure 10, after the SDS washes. The first and/or second wash with a SDS solution seems to remove most of the adsorbed BSA from all the latexes. The subsequent washes have a relatively small effect. This probably indicates the existence of a range of weakly and tightly bound BSA molecules on all the latexes studied.

2.3 (d) *SDS Gel Electrophoresis of BSA Removed from the Latex Surface*

Many proteins, including albumin, form polymeric species in solution and these can be readily detected by sodium dodecyl sulfate-polyacrylamide gel electrophoresis (SDS-PAGE) **[187,188]**. In SDS electrophoresis, proteins are separated on the basis of size alone. The SDS binds to the protein molecules, converting their compact 3-dimensional shape into denatured random coils. Since the SDS molecules often bind to polypeptides with a constant ratio of SDS to polypeptide mass, the charge per unit weight is constant. Thus, the protein's native charge is totally masked with the negative charge of the SDS. When subjected to polyacrylamide gel electrophoresis, the proteins, which are now equal in charge density, are separated purely according to size by the molecular sieving effects of the gel matrix. SDS-PAGE is widely used to estimate the molecular weights of unknown proteins by comparing their relative electrophoretic mobility (R_f) to standard proteins of known

molecular weights.

In order to examine the composition of the adsorbed BSA layer on the latex surface, the latex was washed initially with equilibrium phosphate buffer followed by SDS-PAGE buffer containing 2% SDS, and electrophoresis gels of the removed material run. An attempt to make quantitative comparisons between polymeric contents of the removed (radio iodinated) adsorbed protein exposed to different latex surface areas and the concentration of oligomers present in the original unexposed solution of BSA was made on the basis of SDS-PAGE gel scans since the protein specific activity was too low to produce reliable data by slicing the gels and counting. The bands on gels were recorded by scanning them on a Beckman Model 25 Spectrophotometer with a rod gel scanning adaptor at 590nm. The gel scans were then digitized to a scale approximating the actual length of the gels (10 cm) using a Digi-Pad graphic digitizer Model DP5A-1117A. The area under each peak was obtained by integrating the gel profile over several subintervals using the familiar trapezoid rule: area of a trapezoid is given by its average height times the base. The integrated peak areas from the gel scans represent the amount of each oligomer type present in the electrophoresis sample load. These values were then used to calculate the total amount of each oligomer in the equilibrium BSA solution and that on the surface of the latexes.

The results of SDS-PAGE electrophoresis analysis presented here are those for the proteins removed from the latexes used in : (a) the experiment performed at constant surface areas for the four latexes, as reported in Tables IV and V; and (b) the sulfate (1.073μm) and amidine (0.489μm) latexes of the adsorption experiments whose isotherms are given in Figure 6. For case (b) only the samples with the highest equilibrium concentrations and adsorbed amount per unit area for each case of the

three different surface areas (see Figure 6.) of the two latexes were analyzed. Table VI summarizes the adsorption data for the samples analyzed by SDS-PAGE electrophoresis.

Table VI

Summary of Adsorption Data for samples subsequently washed with 2% SDS and amount of BSA used in SDS-PAGE electrophoresis analysis (a):

Latex type	Surface Area (cm^2)	Amount bound (before buffer wash) ($mg\ m^{-2}$)	Amount bound (after buffer wash) ($mg\ m^{-2}$)
Sulfate	1,967	0.323	0.269
Carboxyl	1,850	0.342	0.287
CML	1,834	0.175	0.119
Amidine (+)	1,756	0.423	0.380

Electrophoresis:		Supernatant(μg)	Pellet(μg)
Sulfate:	(electrophoresis load)	15	26
	(estimated Total BSA)	1420	530
Carboxyl:	(electrophoresis load)	18	50
	(estimated Total BSA)	1420	530
CML:	(electrophoresis load)	18	31
	(estimated Total BSA)	1710	220
Amidine (+):	(electrophoresis load)	12	72
	(estimated Total BSA)	1300	660

The concentration profiles from SDS-PAGE gels of the BSA remaining in the supernatant at equilibrium with the saturated surfaces and of the BSA removed by SDS from the surfaces of the latexes are shown in Figure 12. In these gels the lowest molecular weight species appears farthest to the right. The molecular weights of the BSA monomer and oligomers were confirmed by comparison of the relative mobility of the BSA removed from the latex surface with that of high molecular weight calibration kit (Pharmacia).

Only 44% of adsorbed BSA was removed from the surface of the sulfate latex, 75% from the carboxyl latex, 94% from the carboxyl modified (CML) latex and 76% from the amidine latex under the conditions used here. The concentration profiles given in Figure 12 represent only the above percentages of the total BSA adsorbed to the latexes. It is evident, from the concentration profiles, that there is an enrichment in the higher molecular weight oligomers of BSA removed from the latexes relative to the amounts of these higher molecular weight oligomers in the supernatant or in the original stock BSA solution before exposure to the latexes (see Figure 13.). The percentage values of the concentration profiles of BSA SDS-PAGE gels quoted above and those given below have a considerable amount of uncertainty (15-20%) associated with them due to the difficulty in determining the concentration of BSA used in electrophoresis. However, in an experiment in which BSA was subjected to SDS-PAGE at protein loads ranging from 1 to 50 μg, a plot of the monomer, dimer and total protein peaks versus protein load was linear up to protein load of about 30 μg.

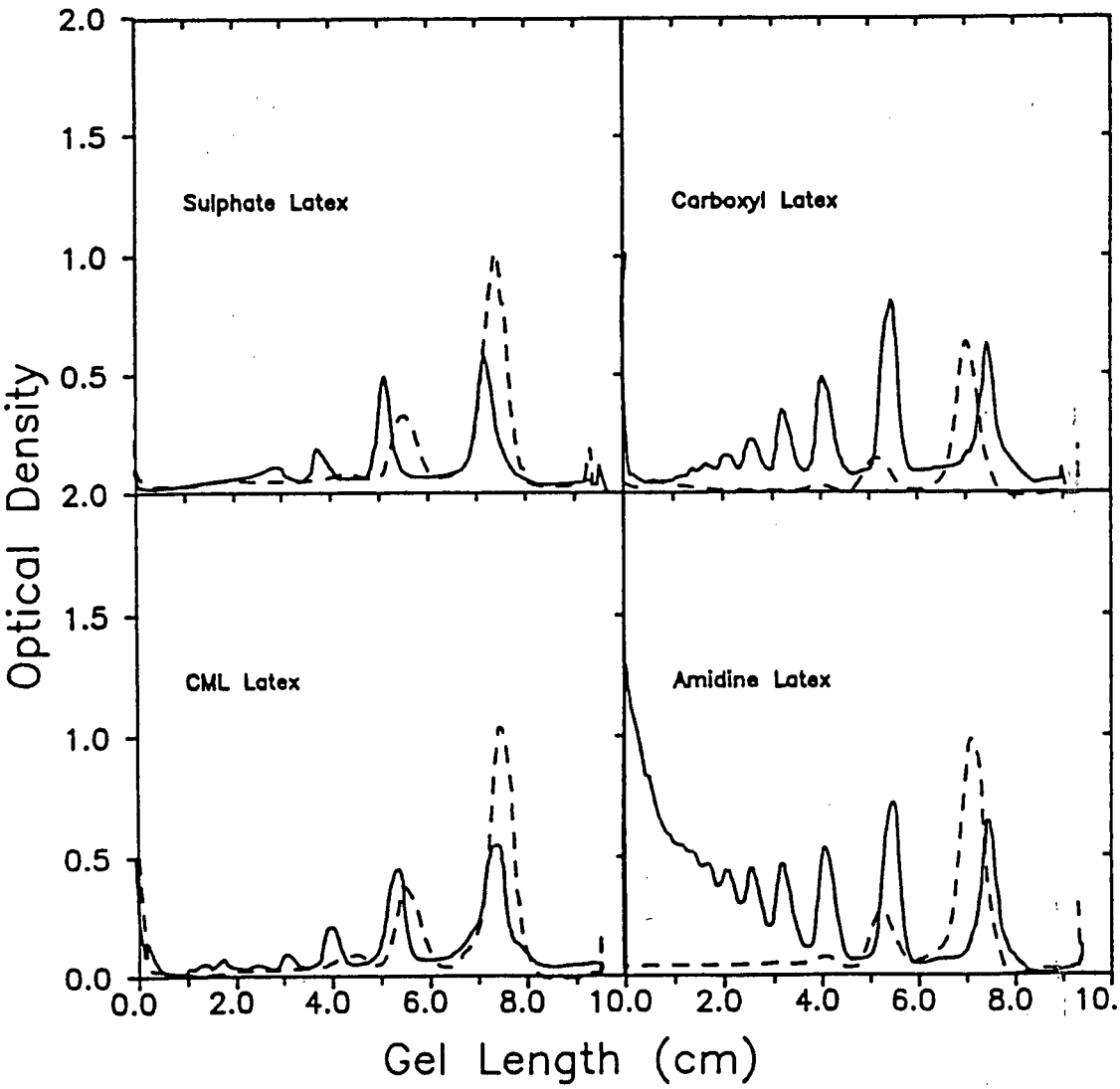

Figure 12. Optical density profile of Coomassie Blue stained SDS 4% polyacrylamide gels of BSA from the supernatant (dashed line) and pellet (solid line)of the adsorption experiment reported in Table IV. The latex pellets were extracted with 2% SDS and the extracts run on SDS-PAGE gels.

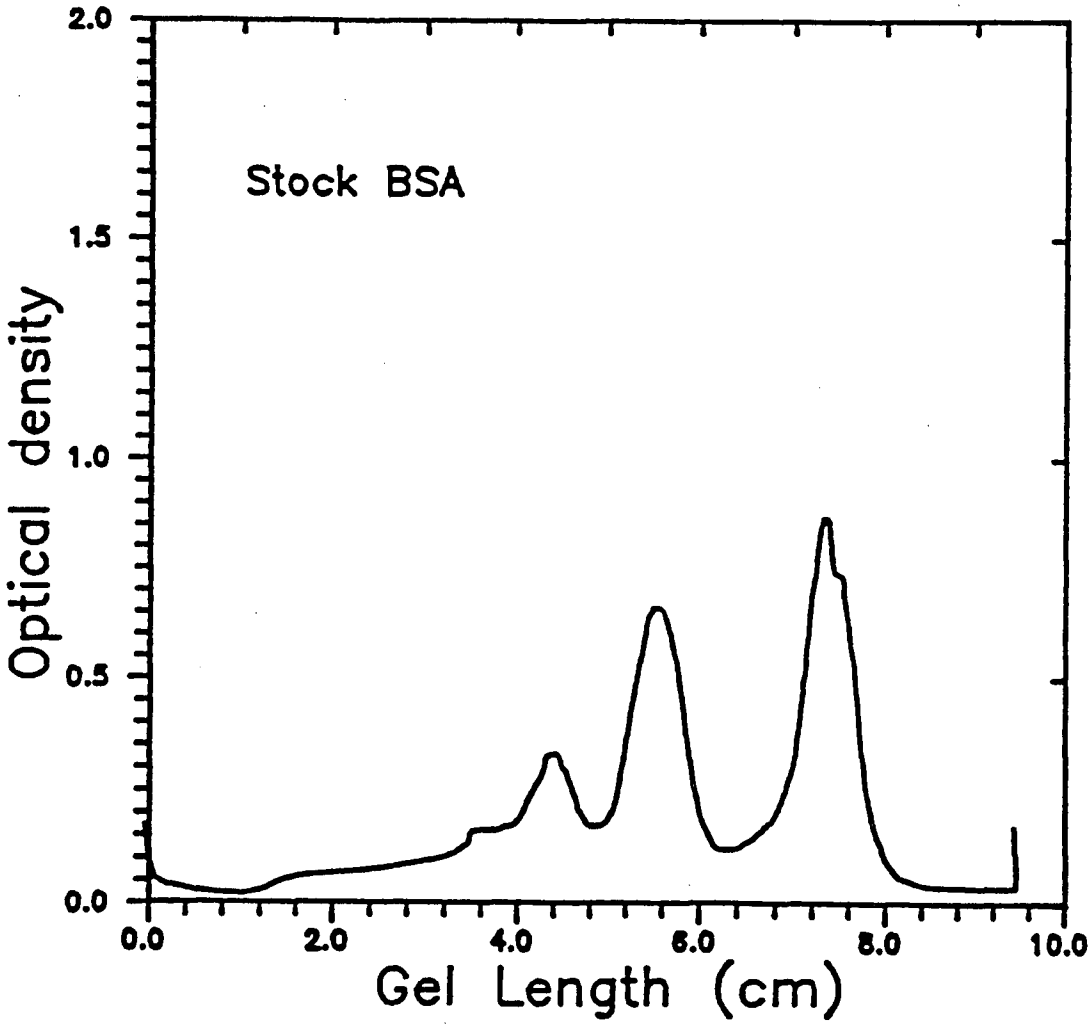

Figure 13. Optical density profiles of Coomassie Blue stained SDS 4% polyacrylamide gel of stock BSA used in the adsorption experiment reported in Table IV. The profile represents the composition of the original BSA that has not been exposed to the latexes. BSA experimental concentration, 0.69 mg/ml; 33 μg protein loaded.

The BSA sample used in these adsorption studies contained approximately 44% monomer, 31% dimer and 15% trimer as determined from the concentration profiles of the SDS-PAGE electrophoresis analysis. Table VII (a) gives the percentage of the polymeric species of the original BSA solution before exposure to the latexes, and the percentages of the polymeric species of BSA in the equilibrium supernatant and that removed from the surface of the latexes which had been equilibrated with BSA solution.

Table VII(a)

The distribution of BSA oligomers in equilibrium solution and on PSL surfaces as a percentage of total BSA in experiment. The adsorption data is summarized in Table VI.

	Original BSA		
	Monomer (%)	Dimer (%)	Trimer (%)
	44	31	15

	BSA in Equilibrium Solution			BSA Adsorbed on PSL and removed with SDS			
	Monomer (%)	Dimer (%)	Trimer (%)	Monomer (%)	Dimer (%)	Trimer (%)	Tetramer (%)
Sulfate	52	18	7	4.7	2.3	1.1	0.6
Carboxyl	41	11	2	4.4	4.0	2.4	1.4
CML	59	23	10	3.1	1.7	0.7	0.2
Amidine	44	12	5	3.2	2.9	2.2	1.9

NB: The percentages given in Table VII(a) are those of the total BSA initially added to the latex suspension.

It can be seen from Table VII(a) that the amount of each polymeric species removed from the surface of the latexes is much less than the corresponding amount in the equilibrium solution, due to the relatively small surface area present. The concentration of monomeric species in the equilibrium solutions is comparable to that in the original unexposed BSA solution, while the concentrations of the dimeric and trimeric species in the equilibrium solutions are considerably reduced. On the other hand, the relative concentrations of oligomers are increased in the material originating from the latex surface. The increase in the concentration of these higher polymeric BSA oligomers on the surface of the latexes does not correspond to the decrease in their concentrations from the original BSA solution, however. Instead, it can be seen from the concentration profiles, particularly from the amidine latex, that higher polymeric species (tetramer, pentamer, etc) were present on the latex surfaces whereas their presence in the original BSA solution and in the equilibrium solution is not observed (Figure 12 and 13).

This is further illustrated in Table VII(b) below in which the concentration of each polymeric species derived from the surfaces of the latexes is now given as a percentage of the total amount of BSA adsorbed at equilibrium. Again it is clear that the monomer:dimer:trimer ratios vary considerably for the different latexes and differ from the BSA stock. The higher polymeric species contribute considerably to the total amount of BSA adsorbed.

Table VII(b)

The distribution of BSA oligomers removed from PSL surfaces as a percentage of BSA adsorbed. The adsorption data is summarized in Table VII.

	BSA Adsorbed on PSL and removed with SDS				
	Monomer (%)	Dimer (%)	Trimer (%)	Tetramer (%)	Pentamer (%)
Sulfate	43.5	22	11	5.4	3.9
Carboxyl	29.5	27	15.8	9.7	7.0
CML	43.5	24	10.5	3.0	2.6
Amidine	12.9	12	8.9	7.8	6.8

Table VIII (a) and (b) summarizes the adsorption data of the second set of samples analyzed by SDS polyacrylamide gels (Figure 6).

Table VIII(a)

Summary of Adsorption Data for samples used in SDS-PAGE electrophoresis analysis (b):

Sulfate Latex (1.073μm)				
Sample	Total Surface Area of Latex (cm^2)	Initial [BSA] (mg/ml)	Amount Adsorbed ($mg\ m^{-2}$)	Amount Adsorbed (mg)
A	242.7	0.793	1.93	0.468
B	696.3	0.796	1.46	1.018
C	1160.3	0.798	1.10	1.273

Table VIII (b)

Summary of Adsorption Data for samples used in SDS-PAGE electrophoresis analysis (b):

Amidine	Latex (0.489μm)			
A	395.4	0.796	1.81	0.715
B	988.6	0.795	1.57	1.547
C	1368.9	0.798	1.32	1.807

The concentration profiles from SDS-PAGE gels of the BSA remaining in the supernatant and of the BSA removed from the surfaces of the two latexes (amidine and sulfate), different areas of which had been equilibrated with BSA, are given in Figures 14 and 15, respectively. It can be seen from the concentration profiles that there is a great enrichment relative to the equilibrium supernatant of the higher molecular weight oligomers of BSA removed from the latex surfaces which becomes more evident as the total surface area of the latexes exposed to the BSA solution increases and larger quantities of protein are recovered. The percentages of the polymeric species of BSA in the supernatant solution and that adsorbed onto the latex surfaces are given in Table IX (a) and (b).

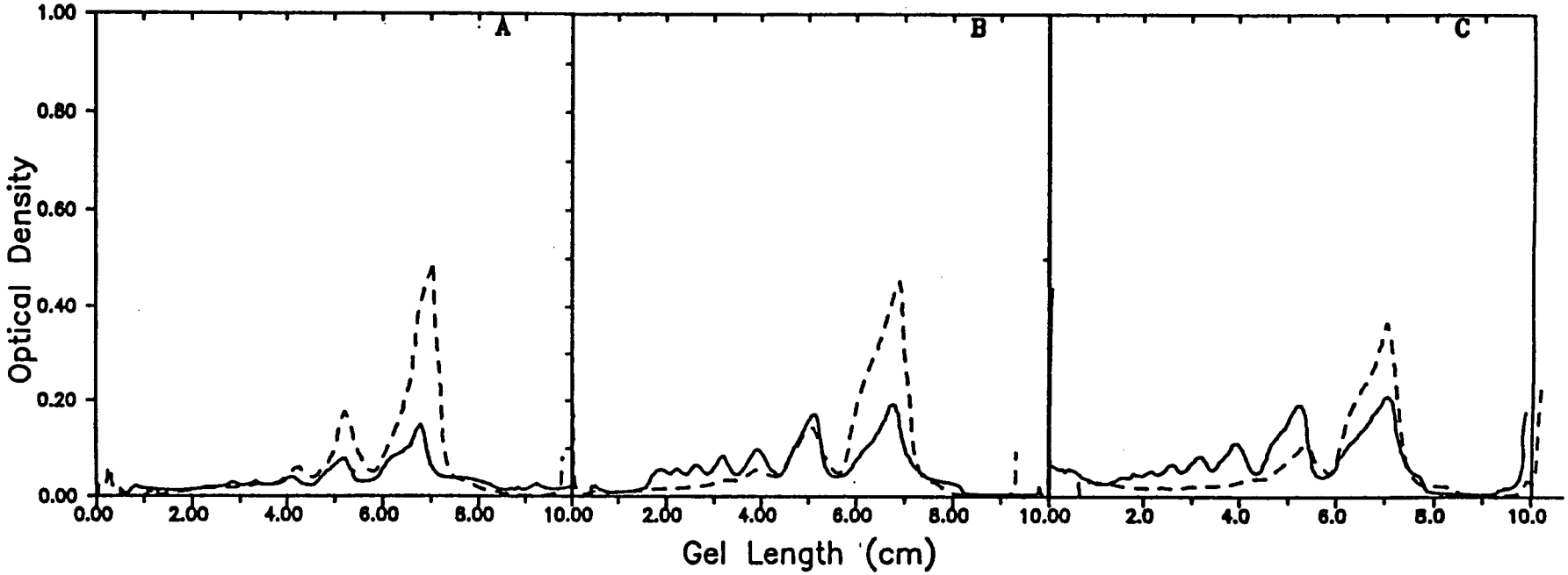

Figure 14. Optical density profiles of Coomassie Blue stained SDS 4% polyacrylamide gels of BSA from the supernatant and pellet of the adsorption experiment on sulfate latex reported in Figure 6. A, B, & C correspond to three different surface area of the latex as indicated in Figure 6 and Table VIII (a). The amount of BSA loaded on each gel and the total amount adsorbed on the latex surface are givenin Table IX.

Table IX

Summary of amount of BSA loaded to each gel, the total amount of BSA adsorbed on the latex surface and the total amount in supernatant solution:

Sulfate latex		Supernatant(μg)	Pellet(μg)
A	Loaded	10	19
	Total	2740	373
B	Loaded	8	39
	Total	2180	780
C	Loaded	7	46
	Total	1940	918
Amidine (+)			
		Supernatant(μg)	Pellet(μg)
A	Loaded	9	32
	Total	2520	642
B	Loaded	6	67
	Total	1640	1340
C	Loaded	5.3	78
	Total	1430	1550

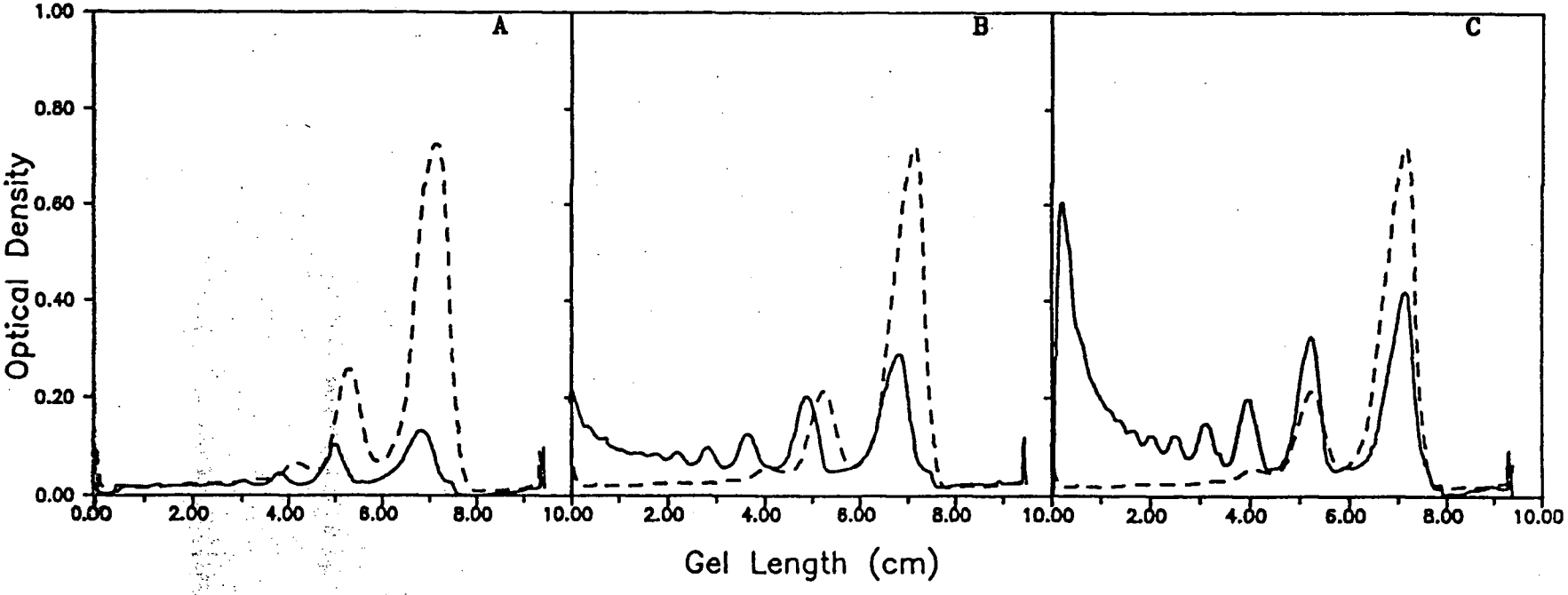

Figure 15. Optical density profiles of Coomassie Blue stained SDS 4% polyacrylamide gels of BSA from the supernatant and pellet of the adsorption experiment on amidine (+) latex reported in Figure 6. **A, B, & C** correspond to three different surface area of the latex as indicated in Figure 6 and Table VIII (b). The amount of BSA loaded on each gel and the total amount adsorbed on the latex surface are given in Table IX.

Similar trends are observed in the distribution of BSA oligomers in the supernatant and in that recovered from the surface of the latexes as seen in the analyses of samples from the adsorption experiments performed at constant surface area. The gel analysis of the samples from adsorption at three different surface areas (Table X (a)) show that, for both the amidine and sulfate latexes, the contribution by the higher polymeric species to the total amount of adsorbed BSA released by SDS increases gradually as the surface area of the latex increases. The decrease in the dimer concentration from the supernatant solution is, again, not reflected by the amount of dimer removed from the latex surfaces. It can be seen from Table X (b) that as the surface area of the latex increases, the percentages of the total BSA adsorbed decreases for the monomeric species, and increases for the higher polymeric species.

It is clear from the above results that the surface area dependence of adsorption is accompanied by a depletion in BSA oligomers from solution and an increase in their concentration in the adsorbed layer, relative to the BSA stock solution. The relative depletion of the oligomer is greater the stronger the adsorption, amidine showing the largest effect and CML the smallest in this regard. These observations suggest that the theoretical model proposed by Cohen Stuart *et al* **[130]** based on the idea that higher molecular weight material adsorbs more strongly and hence will dominate at low surface areas, might explain the data. The good fits to the data reduction scheme proposed in **[130]** (Figure 7) are consistent with this approach. However, the oligomer distribution data given in Table X(b) does not support this interpretation since it does not show a greater relative depletion of the oligomers at low surface area, as predicted. The uncertainty in the

numerical values may mask the depletion difference at low areas but there is no suggestion in the depletion data of a trend in the anticipated direction.

Table X (a)

The distribution of BSA oligomers removed from PSL surfaces as a percentage of BSA added. The adsorption data is summarized in Table VIII (a) and (b).

Amidine latex							
	BSA in Equilibrium Solution			BSA Adsorbed on PSL and removed by SDS			
Sample	Monomer (%)	Dimer (%)	Trimer (%)	Monomer (%)	Dimer (%)	Trimer (%)	Tetramer (%)
A	65.7	19.8	—	0.9	0.5	0.2	0.1
B	62.7	17	—	2.0	1.0	0.7	0.4
C	59.4	16	—	3.2	2.2	1.1	0.8
Sulfate latex							
A	62.2	19.4	—	1.7	0.6	0.4	—
B	61.4	17.6	—	2.3	1.3	0.7	0.4
C	56	15.5	—	2.7	1.8	0.9	0.5

Table X (b)

The distribution of BSA oligomers removed from PSL surfaces as a percentage of BSA adsorbed. The adsorption data is summarized in Table VIII (a) and (b).

Sample	BSA Adsorbed on PSL and removed by SDS				
	Monomer (%)	Dimer (%)	Trimer (%)	Tetramer (%)	Pentamer (%)
Amidine latex					
A	41.8	21.9	9.6	5.2	—
B	31.1	16.4	10.6	5.9	5.2
C	23.8	16.3	8.1	6.3	4.0
Sulfate latex					
A	43.3	14	9.3	—	—
B	40.5	23.4	11.8	7.7	5.1
C	34.1	23	11.5	6.4	4.4

The oligomer distribution of the adsorbed protein removed by SDS is even less supportive of the above model. This is most evident in the molecular weight distribution of Figure 15 C. The high molecular weight species to the left of the profile were never seen in the BSA stock solutions nor in the equilibrium supernatants. The quantities involved are such that they readily would have been detected in these solutions if they were present; their levels are too high to just represent concentration of pre-formed oligomers on the latex surface. Given that the depletion data indicates preferential adsorption of oligomers (in agreement with Zsom **[183]**) the above indicates that the material removed by detergent represents both adsorbed, pre-formed oligomers and species formed by polymerization reactions on the latex surface.

The kinetics and chemical determinants of the surface-catalyzed polymerization are not known at present; it was beyond the scope of this project to characterize it further. It seems likely that the protein left on the latex surface following SDS washing, representing over 20% of the adsorbed BSA, could have a molecular weight distribution shifted to higher oligomers than the released material and that this would contribute to the irreversibility of its binding. The reaction complicates interpretation of the area dependence of adsorption however, since it is enhanced at high surface areas, at least for amidine.

A model which, qualitatively, could explain the observed behavior is as follows. At a given initial protein concentration the amount adsorbed to different surface areas of latex is determined by the molecular weight distribution of the stock, with higher surface concentrations present at low areas due to stronger oligomer adsorption. Higher surface area suspensions would have more monomer adsorbed per unit area, therefore. It is known that monomeric albumin can undergo

conformational changes during adsorption **[76,189-191]**. These changes might be sufficient to open the structure enough to allow for disulfide exchange or other, unknown, polymerization reactions with neighboring molecules on the surface.

If the oligomers formed are linear there would be two sites per oligomer, at either end, available for further reaction. Since this would apply to the monomer as well, there would be more potential reaction sites per unit area in the high area latex suspensions than in the low, even though the total mass adsorbed was somewhat higher (30-40%) in the latter case. The higher concentration of reactable ends could produce higher molecular weight oligomers leading, at equilibrium, to the observed results.

2.4 Summary of BSA Adsorption Studies

1. The mass of BSA adsorbed at saturation depends on the type of polystyrene latex. Latexes with highly hydrophobic surfaces tend to adsorb more BSA molecules than those with with lower hydrophobicity. Electrostatic effects, e.g. electrostatic attraction between (-ve) protein and (+ve) polystyrene latex surface or vice versa, may be superimposed upon the hydrophobic interactions between the hydrophobic amino acids of the protein and the uncharged regions of the latex surface.

2. The desorption of BSA molecules from PSL surfaces is, to a limited extent, dependent on the type of latex. Latexes that maximize adsorption lose the lowest fraction of their bound BSA molecules following extensive pure buffer wash. Partial desorption of BSA from PSL can be achieved by the addition of detergents such as SDS, whereas the addition of more BSA molecules or other macromolecules such as PEG or IgG does not seem to displace the adsorbed BSA molecules from the surface of the latexes over the time courses used in this work.

3. The adsorption of protein containing oligomers to PSL surfaces depends on the concentration of both protein and latex, higher amounts per unit area adsorbing in suspensions containing lower total surface areas. The adsorbed layer is enriched in the higher molecular weight oligomers, relative to their concentrations in the stock solution. This enrichment may be due to preferential adsorption of higher polymeric species or to the formation of these higher polymeric species on the particle surfaces. At equilibrium, higher molecular weight oligomers are prevalent on the surface when higher total areas of the latex are present. This observation is consistent with a model in which adsorbed protein undergoes a conformational change that allows a polymerization reaction to occur from each end of the monomer or oligomer. The higher monomer concentration predicted to be adsorbed initially in suspensions of high total surface area provides a higher surface concentration of reaction sites for polymerization of adsorbed protein, leading to the observed results.

CHAPTER THREE

ANTIBODY BINDING TO ANTIGEN-COATED PSL

3.1 Introduction

Antigens and their corresponding antibodies interact through non-covalent binding in solution to form antigen-antibody complexes which may or may not be soluble. At an optimal antibody-antigen ratio, an insoluble antibody-antigen complex may aggregate by cross linking and/or hydrophobic interactions to form a precipitate. In the region of excess antibody or excess antigen, the aggregates formed become progressively smaller or less easily precipitable **[192]**.

The specificity of the antigen-antibody interaction cannot be explained on the basis of a single type of attractive force or chemical reaction. Nonspecific short range forces, such as van der Waals and Coulombic forces are thought to be important in many antigen-antibody interactions. Other interaction forces such as hydrogen bonding and hydrophobic bonding are also known to play a significant role.

Antigen-antibody interactions depend mainly on a structural complementarity between a determinant on the antigen molecule and a binding site on the antibody. As such, they belong to a large group of noncovalent biological reactions such as the binding of substrate to its enzyme, the binding of a hormone to its receptor, and the binding of ligands to proteins. The antigen-antibody interactions are, however, complicated by the diverse nature of antigens and antibodies. An antigen may have from one to several thousand antigenic determinants, which may differ from each other, while the biological synthesis of antibodies against an individual antigen determinant usually leads to the formation

of a heterogeneous polyclonal antibody population.

Many factors affect the interaction between an antigen and its corresponding antibody **[193]**. The affinity of the antibody for the antigen usually correlates inversely with the reversibility of the interaction; the higher the antibody affinity, the less reversible the reaction. Ionic strength, pH, temperature of the medium and the concentrations of antigenic determinants, and antibody combining sites also influence the outcome of the antigen-antibody interactions.

3.1(a) *Interaction of Monovalent Antibody and Monovalent Antigen in Solution*

The interaction of soluble antigen and its corresponding antibody in solution is theoretically considered as a bimolecular reaction **[120]**:

$$[Ag] + [Ab] \underset{k_r}{\overset{k_f}{\rightleftharpoons}} [AgAb] \quad \ldots\ldots\ldots\ldots\ldots\ldots (3.1)$$

where [Ab] is the concentration of unreacted antibody, [Ag] that of the unbound antigen, [AbAg] the concentration of antigen-antibody complex, and k_f and k_r are the forward and reverse reaction rates, respectively. Equilibrium is reached when the rate of formation of the complex [AbAg] is equal to the spontaneous dissociation of the same complex, implying that the reaction is fully reversible.

The equilibrium constant (binding constant), K is a function of the relative concentrations of the reactants and complex, and is given by the mass action expression:

$$K = \frac{k_f}{k_r} = \frac{[AbAg]}{[Ab][Ag]} \quad \text{.....(3.2)}$$

As expressed above, the equilibrium constant is given as an association constant, with a dimension of litres per mole (M^{-1}). A high numerical value of K corresponds to a high antibody affinity.

In practice, it is usually not possible to estimate the equilibrium concentrations of all three species: the antibody, the antigen, and the antigen-antibody complex. Therefore, Equation 3.2 is usually expressed in terms of the experimentally accessible parameter, υ, defined as the average number of bound antibody molecules per antigen molecule. In this case, the number of moles of bound antibody per unit volume is equal to [AgAb], and the total number of moles of the antigen molecule per unit volume is given by the sum ([Ag] + [AgAb]):

$$\upsilon = \frac{[AgAb]}{[Ag] + [AgAb]} \quad \text{.....(3.3)}$$

and since [AgAb] = K[Ag][Ab],

$$\upsilon = \frac{K[Ab]}{1 + K[Ab]} \quad \text{.....(3.4)}$$

Equation 3.4 gives a typical rectangular hyperbola that is functionally of the same form as the Michaelis-Menten equation of enzyme kinetics and as the Langmiur adsorption isotherm **[194,195]**. Several linear transforms of this equation have been described **[196]**, the most common form being the Scatchard equation , which is obtained by rearranging Equation 3.4 to give:

$$\frac{\upsilon}{[Ab]} = K - K\upsilon \qquad (3.5)$$

A Scatchard plot of $\upsilon/[Ab]$ versus υ will be linear if the above model pertains, and is particularly useful in determining the stoichiometry of binding when more than one antibody is bound per antigenic molecule.

The analysis given above describes the equilibrium reaction between monovalent antibody (Fab fragment) and monovalent antigen. The reaction between divalent antibody and monovalent antigen in solution is more complicated since the geometry of either partner can interfere with binding to the second combining site. Treatments including such effects have been given **[140]** but are difficult to apply and are not useful for the binding of polyclonal antibodies to proteins bearing diverse antigenic sites which is of interest here.

3.1(b) *Multiple Equilibria: General Relationships*

Multiple equilibria between an antibody and a macromolecular antigen with more than one binding site may be formulated in terms of a stoichiometric analysis or on the basis of individual binding sites on the macromolecule **[197]**. The equilibrium expressions for such a system can be written as:

$$Ag + Ab = AgAb_1 \; ; \qquad K_1 = \frac{[AgAb_1]}{[Ag][Ab]}$$

$$AgAb_1 + Ab = AgAb_2 \; ; \qquad K_2 = \frac{[AgAb_2]}{[AgAb_1][Ab]}$$

or in general:

$$AgAb_{i-1} + Ab = AgAb_i \; ; \qquad K_i = \frac{[AgAb_i]}{[AgAb_{i-1}][Ab]} \quad \ldots\ldots\ldots (3.6)$$

where K_1, K_2, and K_i are macroscopic association constants which may be related to the intrinsic association constant in special cases **[193,197]**. For instance, for monovalent Ab binding to bivalent Ag, the above macroscopic constants are related to K, the intrinsic (microscopic) constant defined in Equation 3.2, by $K_1 = 2K$ and $K_2 = 1/2K$.

The binding parameter, υ, the ratio of the total moles of antibody bound to the total moles of antigen, for multiple equilibria may be expressed as follows:

$$\upsilon = \frac{K_1[Ab] + 2K_1K_2[Ab]^2 + ..}{1 + K_1[Ab] + K_1K_2[Ab]^2 + ..} \quad \ldots\ldots\ldots\ldots\ldots (3.7)$$

The site approach focuses on the individual classes of binding sites on the macromolecular antigen. In the simplest case, where the individual classes of sites are assumed to have fixed (although different) affinities which do not change with the extent of occupancy by antibodies, the ratio of the moles of antibodies bound per mole of the total antigen is given as **[197]**:

$$\upsilon = \frac{K_I[Ab]}{1 + K_I[Ab]} + \frac{K_{II}[Ab]}{1 + K_{II}[Ab]} + .. \quad .....(3.8)$$

where K_I and K_{II} are the intrinsic association constants for the binding to each class of antibody binding site. If the antigen molecule is monovalent and the antibody is also monovalent, Equation 3.8 reduces to Equation 3.4 with $K_I = K$, the association constant for the binding of monovalent antibody to monovalent antigen.

3.1(c) *Interaction of Antibody and Particle-bound Antigen*

If the antibody and antigen are monovalent, then there is no difference between their interaction in solution and their interaction when one of the species is particle-bound. This situation is comparable to the binding of small ions or molecules to a protein with multiple, monovalent sites **[143,198,199]**. Because of symmetry one can treat the interaction between monovalent antibody and "*s*" antigenic sites of a particle-bound monovalent antigen in terms of the relation:

$$\upsilon = \frac{sK[Ab]}{1 + K[Ab]} \quad .....(3.9)$$

As expressed above, Equation 3.9 is simply an extension of Equation 3.4, for the interaction of monovalent antibody and monovalent antigen in solution, to cover "*s*" antigenic sites on a particle.

For multiple equilibria involving the interaction of antibodies with particle-bound antigens, the complexity of the equilibrium analysis increases, as does the possibility for diverse types of mechanism of interactions (see Figure 16). This includes the fact that multivalent antibodies can, after the initial binding via one of their binding sites, crosslink to antigenic sites (or antigen molecules) via their secondary binding sites. For IgG with a valency of two, the crosslinking is limited to an antibody-antigen complex consisting of two antigenic sites (or antigen molecules) and one antibody molecule. If the divalent IgG molecule binds to the antigen layer on one particle in a configuration that leaves one of its antigen binding sites free to bind to an antigen molecule on a second particle, then bridging and aggregation of the particles occur due to this specific interaction between antibody in solution and particle-bound antigen. This type of interaction is referred to as particle agglutination.

Because of the crosslinking phenomenon, the lateral antigen density on the particle will have a profound effect on the binding of multivalent antibodies to particle-bound antigens (Figure 16). For example, at high particle surface coverage of antigen and low antibody concentrations, the average number of bound antibody molecules per particles would be small, and the probability that the IgG molecule will bind with both of its binding sites occupied on the same particle surface will be high provided the antigenic sites are sufficiently close together to allow binding by the same IgG molecule.

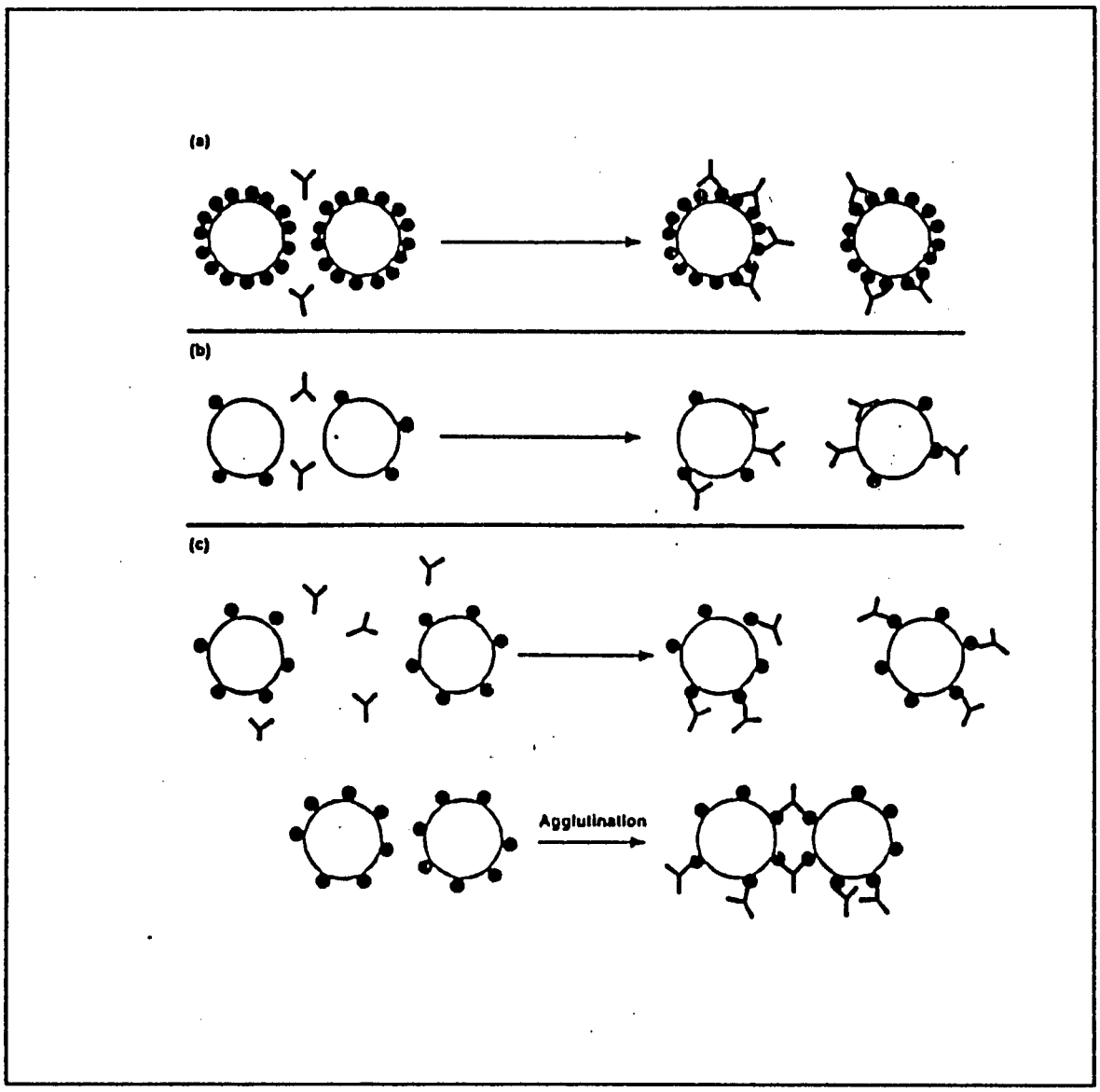

latex particle

antigen

antibody

Figure 16. The possible structures involved in the binding of divalent antibodies with particle-bound antigens. Binding can occur monovalently, divalently , on "naked" particle surface or between particles; depending on surface density of antigen, antibody and particle concentrations.

On the other hand, at high antibody molecule concentrations, the bound antibody will tend to favor configurations in which one binding site is free since there will be more competition for antigenic sites at higher antibody concentrations. Geometric factors and restriction of motion of both surface antigen and bound antibodies means that the effective concentrations of both the surface antigen and bound antibody differ from those in a bulk solution. This leads to further complication in the thermodynamic consideration of such systems. The straightforward relationships obtained in section 3.1(b) for monovalent antibody binding to bivalent antigen (both in solution) are the mathematical result of a known statistical relationship between K_1 and K_2, the macroscopic association constants (equilibrium constants) for such systems. Such a relationship between the sequential equilibrium constants for the binding of ligands to receptors that are otherwise fixed to a particle or cell surface is not predictable from first principles **[199]**, due to orientation factors and restriction of motion of both particle bound receptors and bound ligand (see Chapter One Section 1.4 (d)).

Under certain limiting conditions, simplifying assumptions can be made which allow for thermodynamic expressions to be derived for the interpretation of equilibrium data for such systems **[199]**. However, the present studies utilize a polyclonal IgG fraction which contains antibodies with a variety of association constants. There is no way to interpret the binding of such material in terms of true microscopic association constants.

3.2. Materials and Methods

3.2(a) *Preparation of Antigen-Coated Polystyrene Latexes*

Bovine Serum Albumin, Fraction V, Lot # 388 from Miles Labs., was used as antigen. The polystyrene latexes with different surface functional groups from Interfacial Dynamics Corporation (IDC), Portland, OR. described earlier were used as carrier particles. A large quantity of each latex (6ml of stock suspension) was washed with 0.05M phosphate buffer, pH 7.2 and equilibrated for six to eight hours with unlabeled BSA solutions at four different concentrations, after which the latex suspensions were washed repeatedly in 0.01M phosphate buffer, pH 7.2 and the final suspensions were dispersed in the same buffer solution and stored at $4^{o}C$ until required for agglutination experiments. Duplicate experiments were performed under the same conditions with radiolabeled BSA solution as described in Chapter One to determine the amount of BSA retained on the latex surface.

3.2(b) *Rabbit anti-BSA Immunoglobulin G Antibody:*

(i) Immunisation of Rabbits

Three New Zealand White rabbits were injected subcutaneously with 100μg of antigen (BSA) emulsified in 1.5ml Complete Freund's Adjuvant (1:3 water-in oil emulsion **[200]**). Subsequent boosts at intervals of 3-4 weeks were given in Incomplete Freund's Adjuvant (1:3 water-in-oil emulsion). A week after each boost, approximately 40 ml of blood was drawn from an ear vein of the rabbit. This was repeated to maintain a source of anti-BSA antibodies.

3.2(b) *(ii) Purification of Rabbit anti-BSA Immunoglobulins*

Serum from the rabbit blood was obtained by leaving the blood to clot at room temperature for about one hour, and then at $4^{0}C$ overnight. The serum was recovered by centrifugation (1000g for 10 min) and carefully decanted from the clot. Cold saturated $(NH_4)_2SO_4$ was then added dropwise, while stirring, to the serum to give approximately 40 percent saturation. At this saturation, most of the immunoglobulins were precipitated. The suspension was centrifuged at 10,000g for 10 minutes and the precipitate washed with a solution of cold, 1.75 M $(NH_4)_2SO_4$ until it was white. The final white precipitate was dissolved in 10mM sodium phosphate, pH 7.0 and dialysed overnight against water. The precipitated lipoprotein was removed by centrifugation at 10,000g for 10 minutes. The supernatant was dialysed overnight against 0.02M phosphate buffer, pH 8.0 then loaded onto a column of DEAE Affi-gel Blue (4.5ml per ml of rabbit serum) previously equilibrated with the same buffer. The immunoglobulin G (IgG) fraction was eluted with two bed volumes of 0.02M phosphate buffer, pH 8.0 and the fractions collected were dialysed against water and freeze-dried using a Maxi-Dry freeze dryer (Model FD-4.5-6.0) from FTS Systems, Inc., Stone Ridge, NY. The purity of the IgG fraction collected was checked by SDS-PAGE electrophoresis. This is reported in Appendix 3. The IgG was stored at $-70^{0}C$ and dissolved in a buffer of choice for immunochemical work.

Since the purified rabbit anti-BSA IgG immunoglobulin was used without affinity purification, specific anti-BSA antibodies in the purified fractions represent at most, 20-30% **[201]** of the total immunoglobulin in the binding and agglutination studies.

3.2(c) *Binding Experiments*

Iodinated antibody was prepared as previously described in Chapter Two, **[179]**. A fixed amount (0.5, 1.0, and 2.0ml) of 1% labeled antibody solution in 0.01 M phosphate buffer, pH 7.20 was incubated with increasing concentrations of BSA-coated latex particles. This was to determine an optimal range of concentrations of reactants, required for determining the maximum amount of labeled antibody able to bind to the BSA-coated latex particles. A suitable amount of BSA-coated latex suspension was mixed with the labeled antibody in a final volume of 2 ml. The reaction was performed in 4ml (Evergreen) polystyrene tubes to allow free mixing during equilibration, with gentle shaking, for approximately six hours at room temperature ($\cong 21^0$). The amount of IgG bound per unit area to BSA-coated latex and the estimate of probable error in the measurement were calculated as shown in Appendix 4.

3.3 Results and Discussion

3.3(a) *Polyclonal IgG Antibody Binding to BSA-coated PSL.*

Figure 17 shows the results of binding radioiodinated polyclonal rabbit anti-BSA IgG to sulfate latex bearing the surface concentrations of BSA indicated. In this experiment, the equilibrium IgG concentration was between 6 and 7.00×10^{-3} mg/ml for all latex concentrations indicated. The total antigen (BSA) concentration was increased by increasing the number of particles carrying each of the four BSA surface concentrations.

It can be seen that the total amount of antibody bound decreases rapidly with increasing particle concentration, i.e. there is a strong increase in antibody binding as the latex concentration and hence the surface area per unit volume is reduced. The effect is greatest for latex with the lowest surface concentration of BSA.

This latex concentration effect was demonstrated earlier for BSA adsorption to bare latex surfaces (see Figure 8, Chapter Two). In the case of BSA adsorption, the stronger adsorption at low surface area per unit volume was attributed to preferential adsorption of higher molecular weight BSA oligomers present in the sample.

For IgG binding to PSL bearing different concentrations of antigen (BSA), there are possibly two effects superimposed upon one another: the effect of the range of affinities present in the polyclonal antibody mixture and the surface area dependence of nonspecific adsorption of the antibody mixture to the remaining area of the latex surface unoccupied by antigen.

At low surface density of antigen, the nonspecific adsorption of antibody must dominate since there are many more molecules of IgG present per unit area than BSA; this probably accounts for the stronger increase in the amount of antibody bound. The stronger area dependence observed again implies a wide range of affinities for the bare latex is present in the IgG preparation. Presumably this is due to the inherent variation in structure within the IgG class due to its polyclonal origin, as there was no significant contamination in the IgG preparation by higher molecular weight material (see Appendix 3). On the other hand, at high surface concentration of antigen, nonspecific adsorption of antibody is probably much lower than the antigen-specific reaction since, as will be discussed, the apparent affinity constant is higher. The increase in

binding as the concentration of latex is reduced, at this BSA coverage, therefore, is likely to be due to the range of Ab affinities present in the polyclonal antibody mixture.

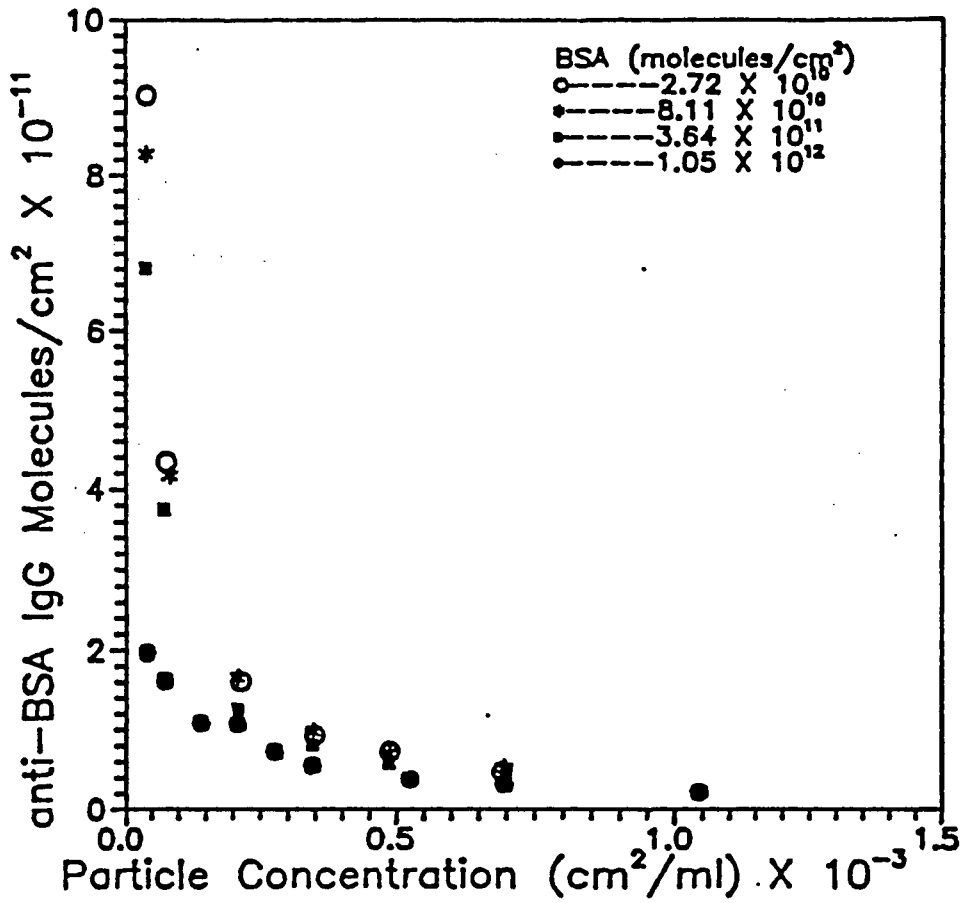

Figure 17. The binding of polyclonal anti-BSA IgG to BSA-coated sulfate PSL at room temperature from 0.01M phosphate buffer, pH 7.20. The PSL concentration was varied to produce the values of surface area per unit volume indicated.

Figure 18 shows the binding isotherms of the polyclonal rabbit anti-BSA IgG fraction to the sulfate latex pre-equilibrated with BSA to give the four different surface concentrations as in Figure 17. Similar data for the carboxyl, carboxyl modified and amidine (+) latexes are shown in Appendix 5.

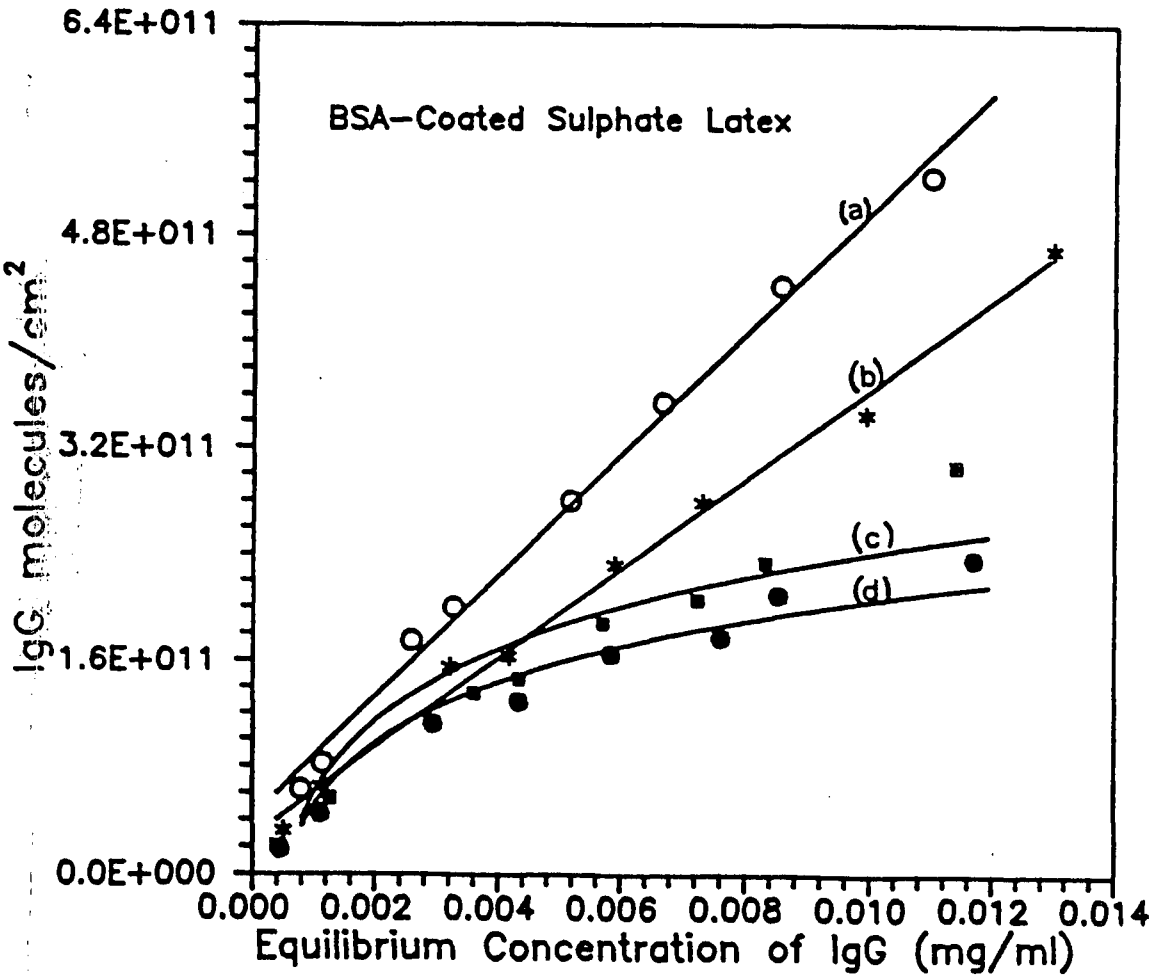

Figure 18. The binding of rabbit anti-BSA IgG to BSA-coated sulfate latexes from 0.01M phosphate buffer, pH 7.20. BSA surface concentrations: (a) 2.72×10^{10}, (b) 8.11×10^{10}, (c) 3.64×10^{11}, (d) 1.05×10^{12} molecules cm^{-2}; PSL surface area = 134 cm^2 ml^{-1}.

In all cases except for the CML, the adsorption and/or binding of antibody at relatively high equilibrium concentrations of antibody increases as the particle surface density of antigen decreases but the total surface area of the latex is held constant. That is, the total amount of IgG bound is greater the smaller the fraction of the PSL surface occupied by BSA and the larger the bare surface area of latex available. Therefore, more non-specific adsorption of antibody to bare PSL occurs than specific binding to antigen (at low BSA coverage; see later discussion).

For the CML, the amount of IgG bound generally increases with the surface density of antigen. It appears that for this latex, adsorption of IgG to the bare surface of the latex is weaker and one observes the effect of specific binding of IgG to the surface-bound antigen at all BSA coverages. This is in all likelihood due to the low hydrophobicity of the CML. It is also consistent with the nature of adsorption of IgG molecules which is believed to occur mainly with the more hydrophobic Fc tail in contact with the latex surface **[202]**.

3.3(b) *Comparison of Amount of Polyclonal IgG Antibody Bound to BSA-coated PSL with Surface Density of BSA.*

In order to compare the amount of polyclonal antibody bound to BSA-coated PSL with the surface density of BSA, the binding isotherms for the sulfate latex shown in Figure 18 were transformed and plotted as Scatchard plots, according to Equation 3.5. Figure 19 shows the Scatchard plots for the sulfate latex in which the ratio of the number of moles of IgG bound per gram of sulfate latex to the molar IgG concentration is plotted against the number of moles of IgG bound per

gram of latex. Similar data for antibody binding to the carboxyl, carboxyl modified, and amidine (+) latexes are shown in Appendix 6.

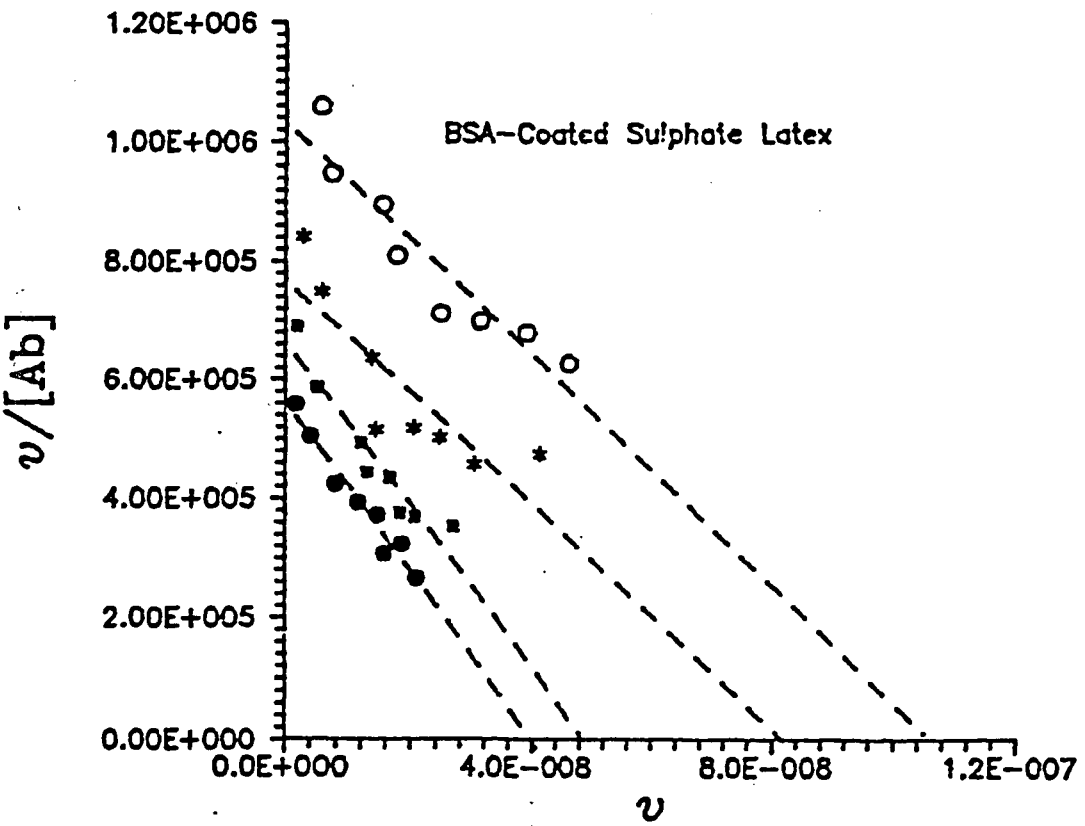

Figure 19. Scatchard graphs of the data for binding of anti-BSA IgG by BSA-coated sulfate latex (data and symbols from Figure 18). υ is moles of IgG bound per gram of latex and [Ab] is moles of IgG/litre of solution.

The intercept on the abscissa indicates the amount of IgG bound at saturation, i.e. the total number of binding sites. The extrapolation to estimate the binding site values assumes that the data obeys simple Langmuir-type behavior over the whole concentration range (described by equations 3.4 and 3.9). All the Scatchard plots indicate that the total amount of IgG bound obey the Langmuir type equations reasonably well over the concentration range studied. At higher concentrations non-linearities might well appear, representing lower affinity constant binding, but this range was not examined.

The value of the intercepts on the abscissa decreases as the surface density of BSA increases, i.e. the total number of sites to which IgG binds decreases with increasing BSA coverage on the PSL surface. Thus, even at saturation values, more binding of polyclonal IgG is predicted to occur to bare PSL than to the BSA-coated latex surface, except for the CML.

The slopes of the Scatchard plots give the apparent binding affinity of the antibodies: more negative slopes mean greater binding affinity. As can be seen from Figure 19 and Appendix 6, except for the CML the slopes increase as the surface concentration of BSA increases. This indicates that high affinity antibody binding increases as the bare latex surface is reduced and BSA coverage on the PSL increased. However, the experimental data on which this conclusion is based was taken over a limited concentration range.

Table XI gives the number of IgG molecules bound at saturation to the various latexes at different BSA surface concentrations, as determined by extrapolation from the Scatchard plots. This data is further illustrated in Figure 20 where the amount of IgG bound at saturation is plotted against the BSA surface coverage.

Table XI

Comparison of amount of anti-BSA IgG bound to latex with different amount of surface bound BSA.

BSA-Coated latex		Amount of BSA Bound (molecules/cm^2)	Amount of anti-BSA IgG Bound (molecules/cm^2)
Sulfate			
(134 cm^2/ml)	(a)	$2.72 \pm 0.15 \times 10^{10}$	$1.20 \pm 0.06 \times 10^{12}$
	(b)	$8.11 \pm 0.23 \times 10^{10}$	$9.32 \pm 0.83 \times 10^{11}$
	(c)	$3.64 \pm 0.17 \times 10^{11}$	$5.57 \pm 0.32 \times 10^{11}$
	(d)	$1.05 \pm 0.14 \times 10^{12}$	$4.55 \pm 0.23 \times 10^{11}$
Carboxyl			
(121 cm^2/ml)	(a)	$2.15 \pm 0.11 \times 10^{10}$	$2.42 \pm 0.09 \times 10^{12}$
	(b)	$7.29 \pm 0.20 \times 10^{10}$	$2.11 \pm 0.05 \times 10^{12}$
	(c)	$3.56 \pm 0.23 \times 10^{11}$	$1.48 \pm 0.06 \times 10^{12}$
	(d)	$9.95 \pm 0.18 \times 10^{11}$	$1.31 \pm 0.04 \times 10^{12}$
CML			
(106 cm^2/ml)	(a)	$3.16 \pm 0.17 \times 10^{9}$	$4.21 \pm 0.14 \times 10^{11}$
	(b)	$4.53 \pm 0.29 \times 10^{9}$	$4.95 \pm 0.18 \times 10^{11}$
	(c)	$2.75 \pm 0.16 \times 10^{10}$	$6.32 \pm 0.24 \times 10^{11}$
	(d)	$2.35 \pm 0.17 \times 10^{11}$	$5.68 \pm 0.15 \times 10^{11}$
Amidine (+)			
(160 cm^2/ml)	(a)	$2.08 \pm 0.10 \times 10^{10}$	$4.61 \pm 0.10 \times 10^{12}$
	(b)	$6.56 \pm 0.15 \times 10^{10}$	$4.25 \pm 0.07 \times 10^{12}$
	(c)	$4.48 \pm 0.18 \times 10^{11}$	$2.95 \pm 0.09 \times 10^{12}$
	(d)	$1.24 \pm 0.09 \times 10^{12}$	$2.59 \pm 0.11 \times 10^{12}$

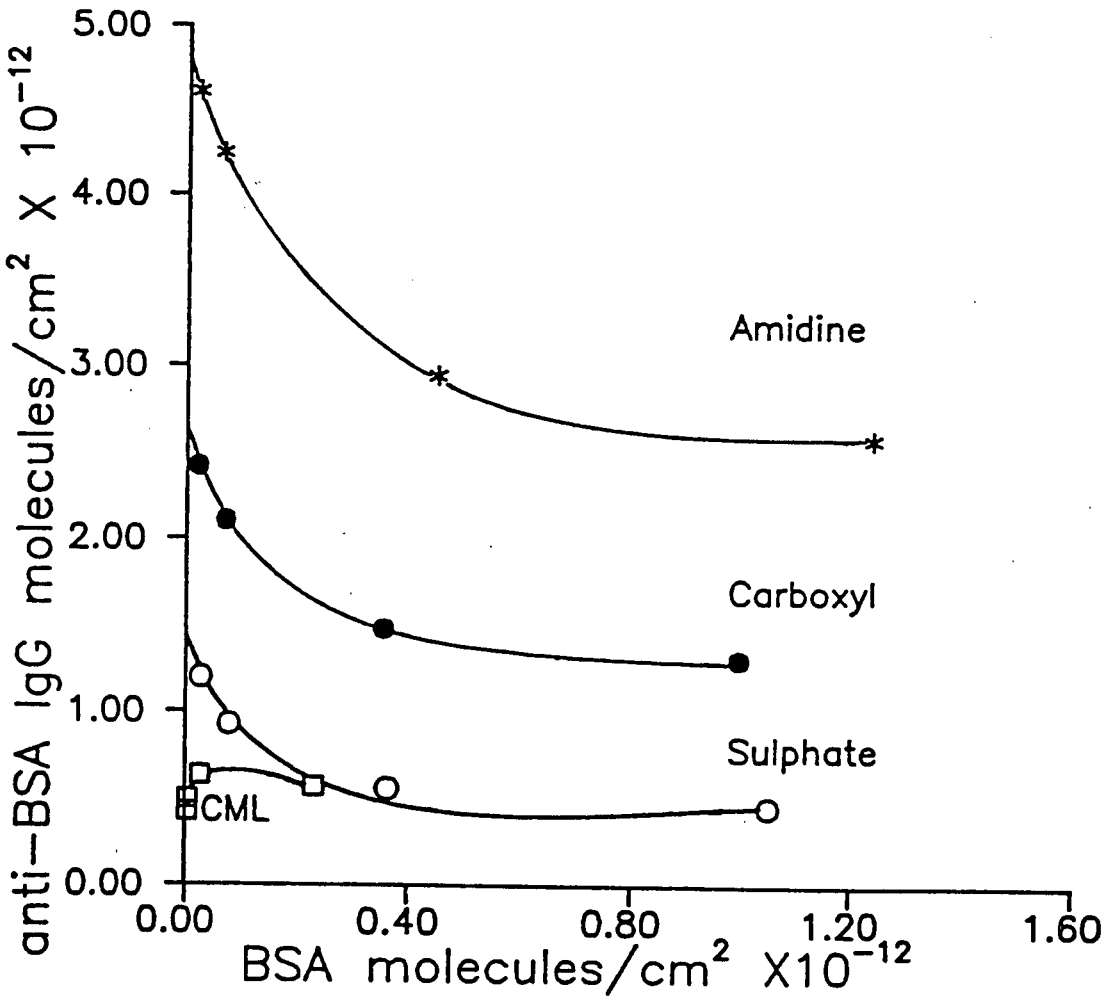

Figure 20. A comparison of relative amounts of rabbit anti-BSA IgG fraction bound to latexes with different amounts of surface bound antigen (BSA) at IgG saturation.

In general, the trend in binding of polyclonal IgG antibody to the various latexes, under the conditions studied, is similar to that of BSA adsorption to the bare surface of the latexes. That is, the amidine (+) latex binds the greatest amount of IgG (at all levels of surface antigen concentrations) followed by carboxyl, sulfate, and carboxyl modified latex. This trend presumably indicates the relative strength in nonspecific adsorption of the IgG molecules to the various surfaces.

As the BSA surface coverage increases, IgG binding to amidine, carboxyl and sulfate latexes generally decreases, consistent with a reduction in the area available for nonspecific binding and in the increasing effect of specific binding to antigen by antibody. The difference in the amount of IgG bound between the latexes at high BSA coverage presumably represents the difference in strength of binding of IgG to the remaining exposed surface of the latexes. The BSA-coated carboxyl modified latex shows a slight increase in the amount of IgG bound with increasing BSA surface density, indicating that nonspecific adsorption of antibody to CML is much lower in this case.

3.3(c) *Binding of Nonspecific IgG Antibody to Bare and BSA-coated PSL*

In order to estimate the extent of adsorption of IgG to the latex surface unoccupied by the antigen, adsorption isotherms for nonspecific IgG (i.e IgG not specific for BSA) were determined for the sulfate PSL at the same surface concentrations of BSA as in Figure 18. The binding isotherms are given in Figure 21 and the corresponding Scatchard plots in Figure 22. It can be seen that there are considerable differences in the amount of nonspecific IgG bound to the latex with different BSA surface coverage. Non-specific binding to bare or "naked" latex is much greater

than non-specific binding to an antigen-covered surface.

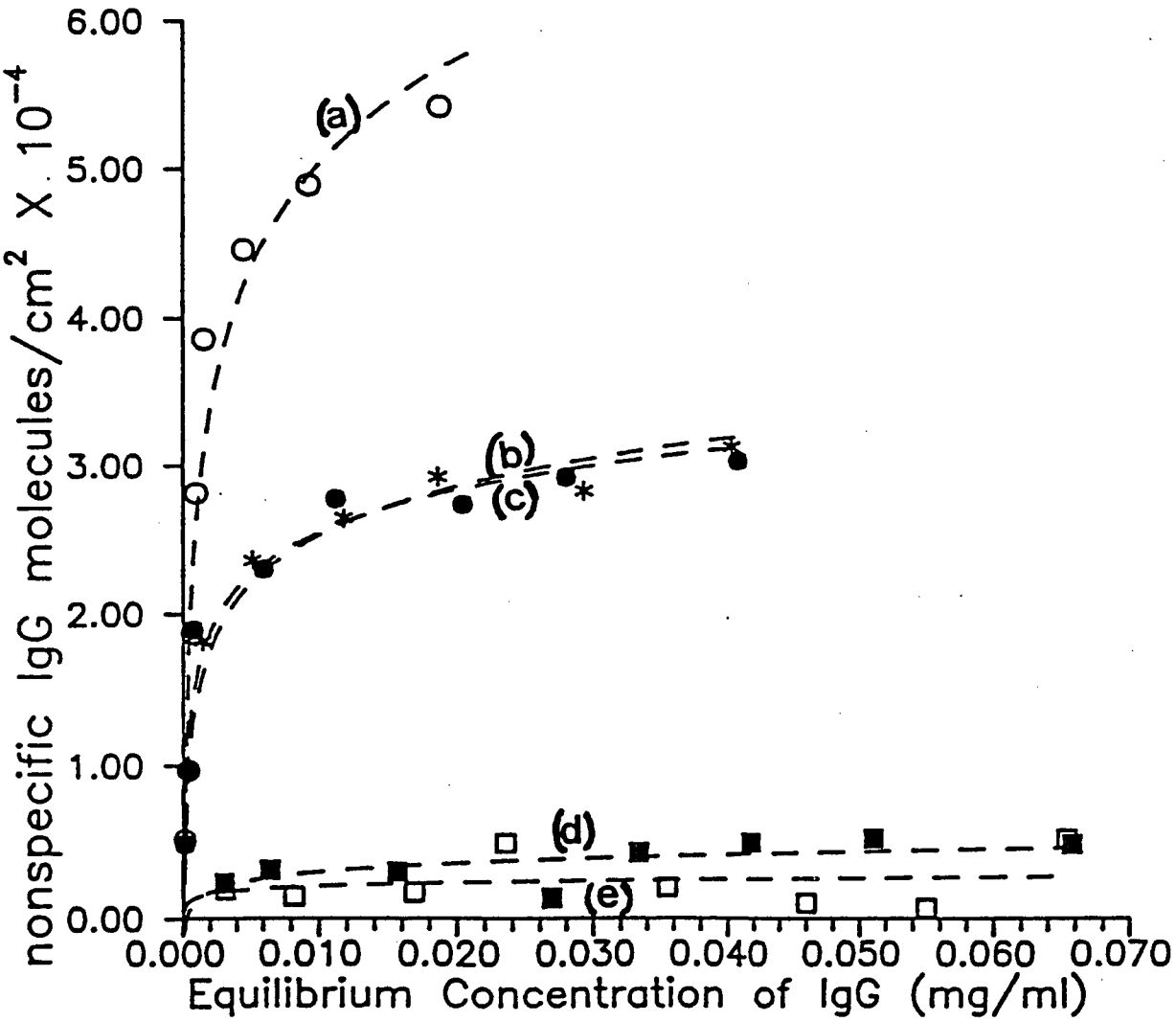

Figure 21. The binding of nonspecific IgG to BSA-coated sulfate latexes from 0.01M phosphate buffer, pH 7.20. BSA surface concentrations: (a) "naked " latex , (b) 2.72×10^{10}, (c) 8.11×10^{10}, (d) 3.64×10^{11}, (e) 1.05×10^{12} molecules cm^{-2}; PSL surface area = 134 cm^2 ml^{-1}.

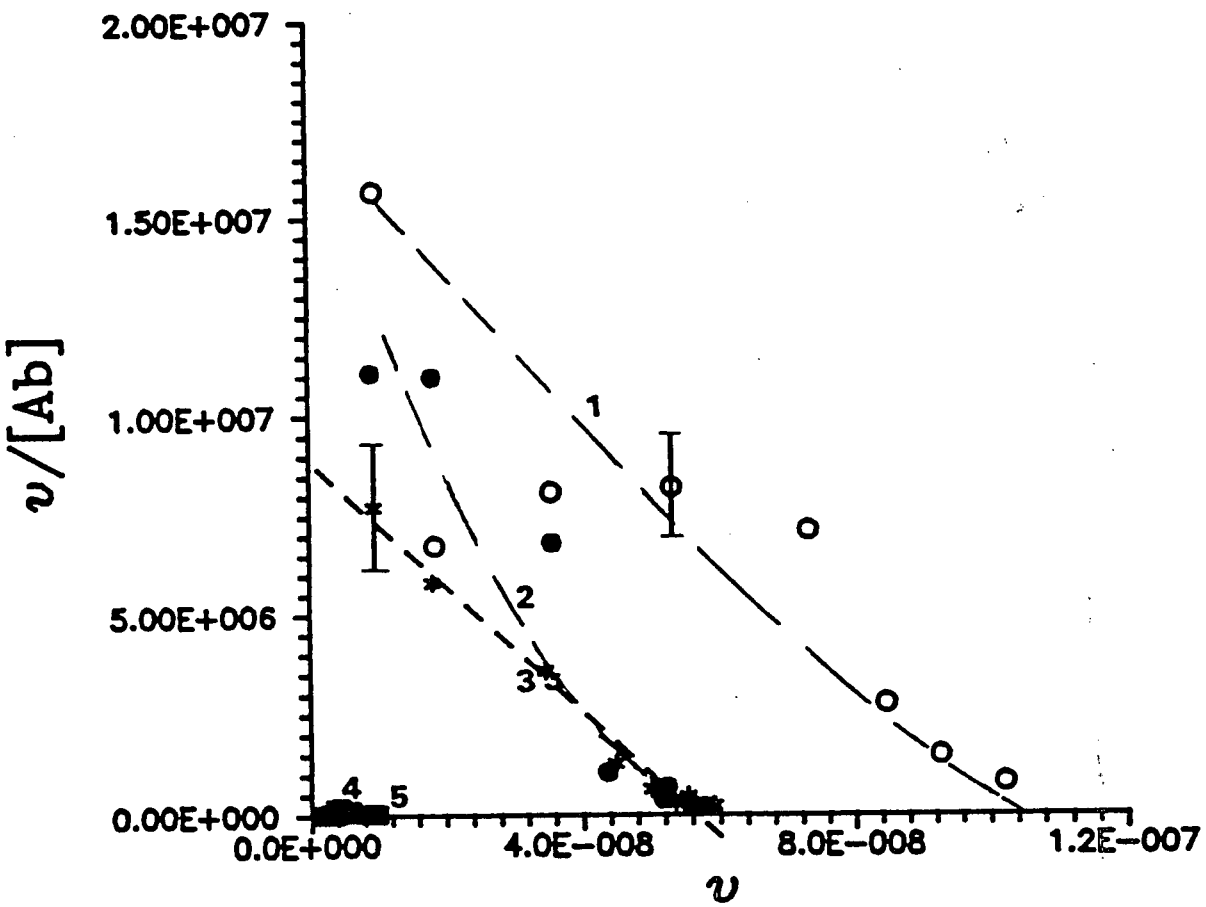

Figure 22. Scatchard plots of data from Figure 21. υ = moles nonspecific IgG bound per gram of sulfate latex; [Ab] = molar IgG concentration.

At high surface antigen concentrations, non-specific binding is extremely low, but nevertheless a finite amount is bound. This suggests that under the conditions of this experiment, saturation of the latex surface by antigen (BSA), even for the highest surface concentration of antigen, was not achieved, consistent with the results shown in Figure 20.

The estimated amount of non-specific IgG together with the amount of anti-BSA bound at saturation to the sulfate PSL with various surface concentrations of BSA is illustrated in Figure 23. It can be seen the nonspecific binding of IgG to the latex surface is strongly reduced by pre-adsorbed BSA whether or not specific antibody to BSA is present in the polyclonal mixture. The data in Figure 23 are saturation values of IgG binding at each equilibrium point. When there is no BSA on the surface of the latex, the IgG adsorbed at saturation to the bare latex surface, Γ^0_{ns}, is estimated to be approximately 1.27×10^{12} IgG molecules/cm^2 whether or not specific antibody is present in the polyclonal mixture. As the coverage of antigen (BSA) on the latex surface increases, both the surface concentration of non-specific IgG, Γ_{ns}, and specific anti-BSA IgG, Γ_{sp}, decrease linearly, i.e. pre-adsorption of BSA replaces the non-specifically adsorbed IgG from the latex surface. However, the rate of decrease of non-specifically adsorbed IgG (represented by the initial slopes of the two curves in Figure 23) is dependent on whether or not the IgG fraction contains antibodies specific for BSA. When there is no specific antibody to BSA present in the polyclonal mixture, approximately 8 molecules of nonspecifically adsorbed IgG are displaced by one molecule of BSA. A model for the stoichiometry of specific and nonspecific binding of polyclonal anti-BSA to latex coated with various surface concentrations

of antigen is given in Appendix 7.

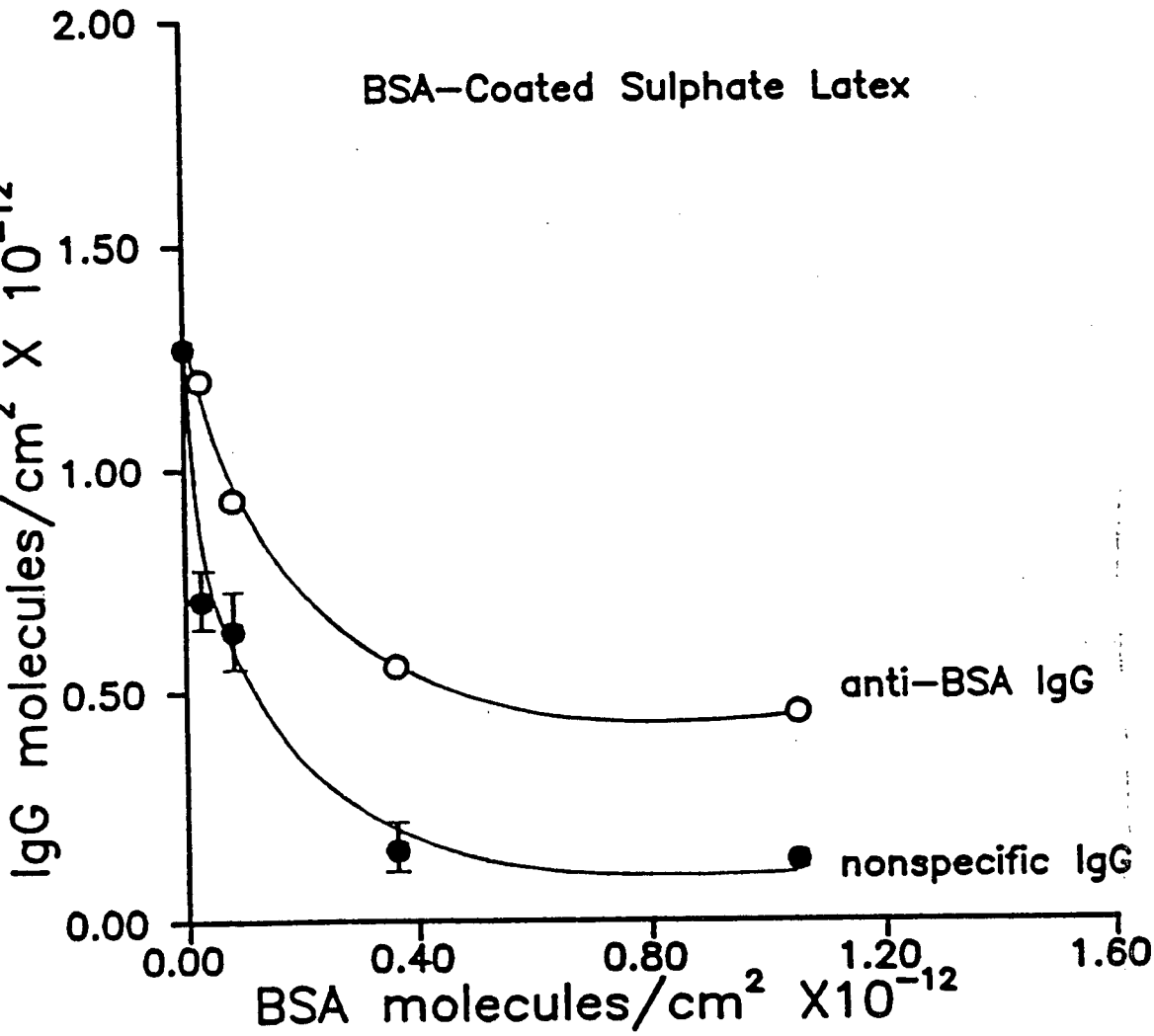

Figure 23. A comparison of relative amounts of specific antibodies (anti-BSA IgG) and nonspecific IgG bound at saturation to sulfate latexes with different amounts of surface bound antigen (BSA).

On the other hand, if the IgG fraction contains antibodies specific for BSA as well, then pre-adsorption of BSA will both displace nonspecifically adsorbed IgG and bind anti-BSA IgG molecules specifically to epitopes on the antigen. The net effect is that approximately 5 molecules of nonspecifically adsorbed IgG are "effectively" displaced by one molecule of BSA.

At higher BSA coverage reduction in nonspecific IgG adsorption saturates above some surface BSA concentration, Γ^{*}_{BSA}, due to overlap of the regions from which BSA excludes IgG molecules. For $\Gamma_{BSA} > \Gamma^{*}_{BSA}$, the surface concentration of IgG containing no Ab against BSA, Γ_{ns}, remains constant as more BSA molecules occupy the surface within the regions from which IgG is excluded (see Appendix 7). Since the BSA packing on the surface of the latex is not regular, nonspecific adsorption of IgG does not go to zero even at very high surface antigen concentration. Thus, there is a small amount of nonspecific adsorption remaining at high Γ_{BSA}, $\Gamma_{ns,s}$. When specific Ab binding is present as well as replacement of Ab, a similar analysis can be applied. At high Γ_{BSA}, IgG binding again saturates, in this case at a higher value, $\Gamma_{sp,s}$, associated with the specific binding of Ab added to the remnant nonspecifically adsorbed IgG molecules.

The Scatchard plots presented in Figures 19 and 22, and Appendix 6 show deviations from the expected linearity (Equation 3.5). These deviations may be due to antibody heterogeneity (polyclonal antibody population with many binding constants), or complex formation (i.e. due to multivalency of the antigen) **[203]**. Since only a limited range of antigen concentration was covered experimentally, the intercepts determined were points with very low accuracy.

3.4 Summary: Antibody Binding to Antigen-coated PSL

(1) Polyclonal antibody binding to antigen-coated PSL is complicated due to the presence of a mixture of antibody species with differing affinities for bound antigen.

(2) The surface concentration of bound antibody depends on the surface concentration of antigen on the latex particles and on the availability of PSL surface area not occupied by antigen to non-specifically adsorb antibody.

(3) In most cases, the adsorption of IgG increases as the surface concentration of antigen is decreased. That is, the total amount of IgG bound is greater the smaller the fraction of PSL surface occupied by antigen and the larger the bare surface area, implying that non-specific binding of antibody to bare PSL surface is more significant than specific binding to antigen at low surface concentration of antigen. As the surface concentration of antigen increases, IgG binding decreases, consistent with the reduction in the area available for non-specific binding and the increasing effect of specific binding of antibody to antigen. While the apparent affinity constant for IgG binding to BSA is higher than for binding to the latex surface, the number of antigenic sites available per unit area is evidently much lower on adsorbed BSA than is the density achievable by nonspecific binding, by a factor of about three. The model in Appendix 7 suggests that approximately 7 molecules of IgG are displaced by one molecules of BSA and that about 3 molecules of anti-BSA IgG bind specifically per molecule of BSA.

(4) If non-specific adsorption to non-antigen occupied surface is weak (e.g CML), then specific binding to antigen becomes a significant fraction of the total and the amount of IgG bound tends to increase with increasing surface coverage of antigen.

(5) The extensive binding of polyclonal IgG to latex surface unoccupied by antigen at low surface concentrations of BSA, results in latex concentration effects as demonstrated for BSA adsorption to bare latex surface in Chapter Two. Such effects decrease as antigen coverage is increased. Latex concentration effects on protein adsorption, therefore, appear to be quite general.

CHAPTER FOUR

ANTIBODY-INDUCED AGGREGATION OF PSL

4.1. Introduction

In practice, a wide variety of techniques is used to assess the degree of aggregation of dispersed particles including light scattering, particle-number counting, sedimentation rate or volume and rheology [204]. However, the two most commonly used methods are direct particle-number counting and light scattering because they yield absolute rate constants which provide the best fundamental basis for comparing the effects of different additives, and additive concentrations.

Particle counting allows the individual concentration of each particular aggregate size to be determined as a function of time. Electrical or optical particle counting instruments such as the Coulter Counter can be used for particle-number counting, provided that the aggregate size is within the resolution limit of the instrument. Particle counting instruments usually require very large dilution of the sample in order to avoid coincidence effects, and also the presence of electrolytes to increase the electrical conductivity. Both these factors are a source of major problems with this method because they affect the state of dispersions in themselves. Another factor is the possible disruption of aggregates on passing through the counter orifice.

Optical methods have the advantage that they do not disturb the system being studied. In general, two types of light-scattering techniques may be used: angular light scattering in which the intensity of the scattered light is measured as a function of the scattering angle, and turbidity τ or optical-density determination, where the intensity of

the transmitted beam is measured. The procedure most widely used is simply to measure the turbidity of an aggregating system at some chosen time interval. One of the problems with turbidity measurements is the difficulty of interpreting unambiguously the change in turbidity in terms of aggregate size distribution, except under very special conditions. Also, partial sedimentation of aggregates out of the light beam may occur. For many situations however, determination of a detailed aggregate size distribution is not necessary. A simple index, related to the state of aggregation of the particles can be used as an empirical indication of aggregation. More quantitative information can be obtained by monitoring turbidity over the initial stages of aggregation at an appropriate wavelength where only scattering occurs [205, 206].

4.2 Materials and Method

Polystyrene latexes, with different surface functional groups from Interfacial Dynamics Corporation, Portland, OR., described earlier were used in the kinetic studies of antibody-induced aggregation. The antigen-coated polystyrene latex samples and the polyclonal antibody preparations used in the study of antibody binding to BSA-coated PSL reported in Chapter Three were used in the kinetic studies at concentration ratios that match the ratios of antigen-coated PSL and antibody concentrations used in the equilibrium studies reported in Chapter Three.

4.2 (a) *Constant Shear rate Aggregometer*

A constant shear rate aggregometer consisting of two transparent cylinders, made of poly(methyl methacrylate), with a gap of 0.149 cm, and an inner rotating 4.128 cm diameter cylinder was constructed. The inner bob is connected to a constant speed motor as shown in Figure 24. Different shear rates were obtained by changing the constant speed motor. The shear rate G was determined by the rate of the rotation of the inner bob and the radial diameters of the cylinders. The rate of shear is given by the relationship for couette flow as **[207]**:

$$G = \left(- \frac{dv}{dr} \right) = \frac{(-2\Omega/r^2)(R_c^2 \times R_b^2)}{(R_c^2 - R_b^2)} \quad \text{.....(4.15)}$$

where;

R_b = radius of bob (inner cylinder)

R_c = radius of cup (outer cylinder)

Ω = angular velocity = $2\pi\omega$, ω is rev per sec

The average shear rates calculated from Equation 4.15 are given in Table XII below, as a function of rotation speed.

The device was designed in such a way that it fit into the light path of an HP 8450 UV/VIS spectrophotometer.

At the start of an experiment, a sample of latex dispersion and distilled water was weighed to a total weight of approximately 4 grams and introduced into the annular gap (8 ml) of the apparatus. The salt or IgG solution was then weighed to approximately 4 g and introduced into the apparatus through a long syringe needle. The mixing ratio of the latex dispersion with the salt or IgG solution was therefore 1:1 by weight.

Table XII

Mean rate of shear in the gap of the coaxial cylinder aggregometer calculated according to Equation 4.15.

Motor Speed	*dv/dr* (at bob)	*dv/dr* (at cup)	*dv/dr* (mean)
10 (rpm)	15 $sec.^{-1}$	13 $sec.^{-1}$	14 $sec.^{-1}$
20 (rpm)	30 $sec.^{-1}$	26 $sec.^{-1}$	28 $sec.^{-1}$
60 (rpm)	87 $sec.^{-1}$	75 $sec.^{-1}$	81 $sec.^{-1}$

After mixing the latex dispersion and the salt solution (or the IgG solution) by plunging the inner bob about three times, the motor was started and the optical absorbance of the dispersion measured. The optical absorbance of the latex sample depends on the latex concentration, particle and/or aggregate size **[208]**, and so an output of absorbance versus time provides a continuous measure of the degree of coagulation or aggregation.

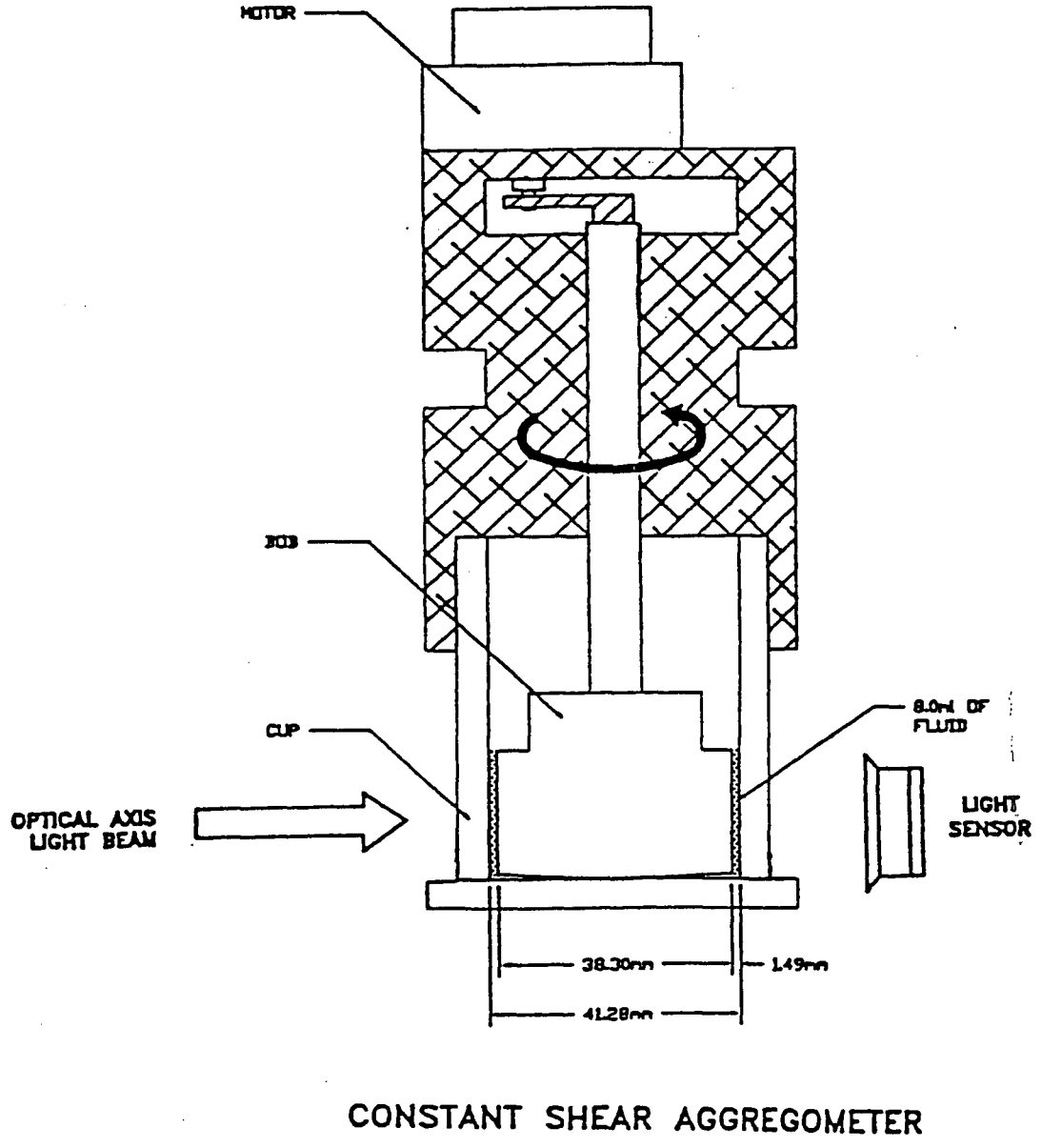

Figure 24. A schematic diagram of the constant shear aggregometer which provides a continuous output of the optical absorbance of a suspension subjected to a steady shear as a function of time.

4.2 (b) *Determination of Rate Constants for Coagulation and Agglutination Kinetics*

In order to relate the absorbance change of coagulating or flocculating latex particles to the kinetics, Oster **[209]** has derived the following expression for the turbidity, τ, of an aggregating system, in which particles are considered to be Rayleigh scatterers, as a function of time, t

$$\tau = \tau_0(1 + 2\rho_0 k_{eff} t) \quad \ldots\ldots\ldots\ldots\ldots\ldots\ldots\ldots (4.17)$$

where τ_0 is the initial turbidity (t = 0) of the stable dispersion and ρ_0 is the initial particle number density ($\rho_0 = \phi/V$, where V is the volume of a singlet particle), and k_{eff} is the effective rate constant.

Turbidity and absorbance (O.D.) are simply related through the expression

$$A = \tau l/2.303 \quad \ldots\ldots\ldots\ldots\ldots\ldots\ldots\ldots\ldots\ldots (4.18)$$

where l is the optical path length through the aggregometer, (l = 0.298cm). Combining Equations (4.17) and (4.18) leads to:

$$d(A/A_0)/dt = 2\rho_0 k_{eff} = k_{eff} \times \text{constant} \quad \ldots\ldots\ldots (4.19)$$

Thus experimental determination of $d(A/A_0)/dt$ enables k_{eff}, the effective rate constant to be obtained. Both the theory of light scattering and the theory of coagulation are best satisfied by making measurements at the early stages of coagulation. Therefore, $(dA/dt)_{t\to 0}$ values were used in determining the experimental rate constants in our studies of coagulation and agglutination kinetics. For cases where there is an initial increase in absorbance followed by a decrease (*cf.* Appendix 11), the (dA/dt) values were determined from the maximum values of the absorbance and used as the initial rate of change in absorbance with time.

4.3 Results and Discussion

4.3 (a) *Absorbance Measurements of PSL*

Measured optical absorption spectra for aqueous suspensions of the four polystyrene latexes used in our studies are shown in Figure 25.

These curves were obtained by measuring the absorbance of latex suspensions in a 1 cm quartz cuvette using an HP 8450 diode array spectrophotometer, a general purpose microprocessor-controlled parallel-detection instrument providing measurements over its full 200nm to 800nm wavelength range with a reproducibility of 0.4% for a one second measurement and a 0.15% for a 10 second measurement over an absorbance range of 0.1 to 1.0.

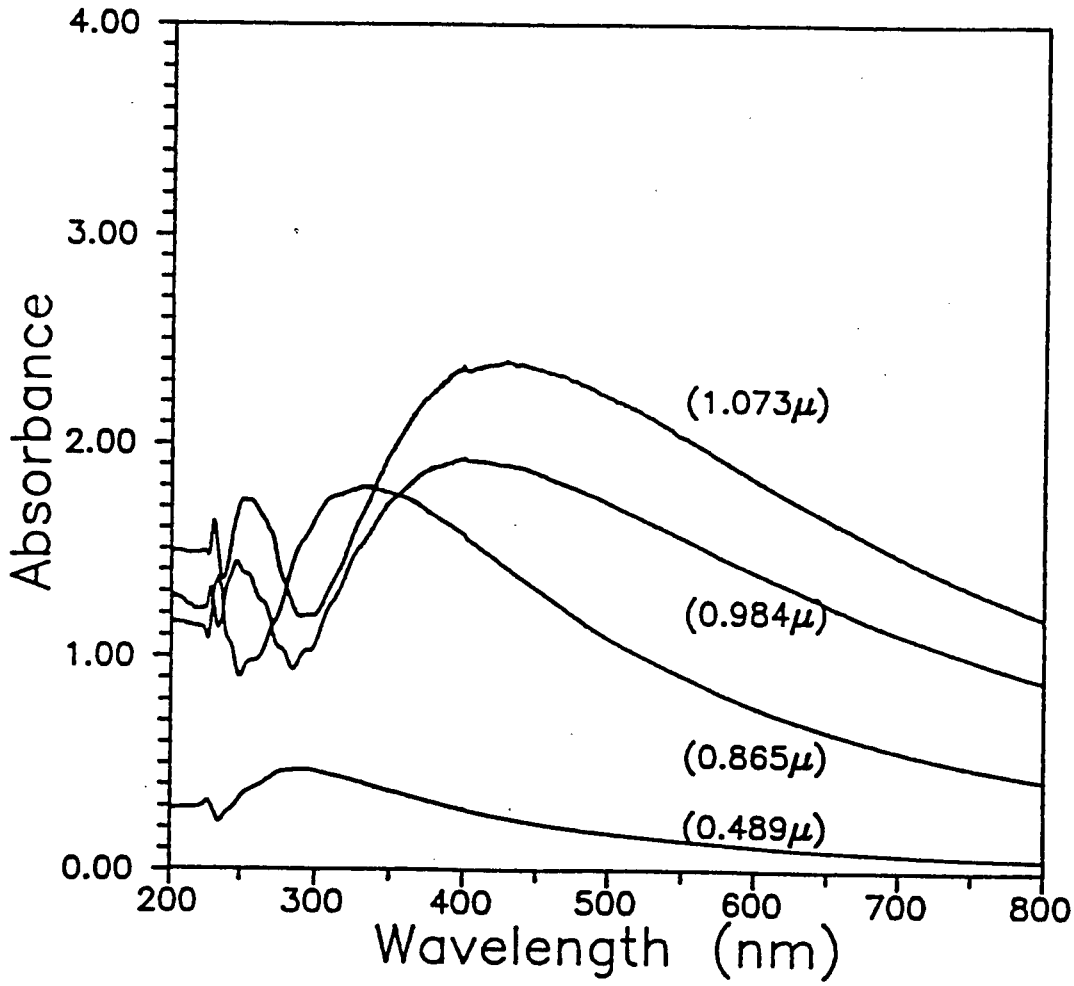

Figure 25. Measured absorbance for aqueous suspensions of sulfate (1.073μm) carboxyl (0.984μm), carboxyl modified (0.865μm), and amidine (0.489μm) latexes.

In practice, the incident light may be absorbed, as well as scattered, by the latex particles. Thus, the measured absorbance, shown in Figure 25 and Appendix 7, is the combined effect of absorption and scattering in all directions by the particle. It is strictly a measure of light lost from the incident beam due to its interaction with the particles in the cuvette. It depends on the chemical composition of the particles, their size, shape, orientation, the surrounding medium, the number of particles, and frequency of the incident beam. The relationship between absorption and particle size as a function of wavelength is very complex **[210]**.

The major features found in the measured optical absorbance curves of the polystyrene latexes are the rising absorbance toward shorter wavelengths, which is a general characteristic of nonabsorbing particles small compared with the wavelength, and interference peaks, the first of which shifts to longer wavelengths with increasing size of the particles **[211]**. The interference peaks arise from interference between the undeviated incident light and forward-scattered light. The optical spectra of all the latexes shown appears to be dominated by scattering since all the particles diameters are about the same or longer than the wavelength. The absorption maximum (major peak) occurs at a specific wavelength, depending on the size of the latex particle (Table XIII).

The biggest change in signal (absorbance) will occur at these major peaks (wavelengths) corresponding to each latex. However, the choice of wavelength for experimental measurement in the sheared system is limited by the fact that the measuring "cell" is made of poly(methyl methacrylate) which absorbs strongly below 400 nm. Thus, all absorbance measurements were made at 450 nm, irrespective of latex size.

Table XIII

Absorption maxima from optical spectra of aqueous suspensions of the four PSL used.

Latex Type	Size (μm)	Absorption maximum (λ-nm)
Sulfate	1.073	428
Carboxyl	0.984	400
CML	0.865	336
Amidine	0.489	290

For a given latex suspension, the absorbance depends on the concentration and light scattering properties of the suspended particles. If the suspension contains only identical particles, then the absorbance is given by:

$$A = \log (1/T) = K'Cl \quad \text{.....(4.16)}$$

where T = transmittance, K' = light extinction cross-section, C is the number of particles per unit volume, and l is the optical path length. Equation 4.16 is known as the Beer-Lambert law **[212]**.

Figure 26 (a) and (b) show the absorption spectra of the sulfate (1.073 μm) at different volume fractions and the corresponding plot of absorbance versus volume fraction at the wavelengths indicated. It can be seen that the absorbance of the sulfate latex suspension obeys the Beer-Lambert law up to a latex volume fraction of approximately 1.05×10^{-3}.

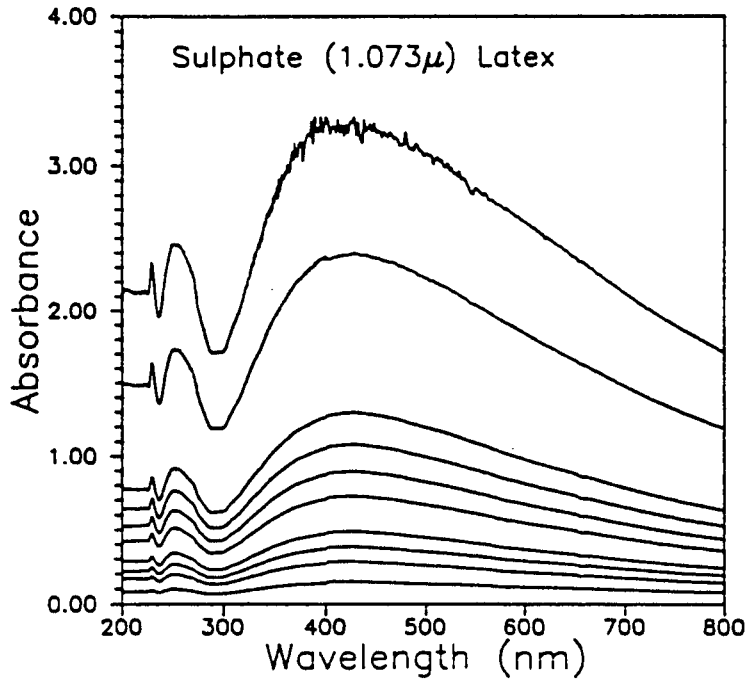

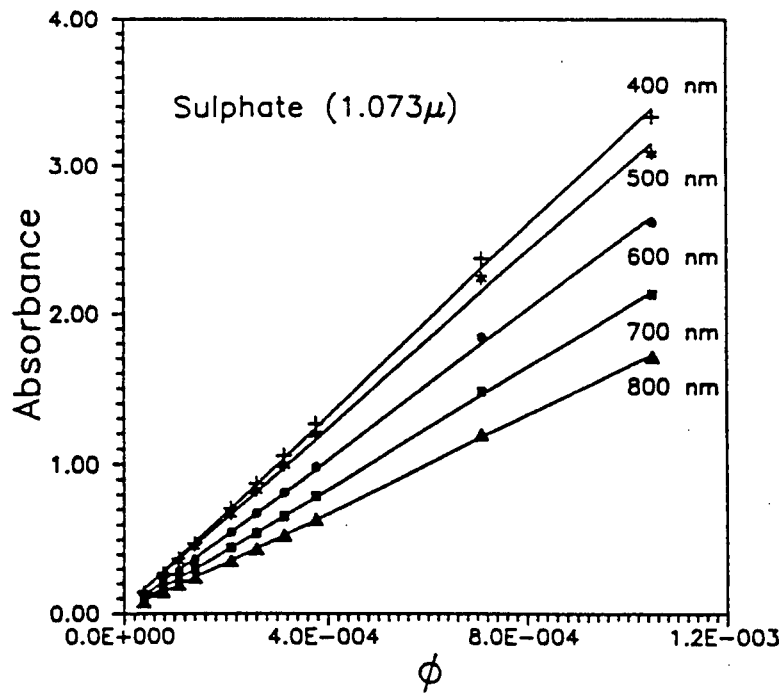

Figure 26. The absorption spectra of sulfate latex at different volume fractions **(a)**, and the corresponding Beer-Lambert's plot of absorbance versus volume fraction at various wavelengths **(b)**.

At higher particle concentrations, the linear dependence of absorbance on particle concentration is no longer observed because of the multiple scattering effect. The results for the other latexes used in our studies are given in Appendix 8; they all show a similar behaviour to that of the sulfate latex.

Changes in the nature of the latex particle suspension, such as aggregation, alter the apparent absorption spectrum of the latex considerably. The effect of particle aggregation on absorbance cannot be predicted easily from light scattering theory **[210]**. For particles smaller than the light wavelength, the absorbance increases with particle size, and the increase in absorbance of an aggregating suspension can be used as a measure of coagulation or flocculation rate **[213]**. However, for particles of size comparable to the wavelength or greater, specific absorbance usually decreases with increasing particle size (hence with aggregation). For such systems, it is usually not possible to obtain quantitative information on the aggregate formation from absorbance measurements. However, when there is significant change (decrease) in absorbance as particles aggregate, it can be used as an empirical indication of aggregation rate. This can be seen in Appendix 8 (a), where the absorbance spectra of coagulating latexes, in a 1 cm × 1 cm cross-section quartz cuvette, at various times after initiation of aggregation are given together with a plot of the absorbance of coagulating latexes as a function of time at different wavelengths (Appendix 8 (b)). For a given particle the degree of linearity of absorbance with time varies for different wavelengths. The change in absorbance as particles aggregate also varies with wavelength for a given particle.

4.3 (b) *Stability of BSA-coated PS latexes under shear*

Figure 27 shows the stability of unsheared PS latex suspensions in the absence of added protein at various concentrations of sodium chloride. The results were obtained by a centrifugal/optical absorbance method in which equal volumes (1.0 ml) of latex dispersion (mass fraction = 0.1%) and electrolyte solutions (NaCl), of varying concentration, were pipetted into each of a series of tubes. The dispersions were shaken and allowed to stand for 2 hours, after which they were centrifuged for 10 minutes at 3000 × g **[214]**. This centrifugation caused any coagulated material to sediment, considerably reducing the concentration of the latex in the supernatant dispersion. At the end of the centrifugation the absorbance of the supernatant was determined with a spectrophotometer (HP 8450 UV/VIS) using a 1 cm × 1 cm quartz spectrophotometer cell.

The critical coagulation concentration (CCC) values for the latexes were identified as the break points in the plots of supernatant absorbance against sodium chloride concentration and are given in Table XIV.

The critical coagulation concentration values for the sulfate, carboxyl, and amidine latexes are typical for coagulation of charge stabilized latexes **[215]**. The modified latex is substantially more stable (CCC = 0.68 mole/l) than the other latexes. This is due to the high density of carboxyl groups chemically bound to the surface of the particles.

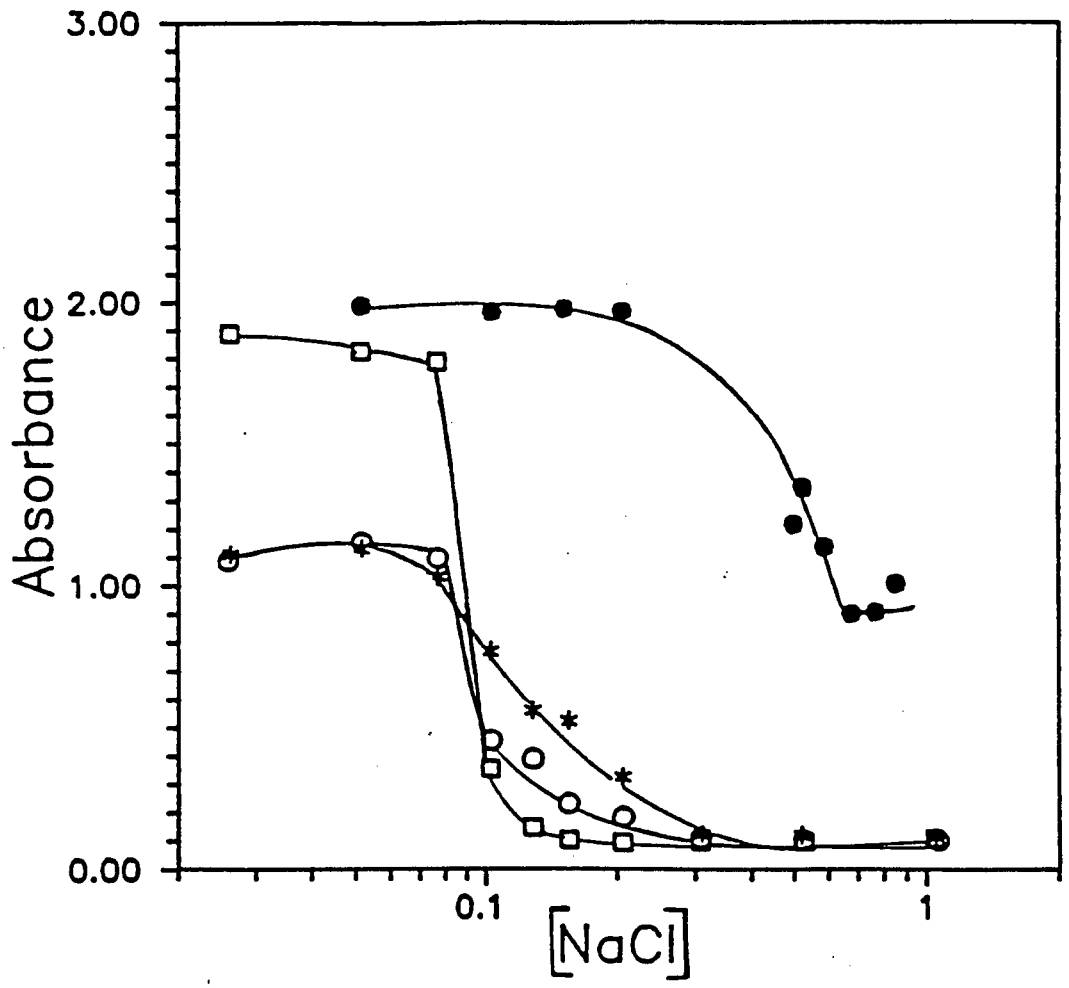

Figure 27. Optical absorbance of supernatant vs concentration of NaCl for the sulfate (○), carboxyl, (✳), carboxyl modified (●) and amidine (+) (□) latexes.

Table XIV

Critical coagulation concentration of the latexes as estimated from supernatant absorbance readings:

Latex Type	Surface Charge density ($\mu C\ cm^{-2}$)	CCC (moles/litre)
Sulfate (1.073 μm)	6.70	0.15
Carboxyl (0.984 μm)	2.88	0.30
CML (0.865 μm)	30.7	0.68
Amidine (+) (0.489μm)	12.2	0.12

The critical coagulation value for the sulfate latex with surface charge density of 6.70 $\mu C\ cm^{-2}$, is found to be lower than that of carboxyl latex with a surface charge density of 2.88 $\mu C\ cm^{-2}$. This difference is presumably due to the difference in specific adsorption of Na^+ ions. As the interaction of Na^+ ion with SO_4^- groups is likely to differ from its interaction with —COO^- groups, differences in the specific adsorption of Na^+ between the two latexes, implying differences in effective surface charge, would be expected.

The results of stability measurements on sulfate latex coated with BSA at (a) 2.72×10^{10}, (b) 8.11×10^{10}, (c) 3.64×10^{11}, and (d) 1.05×10^{12} molecules cm^{-2} are illustrated at a fixed ionic strength of 0.5 M NaCl in Figure 28. It is seen that the stability of BSA-coated latex increases with surface coverage, the saturated latex suspension being completely stable at all shear rates. At low coverage, (results not shown) latex dispersions are unstable at all ionic strengths. At intermediate coverage, the latex dispersions are stable at low ionic strengths but unstable at high ionic strengths. At high surface coverage, latex dispersions are stable at all ionic strengths.

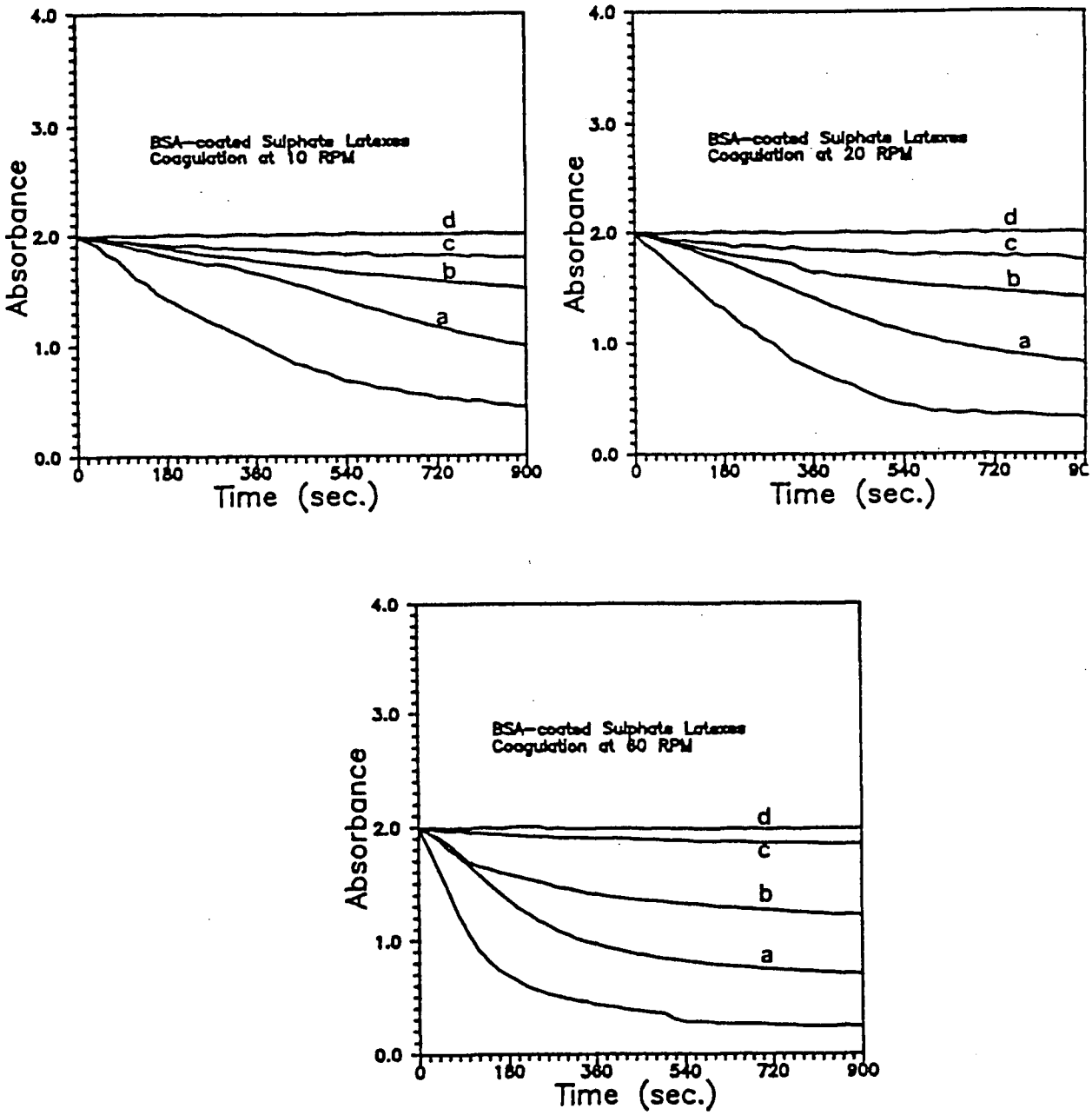

Figure 28. Absorbance change with time for shear flocculation in 0.5M NaCl at 14, 28 & 81 s^{-1} of BSA-coated sulfate latex with surface coverages: (a) 2.72×10^{10} , (b) 8.11×10^{10} , (c) 3.64×10^{11} , and (d) 1.05×10^{12} molecules cm^{-2}. The unlabeled lines refer to bare latex.

The instability at low surface coverage is probably due to a combination of electrostatic and macromolecular factors. At low coverage, the adsorbed protein is thought to reduce the particle surface potential to an extent that the basic DLVO mechanism probably still operates, but with some perturbation of the electrostatic environment near the surface of the particle due to the presence of the adsorbed protein **[216]**. Macromolecular bridging due to protein molecules on one particle adsorbing to a bare patch on another particle in close proximity is also considered a possible explanation for latex destabilisation at low salt and protein concentrations **[217]**.

At the opposite extreme of high protein coverage (saturation) the coated latex particle becomes hydrophilic, and its stability is no longer governed by the DLVO mechanism alone. Both steric factors and electrostatic repulsion between the adsorbed protein layers on the particles likely contribute to the high stability exhibited at higher surface coverage of PSL.

Under shear, the experimental rate constants for coated latexes are always lower than that for the bare particles (Figure 29 & 30). The rate constants decrease with increasing surface coverage of BSA, since the effective collisions between the particles are progressively reduced with surface coverage of BSA. At high protein coverage (saturation coverage) there is virtually no flocculation observed, and the experimental flocculation rate constant slightly decreases with increasing shear rate. This is illustrated in Figure 30, in which the experimental flocculation rate constants are plotted against shear rates for the bare sulfate latex and the various sulfate latexes coated with BSA at concentrations as given in Figure 27.

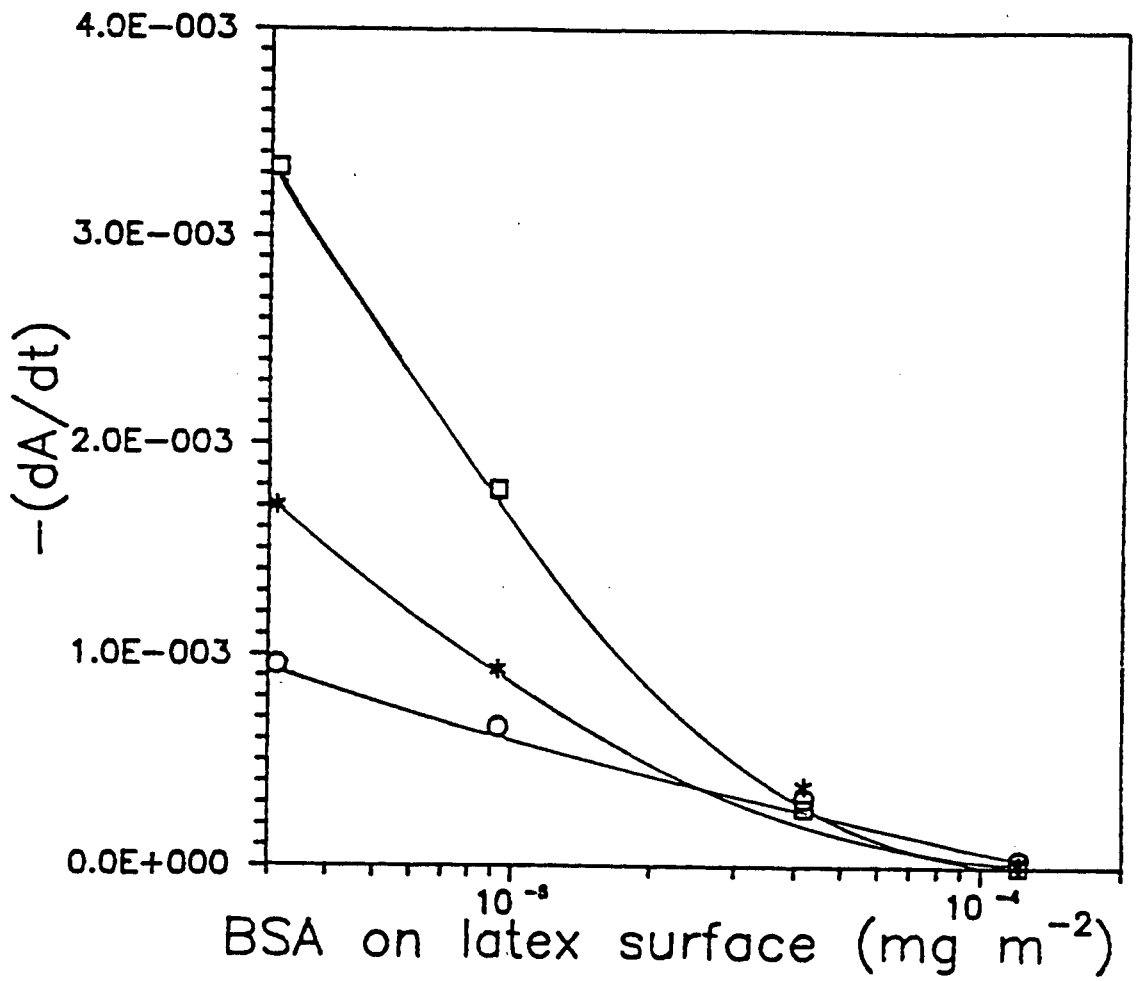

Figure 29. Stability of BSA-coated sulfate latex at ionic strength 0.5M as a function of protein concentration at different shear rates. The experimental rate constants $(-dA/dt)_{t=0}$ is plotted against protein concentration per unit area of particle surface: (O) 14 s^{-1}, (✳) 28 s^{-1}, and (□) 81 s^{-1}.

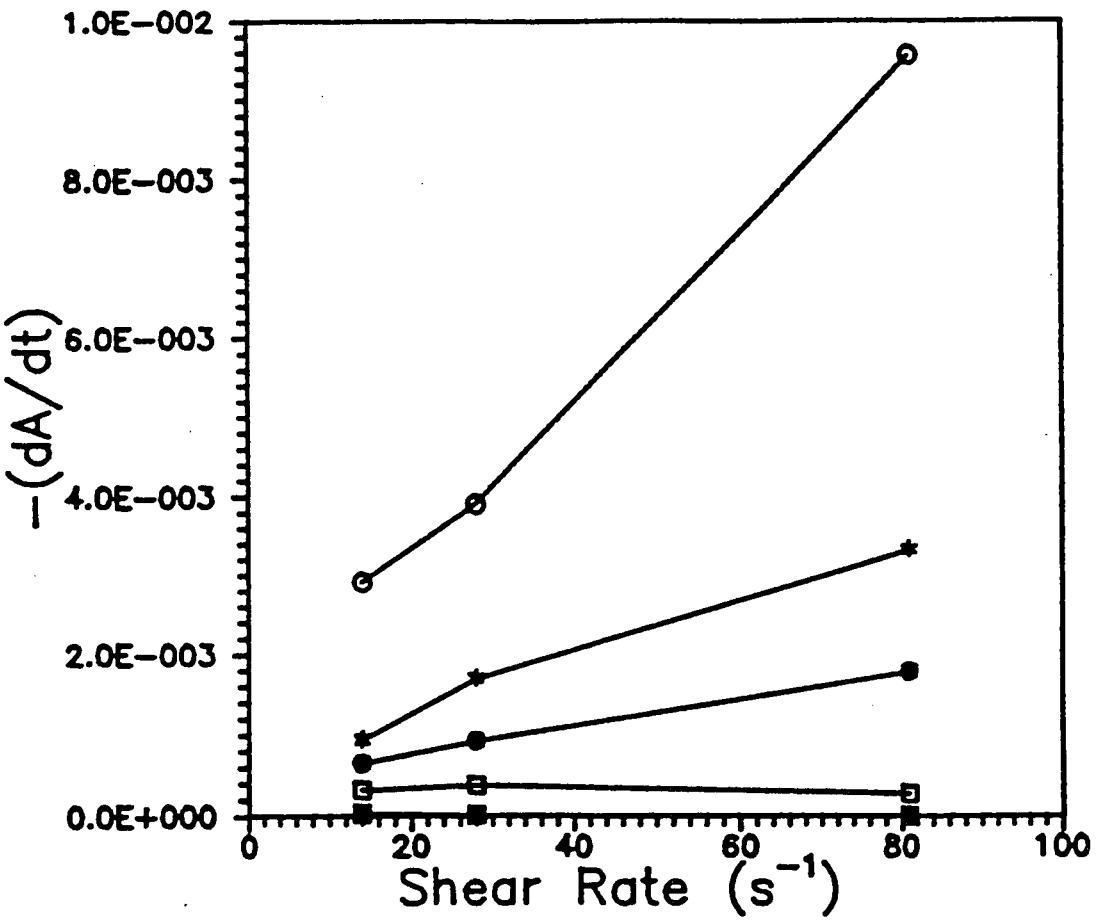

Figure 30. Stability of bare sulfate latex and BSA-coated sulfate latexes at ionic strength 0.5M as a function of shear rate. The experimental rate constants $(-dA/dt)_{t=0}$ are plotted against shear rates for: (O) bare latex; and for BSA-coated sulfate latex with surface coverages; (✱) 2.72×10^{10} , (●) 8.11×10^{10} , (□) 3.64×10^{11} , and (■) 1.05×10^{12} molecules cm^{-2}.

This is the reverse of the trend for flocculation rate constants at surface coverages that are intermediate and/or below saturation, in which the rate constants increase with increasing shear rate. Presumably this is due to a complete transition of the coated particle from a hydrophobic to a hydrophilic one, and may represent shear-induced breakdown of the weak flocs formed.

4.3 (c) *Agglutination of BSA-coated PSL under Shear:*

The results presented in this section are those for the BSA-coated sulfate latex only. The data for agglutination experiments for the other latexes are included in Appendix 11.

4.3 (c) *(i)* *The Effect of varying Anti-BSA IgG Concentration*

Figure 31 shows the effect of varying BSA-coverage and anti-BSA antibody concentration on the rate of agglutination in a sulfate PSL suspension in 0.01M phosphate buffer, pH 7.2. The sulfate latex suspension was first equilibrated with different amounts of BSA to give different degrees of coverage after extensive buffer washes. A polyclonal rabbit anti-BSA IgG preparation was then introduced into the aggregometer and the optical absorbance as a function of time after mixing the BSA-coated sulfate latex suspension and the antibody was measured.

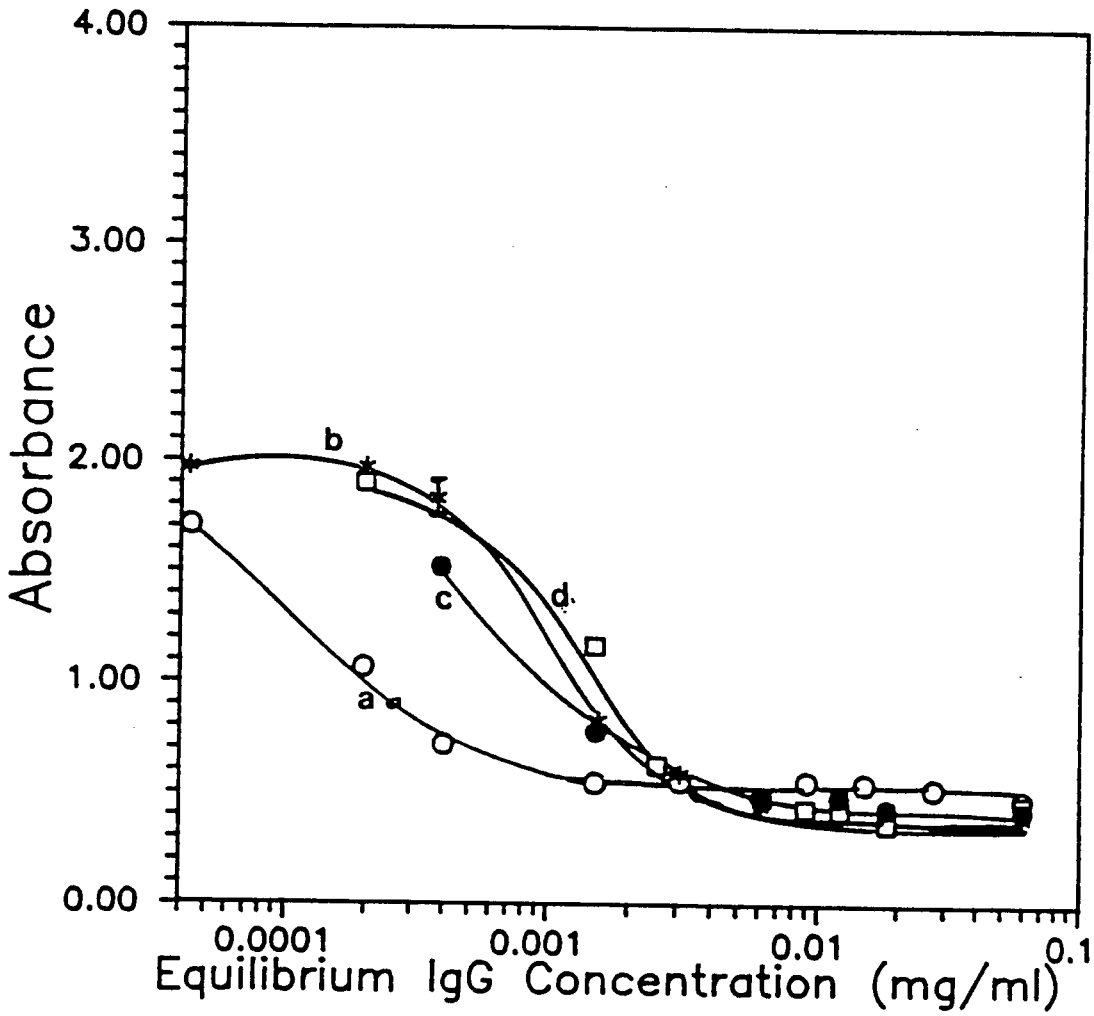

Figure 31. Absorbance (at 900 seconds) as a function of equilibrium IgG concentration for shear agglutination at 28 s^{-1} for BSA coated sulfate latex with surface coverages: (O) 2.72×10^{10} , (✳) 8.11×10^{10} , (◐) 3.64×10^{11} , and (□) 1.05×10^{12} molecules cm^{-2}.

The optical absorbance vs time plots are given in Appendix 10 (a), from which the absorbance at 900 seconds after mixing the antibody and latex suspension is plotted as a function of equilibrium antibody concentration in Figure 31. This time point was chosen as it represents a practical limit to the time over which agglutination assays are performed. Similar plots for earlier times are given in Appendix 10 (b). All the BSA-coated samples used in these studies were stable in the absence of anti-BSA antibody, i.e., the absorbance was constant with time. Addition of non-specific antibody to the system did not produce any nonspecific agglutination response, in spite of the adsorption shown earlier to occur.

It can be seen from Figure 31 that for the lowest surface coverage of BSA (2.72×10^{10} molecules cm^{-2}) a very small amount of anti-BSA antibody (<0.6 μg/ml) is sufficient to induce agglutination, and a maximum rate of agglutination ($-(dA/dt) \cong 3.8 \times 10^{-3}$) is attained at an antibody concentration of approximately 1.0 μg/ml (as determined from the inflection points of the curves in Figure 31 above).

Comparison with Figure 18 shows that agglutination is caused by very low numbers of bound antibodies of the order of 6×10^{10} molecules/cm^2, and that the rate saturates when about 1×10^{11} molecules/cm^2 are present. That is, a very small fraction (≈5% of saturation) of antibody can cause agglutination, implying that few Ab bridges are required to hold the aggregates involved together. The proportion of the bound Ab molecules involved in bridge formation cannot be estimated from this data, hoewver. As the BSA surface coverage of the latex increases, significantly higher concentrations of anti-BSA antibody are required to produce agglutination.

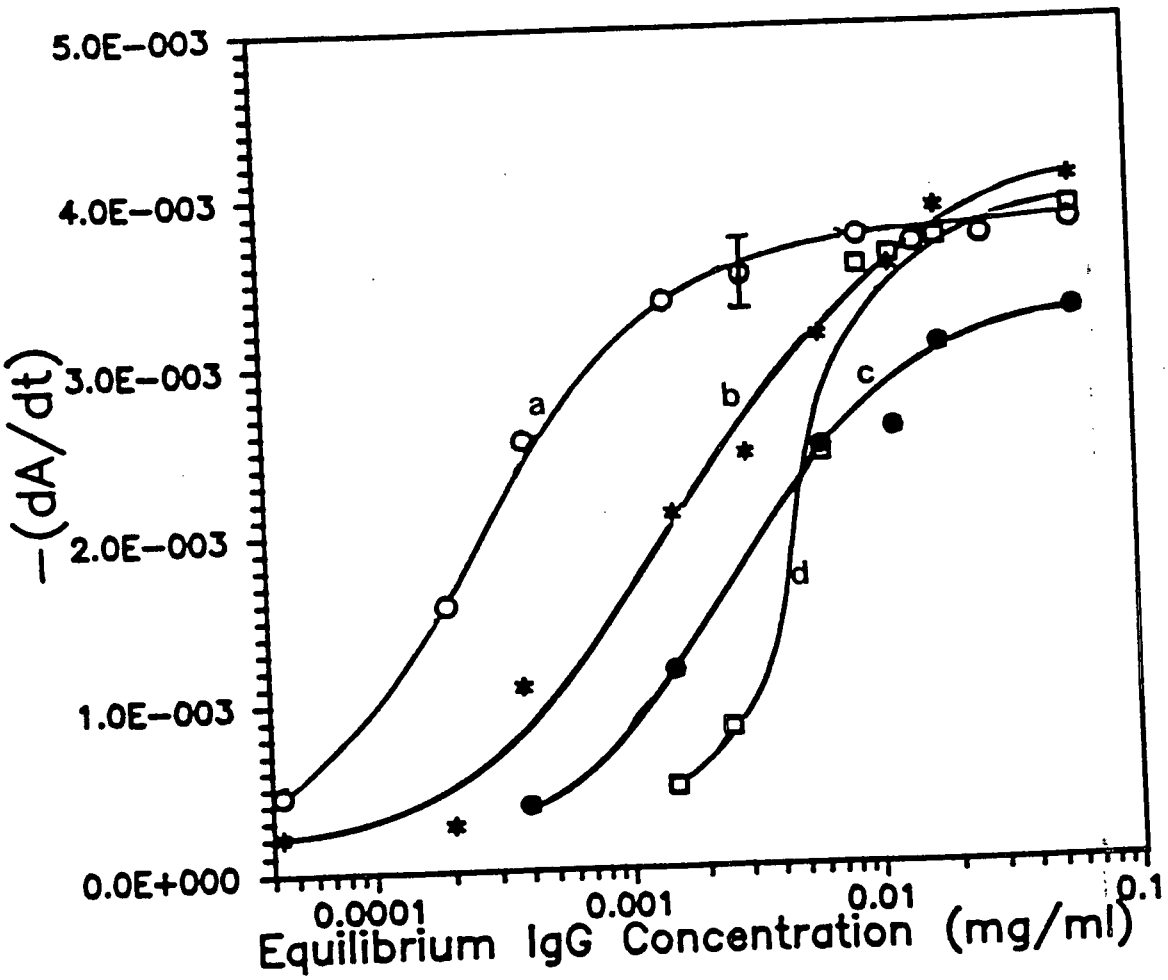

Figure 32. Plots of initial rate of change of absorbance at 28 s^{-1} vs equilibrium antibody concentrations for various BSA coverage as given in Figure 31.

The IgG concentrations at which the maximum rates of agglutination occur at increasing surface coverage also increases, to 2.4, 3.0, and 3.2 μg/ml as the BSA coverage increases. This is consistent with the view that at low surface concentrations of BSA, a significant fraction of antibody binds in a configuration that leaves one of its binding sites free to bridge and bind to another BSA molecule on a second latex particle, thus enabling agglutination to occur at relatively low antibody concentration. Higher BSA coverage requires more antibody molecules to effect agglutination, presumably because at low concentrations the antibody molecules would likely bind with both sites occupied on the same surface, reducing the probability of a bridging configuration.

The initial agglutination rates, as estimated by the initial slopes of the absorbance-time curves are given in Figure 32 at different equilibrium antibody concentrations for the various BSA surface coverage.

The semilogarithmic plots show that the initial rates vary weakly with equilibrium concentration of antibody. Increasing the density of BSA coverage on the particle surface shifts the curves to higher equilibrium concentration of antibody, again indicating that significantly higher concentrations of antibody are required to produce agglutination of a given rate as the BSA coverage on the particle surface increases. All the curves appear to reach the same maximum value at this shear rate, however. Some of this data is presented numerically in Table XV. For a given equilibrium concentration of antibody, the difference in initial agglutination rates for the various BSA coverage on the particle surface is significantly higher at low equilibrium antibody concentrations than at high equilibrium antibody concentrations. This can be clearly seen in Figure 32 and is further illustrated in Table XV below, for two different equilibrium concentrations.

Table XV

Initial rate of change of absorbance at two equilibrium antibody concentrations for different BSA surface coverages as given in Table X (Chapter Three) for the sulfate latex.

Equilibrium IgG (mg/ml)	Initial rate of change of absorbance at given BSA surface coverage			
	2.72×10^{10} (molec/cm^2)	8.11×10^{10} (molec/cm^2)	3.64×10^{11} (molec/cm^2)	1.05×10^{12} (molec/cm^2)
	-(dA/dt)	-(dA/dt)	-(dA/dt)	-(dA/dt)
1.5×10^{-3}	3.36×10^{-3}	2.10×10^{-3}	1.17×10^{-3}	4.80×10^{-4}
6.0×10^{-2}	3.79×10^{-3}	4.05×10^{-3}	3.27×10^{-3}	3.87×10^{-3}

The maximum degree of agglutination, as represented by the minimum absorbance, is not as sensitive to IgG concentration at different BSA coverages as is the initial agglutination rate. Evidently there is sufficient Ab bridging at long times to allow equivalent sized aggregates to form. The initial rates suggest the probability of bridge formation at short times is strongly dependent on Ag coverage, however. Apparently 900 seconds is sufficient time to allow either lower probability bridges to form at higher BSA coverages, or is sufficient to allow some rearrangement of bound Abs to allow interparticle bonds to form. The fact that the initial agglutination rate at high BSA coverage (Figure 32) can be increased to the same level as that observed at low Ag surface concentrations if enough IgG is present supports the former explanation, however. The rate at which lower probability events occur would be expected to increase as the concentration of potential bridging molecules is increased at constant Ag coverage, as observed.

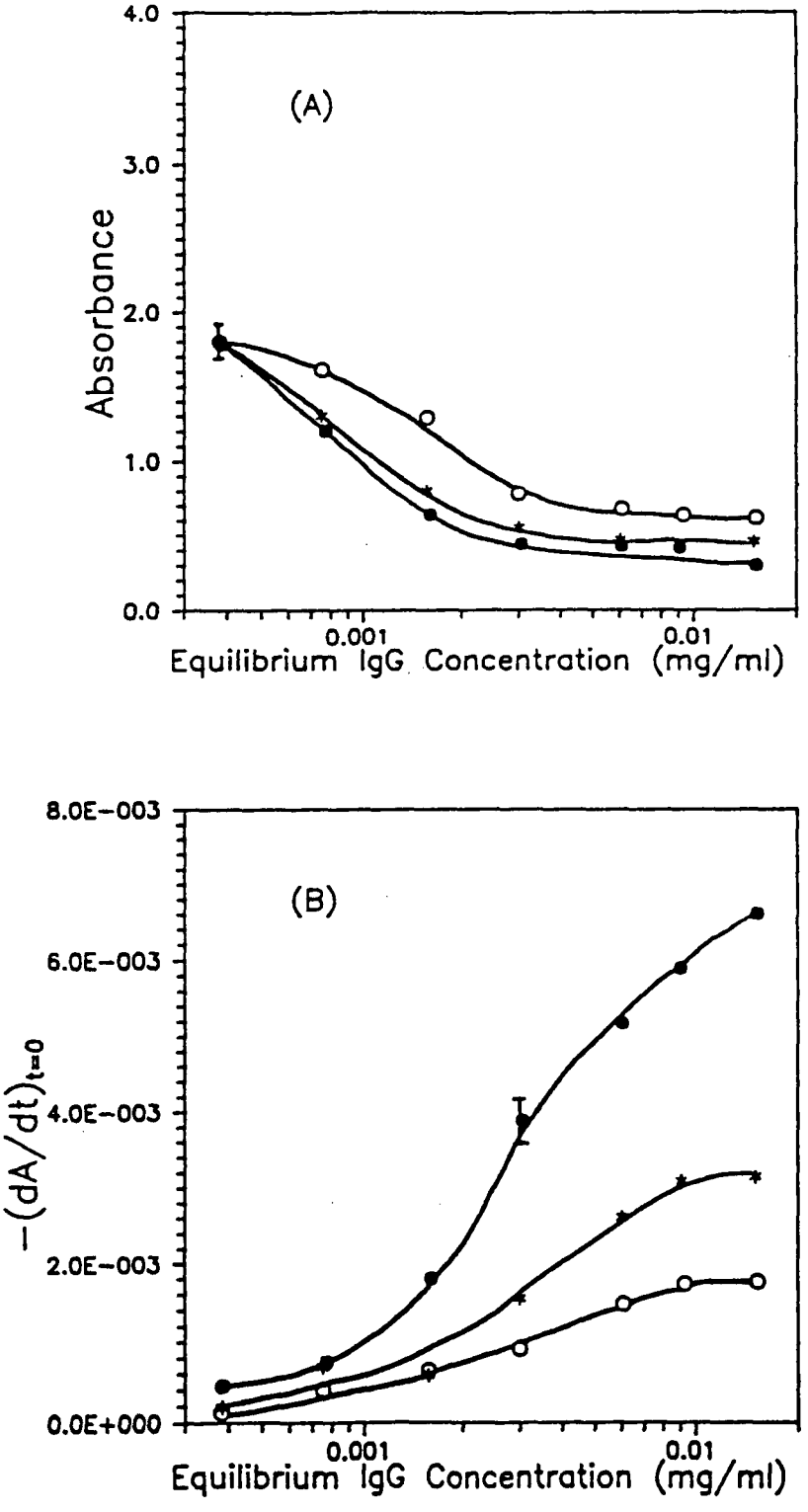

Figure 33 (a) and (b). Plots of absorbance (900 seconds) (a) and initial agglutination rate (b) vs equilibrium antibody concentration for shear agglutination at (○) 14, (✳) 28 and (●) 81 s^{-1} of sulfate latex with BSA coverage of 1.05×10^{12} molecules cm^{-2}.

4.3 (c) *(ii)* *The Effect of Varying Shear Rate*

Figures 33 (a) and (b) illustrate the effect of shear rate on agglutination reaction of sulfate latex with a BSA surface density of 1.05×10^{12} molecules cm^{-2}. The absorbance (at 900 seconds) and initial rates plotted against equilibrium antibody concentrations in Figure 33 (a) and (b) were obtained from the optical absorbance vs time plots of Appendix 10 (c). The agglutination at each antibody concentration was studied for three different shear rates: 14 s^{-1}, 28 s^{-1}, and 81 s^{-1}.

The results show that doubling the shear rate from 14 s^{-1} to 28 s^{-1} significantly reduces the Ab concentration at which the degree of agglutination at 900 seconds is half maximum. However at earlier times, the degree of agglutination is much more reduced at 81 s^{-1} than between 14 s^{-1} and 28 s^{-1} (see Appendix 10 (c)). Thus for a given surface coverage of BSA, increasing the shear rate in this range decreases the Ab concentration necessary to produce a given degree of agglutination. It seems unlikely shear would alter the binding of Ab, since no dependence on stirring rate was observed. It is possible that the more energetic interparticle collisions that occur at higher shear rates allow configurations of bound Ab to bridge that would be ineffective at lower shear rates. In effect, smaller energy barriers to agglutination could be overcome by shear. The further increase in shear rate to 81 s^{-1} did not appreciably increase the sensitivity to Ab concentration, however, so the above effect occurs only at relatively low shear rates.

As the shear rate is raised both energy and frequency of interparticle collisions is increased. If the collision efficiency is independent of shear rate the initial collision rate should be directly proportional to it **[218]**. The data in Figure 33 (b) does not show this

proportionality, however. For instance at $\approx 6 \times 10^{-3}$ mg/ml IgG the rates are 1:1.8:3.5, while the shear rates increased as 1:2:5.8. The effect of shear rate appears to be a roughly equal factor at all IgG concentrations within the uncertainty of the data, the relative increase in sensitivity to Ab between 14 s^{-1} and 28 s^{-1} observed if Figure 33 (a) not being in evidence in the rate data. The reason for this difference is not clear.

Although higher shear rates mean more frequent collisions and greater chances of antibody bridge formation, there will be some value of shear rate above which the rate of aggregate formation will not increase since large shear forces in the fluid will tend to disrupt the aggregates. The value will depend on the strength of the interparticle bonds and their ability to resist the forces which shear exerts on the aggregates as they grow. Up to this point, however, it is to be expected that increasing the shear rate will increase the agglutination rate. Based on the absorbance values in Figure 33 (a), it is evident that larger aggregates are formed at the higher shear rate 28 and 81 s^{-1} than at the lower shear rates 14 s^{-1} if comparisons are made after the same length of shear exposure.

4.3 (c) *(iii)* *The Effect of varying BSA-coated Latex Concentration*

The effect of varying the amount of BSA-coated latex was studied at a constant shear rate of 28 s^{-1} for sulfate latex with BSA surface density of 1.05×10^{12} molecules cm^2 at five different equilibrium antibody concentrations ranging from 3.0×10^{-3} mg/ml to 6.0×10^{-2}mg/ml. The experimental data of absorbance vs time plots are given

in Appendix 10 (d), and the plots of initial agglutination rates vs equilibrium antibody concentrations are given in Figure 34.

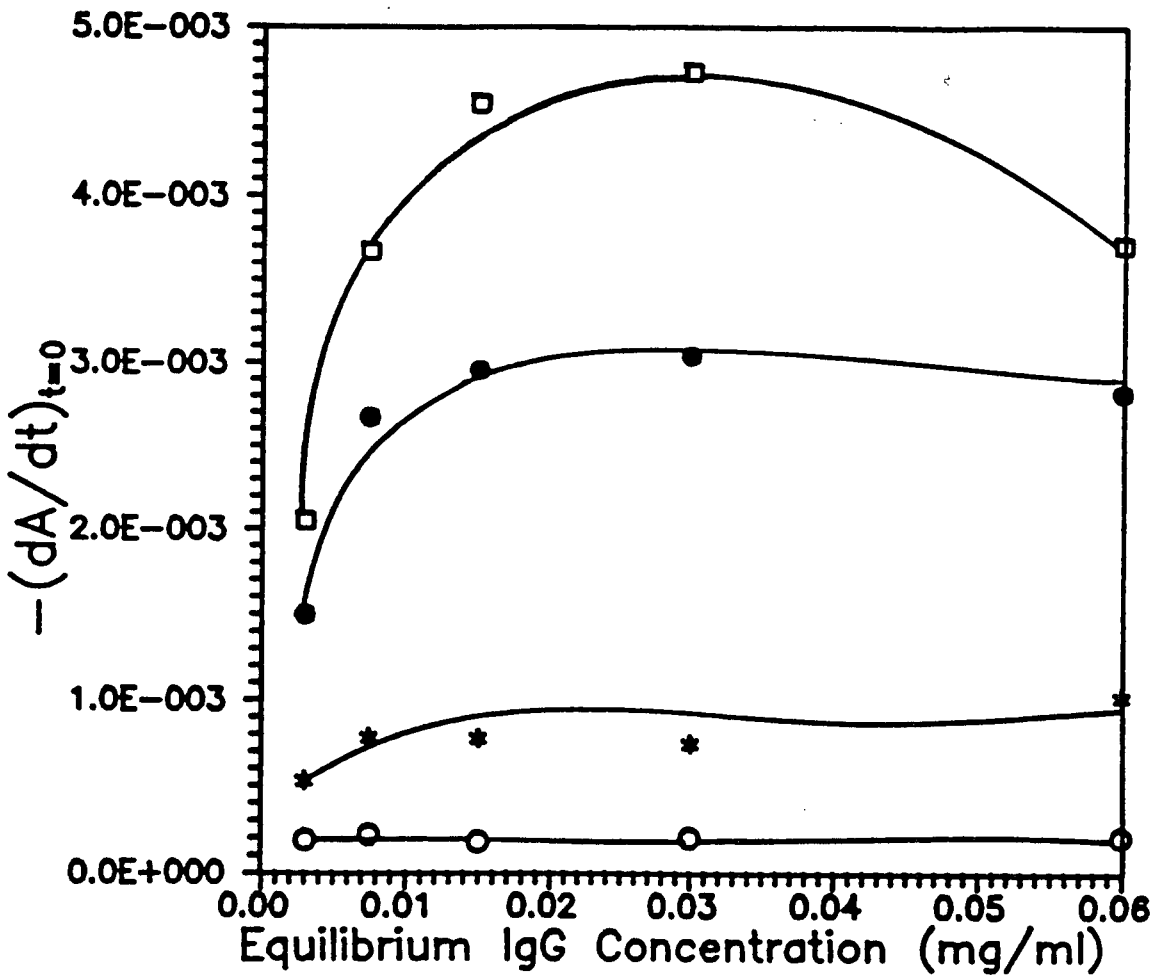

Figure 34. Plots of initial rate of change of absorbance vs equilibrium antibody concentrations for different concentration of particle per unit volume: (○) 4.59×10^9, (✳) 9.09×10^9, (●) 1.82×10^{10}, (□) 2.69×10^{10} molecules per cm^2.

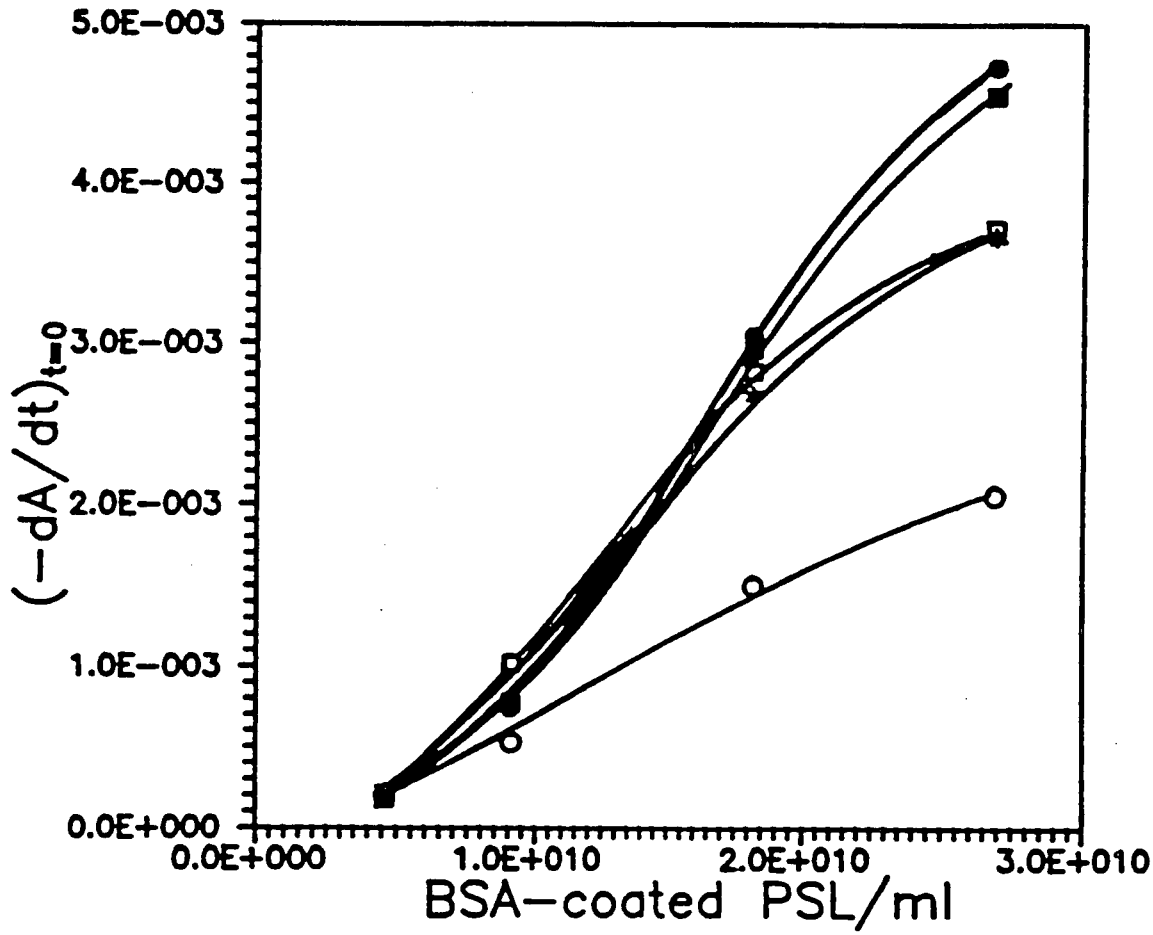

Figure 35. Plots of initial rate of change of absorbance vs number of particles per unit volume for different equilibrium antibody concentrations : (○) 3.0×10^{-3}, (✱) 7.50×10^{-3}, (■) 1.5×10^{-2}, (●) 3.0×10^{-2}, (□) 6.0×10^{-2} mg/ ml.

It can be seen that when the number of BSA-coated latex particles per unit volume is very low, the initial rate of absorbance change is virtually unaffected by an increase in equilibrium concentration of antibodies. At a low ratio of antibody molecules to number of BSA-coated particles per unit volume, there is a rapid increase in the rate. As this ratio increases, the rate levels off over a wide range of equilibrium antibody concentrations.

At higher ratio of the antibody molecules to number of BSA-coated particles per unit volume, the rate of change of absorbance begins to decrease, suggesting that there is an optimal antibody concentration at a given number of coated particles per unit volume for which agglutination attains a maximum rate. This optimal value is probably dependent on particle surface coverage and shear rate. The data is replotted in Figure 34, specifically illustrating the particle concentration dependence. The tendency towards saturation at high particle concentration is likely due to the complex optical path and the increase in overlap of aggregates in the light beam as the fraction of solids increases.

4.4 *Structure Formation in PSL Dispersions*

In the course of our studies with PSL, we have observed a new type of structuring in particle suspensions undergoing simple shear flow in the concentric cylinder device (aggregometer) used in our kinetic studies of latex coagulation and agglutination.

It was observed that when a dilute suspension of polystyrene latex spheres containing a sufficient amount of salt to cause aggregation was subjected to a uniform shear flow of 14 $s^{-1}$and 28 s^{-1} in our shearing device, the randomly distributed, freely-moving particles produced an initially cloudy suspension. As the shearing was continued, however, small aggregates began to form as a result of collisions taking place between particles. The aggregates continued to build as more single particles and smaller aggregates collected in the growing masses. After a characteristic time lag that was dependent on the shear rate and latex concentration such that the aggregates had attained a certain size (~ 0.5mm), they began to arrange themselves into lines of approximately equally spaced aggregates that were roughly parallel to the stream lines in the shearing device. A steady state was observed at roughly 10 minutes after the onset of structuring. Thereafter the pattern gradually degraded as the aggregates sedimented. The size of the aggregates in the structure increased with an increase in latex and/or salt concentrations, but decreased with an increase in shear rate. Although the structure became more defined at higher shear rates, for example at 28 s^{-1} compared to 14 s^{-1}, it was completely lost at 81 s^{-1}, presumably due to shear-induced breakdown of the aggregates.

An example of the development of the structure formation is given in Figure 36 for coagulation of sulfate latex (diameter = 1.073 μm), concentration 0.05% latex in 1.44M NaCl at a shear rate of 21.6 s^{-1}.

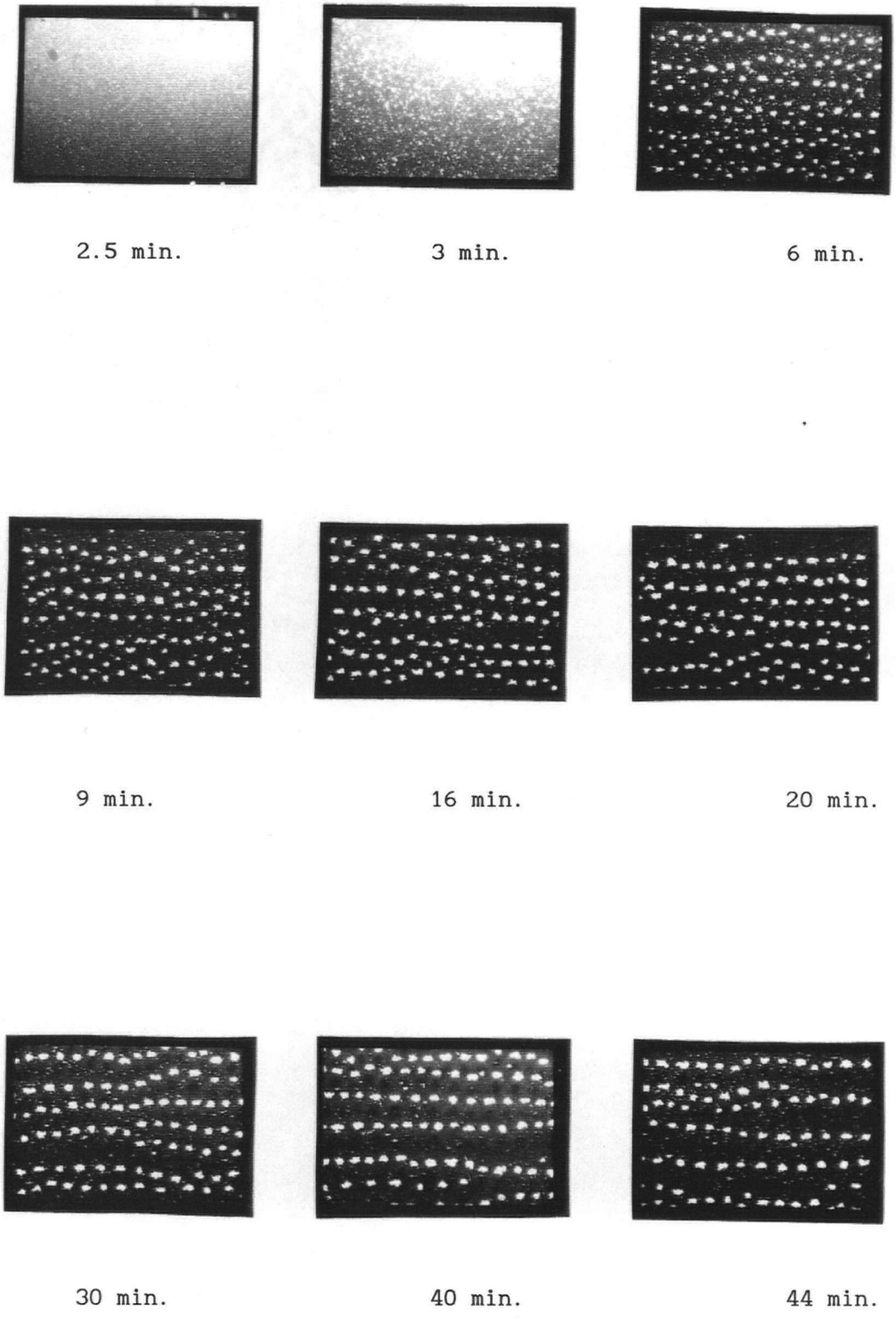

Figure 36. Structure formation in coagulating sulfate latex suspension under shear (21.6 s^{-1}) at room temperature.

Comparison is made in Figure 37 with formation of aggregates during shear agglutination of BSA-coated sulfate latex, concentration 0.05% BSA-coated latex at 21.6 s^{-1} in 0.06 mg/ml anti-BSA IgG, after the same length of shear exposure. It can be seen that under these conditions no pattern appears. This may be because agglutination does not lead to formation of aggregates large enough to produce pattern formation, as observed with coagulating sulfate latex, even after long periods of shearing. Instead many more smaller aggregates are formed, as can be seen in Figure 37.

This may be because the aggregates formed under agglutination by antibody bridges are more shear sensitive due to their open structure, than aggregates formed by coagulation, low shear (21.6 s^{-1}) being sufficient to break down the aggregates. Increasing the concentration of BSA-coated latex does not significantly increase the aggregate size formed during agglutination and no structuring is observed at higher concentrations of BSA-coated latex. At extremely low shear rates the aggregates formed during agglutination are slightly bigger, and coarser in shape (see Appendix 12), but no structuring is observed at this shear rate either. Similar behaviour is observed for flocculation of BSA-coated latexes with salt solutions, i.e., no structure formation is observed at all, although the absorbance signal indicates that flocculation is still occurring; the size of the aggregates formed are small compared with those for naked latex coagulating at similar volume fractions. It appears, therefore, that adsorbed protein or macromolecules on the surface of latexes greatly affects the formation of aggregate structures and patterns that are observed with coagulation of naked latexes. The presence of protein or macromolecules on the surface of particles apparently hinders the growth of aggregate size and this

probably explains the failure of structure formation under these conditions.

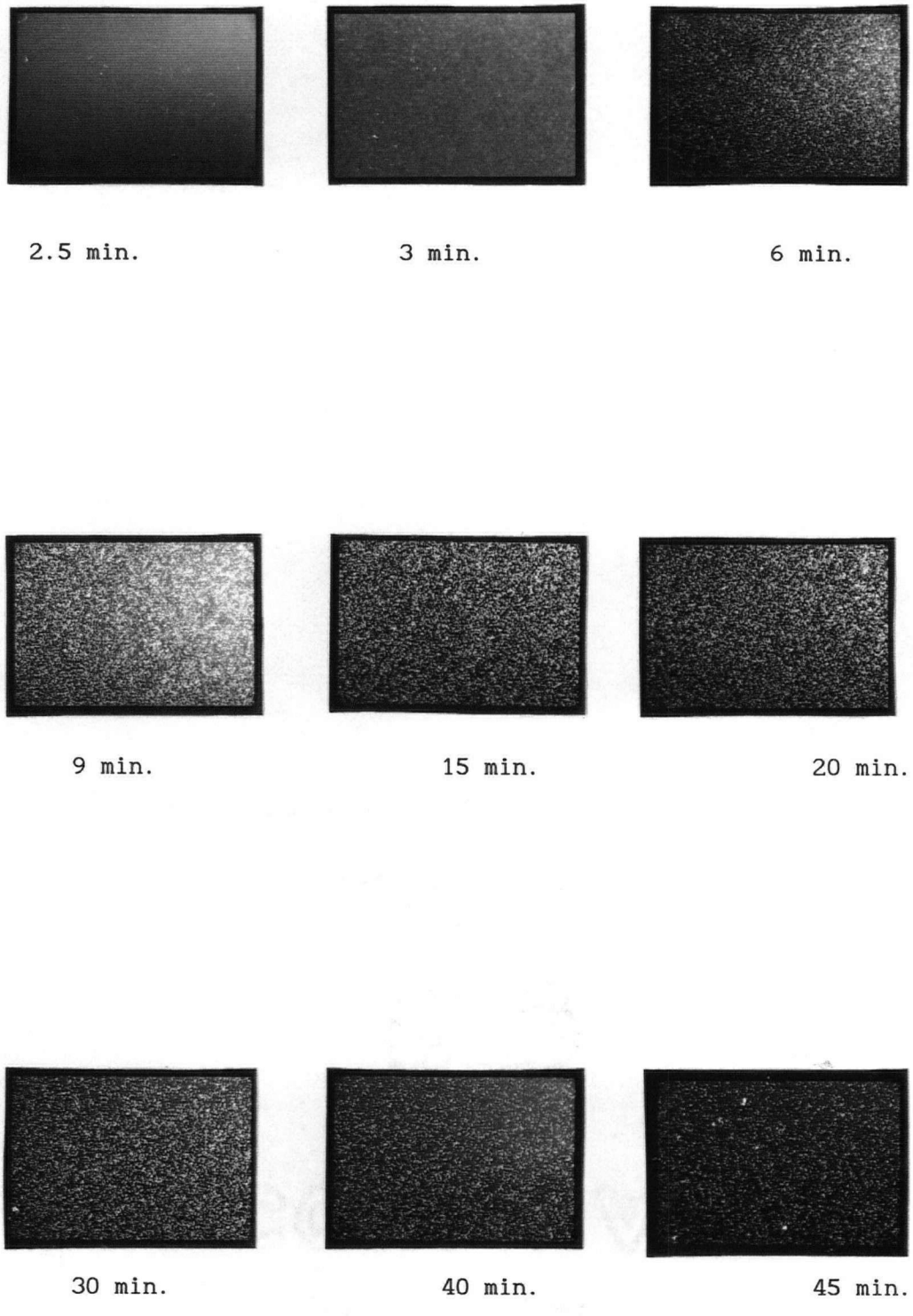

Figure 37. Floc formation in agglutinating BSA-coated sulfate latex suspension under shear (21.6 s^{-1}) at room temperature.

Although different size aggregates and patterns were observed for the coagulation and flocculation of latex particles by salt and antibodies, the absorbance signal did not show any effect of pattern formation. This is probably due to the large optical source slit of the HP 8450A UV/VIS Spectrophotometer (50 micrometer wide) and the fact that each absorbance reading recorded was an average of ten one-second measurements.

4.5. Summary: Antibody-induced Aggregation of PSL

(1). Low surface coverage of latex particles by protein may cause latex instability by both bridging and charge neutralization mechanisms. Increasing surface density of protein on latex particles increases the stability of the particles.

(2). Addition of a sufficient amount of specific antibody to antigen-coated latex suspensions causes agglutination to occur. Non-specific antibody does not cause agglutination at any concentration.

(3). For low surface coverage of latex particles by protein antigen, relatively low concentrations of specific antibodies are required to cause agglutination. The numbers of antibodies bound under thses conditions represent a small fraction (≈5%) of Ab saturation, and demonstrating that very few Abs per unit area can cause agglutination.

(4). Increasing surface density of protein antigen on latex surface requires significantly higher concentrations of specific antibodies to produce agglutination, presumably because at higher protein surface density, antibody binding occurs with both sites occupied on the same surface, reducing the probability of a bridging configuration.

(5). Fluid motion caused by shear is an important factor in agglutination reactions, because of the increase in number of collisions between particles. However, high shear rates may cause aggregate break-up, thus producing smaller aggregates that may not be clearly visible and higher optical absorbance.

(6). There is a remarkable structure formation that is exhibited by latex coagulation in salt under intermediate shear rates. This structure formation does not occur during antibody-induced agglutination under shear probably because the aggregates formed are relatively easily broken down by shear.

CHAPTER FIVE

GENERAL CONCLUSIONS

This study was designed to provide some general information on the physicochemical factors important in latex agglutination caused by Ag-Ab reactions. The results delineated some interesting effects both in protein adsorption and the agglutination response. It was found that Ag adsorption, in this case BSA, is markedly influenced by the properties of the latex surface. In most cases hydrophobic interactions between the hydrophobic amino acids of the protein and the hydrophobic regions of the PSL surface are responsible for protein adsorption. Hence latexes with high hydrophobic surface areas maximize adsorption. Latexes with opposite charge to that of the adsorbing protein may show enhanced adsorption due to superimposition of electrostatic and hydrophobic effects. Although the amount of protein adsorbed will vary with the protein used, these findings have practical implications when considering the the use of latex particles for applications that require immobilization of proteins onto the latex surface, such as in immunological procedures. There is a clear need to establish in each the most appropriate latex to be used.

Desorption or exchange of proteins during storage of prepared reagents will obviously affect results obtained by solid-phase immunoassay. The desorption of albumin molecules from PSL surfaces was found, to a limited extend, to be dependent on the type of latex. Latexes that maximize adsorption lose the lowest fraction of molecules following extensive pure buffer wash. The addition of more protein or other macromolecules did not displace the adsorbed albumin from the

surface of the latexes over a relatively short period of time. However, partial desorption was achieved by the addition of the surface active agent, sodium dodecyl sulfate. It appears that proteins pre-adsorbed to hydrophobic surfaces remain stably bound, at least over the time courses used in this study, so that desorption and/or exchange, being slow processes do not occur significantly over this time period. Since surface active agents such as SDS can displace and solubilize proteins from the surface of latex, the use of surfactant stabilized latex preparations could reduce the adsorption of proteins because of competition between the surface active agents and proteins.

The adsorption of proteins containing oligomers and or mixtures to PSL depends on the concentration of both the proteins and latex. For proteins containing oligomers, this study shows that higher amounts per unit area adsorb in suspensions containing lower total surface areas. The adsorbed layer is enriched in the higher molecular weight oligomers, relative to their concentrations in the stock solution. This enrichment may be due to preferential adsorption of higher polymeric species or to the formation of these higher polymeric species on the particle surfaces as a consequence of conformational changes occurring upon adsorption. This result further complicates the analysis of protein adsorption on polystyrene latexes. However, the presence of oligomers or competing proteins on the latex surface may have no effect on the immunoassay of a protein of interest as long as that protein is present in sufficient amounts.

The binding of polyclonal antibodies to antigen immobilized on the surface of latexes is complicated by the fact that polyclonal antibody preparations contain a mixture of species with different affinities for bound antigen and/or the bare surface of latexes. A consequence of this

is that a variety of effects can be expected, depending on the concentration of antigen on the PSL surface and on the availability of the area not occupied by the antigen to nonspecifically adsorb antibody molecules.

The results of binding studies show that the adsorption at all but the lowest antibody concentrations increases as the surface concentration of antigen is decreased, i.e. the amount of IgG bound is greater the smaller the fraction of the PSL surface occupied by the antigen and the larger the bare surface area. This implies that more nonspecific binding of antibody to bare PSL occurs than specific binding to antigen at most antibody concentrations. As the surface concentration of antigen increases, antibody binding decreases, consistent with the reduction in the area available for nonspecific binding and the increasing effect of specific binding of antibody to antigen. At higher surface antigen concentrations the slopes of the Scatchard plots increase meaning that the affinity of antibody binding increases. This is consistent with the contribution of high affinity antibody binding increasing as bare surface area of latex is reduced. This superimposition of nonspecific adsorption of antibody on the specific binding to antigen means that a direct binding measurement of the total antigenic binding sites per latex particles becomes ambiguous, since different results can be obtained in the same system depending on the magnitudes of the different affinities present. It also complicates comparisons of the number of surface antigenic sites on different latex particle types using, say, the same antibody preparation, since the nonspecific adsorption is dependent on the hydrophobicity of the latex surfaces. Estimates of the number of antigenic sites available per particle for a given antigen surface concentration are of importance in determining the number of antibody

molecules required to effect agglutination which, in turn, subsequently determines the ultimate sensitivity achievable by latex immunoassys. While the apparent affinity constant for antibody binding to BSA is higher than for binding to the bare latex surface, the number of antigenic sites available per unit area is evidently much lower on adsorbed BSA than is the density achievable by nonspecific binding, by about a factor of three according to the model presented in Appendix 7. Only three molecules of antibody bind specifically per molecule of BSA.

The kinetic results in this study show that very low surface coverage of latex surface by protein may cause latex instability and the addition of any level of antibody to such systems produces an agglutination response that is indistinguishable from the nonspecific flocculation caused by bridging and charge neutralization by the antigen molecules in the absence of antibody. At higher antigen surface coverage, the latex is stable in the absence of the antibodies. This indicates the importance of distinguishing pure immunochemical effects (agglutination) from non-specific aggregation caused by flocculation or coagulation.

For surface coverage of latex particles by protein antigen which is low but sufficient to produce a stable suspension, relatively low concentrations of specific antibodies are required to to cause agglutination. Increasing the surface density of protein antigen on the latex surface requires significantly higher concentrations of specific antibodies to produce agglutination. Presumably the difference is due to the nature of antibody binding, i.e. whether it increases or reduces the probability of bridge formation. These results indicate that antigen adsorption effective for agglutination is achieved at concentrations much lower than that necessary to saturate the latex particle surfaces.

Therefore, for a given protein antigen, it is desirable to establish the concentration at which stability of the latex is achieved and above which it reduces the probability of a bridging configuration.

The results of agglutination of latexes at different shear rates illustrate the strong effects that local flow conditions can have on the rate at which agglutination occurs. Increasing shear rates increase the number of collisions between particles, thus increasing the probability of bridge formation. However, extremely high shear rates may cause aggregate break-up. The initial rates suggest that the probability of bridge formation is strongly dependent on antigen coverage. The maximum degree of agglutination, as represented by minimum absorbance, is not as sensitive to antibody concentrations at different BSA coverages as is the initial agglutination rate. Under shear conditions lower probability bridges form in relatively short periods of time if sufficient antibody is present. Thus under shear agglutination may include contributions from antibody molecules of low affinities, which are normally assumed to contribute only to equilibrium titres.

Glossary of Terms

Adsorption

The spontaneous enrichment (accumulation) of one or more components at a surface or in an interfacial layer.

Adsorption Isotherm

The relation between the quantity adsorbed and the composition of the bulk phase under equilibrium conditions at constant temperature.

Affinity

The number and total strength of the bonds between an individual antibody binding site and antigenic determinant.

Agglutination

The process by which suspended particles (bacteria, cells, latex, etc) are caused to adhere and form into clumps due to specific macromolecular briding, as in the case of antibody-antigen interaction.

Antibody

Antibody is one of many classes of immunoglobulins present in blood serum or body fluids of an animal, which are produced in response to an antigenic stimulus.

Antigen

Is any foreign substance (e.g. microorganism) that, as a result of comning into contact with appropriate tissues of an animal, induces the body to produce another substance (an antibody) which reacts with the antigen.

Coagulation and Flocculation

The formation of aggregates is called coagulation or flocculation. Coagulation implies the formation of compact aggregates and flocculation implies the formation of loose or open network aggregates (or flocs).

Colloidal

Refers to a state of subdivision, implying that the molecules or polymolecular particles dispersed in a medium have at least in one direction a dimension roughly between 1nm and 1μm.

Colloidal Aggregate

An aggregate is, in general, a group of particles (atoms or molecules) held together in any way. Colloidal aggregates describe the structure formed by the cohesion of colloidal particles.

Colloidal Dispersion

A system in which particles of colloidal size of any nature (gas, liquid or solid) are dispersed in a continous phase of a different composition (or state).

Collodal Stability

Implies the particles in a colloidal system do not aggregate at a significant rate.

Colloidal Suspension

A suspension is solid particles dispersed in a liquid; a colloidal suspension is one in which the size of the particles lie in the colloidal range.

Emulsion

Liquid droplets dispersed in a liquid.

Latex

(plural = latices or latexes) is an emulsion or sol in which each colloidal particle contains a number of macromolecules.

Lyophobic and Lyophilic

Terms used to describe the character of interaction of a material with the medium. Qualitatively, lyophobic means "solvent rejecting" and lyophilic means "solvent prefering". Colloidal dispersions may be lyophobic (hydrophobic, if the dispersion medium is an aqueuos solution) or lyophilic (hydrophilic).

Monodisperse

If all particles in a colloidal system are of (nearly) the same size the system is called monodisperse. If they are not of (nearly) the same size, it is called heterodisperse and if many particles sizes occur polydisperse.

Perikinetic and Orthokinetic aggregation

The rate of aggregation is in general determined by the frequency of collisions between the particles and the probability of cohesion during collision. If the collisions are caused by Brownian motion, the process is called perikinetic aggregation; if by hydrodynamic motions (e.g. convection, sedimentation or shear forces) then the process is called orthokinetic aggregation.

Sentitization and Protective Action

Addition of small amounts of a hydrophilic colloid to a hydrophobic colloid sol may make the hydrophobic sol sensitive to flocculation by electrolyte. This phenomenon is called sentitization. When higher concentration of the hydrophilic colloid protects the hydrophobic sol from flocculation, then the phenomenon is called protective action.

Sol

Colloidal system composed of two or more componenets, e.g. protein sol, gold sol and an emulsion.

Surface active agent (= surfactant)

A substance which lowers the surface tension of the medium in which it is dissolved and/or the interfacial tension with other phases.

Glossary of Symbols and Abbreviations

a radius of particle

a and b major and minor semi-axes of prolate spheroid

a_s specific surface area of latex (cm^2/g)

A Absorbance (A_0, initial absorbance at t = 0)

A_{11} Hamaker constant of particles

A_{22} Hamaker constant of medium

Ab antibody

Ag antigen

BSA bovine serum albumin

C_i molar concentration of the ith ionic species

C_i initial concentration of BSA ($mg/g_{soln.}$)

C_e equilibrium concentration of BSA (mg/g_{soln})

C_p equilibrium protein concentration

C number of particles per cm^3

CCC critical coagulation constant

c.f.c. critical flocculation concentration

c.f.T. critical flocculation temperature

CMC critical micelle concentration

CML carboxyl modified latex

D_i diffusion constant of a spherical particle

DEAE diethylaminoethyl

$-(dn)/(dt)$ rate of diffusion-controlled coagulation

(dA/dt) rate of change of absorbance with time

DNA deoxyribonucleic acid

FPLC fast protein liquid chromatography

G = (dv/dr) velocity gradient (shear rate)

ΔG_A free energy of attraction

ΔG_R free energy of repulsion

ΔG_T Total free energy of interaction between two particles

H distance of separation between the centres of particles

hCG human chorionic gonadotropin

HSA human serum albumin

$I = 1/2\ \Sigma z_i^2\ C_i =$ ionic strength

IgG immunoglobulin G

J_B^0 Brownian collision frequency

J_S^0 Shear-induced collision frequency

k Boltzmann's constant

k rate constant for diffusion-controlled coagulation

k_f rate constant for fast coagulation

k_s rate constant for slow coagulation

$k_{\rightarrow}$ forward reaction rate

$k_{\leftarrow}$ reverse reaction rate

k_{eff} efective rate constant
k_{exp} experimental rate constant
K_1, K_2, & K_i are the intrinsic association constants for the binding of each class of antibody binding site
K equilibrium binding constant
K_I and K_{II} intrinsic association constants
K' light extinction cross-section
l optical path length
M monomer
m mass of latex (g)
M_1 primary minimum
M_2 secondary minimum
M_r relative molar mass
N_A Avogadro's number
n number of particles per unit volume
P primary maximum
PCS photon correlation spectroscopy
PDMS polydimethylsiloxane
PS polystyrene
PSL polystyrene latex
PVT polyvinyl toluene
R_b radius of bob (inner cylinder)
R_c radius of cup (outer cylinder)
R_f relative electrophoretic mobility
RNA ribonucleic acid
s number of antigenic binding sites
S surface area of adsorbent
S_{el} geometric function
S_{mix} geometric function
SDS sodium dodecyl sulfate
SANS small-angle neutron scattering
t time
T Absolute Temperature
T Transmittance
TCA trichloroacetic acid
TEMED tetramethylethylne diamine
V potential energy of interaction
V solution volume
ΔV energy barrier to coagulation
V_R^s steric interaction energy
V_1 solvent molecular volume
V_2 polymer molecular volume
W coagulation stability ratio
W_A^p polar component of work of adhesion

W_A^d dispersion component of the work of adhesion

z_i valency of the ith ionic species

Γ amount adsorbed per unit area

Γ_{max} plateau adsorption value (mg/cm^2)

Γ_{ns} amount of nonspecific IgG bound to BSA-coated latex per unit area

Γ_{ns}^0 amount of nonspecific IgG bound to naked latex per unit area

$\Gamma_{ns,s}$ amount of nonspecific IgG adsorbed at high Γ_{BSA}.

Γ_{sp} amount of specific anti-BSA IgG bound to BSA adsorbed on latex particle

$\Gamma_{sp,s}$ amount of specific anti-BSA bound to BSA adsorbed on PSL plus nonspeifIc adsorption of anti-BSA IgG to bare surface of PSL

Γ^* nonadsorbed amount per unit area (mg/cm^2)

Γ_{BSA}^* surface BSA concentration above which nonspecific and specific IgG binding to PSL saturates

ε_s dielectric permittivity of medium

ε_0 permittivity of free space

ζ zeta potential

η viscosity of continous phase

κ reciprocal Deby-Hückel electrical double layer thickness

ν moles of IgG bound per gram of latex

ρ density of latex (g/cm^3)

$\rho(z)$ adsorbed polymer segment concentration profile

τ turbidity (τ_0 initial turbidity)

χ Flory polymer/solvent interaction parameter.

ω revolution per second

Ω angular velocity

ψ_0 surface electrostatic potential

ϕ volume fraction of particles

Appendix 1

Procedure for electrophoretic analysis of BSA samples in the stock solution, supernatant solution, and that eluted from latex surfaces.

The overall approach to gel preparation was that due to Fairbanks *et. al* **[75]**. Concentrated stock solutions were prepared in the proportions given in Table IA. The 4% gel stock solution was then poured into glass tubes of 5mm inner tube diameter, 12.5 cm long, that had been cleaned by soaking in chromic acid , rinsed thoroughly in distilled water and dried in an oven. Each gel column was overlaid gently with overlay solution (Table IA) and when polymerization was complete (about one hour at room temperature), the tops of the gels were rinsed with distilled water and overlaid with electrophoresis buffer.

The supernatant and stock BSA solution from adsorption studies were prepared for electrophoresis by mixing 100μl of the protein solution with 100μl of Fairbanks sample reagent (Table IA). The BSA adsorbed onto the latex surface was either eluted with 200μl portions of 2% SDS and then mixed with an equal portion of Fairbanks sample reagent for electrophoresis analysis, or directly eluted, from the latex surface, with 200μl portions of Fairbanks sample reagent. These samples were then boiled for 5 minutes and allowed to cool to room temperature, and 20μl of each were, separately, discharged gently to the top of a gel, using a micropipette. Normally, electrophoresis was performed at a constant current of 3 mA/gel for about 2.5 hr. When the tracking dye band, pyronin Y, had come to the bottom of the gels, the electrophoresis was stopped and the tubes removed from the electrophoresis apparatus. The gels were removed from the tubes and the position of the tracking dye was

marked in each gel by pricking it with a needle dipped in black ink. The gels were then stained as described below.

Table IA

Solutions used to make 4% SDS PAGE gels

FAIRBANKS SAMPLE REAGENT			10X TRIS-HCL BUFFER		
Tris-HCl	0.02	M	Tris-HCl	24.23	g
EDTA	0.002	M	S odium Acetate	13.61	g
SDS	2.0%	w/w	EDTA	3.72	g
Sucrose	14.0	%	H_2O up to	500	ml
Pyronin Y	0.004	%			
4% GEL STOCK			**10X ACRYLAMIDE:BIS**		
10X Acrylamide:bis	4	ml	Acrylamide	40	g
10X Tris-HCl buffer	3	ml	Bis	1.5	g
H_2O	17	ml	H_2O up to	100	ml
4% SDS	1.5	ml			
0.5% TEMED	1.5	ml			
1.5% Ammonium Persulphate	3	ml			
OVERLAYING SOLUTION			**RESERVOIR BUFFER**		
This was made as the 4% gel solution with the acrylamide:bis replaced with H_2O.			10X Tris-HCl	200	ml
			4% SDS	100	ml
			H_2O	1700	ml

The gels were stained for protein with coomassie blue. They were placed in a gel stain/destainer plastic mold with a compartment slotted to hold 12 gel rods; to which was added the staining, fixing and destaining solutions given below:

Table IB

Solutions for staining, fixing and destaining electrophoretic gels

Coomassie Blue Stain:		
Coomassie Blue G-250	0.200	g
Methanol	28	ml
Glacial Acetic acid	5	ml
Perchloric acid	25	ml
H_2O.....up to	500	ml
Methanol Fix Solution:		
Methanol	300	ml
Acetic acid	50	ml
H_2O	650	ml
Destaining Solution (7% Acetic acid):		
Acetic acid	70	ml
H_2O	930	ml

The gels were stained in coomassie blue stain solution for ≤ 1 hr., followed by ≅ 1hr. of methanol fix solution and then destained in 7% acetic acid until a clear background was obtained. They were then stored in glass tubes filled with water.

The bands on the gels were recorded by scanning them on a Beckman Model 25 Spectrophotometer with a rod gel scanning adaptor at 590nm and integrated as described in Chapter 2, section 2.3 (d).

Appendix 2a

The following is an outline of the procedure used to calculate the amount of BSA adsorbed per unit area of PSL and error estimates associated with the calculations.

The amount of BSA adsorbed per unit area of latex is given by:

$$\Gamma = \frac{C \times V}{a_s \times m} \qquad (2A)$$

where Γ = amount of protein adsorbed per unit area (mg cm^{-2})

$C = C_i - C_e$

C_i = initial concentration of BSA before binding ($mg/g_{soln.}$).

C_e = equilibrium concentration of BSA ($mg/g_{soln.}$).

V = amount of liquid phase (g).

a_s = specific surface area of latex (cm^2/g).

m = mass of latex (g).

Measured Quantities:

A_c = CPM/g solution of BSA for calibration

A_i = CPM/g solution of BSA before adding latex

A_e = CPM/g solution of BSA in supernatant

W_i = wt. of BSA stock solution

W_e = wt. of BSA solution + wt. of latex suspension

W_f = total wt. of fluid

W_b = wt. of buffer

W_l = wt. of stock latex suspension

w_s = wt. of supernatant for counts

β_i = mass fraction of stock latex suspension

β_e = equilibrium mass fraction of latex suspension

(a) The initial concentration of BSA in each sample was determined from the amount of BSA solution added in each sample and the specific radioactivity of stock BSA:

The specific activity of BSA is given by:

$A_{BSA} = A_c/C_{BSA}$, (C_{BSA} = concentration of BSA ($g_{BSA}/g_{soln.}$).

The initial concentration of BSA is then given by:

$C_i = A_i/A_{BSA}$ ($g_{BSA}/g_{soln.}$).

(b) The equilibrium concentration of BSA in each sample was determined from the activity of the supernatant of each sample and the specific radioactivity of the stock BSA:

$C_e = A_e/A_{BSA}$ ($g_{BSA}/g_{soln.}$).

(c) The mass of latex in each sample was determined from the mass fraction of the stock latex suspension:

$m = (\beta_e \times W_e)$.

(d) The specific area of the latex was determined from:

$a_s = 6 \times 10^4/d\rho$, $\rho = 1.055$ g cm^{-3}, d = diameter of latex particle.

The probable error in the amount of BSA adsorbed per unit area, $\Delta\Gamma$, as calculated by Equation 2A is given by:

$$\Delta\Gamma \approx \left[(V/a_s m)^2(\Delta C)^2 + (C/a_s m)^2(\Delta V)^2 + (CV/a_s^2 m)^2(\Delta a_s)^2 + (CV/a_s m^2)^2(\Delta m)^2 \right]^{1/2}$$

where ΔC is the uncertainty in the difference in the initial concentration of BSA before adsorption and the equilibrium concentration of BSA, ΔV is the uncertainy in amount of fluid, Δa_s is the uncertainty in the specific surface area of latex, and Δm is the uncertainty in the mass of latex used in each sample.

Appendix 2b

Adsorption isotherms of repeated measurements of BSA adsorption to sulfate latex under similar conditions as those given in Figure 6, Chapter Two. The error bars shown are the standard deviation of the mean values of amount adsorbed per unit area as obtained from repeated measurements. It can be seen that the reproducibility is low for isotherms obtained at relatively low total surface areas: Appendix 2b (I) and (II) where the standard deviation of the mean range from ~ ±2-15%. This probably reflects the uncertainty in determining the relatively small change in the concentration of BSA solution due to the fact that there is relatively low surface area exposed for protein adsorption.

On the other hand, when relatively high surface are of latex is exposed to the same BSA solution, the reproducibility of the adsoption isotherms is much improved as indicated by the low values of the standard deviation of the mean (< ±3.5%): Appendix 2b (III).

Appendix 2b (I)

Repeated adsorption isotherms for BSA to sulfate latex at room temperature from 0.01M phosphate buffer, pH 7.20. The total surface area used is 240 cm^2.

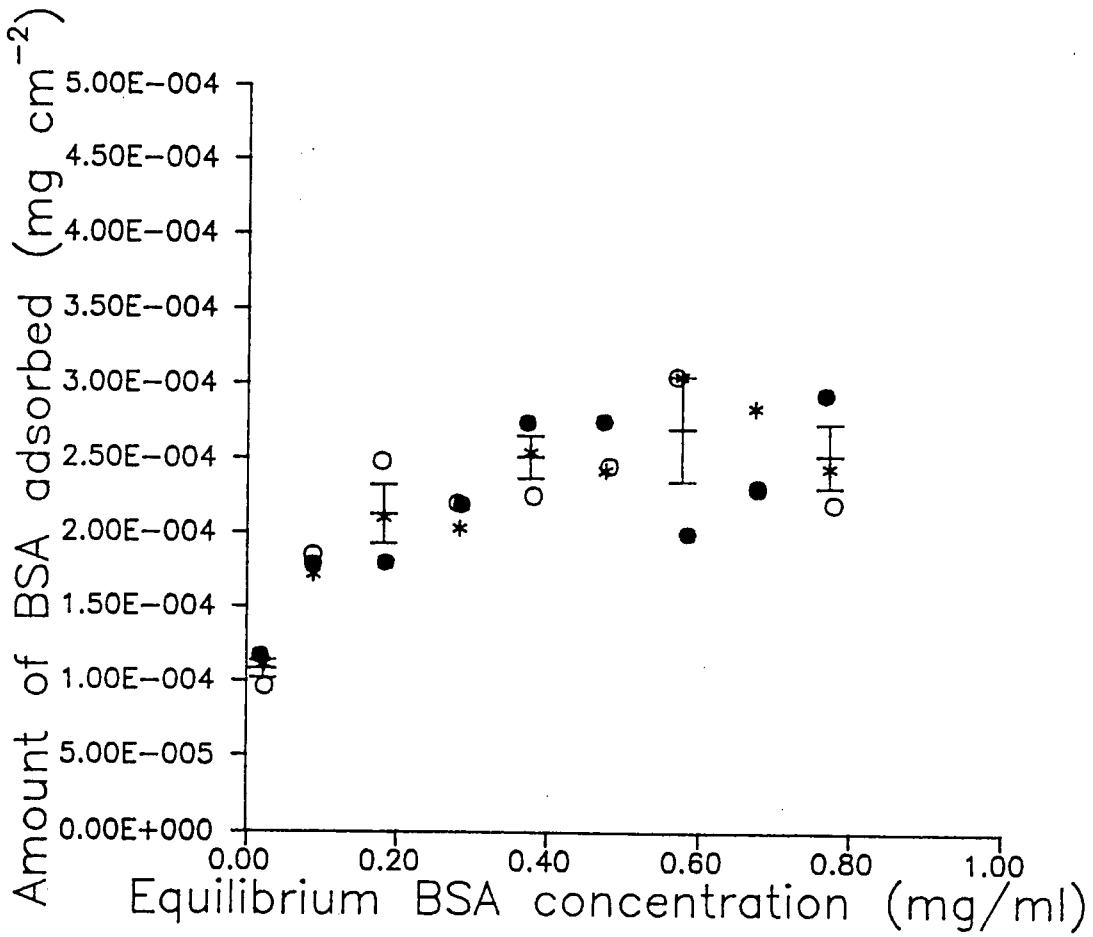

Appendix 2b (II)

Repeated adsorption isotherms for BSA to sulfate latex at room temperature from 0.01M phosphate buffer, pH 7.20. The total surface area used is 712 cm^2.

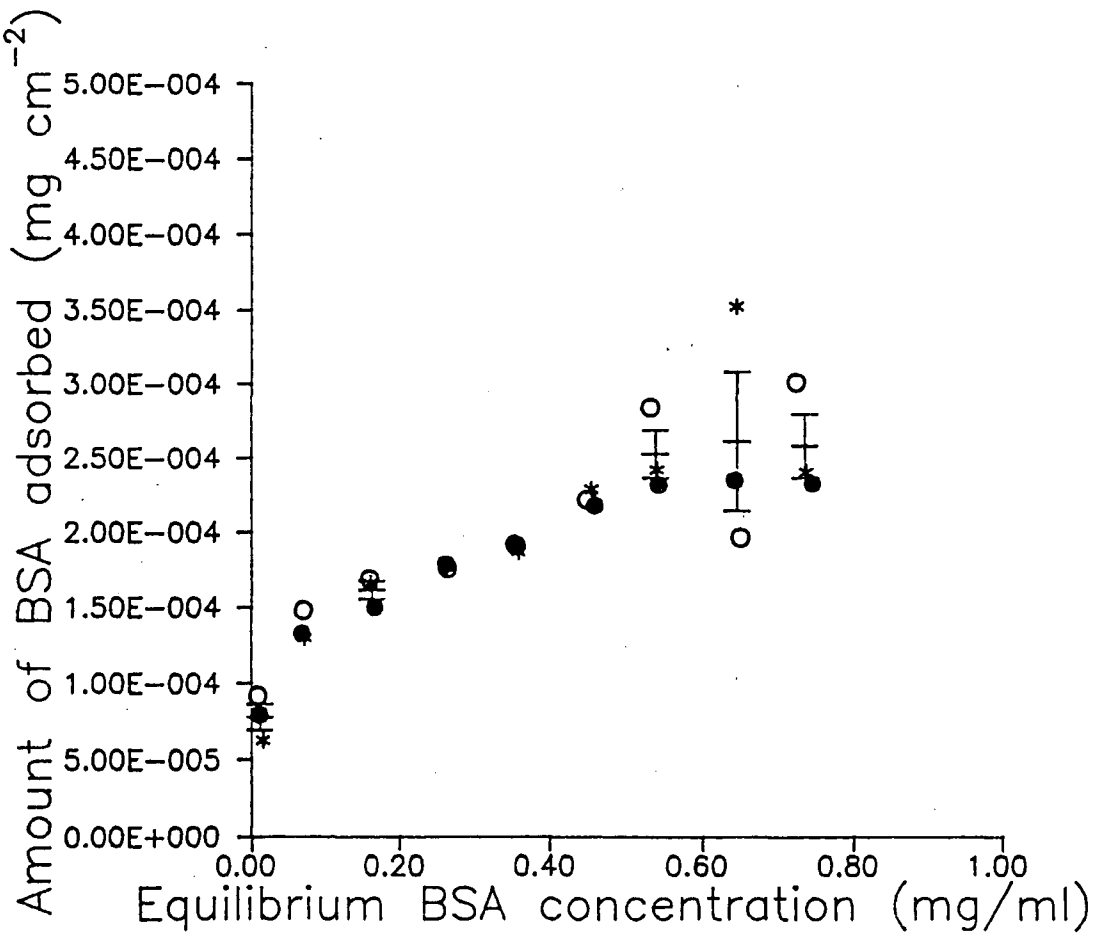

Appendix 2b (III)

Repeated adsorption isotherms for BSA to sulfate latex at room temperature from 0.01M phosphate buffer, pH 7.20. The total surface area used is 1200 cm^2.

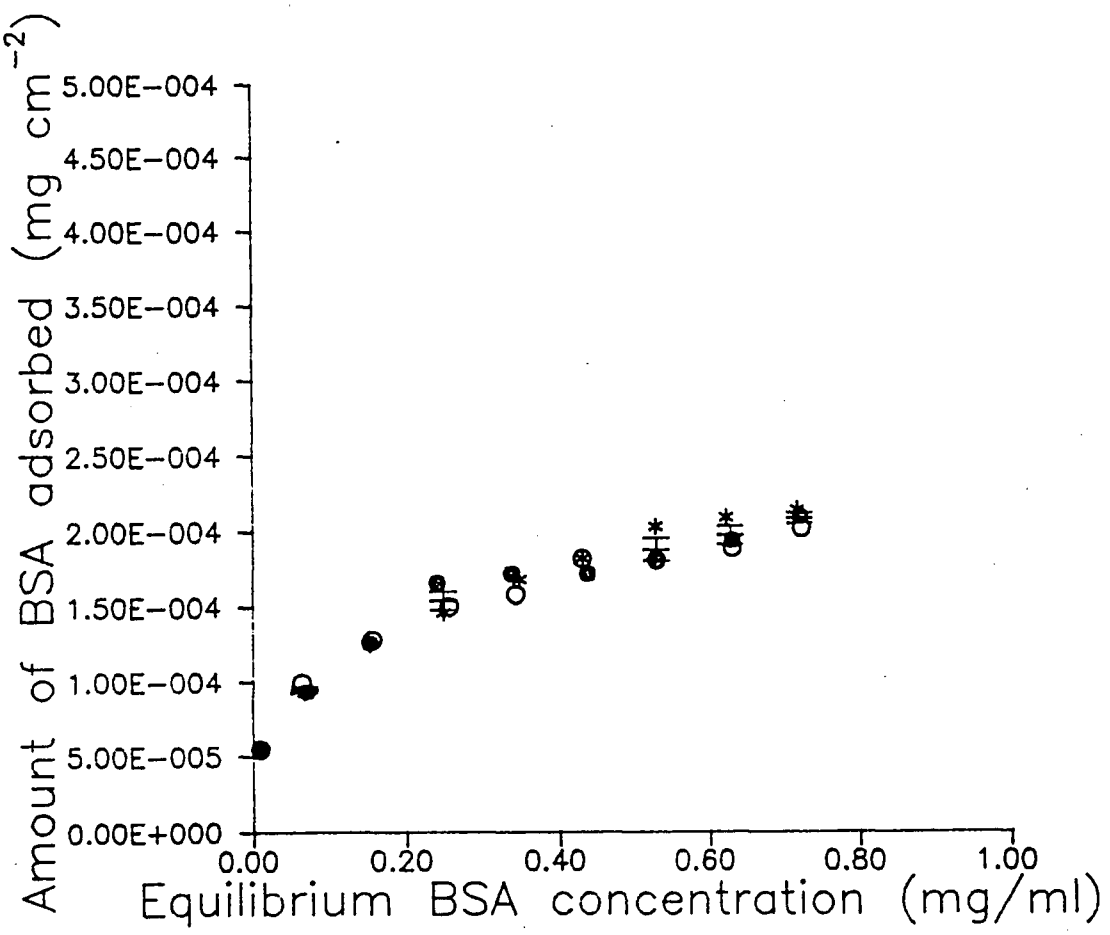

Appendix 3

4% SDS-PAGE electrophoresis of polyclonal IgG fraction used in antibody binding to antigen-coated PSL and agglutination of antigen-coated PSL. All protein samples were reduced with 5mM 2-mercaptoethanol.

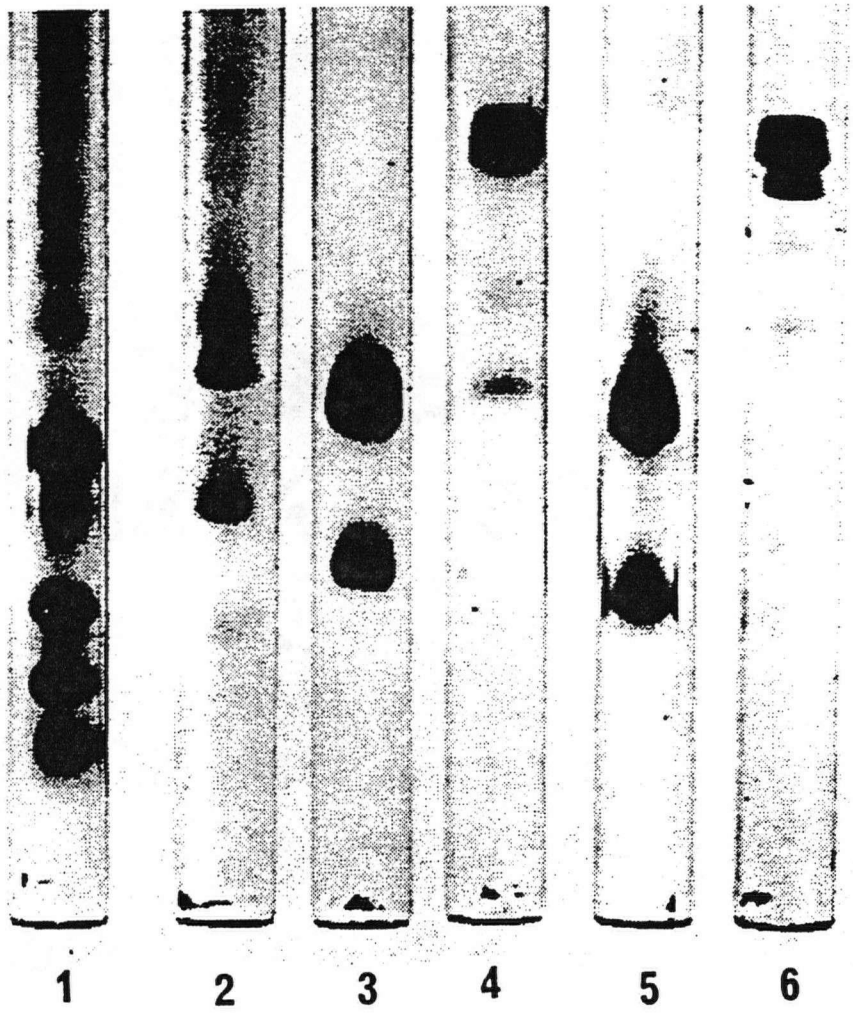

Lane 1. Low molecular weight standards.
Lane 2. High molecular weight standards.
Lane 3. Reduced polyclonal (anti-BSA) IgG preparation.
Lane 4. Non-reduced polyclonal (anti-BSA) IgG preparation.
Lane 5. Reduced nonspecific IgG.
Lane 6. Non-reduced nonspecific IgG.

Appendix 4

Calculation of amount of polyclonal anti-BSA IgG bound per unit area of BSA-coated PSL.

(1). The procedure outlined in Appendix 2 (see above) for the calculation of the amount of BSA adsorbed per unit area of latex was used to calculated the amount of IgG bound per unit area of latex.

(2). For the Scatchard plots the values ν = moles of IgG bound per gram of PSL and the ratio ν/[Ab] were calculated from the amount of IgG bound per unit area of latex and equilibrium concentration of IgG (M_r = 1.5×10^5) as follows:

$$\nu = (\Gamma \times 10^{-3} / 1.5 \times 10^5) \times a_s \quad \text{(moles of IgG/g}_{latex}\text{)}$$

and

$$[Ab] = C/1.5 \times 10^5 \quad \text{(moles/litre)}$$

(3). The amount of IgG bound at saturation was estimated from the intercept of the Scatchard plots and converted into molecules of IgG bound per unit area as follows:

Amount bound (molecules/cm^2) = Intercept (moles of IgG/g_{latex}) $\times$ 1/specific surface area of latex (cm^2/g_{latex}) $\times$ 6.023 $\times$ 10^{23} (molecules/mole of IgG).

(4). The probable error in the amount of IgG bound (molecules/cm^2), as estimated from the intercepts of the Scatchard plots, was estimated using the standard deviation of the residuals assuming that the residuals are a sample of actual experimental errors.

The standard deviation of N residuals is given by

$$s_r = \left(\frac{1}{N-2} \sum_{i=1}^{N} r_i^2 \right)^{1/2}$$

where N is the number of data points, r is the residual of the i^{th} data point and is defined for a linear function as:

$$r_i = y_i - a_1 x_i - a_2$$

where a_1 and a_2 are the slope and intercept of the linear function respectively. Using the fact that at the 95% confidence level, the error in the dependent variable, Δy, lies within 1.96 standard deviation of the mean if the standard normal distribution holds, the expected error in the intercept of the Scatchard plots assuming that the error in the dependent variable is not known is given by

$$\Delta a_2 = \left(\frac{1}{D} \sum_{i=1}^{N} x_i^2 \right)^{1/2} (1.96 s_r)$$

where

$$D = N S_{x2} - S_x^2;$$

$$S_x = \sum_{i=1}^{N} x_i; \text{ and}$$

$$S_{x2} = \sum_{i=1}^{N} x_i^2$$

Appendix 5

Binding isotherms of polyclonal rabbit anti-BSA IgG to BSA-coated PSL with different surface coverage of BSA. The labels (a), (b), (c), and (d) correspond to the number of molecules of BSA bound per cm^2 for each latex type as given in Table XVI (see page 202).

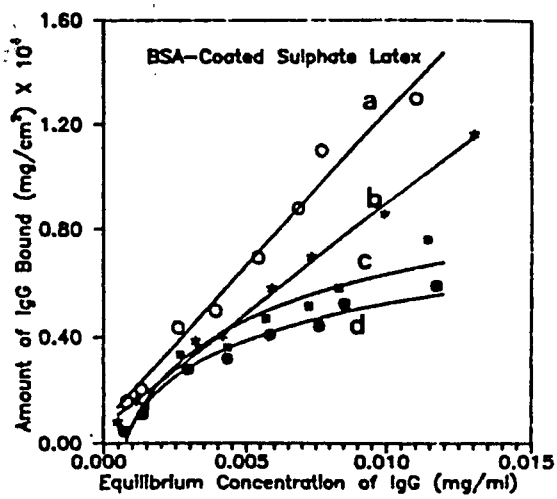

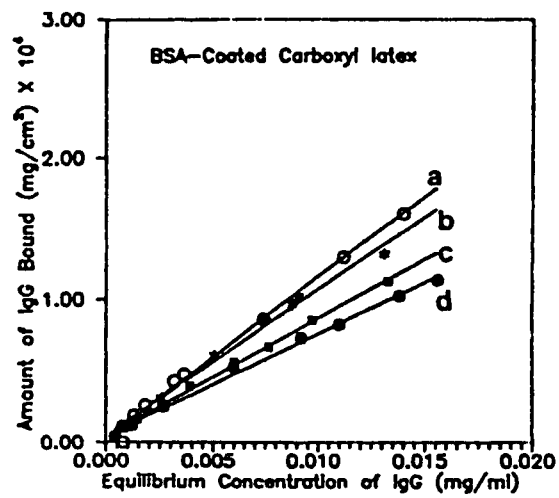

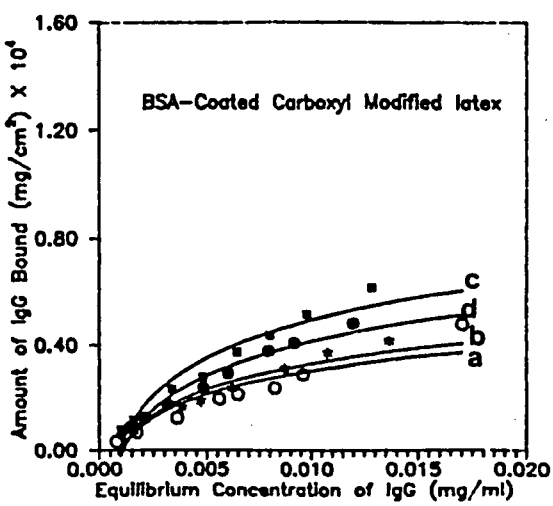

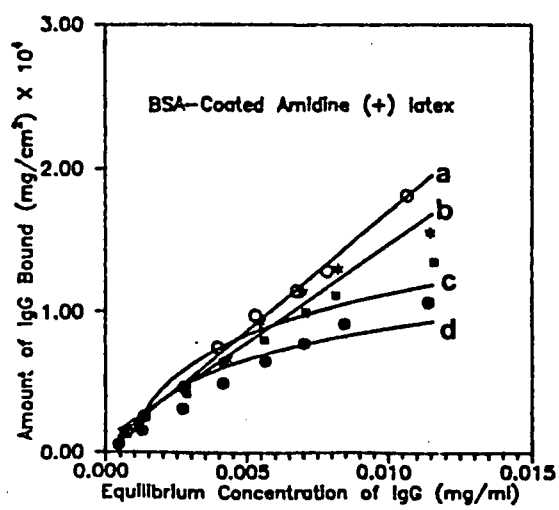

Appendix 6

Scatchard plots of isotherms given in Appendix 5. The labels (a), (b), (c), and (d) correspond to the number of molecules of BSA bound per cm^2 for each latex type as given in Table XVI (see page 202).

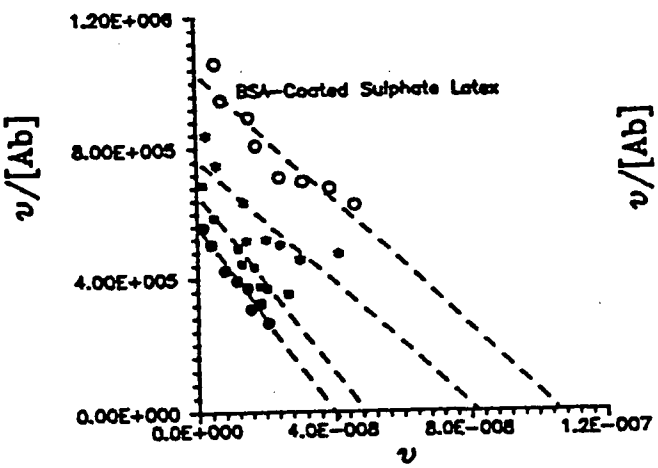

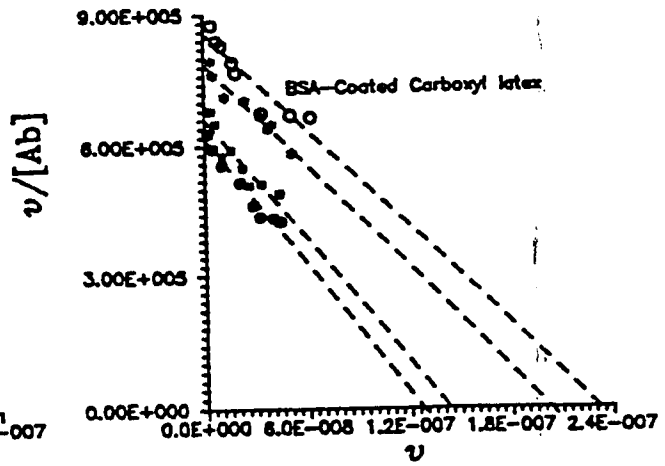

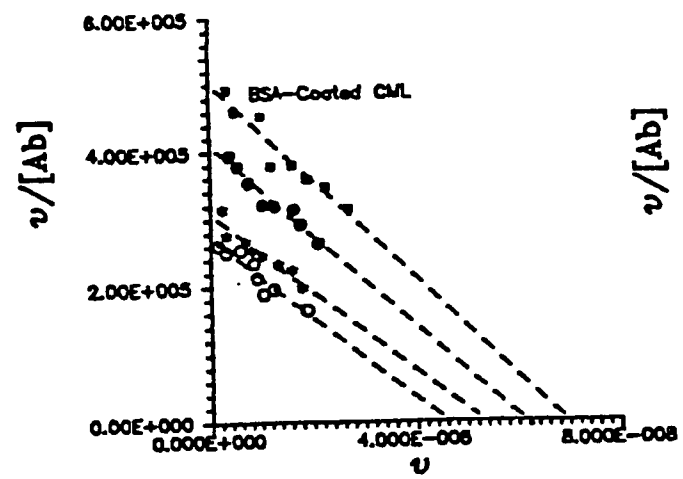

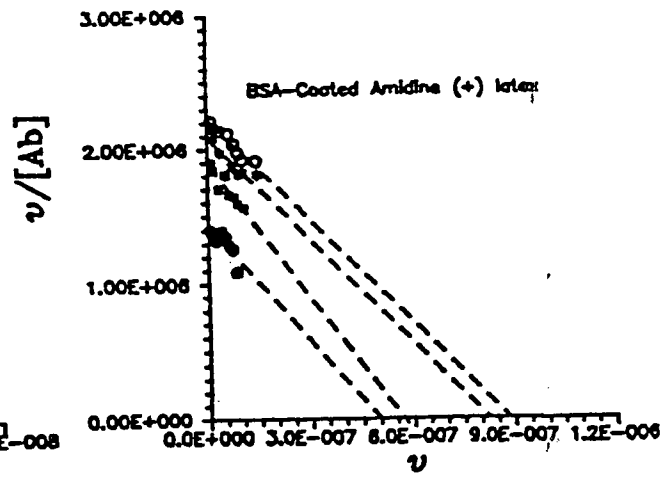

Table XVI

Amounts of BSA and IgG bound per cm^{-2} for the data plots in Appendix 5 and 6.

BSA-Coated latex	Amount of BSA Bound.	Amount IgG bound at saturation. (from Scatchard plots)
	(molecules/cm^2)	(molecules/cm^2)
Sulfate		
(134 cm^2/ml)	(a) $2.72 \pm 0.15 \times 10^{10}$	$1.20 \pm 0.06 \times 10^{12}$
	(b) $8.11 \pm 0.23 \times 10^{10}$	$9.32 \pm 0.83 \times 10^{11}$
	(c) $3.64 \pm 0.17 \times 10^{11}$	$5.57 \pm 0.32 \times 10^{11}$
	(d) $1.05 \pm 0.14 \times 10^{12}$	$4.55 \pm 0.23 \times 10^{11}$
Carboxyl		
(121 cm^2/ml)	(a) $2.15 \pm 0.11 \times 10^{10}$	$2.42 \pm 0.09 \times 10^{12}$
	(b) $7.29 \pm 0.20 \times 10^{10}$	$2.11 \pm 0.05 \times 10^{12}$
	(c) $3.56 \pm 0.23 \times 10^{11}$	$1.48 \pm 0.06 \times 10^{12}$
	(d) $9.95 \pm 0.18 \times 10^{11}$	$1.31 \pm 0.04 \times 10^{12}$
CML		
(106 cm^2/ml)	(a) $3.16 \pm 0.17 \times 10^{9}$	$4.21 \pm 0.14 \times 10^{11}$
	(b) $4.53 \pm 0.29 \times 10^{9}$	$4.95 \pm 0.18 \times 10^{11}$
	(c) $2.75 \pm 0.16 \times 10^{10}$	$6.32 \pm 0.24 \times 10^{11}$
	(d) $2.35 \pm 0.17 \times 10^{11}$	$5.68 \pm 0.15 \times 10^{11}$
Amidine (+)		
(160 cm^2/ml)	(a) $2.08 \pm 0.10 \times 10^{10}$	$4.61 \pm 0.10 \times 10^{12}$
	(b) $6.56 \pm 0.15 \times 10^{10}$	$4.25 \pm 0.07 \times 10^{12}$
	(c) $4.48 \pm 0.18 \times 10^{11}$	$2.95 \pm 0.09 \times 10^{12}$
	(d) $1.24 \pm 0.09 \times 10^{12}$	$2.59 \pm 0.11 \times 10^{12}$

Appendix 7

A model for the stoichiometry of specific and non-specific binding of polyclonal anti-BSA IgG to latex coated with various surface concentrations of antigen. (Personal communication, D.E Brooks, Departments of Pathology and Chemistry, University of British Columbia, B.C., Canada.)

It is evident from Figure 22 that the non-specific binding of IgG to the latex surface is strongly reduced by pre-adsorbed BSA whether or not specific antibody to BSA is present in the polyclonal mixture. In the following model it is assumed that the IgG binding is saturated at each equilibrium point and that depletion effects and binding differences due to variations in affinity within the IgG fraction are negligible.

When the BSA surface concentration, Γ_{BSA}, is low, assume that a constant number of molecules of non-specific IgG, n_{ns}, is displaced per molecule of pre-adsorbed BSA. Near the origin of Figure 22, then, the surface concentration of IgG containing no Ab against BSA, Γ_{ns}, will be given by:

$$\Gamma_{ns} = \Gamma^{0}_{ns} - n_{ns}\Gamma_{BSA} \quad \text{.....(A7.1)}$$

where Γ^{0}_{ns} is the surface IgG concentration adsorbed at saturation to the bare latex surface. If the IgG fraction contains antibodies specific for BSA, assume n_{sp} IgG molecules bind specifically to epitopes on the antigen. In this case, again when Γ_{BSA} is low, pre-adsorption of BSA will both replace non-specifically adsorbed IgG and bind n_{sp} IgG molecules per BSA molecule. Therefore, the total amount of IgG bound per unit area, Γ_{sp}, will be:

$$\Gamma_{sp} = \Gamma^{o}_{ns} - n_{ns}\Gamma_{BSA} + n_{sp}\Gamma_{BSA} \quad \text{.....(A7.2)}$$

Hence, the initial slopes $\left(\frac{\Delta\Gamma_{ns}}{\Delta\Gamma_{BSA}} \right)$ and $\left(\frac{\Delta\Gamma_{sp}}{\Delta\Gamma_{BSA}} \right)$ provide estimates for n_{ns} and n_{sp}, since from Equations (A7.1) and (A7.2) above:

$$\left(\frac{\Delta\Gamma_{ns}}{\Delta\Gamma_{BSA}} \right) = -n_{ns} \quad \text{.....(A7.3)}$$

and

$$\left(\frac{\Delta\Gamma_{sp}}{\Delta\Gamma_{BSA}} \right) = (n_{sp} - n_{ns}) \quad \text{.....(A7.4)}$$

The initial slopes in Figure 22 give:

$$n_{ns} \cong 8 \quad \text{and} \quad n_{sp} \cong 3$$

At high BSA coverage, since each BSA molecule replaces about 8 IgG molecules from the surface, the regions from which they exclude IgG will overlap and reduction in IgG binding saturate above some surface BSA concentration, Γ^{*}_{BSA}. For $\Gamma_{BSA} > \Gamma^{*}_{BSA}$, Γ_{ns} will remain constant as more BSA is put on the surface within the regions from which IgG is excluded. If BSA packing on the surface was perfectly regular, Γ_{ns} would be zero above Γ^{*}_{BSA}. However, this is not the case and there is a small amount of non-specific adsorption remaining at high Γ_{BSA}, $\Gamma_{ns,s}$.

Due to statistical and geometric effects the transition between the linear decrease in Γ_{ns}, and its saturation at $\Gamma_{ns,s}$ is not sharp, but Γ^{*}_{BSA} can be estimated by making the simplifying assumption that Γ_{ns} obeys

the following conditions:

$$\Gamma_{ns} = \Gamma^{*}_{ns} - n_{ns}\Gamma_{BSA}; \quad \text{for } \Gamma_{BSA} \ll \Gamma^{*}_{BSA} \quad \text{.....(A7.5)}$$

$$\Gamma_{ns} = \Gamma_{ns,s}; \quad \text{for } \Gamma_{BSA} \gg \Gamma^{*}_{BSA} \quad \text{.....(A7.6)}$$

Hence Γ^{*}_{BSA} can be estimated from the intersection of the two lines to be

$$\Gamma^{*}_{BSA} \approx 0.15 \times 10^{12} \text{ molecules/cm}^2$$

In the case in which specific Ab binding is present as well as replacement a similar analysis can be applied. At low Γ_{BSA}, Γ_{sp} is assumed to decrease linearly with increasing Γ_{BSA}. At high Γ_{BSA}, IgG binding again saturates, in this case at the higher value , $\Gamma_{sp,s}$, associated with the specific binding of Ab added to the remnant non-specifically bound material. That Γ_{sp} approaches the constant value $\Gamma_{sp,s}$ suggests that surface bound BSA can exclude specifically bound IgG as well as non-specifically adsorbed antigen. Again, the transition of Γ_{sp} from a linear decrease to a constant value is assumed to occur at the some value Γ'_{BSA}. Intersection of the appropriate linear regions on Figure 22 gives:

$$\Gamma'_{BSA} \approx 0.15 \times 10^{12} \text{ molecules/cm}^2$$

This is in good agreement with Γ^{*}_{BSA}, suggesting that the above model is reasonable. It follows that the difference ($\Gamma_{ns} - \Gamma_{sp}$) represents the amount of antibody specifically bound to surface adsorbed Ag; its concentration dependence is shown as the solid line in Figure A7 below.

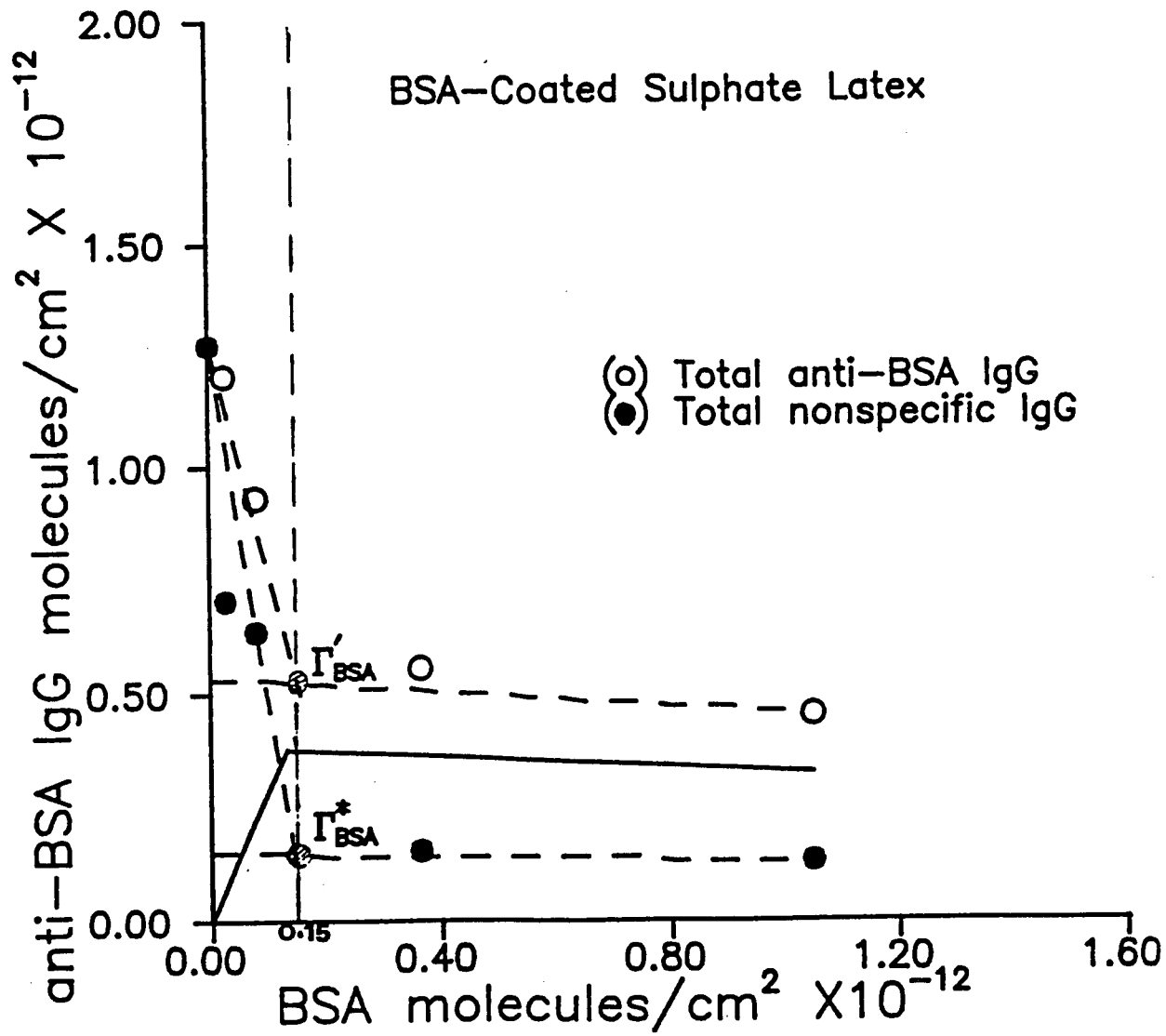

Figure A7. Plots according to Equations A7.1 and A7.2.

Appendix 8 (a)

Absorption spectra of PSL at different volume fractions. The range of volume fractions for each latex type can be seen from the abscissa of the Beer-Lambert plots of the same data in Appendix 8 (b).

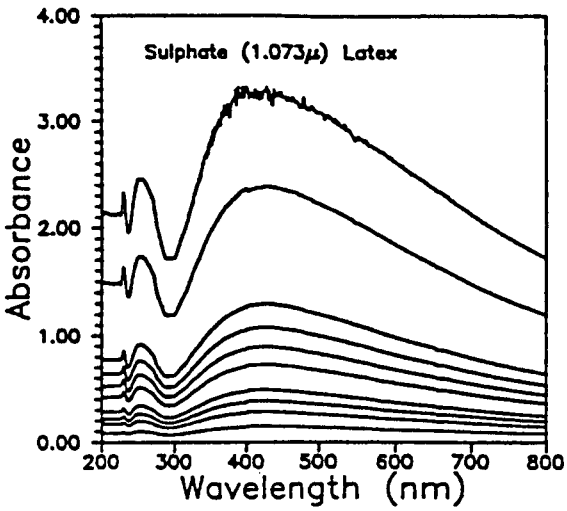

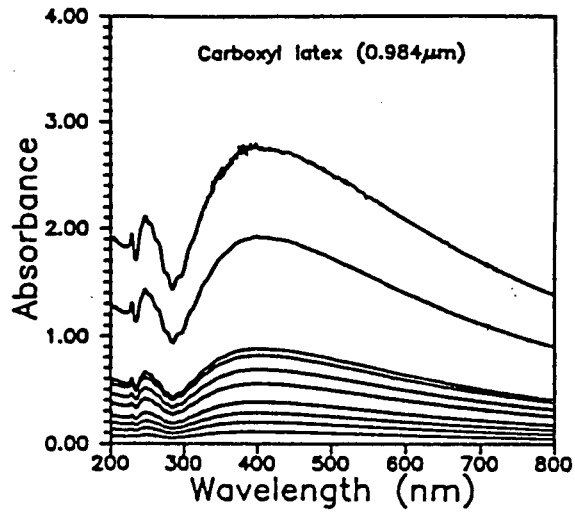

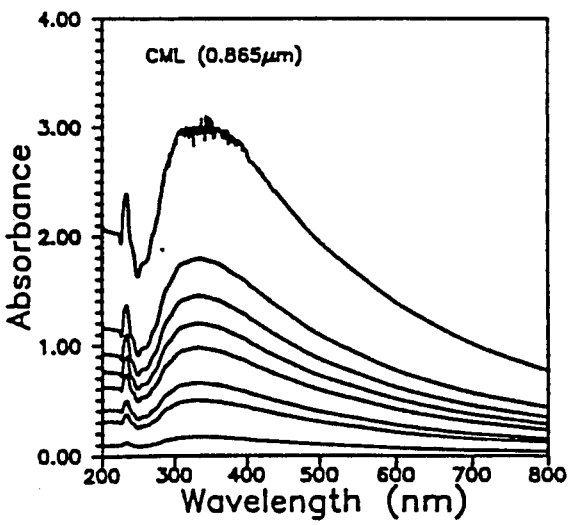

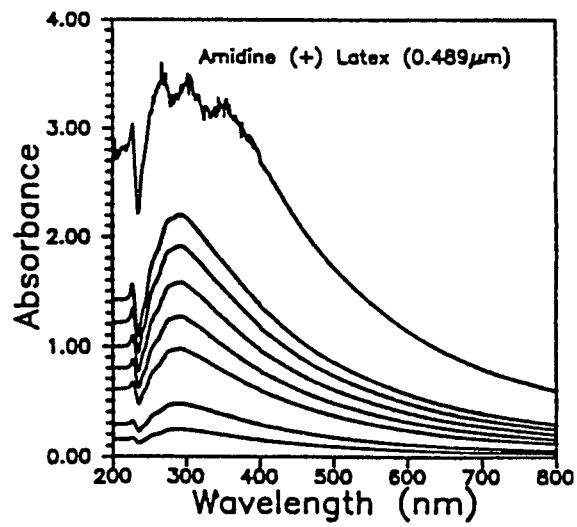

Appendix 8 (b)

Beer-Lambert plots at different wavelengths (400-800nm) for plots of absorption spectra of different PSl given in Appendix 8 (a).

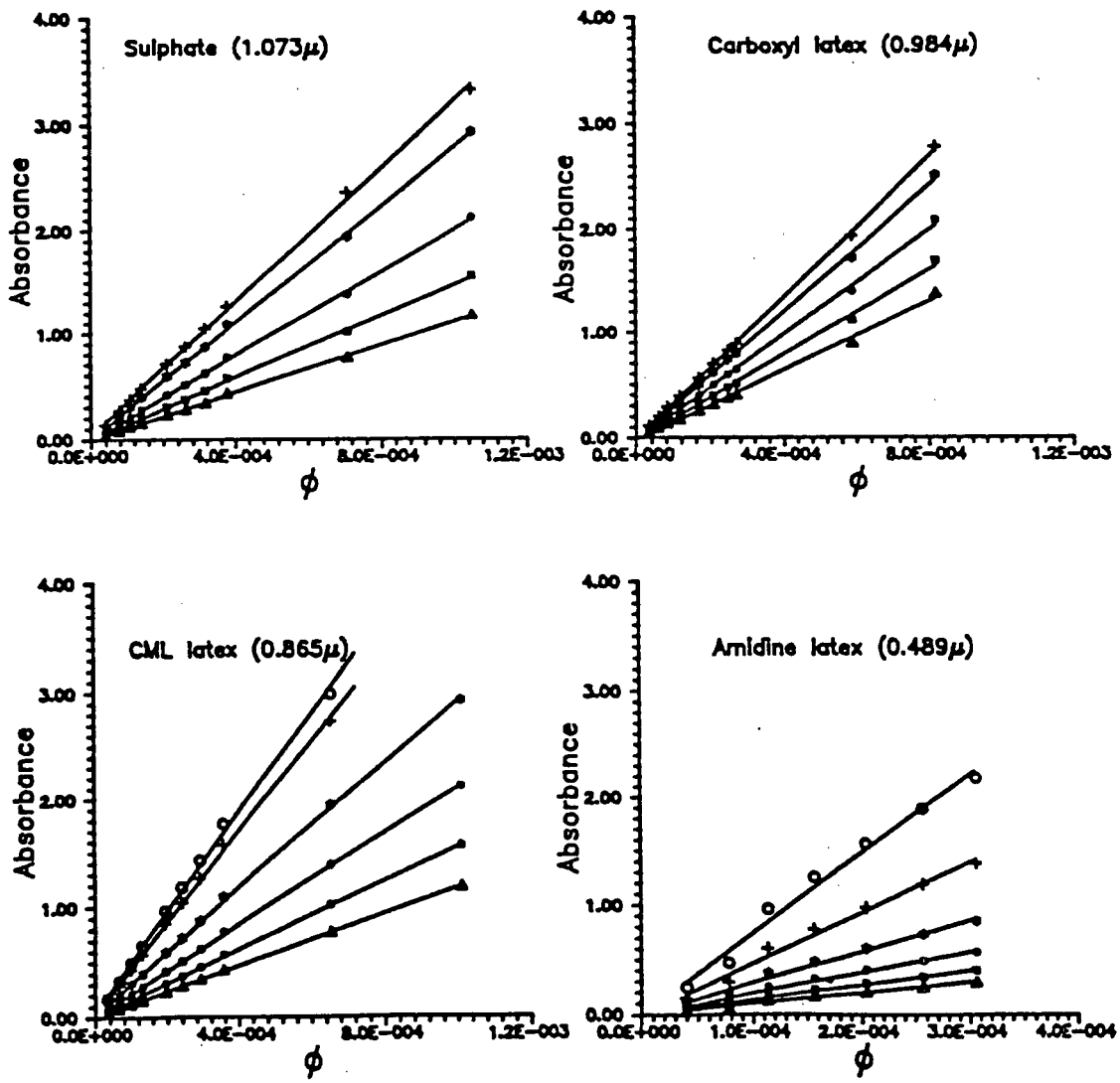

Appendix 9 (a)

Plots of optical absorbance at various times (0-180 min.) *vs* wavelength for coagulating PSL, in the absence of shear. Each curve represents a 20 minute interval.

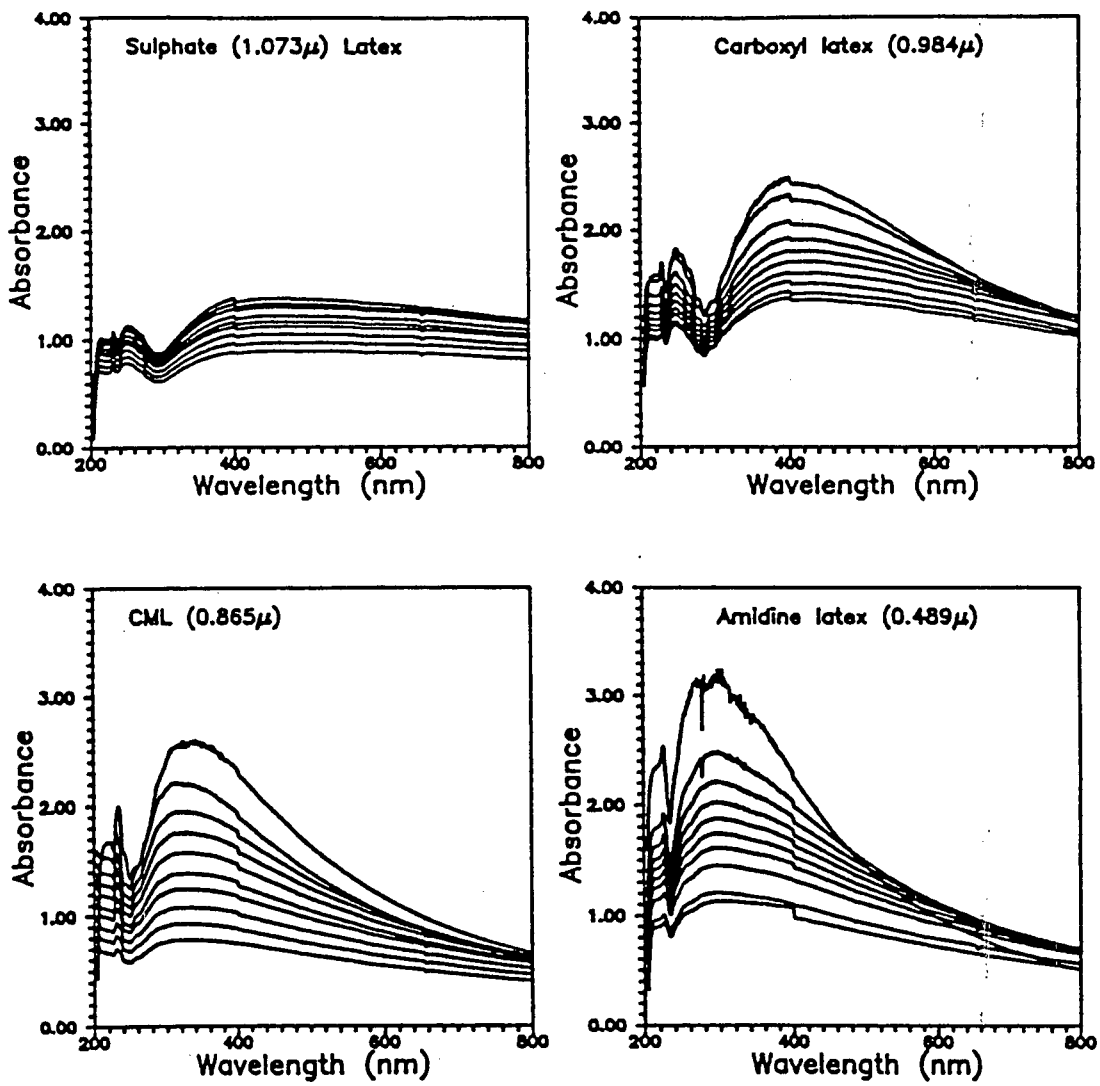

Appendix 9 (b)

Plots of optical absorbance at different wavelengths *vs* time (min.) for coagulating PSL in a 1 cm × 1 cm quartz cuvette.

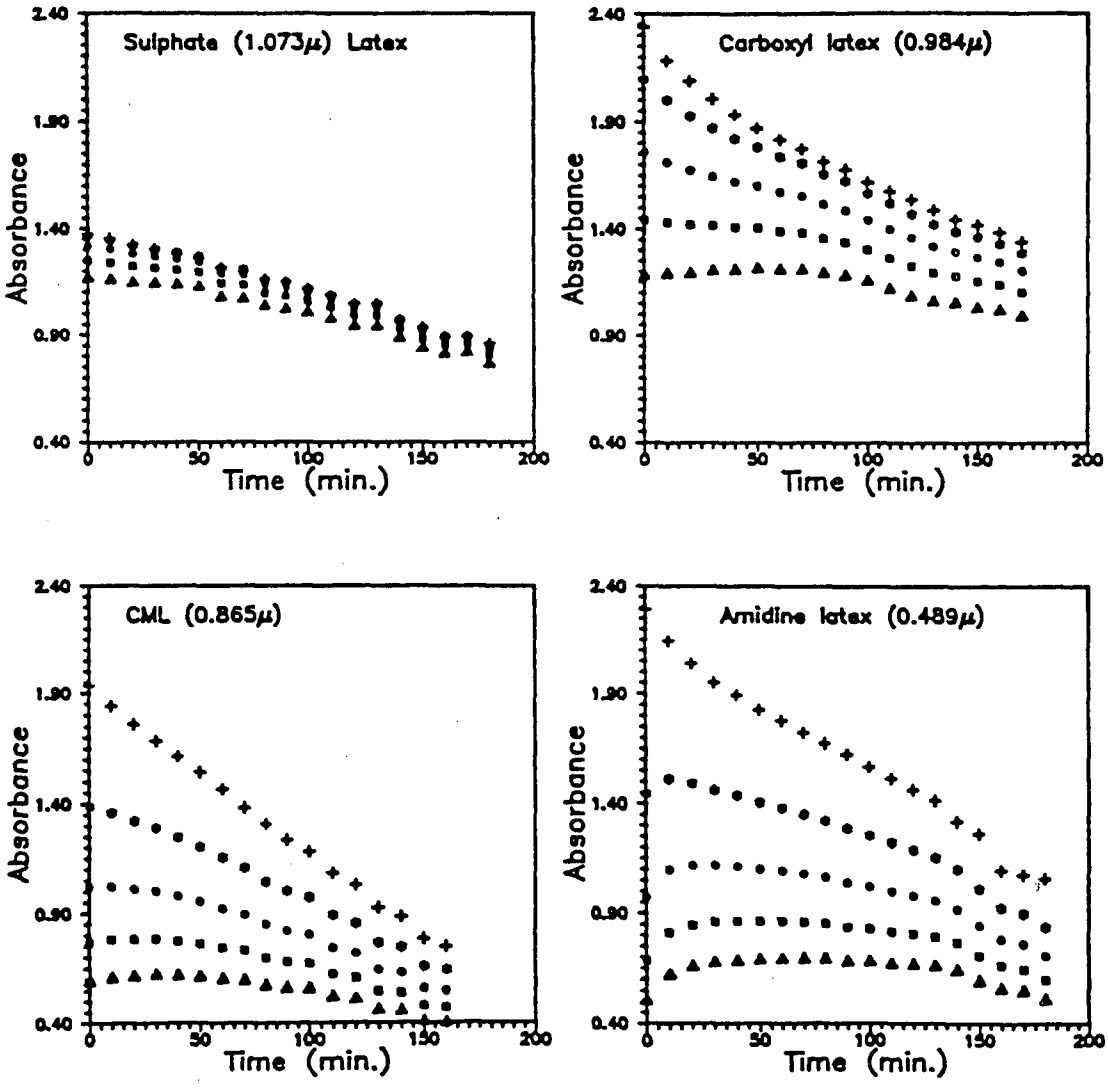

(+) 400 nm, (✳) 500 nm (●) 600 nm (■) 700 nm (▲) 800 nm)

Appendix 10 (a)

Optical absorbance *vs* time (sec.) plots for agglutination of BSA-coated sulfate latexes with different surface densities of BSA: (A) 2.72×10^{10}, (B) 8.11×10^{10}, (C) 3.64×10^{11}, and (D) 1.05×10^{12} molecules cm^{-2}. The effect of varying anti-BSA IgG concentration. The equilibrium concentration of antibodies for the curves identified are given on page 212.

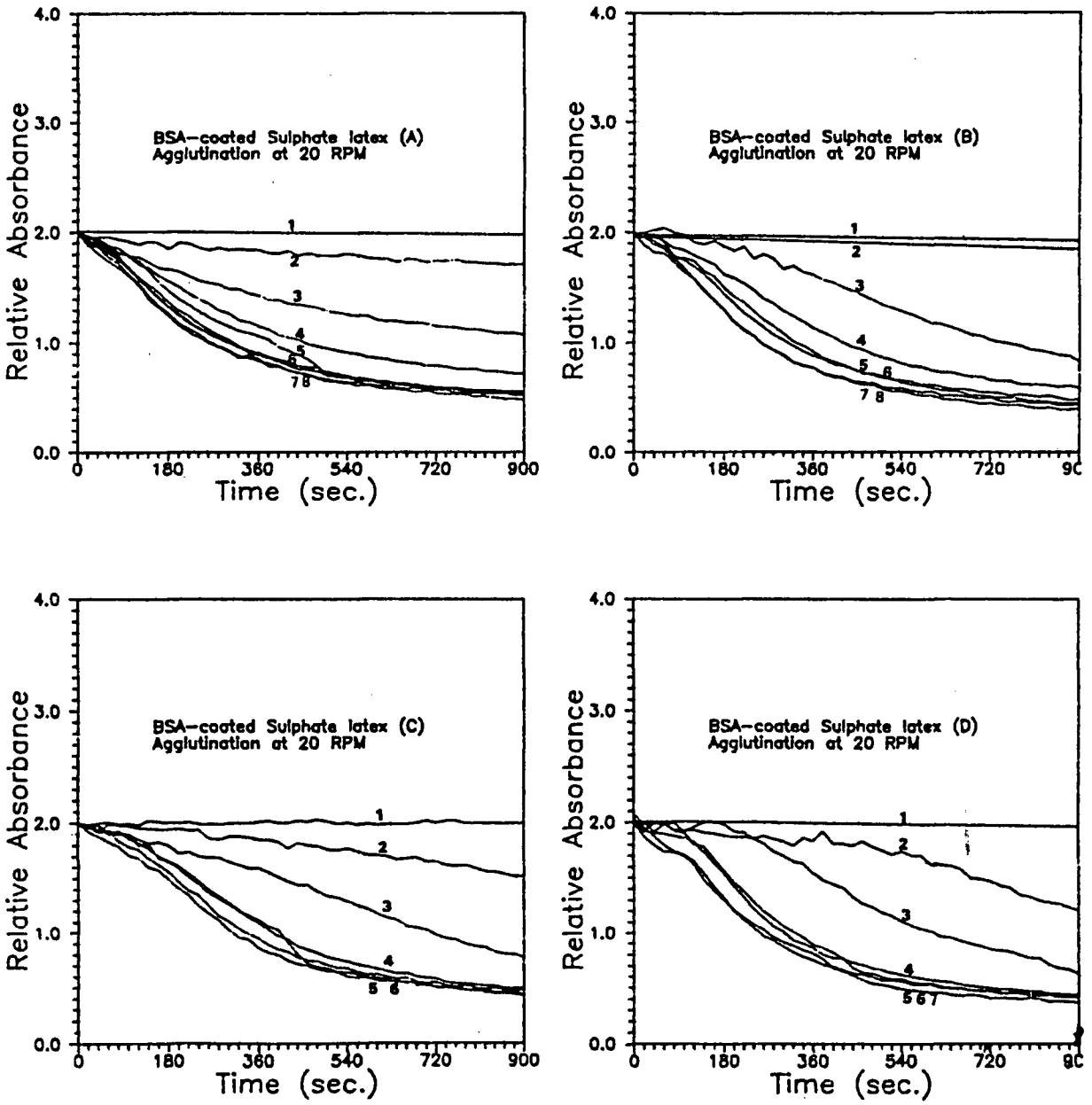

Summary of equilibrium concentrations of IgG for data shown in Appendix 10 (a).

Sample: (A)

(1) 4.3×10^{-5}, (2) 1.95×10^{-4}, (3) 3.99×10^{-4}, (4) 1.5×10^{-3}, (5) 3.08×10^{-3}, (6) 9.05×10^{-3}, (7) 1.48×10^{-2}, (8) 2.72×10^{-2}, (9) 5.99×10^{-2} (mg/ml).

Sample: (B)

(1) 4.3×10^{-5}, (2) 1.99×10^{-4}, (3) 3.76×10^{-4}, (4) 1.54×10^{-3}, (5) 3.07×10^{-3}, (6) 6.15×10^{-3}, (7) 1.19×10^{-2}, (8) 1.82×10^{-2}, (9) 5.99×10^{-2} (mg/ml).

Sample: (C)

(1) 3.9×10^{-4}, (2) 1.52×10^{-3}, (3) 6.17×10^{-3}, (4) 1.2×10^{-2}, (5) 1.82×10^{-2}, (6) 6.01×10^{-2} (mg/ml).

Sample: (D)

(1) 1.9×10^{-4}, (2) 1.5×10^{-3}, (3) 2.54×10^{-3}, (4) 6.2×10^{-3}, (5) 8.97×10^{-3}, (6) 1.21×10^{-2} (7) 6.011×10^{-2} (mg/ml).

Appendix 10 (b)

Plots of optical absorbance at various agglutination times as a function of equilibrium IgG concentrations for shear agglutination at 28 s^{-1} of BSA-coated sulfate latex with surface coverage (a), (b), (c), and (d) as given in Figure 28 (see page 156).

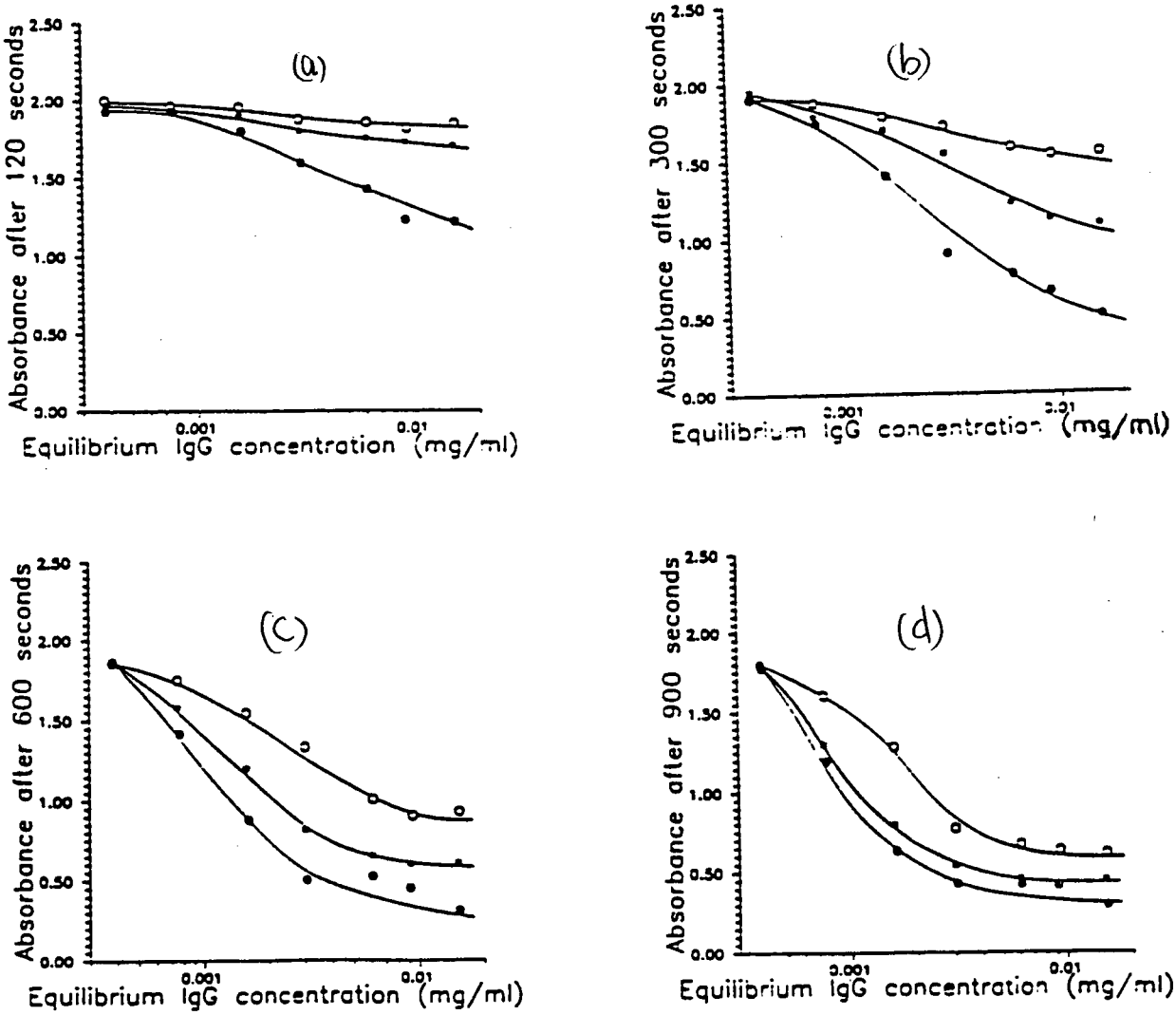

(O) 120 min., (✱) 300 min. and (●) 900 min.

Appendix 10 (c)

Optical absorbance vs time (sec.) plot for agglutination of BSA-coated sulfate latex (1.05×10^{12} molecules cm^{-2}). The effect of varying shear rates. The equilibrium concentrations of antibodies for the curves identified are given on page 215.

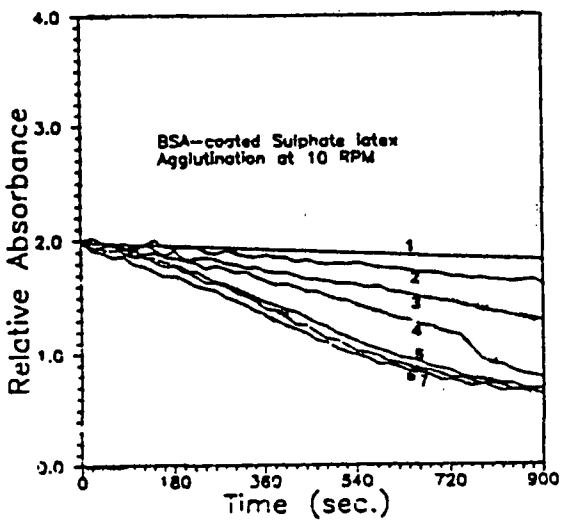

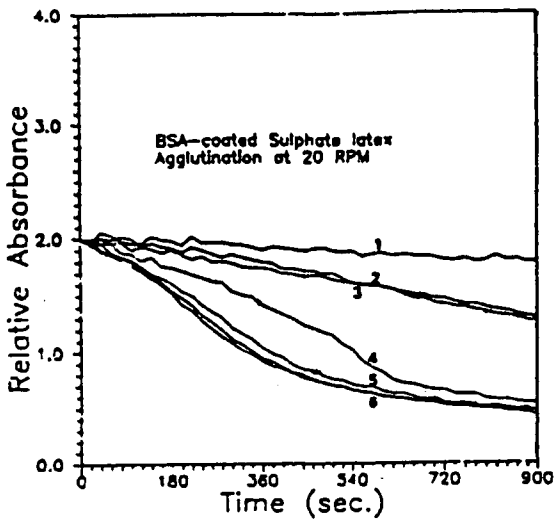

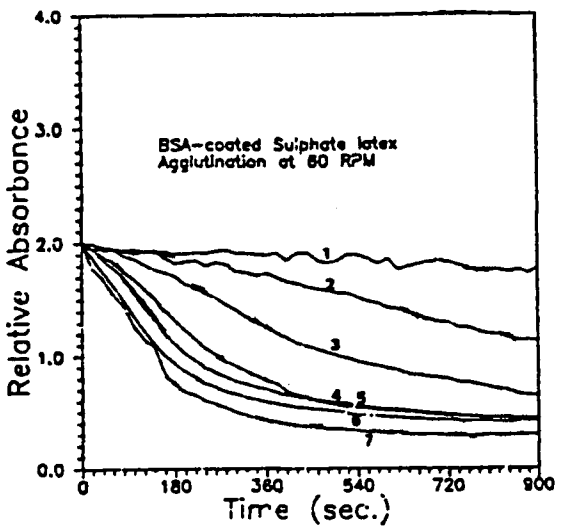

Summary of equilibrium concentrations of IgG for data shown in Appendix 10 (c).

Data for agglutination at 10 rpm (14 s^{-1})

(1) 3.8×10^{-4}, (2) 7.5×10^{-4}, (3) 1.57×10^{-3}, (4) 3.0×10^{-3}, (5) 6.03×10^{-3}, (6) 9.1×10^{-3} (7) 1.50×10^{-2} (mg/ml).

Data for agglutination at 20 rpm (28 s^{-1})

(1) 3.84×10^{-4}, (2) 7.5×10^{-4}, (3) 1.57×10^{-3}, (4) 3.0×10^{-3}, (5) 6.03×10^{-3}, (6) 9.1×10^{-3} (7) 1.50×10^{-2} (mg/ml).

Data for agglutination at 60 rpm (81 s^{-1})

(1) 3.85×10^{-4}, (2) 7.7×10^{-4}, (3) 1.6×10^{-3}, (4) 3.05×10^{-3}, (5) 6.07×10^{-3}, (6) 9.08×10^{-3} (7) 1.53×10^{-2} (mg/ml).

Appendix 10 (d)

Optical absorbance *vs* time (sec.) plots for agglutination of BSA-coated sulfate latex (1.05×10^{12} molecules cm^{-2}). The effect of varying BSA-coated latex concentration and equilibrium IgG concentration: (1) 4.59×10^{9}; (2) 9.09×10^{9}; (3) 1.82×10^{10} and (4) 2.69×10^{10} BSA-coated particles/ml.

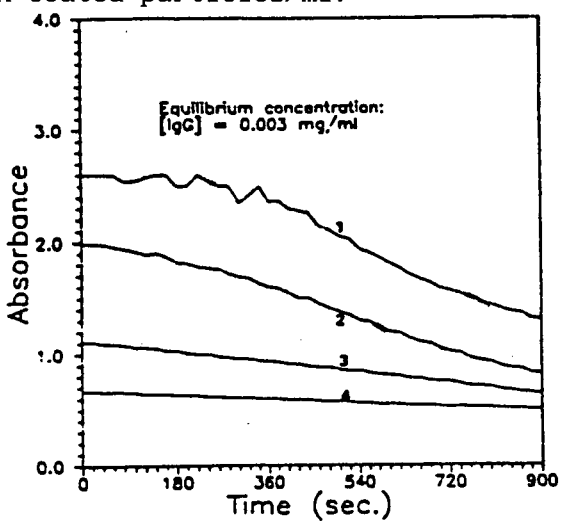

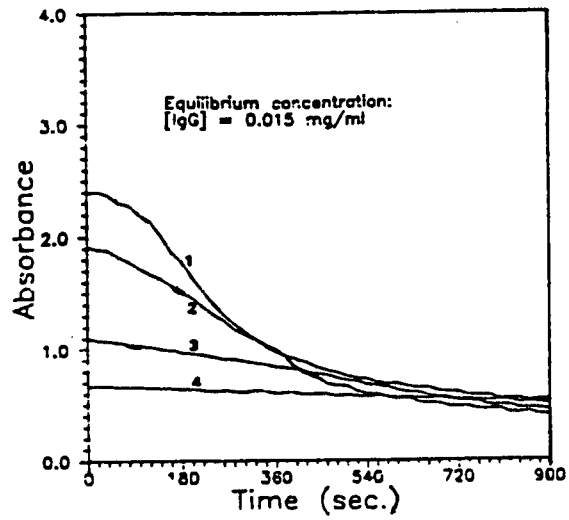

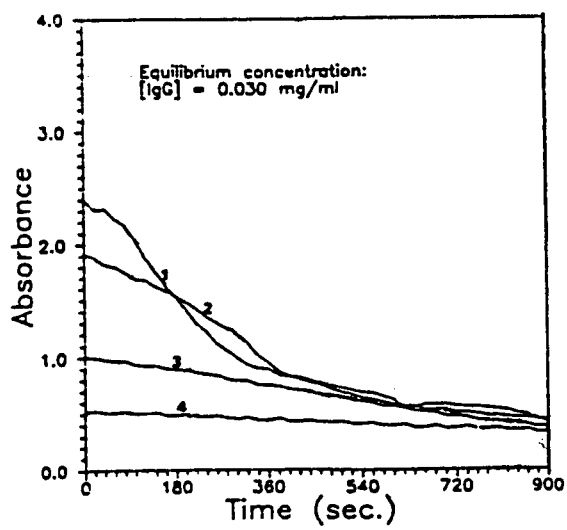

Appendix 11 (a)

Optical absorbance *vs* time (sec.) plot for agglutination of BSA-coated amidine (+) latex (0.45 mg m^{-2}). The effect of varying shear rates.

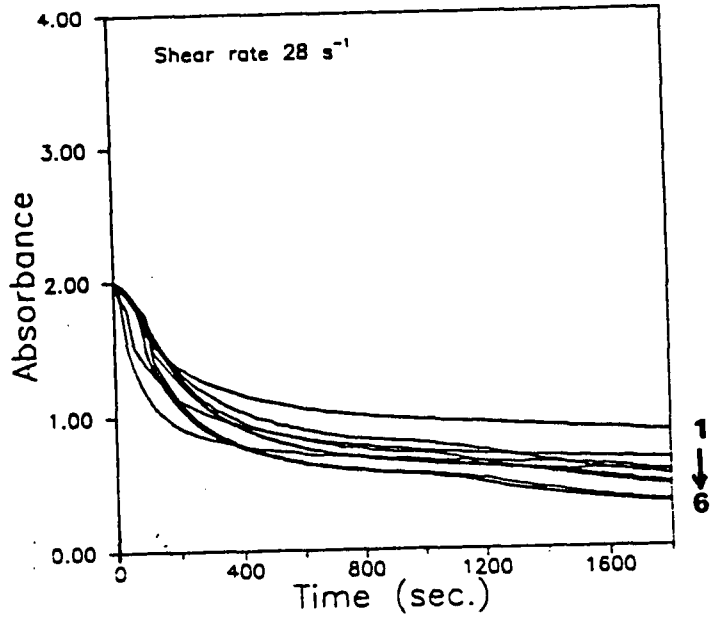

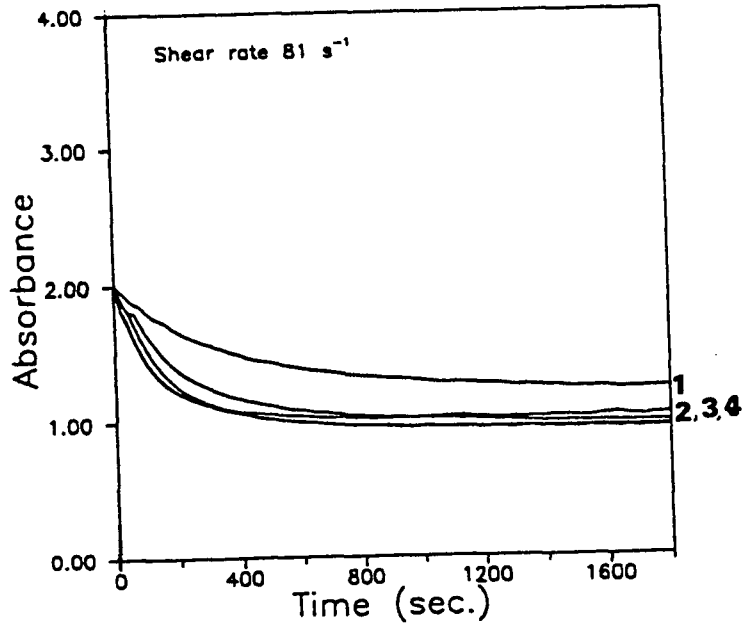

1. Apendix 11 (a):Amidine (+) latex: BSA surface coverage ≈ 0.45 mg m^{-2}.

Equilibrium concentration of IgG (mg/ml) for agglutination at 28 s^{-1}:

(1) 0.0048; (2) 0.0097; (3) 0.0188; (4) 0.028; (5) 0.0470 and (6) 0.0940

Equilibrium concentration of IgG (mg/ml) for agglutination at 81 s^{-1}:

(1) 0.0048; (2) 0.0097; (3) 0.0188; (4) 0.028.

Appendix 11 (b)

Optical absorbance vs time (sec.) plot for agglutination of BSA-coated amidine (+) latex (0.60 mg m^{-2})). The effect of varying shear rates.

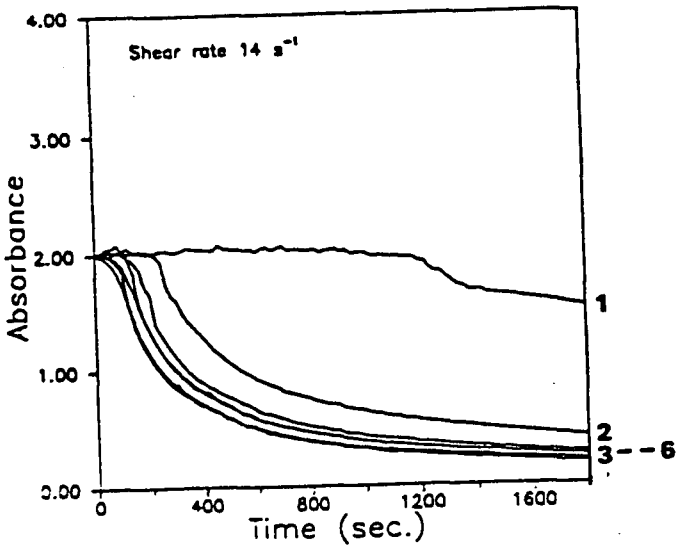

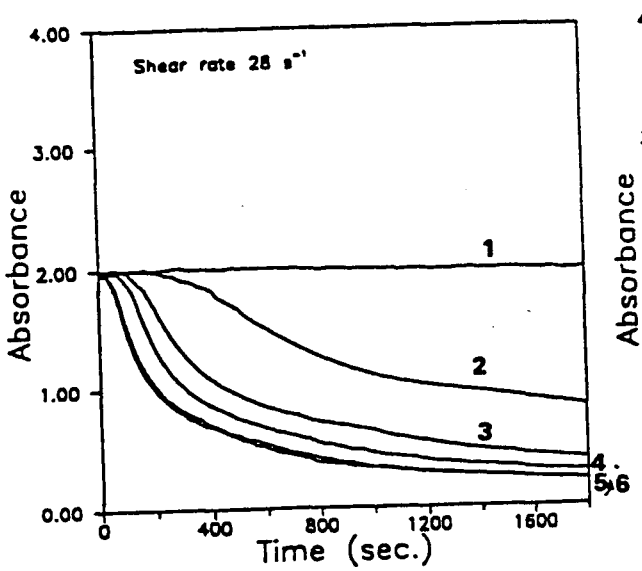

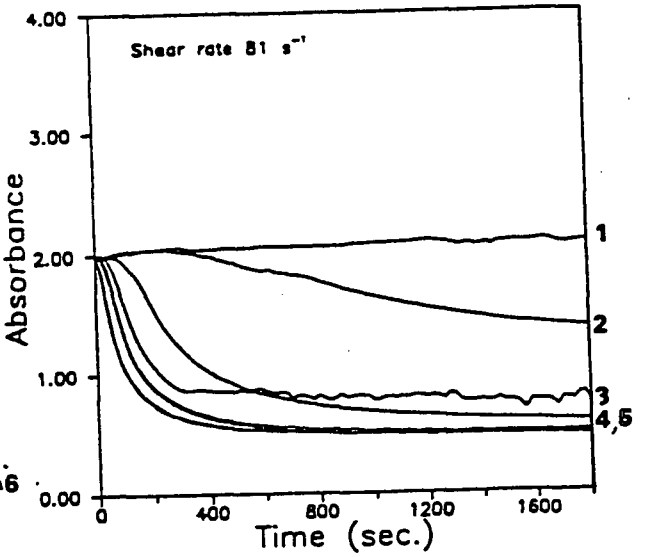

2. Apendix 11 (b):Amidine (+) latex: BSA surface coverage ≈ 0.60 mg m^{-2}.

Equilibrium concentration of IgG (mg/ml) for agglutination at 14 s^{-1}:

(1) 0.0000; (2) 0.0016; (3) 0.0056; (4) 0.0116; (5) 0.0226; (6) 0.0336

Equilibrium concentration of IgG (mg/ml) for agglutination at 28 s^{-1}:

(1) 0.0000; (2) 0.0016; (3) 0.0056; (4) 0.0116; (5) 0.0226; (6) 0.0336

Equilibrium concentration of IgG (mg/ml) for agglutination at 81 s^{-1}:

(1) 0.0000; (2) 0.0016; (3) 0.0056; (4) 0.0116; (5) 0.0226

Appendix 11 (c)

Optical absorbance vs time (sec.) plot for agglutination of BSA-coated amidine (+) latex (0.75 mg m^{-2}). The effect of varying shear rates.

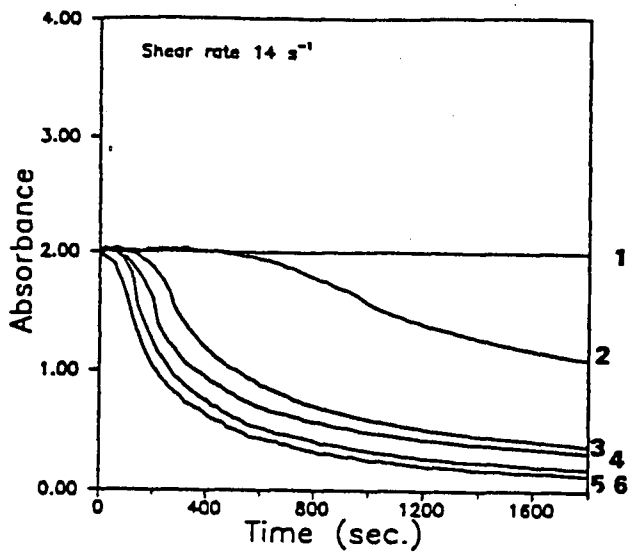

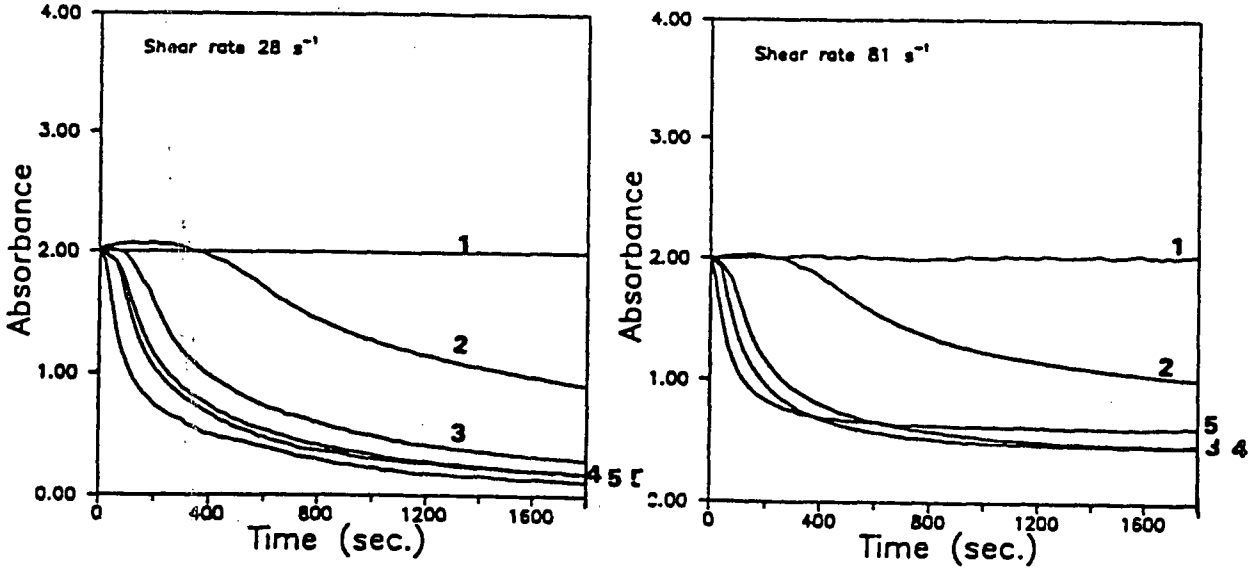

3. Appendix 11 (c):Amidine (+) latex: BSA surface coverage ≈ 0.75 mg m^{-2}.

Equilibrium concentration of IgG (mg/ml) for agglutination at 14 s^{-1}:

(1) 0.00 (2) 0.002 (3) 0.009 (4) 0.018 (5) 0.035 (6) 0.173

Equilibrium concentration of IgG (mg/ml) for agglutination at 28 s^{-1}:

(1) 0.000 (2) 0.002 (3) 0.009 (4) 0.017 (5) 0.035 (6) 0.174

Equilibrium concentration of IgG (mg/ml) for agglutination at 81 s^{-1}:

(1) 0.00 (2) 0.0017 (3) 0.087 (4) 0.0175 (5) 0.174

Appendix 11 (d)

Optical absorbance vs time (sec.) plot for agglutination of BSA-coated amidine (+) latex (1.8 mg m^{-2}). The effect of varying shear rates.

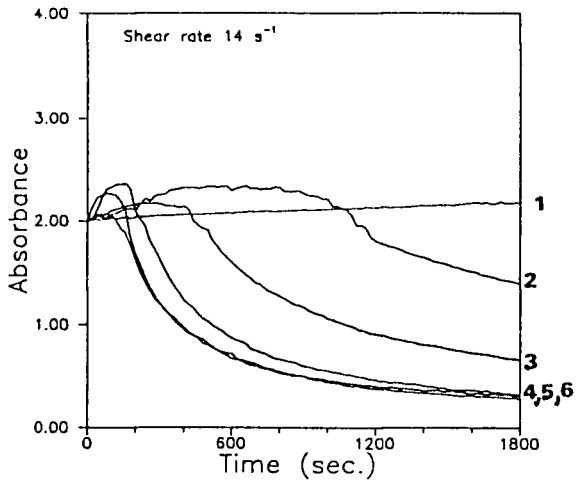

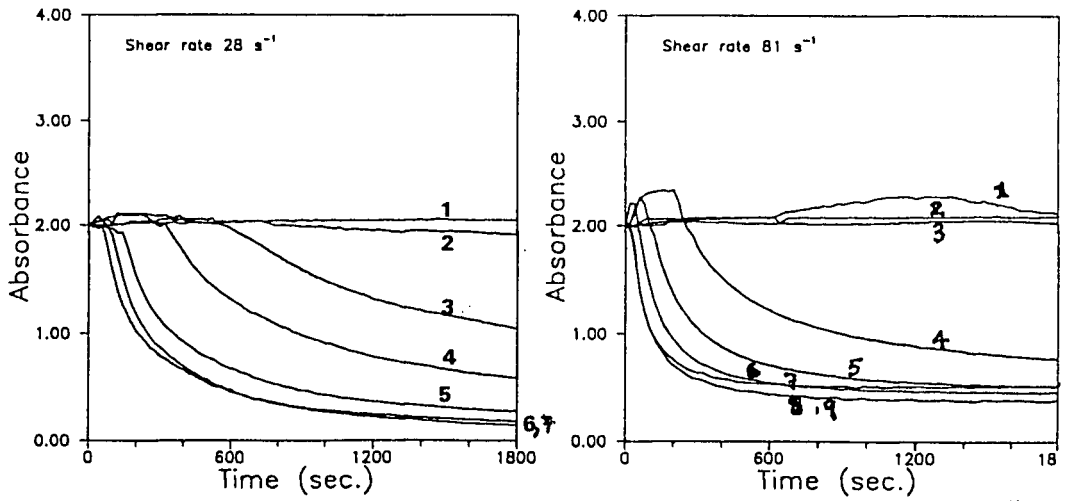

4. Appendix 11 (d):Amidine (+) latex: BSA surface coverage ≈ 1.80 mg m^{-2}.

Equilibrium concentration of IgG (mg/ml) for agglutination at 14 s^{-1}:

(1) 0.012; (2) 0.018; (3) 0.024; (4) 0.036; (5) 0.048; (6) 0.121

Equilibrium concentration of IgG (mg/ml) for agglutination at 28 s^{-1}:

(1) 0.006 (2) 0.012; (3) 0.0318; (4) 0.024; (5) 0.036; (6) 0.048; (7) 0.121.

Equilibrium concentration of IgG (mg/ml) for agglutination at 81 s^{-1}:

(1) 0.00; (2) 0.0088; (3) 0.018; (4) 0.035; (5) 0.052; (6) 0.070; (7) 0.070, (8) 0.084; (9) 0.173.

Appendix 12

Floc formation in agglutinating BSA-coated sulfate latex at constant volume fraction but different shear rates : 3.7 s^{-1} and 21.6 s^{-1}.

Agglutination at 3.7 s^{-1}:

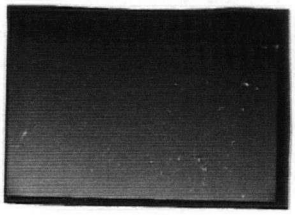

1.2 min.

4 min.

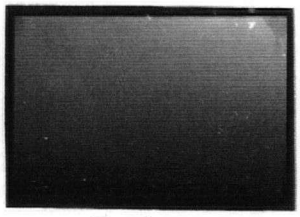

7 min.

10 min.

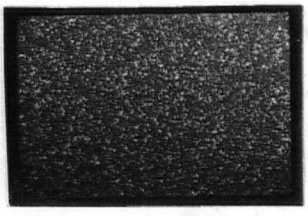

15 min.

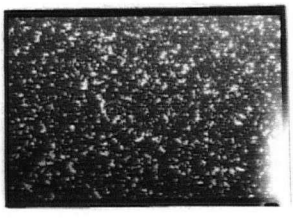

30 min.

Agglutination at 21.6 s^{-1}:

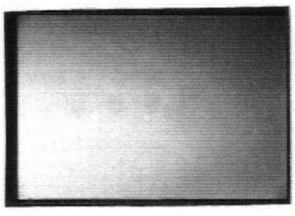

1.2 min.

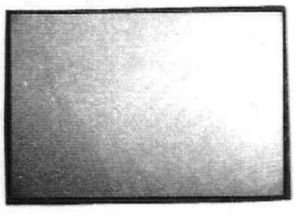

4 min.

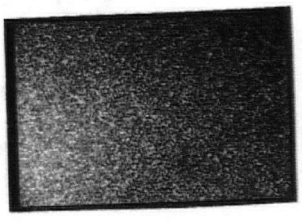

7 min.

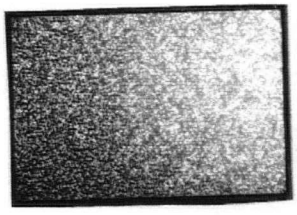

10 min.

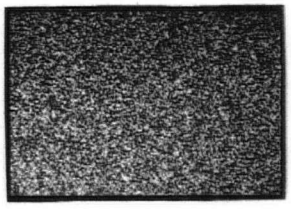

15 min.

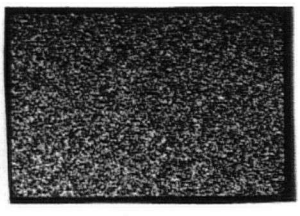

30 min.

References

1. Singer, J.M. and Plotz, C.M. (1956). The latex fixation test. I. Apllication to the serological diagnosis of rheumatoid arthritis. *Am. J. Med.*, **21**, 888.

2. Hechemy, E.K., and Michaelson, E.F. (1984). Latex Particle Assays. *Laboratory Management*, **22(6)**, 27, ff(part 1) and **22(7)**, 26 ff(part II).

3. Singer, J.M., (1987). The use of polystyrene latexes in Medicine. In: *"Future Directions in Polymer Colloids"* p. 371. Eds. El-Aasser, M.S. and Fitch, R. (Martinus Nijhoff Publishers, Dordrecht, The Netherlands).

4. Leigh B. Bangs. (1984). *Uniform Latex Particles*. Seradyn Diagnostic Inc.

5. Nato, T.A. and Miale, J.B. (1960). New immunological test for pregnancy. *Am. J. Clin. Pathol.* **44**, 273-278.

6. "Biomedical Applications of polymer colloids: Future Directions. Position Paper #1. (1987). In:*"Future Directions in Polymer Colloids"*. p. 307-313. Eds. El-Aasser, M.S. and Fitch, R. (Martinus Nijhoff Publishers, Dordrecht, The Netherlands).

7. "Future Directions in Latex Agglutination Assays. Position Paper #2. (1987). In: *"Future Directions in Polymer Colloids"*. p. 315-319. Eds. El-Aasser, M.S. and Fitch, R. (Martinus Nijhoff Publishers, Dordrecht, The Netherlands).

8 **(a)**. Ottewill, R.H. and Shaw, J.N. (1967). Studies on the preparation and characterization of monodisperse polystyrene latices. I. Preparation. *Kolloid Z u. Z. Polymere,* **215**, 161-166.

(b). Woods, M.E., Dodge, J.S., Krieger, I.M., Pierce, P.E. (1968). Monodisperse Latices. I. Emulsion polymerization with mixtures of anionic and nonionic supernatants. *J. Paint Technol.,* **40**, 541-548.

9. Magawinata, T., El-Aasser, M.S., Klein, A. and Vanderhoff, J.W. (1984). Kinetic Studies of Semi-batch Emulsion Copolymerization of 80:20 vinyl acetate-butyl acrylate. *J. Dispersion Sci. Technol.* **5**, 301.

10. Vanderhoff, J.W., van den Hul, H.L., Tansk, R.J.M., and Overbeek, J.Th.G. (1970). *Clean Surfaces: Their Preparation and Characterization for Interfacial Studies.* Ed. Goldfinger, G. (Mercel Dekker, New York).

11. Harkins, D. (1947). A General Theory of the Mechanism of Emulsion Polymerization. *J. Am. Chem. Soc.* , **69**, 1428.

12. Smith, W.V. and Ewart, R.H., (1948). Kinetics of Emulsion Polymerization. *J. Chem. Phys.,* **16**, 592.

13. Priest, W.J. (1952). Particle growth in the Aqueous Polymerization of vinyl acetate. *J. Phys. Chem.* **56**, 1077.

14. Patsiga, R., Litt, M. and Stannett, V. (1960). The Emulsion Polymerization of vinyl acetate. Part 1. *J. Phys. Chem.*, **64**, 801.

15. Fitch, R.M. (1971). "*Polymer Colloids*" Ed. Fitch, R.M., Plenum, New York, p. 73.

16. **(a)** Kotera, A., Furusawa, K. and Takeda, Y. (1970). Colloid Chemical Studies of Polystyrene latices polymerize without any surface active agents. I. Method for preparing monodisperse latices and their characterization. *Kolloid Z. u. Z.. Polymere*, **239**, 677.
(b) Goodwin, J.W. Ottewill, R.H. Pelton, R., Vianell, G. and Yates, D.E. (1978). Control of Particle Size in the Formation of Polymer Latexes. *Brit. Polym. J.* **10**, 179.

17. Vanderhoff, J.W. (1987). Semi-Continous Emulsion polymerization. In:"*Future Directions in Polymer Colloids*" Eds. El-Aasser, M.S. and Fitch, R. Martinus Nijhoff Publishers, Dordrecht, The Netherlands, p. 23.

18. Uglelstad, J., Berge, A., Ellingsen, T., Bjorun, J., Schmid, R., Stenstad, P., Aume, O., Nilsen, T.N., Fundernd, S. and Nustad, K. (1987). Biomedical applications of monodisperse magnetic polymer particles. In:"*Future Directions in Polymer Colloids*" Eds. El-Aasser, M.S. and Fitch, R. Martinus Nijhoff Publishers, Dordrecht, The Netherlands, p. 23.

19. Overbeek, J. Th. G. (1978). Technical Applications of Colloid Science In: "*Emulsions, Latices, Dispersions*". Ed Becher, P.Yadenfreund, M.N., Dekker, New York, p. 1.

20. Osmond D.W.J., (1974). The Impact of Colloid Science on Paint Industry. *Chem. Ind. (London),* 891.

21. Kitchener, J.A., (1975). Surface Chemistry in Mineral Processing. *Chem. Ind. (London),* 54.

22. Arnold, C.W. (1977). Enhanced Oil Recovery. *Chem. Technol.*, **7**, 762.

23. Goodwin, J.W. (1982). Some uses of Rheology in Colloid Science. In:"*Colloidal Dispersions*", Chap. 8. Ed. Goodwin, J.W., Special Publication No. 43., The Royal Society of Chemistry, London.

24. Overbeek, J. Th. G. (1982). Monodisperse Sytems, Fascinating and Useful. *Adv. Colloid Interface Sci.* **15**, 251.

25 **(a).** Dicke, K.A., Van Hooft, J., and Van Bekkum, D.W. (1968). The selective elimination of immunologically competent cells from bone marrow and lymphatic cell mixtures. *Transplantation*, **6**, 562.

(b). Dicke, K.A., McCredie, K.B., Spitzer, G., *et al.* (1978). Autologous marrow transplantation in patients with adult acute leuklemia. *Transplantation*, **26**, 169.

(c). Dicke, K.A., Zander, C., Spitzer, C., *et al.* (1979).Autologous bone marrow transplantation in adult leukemia in relapse. *Lancet*, **1**, 514.

26. Widder, K.J. and Green, R. (1985). Drug and Enzyme Targeting. *Methods in Emzymology.* **112**, Acedemic Press, Inc., Orlando, New York.

27. Davis, S.S., Illum, L., McVie, J.G. and Tomlinson, E. (Eds.). (1984). *Microspheres and Drug Therapy.* Pharmaceutical, Immunological and Medical Aspects. Elsevier, Amsterdam, New York, p. 448.

28. Ugelstad, J., Soderberg, L., Berge, A., and Bergstrom, J. (1983). Monodispersed polymer particles——a step forward for chromatography. *Nature,* **303**, 96.

29. Lyklema, J. (1982). Fundamentals of Electrical Double Layers in Colloidal Systems. Chap. 3. Ed. Goodwin, J.W. *The Royal Society of Chemistry Special Publication No. 43,* p. 47-70.

30 (a). Gouy, G. Sur la constitution de la charge életrique a la surface d'un électrolyte. (1910). *J. Phys. Theor. Appl.* **(4)**, *9*, 457-467.
(b). Chapman, D.L. (1913). A contribution to the theory of electrocapillarity. *Phil. Mag.* **(6)**, *25*, 475-481.

31. Stern, O. (1924). Zur Theorie der elektrolyischen doppelschicht, *Z. Elektrochem. Angew. Phys. Chem.* **30**, 508-516.

32. Hartley, G.S. and Roe, J.W. (1940). Ionic concentrations at interfaces. *Trans. Faraday Soc.*, **36**, 101-109.

33. Bradford, E.B., Vanderhoff, J.W. and Alfrey, T. Jr. (1956). The use of monodisperse latexes in an electron microscope: An investigation of the mechanism of emulsion polymerization. *J. Colloid Sci.*, **111, 135-149.**

34. Cooke, D.D. and Kerker, M. (1973). Particle size distribution of colloidal suspensions by light scattering based upon single particle counts—polystyrene latex. *J. Colloid Interface Sci.*, **42**, 150-155.

35. McCann, G.D., Vanderhoff, J.W., Strickler, A. and Sacks, T.I. (1974). Separation of latex particle according to size by continous electrophoresis. In:"*Separation and Purification Methods*". Eds. Perry, E.S., Van Oss, C.J. and Grushka, E. New York, Mercel Dekker, Inc., p. 153-198.

36. Small, H., (1974). Hydrodynamic Chromatography. A Technique for size Analysis of Colloidal Particles. *J. Colloid Interface Sci.* **48**, 147.

37. Cooper, W.D. and Parfitt, G.D. (1968). Comparison of Particle size distribution of "monodisperse" particles from 0.8 to 3.5 μm in diameter using Coulter Counter and electron microscopy. *Kolloid Z u. Z. Polymere*, **223**, 160-166.

38. Sharp, D.G. and Beard, J.W. (1950). Size and density of polystyrene particles measured by ultracentrifugation. *J. Biol. Chem.*, **185**, 247-253.

39. Knight, R.A., Fiore, J.V., and Rossito, J.V. (1982). Harnessing Theory for Practical Applications. In:"*World Filtration Congress III, Sept. 13-17, The Filtration Society, Cryodon, England, Vol. II,* 472-483.

40. Israelachvilli, J.N. and Ninham, B.W. (1977). Intermolecular Forces—the long and short of it. *J. Colloid Interface Sci.* **58**, 14.

41. Everett, D.H. (1988). *Basic Principles of Colloid Science.* The Royal Society of Chemistry Paperbacks, London.

42. Napper, D.H. (1970). Colloid Stability. *Ind. Eng. Chem. Prod. Develop.*, **9**(4), 467-478.

43. Derjaguin, B.V. and Landau, L. (1941). Theory of the stability of strongly charged hydrophobic sols and the adhesion of strongly charged particles in solutions of electrolytes. *Acta Physicochim., URSS*, **14**, 733-762.

44. Verwey, E.J. and Overbeek, J. Th. G. (1948). *Theory of Stability of Lyophobic Colloids.* Elsevier, Amsterdam.

45. Derjaguin, B.V. (1939). A Theory of interaction of particles in the presence of electric double layers and the stability of lyophobic colloids and disperse systems. *Acta Physicochim. U.R.S.S.* **10**, 333-346.

46. Hamaker, H.C. (1937). The London-Van der Waals attraction between particles, *Physica (Utrecht)*, **4**, 1058-1072.

47. Mahanty, J. and Ninham, B. W. (1976). *Dispersion Forces.* Academic Press, London.

48. Lifshitz, E.M. (1956). The theory of molecular attractive forces between solids. *Sov. Phys. JEPT (Eng. Trans.)* , **2**, 73-83.

49. Vincent, B. (1987). The stability of solid/liquid dispersions in presence of polymers. In:"*Solid/Liquid Dispersions*". Chap. 7. Ed. Tadros Th. F. (Academic Press, London).

50. Napper, D.H. (1983). *Polymeric Stabilization of Colloidal Dispaersions.* (Academic Press, London).

51. Vincent, B. (1973). The van der Waals Attraction Between Colloid Particles Having Adsorbed Layers. II. Calculation of Interaction Curves. *J. Collod Interace Sci.*, **42**, 270.

52 **(a)**. Gregory, J. (1976). The effect of cationic polymers on the colloidal stability of the latex particles. *J. Colloid Interface Sci.*, **55**, 35-44.

(b). Vincent, B. (1974). The Effect of Adsorbed Polymers on Dispersion Stability. *Adv. Colloid Interface Sci.*, **4**, 193.

(c). Kitchener, J.A (1972). Principles of Action of Polymeric Flocculants. *Brit. Polym. J.*, **4**, 217.

53. Hardy, W.B. (1900). A preliminary investigation of the conditions that determine the stability of irreversible hydrosols. *Proc. Roy. Soc., London*, **66**, 110-125.

54. von Smoluchowski, M. (1917). (Mathematical theory of the kinetics of the coagulation of colloidal solutions). *Z. Physic. Chem., Stoechiom, Verwanschaftsl*, **92**, 129-168.

55. Batchelor, G.K. and Green, J.T. (1972). The hydrodynamic interaction of two small freely-moving spheres in a linear field. *J. Fluid Mech.*, **56**, 375.

56. Curtis, A.S.G and Hocking, L.M. (1970). Collision Efficiency of Equal Spherical Particles in a Shear Flow. *Trans. Faraday Soc.*, **66**, 1381.

57. van der Ven, T.G.M. and Mason, S.G. (1976). The microrheology of colloidal Dispersions. IV. Pairs of Interacting Spheres in a Shear flow and V. Primary and Secondary Doublets of spheres in Shear flow. *J. Colloid Interface Sci.*, **57**, 505 and 517.

58. Zeichner, G.R. and Schowalter, W.R. (1979). Effects of hydrodynamic and colloidal Forces on the coagulation of Dispersions. *J. Colloid Interface Sci.*, 71, 237.

59 (a). Chandrasekar, S. (1943). Stochastic problems in Physics and Astronomy. *Rev. Mod. Phys.* **15**, 59.

(b). Manley, R. St. J., and Mason, S.G. (1952). Particle motions in sheared suspensions. II. Collisions of uniform spheres. *J. Colloid Sci.* **7**, 354-369.

60. (See Kruyt, H.R. (ed.) (1952)). *Colloid Science*, Vol. I. Elsevier, Amsterdam.

61. Reernik, H. and Overbeek, J.Th.G. (1954). The rate of coagulation as a measure of the stability of silver iodide sols. *Discuss. Faraday Soc.*, **18**, 74-84.

62 (a). Forbes, E.S, Groszek, A.J. Neustadter, E.L. (1970). Adsorption Studies on Lubricating Oil Additives. *J. Colloid Interface Sci.* **33**, 629.

(b). Graham, D.E. (1983). Chemistry and Technology of Water-Soluble Polymers. Ed. Finch, C.A., p. 321-340. (Plenum Press, New York).

(c). Klein, J., Kulicke, W.M. (1980). Paper SPE 8990. 5th Intern. Symp. Oilfield Chemistry, p. 51-58. (Standford, California).

(d). Hoyt, J.W., Wade, R.H., Ting, R.Y., Kim, O.K., MacWilliams, D.C., Rogers, J.H. and West, T.J. (1973). Water-Soluble Polymers. Ed. Bikales, N.M. P. 137-150, 151-160, 105-126. (Plenum Press, New York).

(e). Bailey, F.E. Jr, and Koleske, J.V. (1976). *Polyethyleneoxide.* (Academic Press).

(f). Cohen, Y. and Metzner, A.B. (1985). Apparent Slip Flow of Polymer Solutions. *J. Rheol.* **29**, 67-102.

63 (a). Vroman, L. and Adams, A.L. (1971). Peculiar behaviour of Blood at Solid Interfaces. *J. Pol. Sci. Part C, Polm. Symp.* **34**, 159-165.
(b). Hutchinson, F.G. (1983). Chemistry and Technology of Water-Soluble Polymers. Ed. Finch, C.A. p. 267-286. (Plenum Press, New York).
(c) Regelson W. (1973) Water-Soluble Polymers. Ed. Bikales. N.M. p.161-178. (Plenum Press, New York).

64. Andrade, J.D. (Ed). (1985). "*Surface and Interfacial Aspects of Biomedical Polymers*". Vol. **2**. (Plenum, New York).

65. Cooper, S.L., and Peppas, N. A. (Eds.) (1982). "*Biomaterials: Interfacial Phenomena and Applications*". *ACS. Advances in Chemistry Series, Vol.* **199**, Am. Chem. Soc., Washington, D.C.

66. Brash, J.L. and Horbett, T.A. (Eds.) (1987). "*Proteins at Interfaces. Physicochemical and Biochemical Studies*". *ACS Symposium Series* **343**. (Am. Chem. Soc., Washington, DC).

67. Salzman, E.W. (Ed.) (1981). "*Interaction of Blood with Natural and Artificial Surfaces*". (Mercel Dekker, New York).

68. McRitchie, F. (1978). Proteins at Interfaces. *Adv. Protein Chem.*,

69. Lyklema, J. (1984). Proteins at solid-liquid Interfaces. A Colloid-Chemical Review. *J. Colloids Surf.*, **10**, 33.

70. Seventh International Symposium on Affinity Chromatography and Interfacial Macromolecular Interactions. (1988). (Eds.) Jennissen, H.P. and Müller, W. *Makromol. Chem.,Macromol. Symp.* **17**.

71. Norde, W. (1986). Adsorption of Proteins from solution at the solid-liquid Interface. *Adv. Colloid Interface Sci.* **25**, 267-340.

72. Norde, W. (1983) Physicochemical aspects of the behaviour of biological components at solid/liquid interfaces. In: *Microspheres in Drug Therapy: Pharmacuetical, Immunological and Medical Aspects.* Ed. Davis Stanley S.; Chap. 3,. p. 39-59. (Elsevier, Amsterdam, The Netherlands).

73. Morrissey, B.W. (1977). The Adsorption and Conformation of Plasma Proteins. A Physical Approach. *Ann. N.Y. Acad. Sci.* **283**, 50.

74. Ivarsson, B., and Lundstrom, I. (1986). Physical Characterization of Protein adsorption on metal and metal surfaces. *CRC Crit. Rev. Biocompat.* **2(1)**, 1-96.

75. Brash, J.L. and Lyman, D.J. (1971). Adsorption of Proteins and Lipids to Nonbiological Surfaces. In: "*The Chemistry of Bio-Surfaces*". Ed. Hair, M.L. p. 177-229. (Dekker, New York).

76 (a). Norde, W. and Lyklema, J. (1978). The Adsorption of Human Plasma Albumin and Bovine Pancrease Ribonuclease at Negatively Charged Polystyrene Surfaces. I. Adsorption Isotherms. Effects of Charge, Ionic Strength, and Temperature. *J. Colloid Interface Sci.*, **66**, 257.

(b). Norde, W. and Lyklema, J. (1978). The Adsorption of Human Plasma Albumin and Bovine Pancrease Ribonuclease at Negatively Charged Polystyrene Surfaces. II. Hydrogen Ion Titrations. *J. Colloid Interface Sci.*, **66**, 266.

(c). Norde, W. and Lyklema, J. (1978). The Adsorption of Human Plasma Albumin and Bovine Pancrease Ribonuclease at Negatively Charged Polystyrene Surfaces. III. Electrophoresis. *J. Colloid Interface Sci.*, **66**, 277.

(d). Norde, W. and Lyklema, J. (1978). The Adsorption of Human Plasma Albumin and Bovine Pancrease Ribonuclease at Negatively Charged Polystyrene Surfaces. IV. The Charge Distribution in the Adsorbed State. *J. Colloid Interface Sci.*, **66**, 285.

(e). Norde, W. and Lyklema, J. (1979). The Adsorption of Human Plasma Albumin and Bovine Pancrease Ribonuclease at Negatively Charged Polystyrene Surfaces. V. Microcalorimetry. *J. Colloid Interface Sci.*, **71**, 350.

77. Suzawa, T. and Murakami, T. (1980). Adsorption of Bovine Serum Albumin on Polymer Latices. *J. Colloid Interface Sci.* **78**, 266-268.

78. Bornzin,G.A. and Miller, I.F. (1982). The Kinetics of Protein Adsorption on Synthetics and Modified Natural Surfaces. *J. Colloid Interface Sci.* **86**, 539-558.

79. Young, B.R., Pitts, W.G., and Cooper, S.L. (1988). Protein Adsorption on Polymeric Biomaterials. I. Adsorption Isotherms. *J. Colloid Interface Sci.* **124**, 28-43.

80. Penners, G. Priel, Z. and Silberberg, A. (1982). Irreversible Adsorption of Triple-Helical Soluble Collagen Monomers from solution to Glass and other surfaces. *J. Colloid Interface Sci.*, **80**, 437-488.

81. Ito, Y., Sisido, M., and Imanishi, Y. (1986). Synthesis and antithrombogenicity of anionic polyurethanes and heparin-bound polyurethanes. *J. Biomed. Mater. Res.* **20**, 1157.

82. Nyilas, E. Chi, T.H., and Herzlinger, G.A. (1974). Thermodynamics of native protein/foreign surface interactions. I. Calorimetry of the Human γ-globulin/glass system. *Trans. Amer. Soc. Artif. Intern. Organs.* **20**, 480.

83. Gendreau, R.M. and Jakobsen, R.J. (1979). Blood-Surface Interaction: Fourier Transform Infrared Studies of Protein Surface Adsorption from Flowing Blood Plasma and Serum. *J. Biomed. Mater. Res.* **13**, 893.

84. Burghardt, T.P. and Axelrod, D. (1981). Total Internal Reflection Fluorescence photobleaching recovery study of serum albumin adsorption dynamics. *Biophys. J.* **33**, 455.

85. Bagnall, R.D. (1977). Adsorption of Plasma Proteins on Hydrophobic Surfaces. I. Albumin and γ-Globulin. *J. Biomed. Mater. Res.* **11**, 947.

86. Roe, R.J. (1980). Adsorption of Bovine Serum Albumin (BSA) on Polyoxymethylene Single crystals. *Polym. Sci. Technol. B* **12.**

87. Fleer, G.J. and Lyklema, J. (1985). Forces and Mechanisms in the Adsorption of Uncharged and Ionizable Macromolecules and of Proteins. *Makromol. Chem., Macromol. Symp.* **17**, 39-56.

88. Lee, S.H. and Ruckenstein, E. (1988). Adsorption of proteins onto polymeric surfaces of different Hydrophilicities. A case study with Bovine Serum Albumin. *J. Colloid Interface Sci.* **125**, 365-375.

89. Jönsson, U., Lunström, I. and Rönnberg, I. (1987). Immunoglobulin G and Secretory Fibronectin Adsorption to Silica. *J. Colloid Interface Sci.* **117**, 127.

90. McRitchie, F. (1972). The adsorption of Proteins at the Solid/Liquid Interface. *J. Colloid Interface Sci.* **38**, 484.488.

91. Shirahama, H. and Suzawa, T. (1985). Adsorption of Bovine serum Albumin onto Styrene/2-hydroxyethyl Metacrylate Copolymer Latex. *J. Colloid Interface Sci.* **104**, 416.

92. Suzawa, T., Shirahama, H., and Fujimoto, T. (1982). Adsorption Bovine Serum Albumin onto Homo–and Copolymer Latices. *J. Colloid Interface Sci.***86**, 144.

93. Mizutani, T. (1981). Adsorption of Proteins on silicone-coated Glass Surfaces. *J. Colloid Interface Sci.* **82**, 162.

94. Jönsson, U., Ivarsson, B., Lundström, I., and Berghem, L. (1982). Adsorption Behaviour of Fibronectin on Well-Characterised Silica Surfaces. *J. Colloid Interface Sci.* **90**, 148.

95. Fletcher, M., and Pringlwe, J.H. (1985). The effect of Surface Free energy and Medium Surface Tension on Bacterial Attachment to Solid Surfaces. *J. Colloid Interface Sci.* **104**, 5.

96. Cuypers, P.A., Hermens, W.T., and Heneker, H.C. (1977). Ellipsometric Study of Protein Film on Chromium. *Ann. N. Y. Acad. Sci.* **283**, 77.

97. Paul, L., and Sharma, C.P. (1981). Preferential Adsorption of Albumin onto Polymeric Surface: An Understanding. *J. Colloid Interface Sci.* **84**, 546.

98. Dillruan, W.J. Jr, (1972). On the Adsorption of Serum Proteins on Polymer Membrane Surfaces.. *J. Colloid Interface Sci.* **44**, 221.

99. Dulm, P. and Norde, W. (1983). The Adsorption of Human Plasma Albumin on solid surfaces, with special attension to the Kinetic Aspects. *J. Colloid Interface Sci.* **91**, 248-255.

100. Cantarero, L.A., Bulter, J.E., and Osborne, J.W. (1980). The Adsorptive Characteristics of Proteins for Polystyrene and their Significance in Solid-Phase Immunoassays. *Anal. Biochem.* **105**, 375-382.

101. Schmitt, A., Varoqui, R., Uniyal, S., Brash, J.L., and Pusineri, C. (1983). Interaction of Fibrinogen with solid surfaces of varying charge and Hydrophobic-Hydrophilic Balance. *J. Colloid Interface Sci.*, **92**, 25.

102. Norde, W. (1984). Ion Participation in Protein Adsorption at solid surfaces. *Colloids and Surfaces*, **10**, 33-42.

103. Baszkin, A. and Lyman, D.J. (1980). The interaction of plasma proteins with polymers. I. Relationship between polymer surface energy and protein adsorption/desorption. *J. Biomed. Mater. Res.* **14**, 393.

104. Andrade, J.D. (1973). Interfacial phenomena and biomaterials. *J. Med. Instrum.* **7**, 110-120.

105. Ruckenstein, E. and Gourisankar, S.V. (1984). A Surface Energetic Criterion of Blood Compatibility of Foreign Surfaces. *J. Colloid Interface Sci.* **101**, 436.

106. Horbett, T.A.,and Brash, J.L. (1987). In:*"Proteins at Interfaces. Physicochemical and Biochemical Studies"*. Brash, J.L. and Horbett, T.A. (Eds). Chap. 1., p. 1-33. *ACS Symposuim Series* **343**. (Am. Chem. Soc., Washington, DC).

107. Horbett, T.A.,(1987). Adsorption to Biomaterials from Protein Mixtures. In:*"Proteins at Interfaces. Physicochemical and Biochemical Studies"*. Brash, J.L. and Horbett, T.A. (Eds). Chap. 16., p. 239-260. *ACS Symposuim Series* **343**. (Am. Chem. Soc., Washington, DC). (And References therein).

108. Brash, J.L. (1987). Protein Adsorption at the Solid-Solution Interface in Relation to Blood-Material Interactions. In:*"Proteins at Interfaces. Physicochemical and Biochemical Studies"*. Brash, J.L. and Horbett, T.A. (Eds). Chap. 1., p. 1-33. *ACS Symposuim Series* **343**. (Am. Chem. Soc., Washington, DC). (And References therein).

109. Goudsward, J. van der Donk, T.A., and Noordzij, A. (1978). Protein A Reactivity of Various Mammalian Immunoglobins. *Scand. J. Immunol.* **8**, 21.

110. Farooqui, A.A. (1980). Purification of Enzymes by Heparin-Sepharose Affinity Chromatography. *J. Chromatogr.* **184**, 335.

111. Gianazza, E. and Arnand, P. (1982). A General Method for fractionation of plasma proteins. Dye-Ligand affinity chromatography on immobilized Cibacron Blue F3-GA. *Biochem. J.* **201**, 129.

112. Vroman, I. and Adams, A.L. (1987). Why Plasma Proteins Interact at Interfaces. In:*"Proteins at Interfaces. Physicochemical and Biochemical Studies"*. Brash, J.L. and Horbett, T.A. (Eds). Chap. 10., p. 154-164. *ACS Symposuim Series* **343**. (Am. Chem. Soc., Washington, DC).

113 (a). Brash J.L., and Samak, Q.M. (1978). Dynamics of Interactions between Human Albumin and Polyethylene Surface. *J. Colloid Interface Sci.* **65**, 495-504.

(b). Chan, B.M.C. and Brash, J.L. (1981). Adsorption of Fibrinogen on Glass: Reversibility Aspects. *J. Colloid Interface Sci.* **82**, 217-225.

(c). Schmitt, A. Varoqui, R., Uniyal, S., Brash, J.L., and Pusineri, C. (1983). Interaction of Fibrinogen with Solid Surfaces of varying Charge and Hydrophobic-Hydrophilic Balance. I. Adsorption Isotherms. *J. Colloid Interface Sci.* **92**, 25-30.

(d). Uniyal, S., and Brash, J.L. (1982). Patterns of Adsorption of Proteins From Human Plasma Onto Foreign Substances. *Thromb. Haemostas. (Stuggart).* **47***(3)*, 285-290.

114 (a). Price, T.M. and Rudee, M.L. (1987). Early Stages of Plasma Protein Adsorption. In:*"Proteins at Interfaces. Physicochemical and Biochemical Studies"*. Brash, J.L. and Horbett, T.A. (Eds). Chap. 3. p. 48-62. *ACS Symposuim Series* **343**. (Am. Chem. Soc., Washington, DC).

(b). Rudee, M.L. and Price, T.M. (1985). Adsorption of Plasma-Derived Proteins on Artificial Surfaces in a controlled flow Environment. *J. Biomed. Mater. Res.* **19**, 57.

115. Cheng, Y. L., Darst, S.A., and Robertson, C.R. (1987). Bovine Serum Albumin Adsorption and Desorption Rates on Solid Surfaces with Varying Surface Properties. *J. Colloid Interface Sci.* **118**, 212-223.

116. Katsunori, N., Youkei, H. Hiromi, K., and Norio, I. (1987). Dynamic analysis of irreversible adsorption of proteins on porous polymer resins as studied by pulse injection method. *Biotech. Bioeng.* **30***(2)*, 216-224.

117. Simha, R. Frisch, H.L., Eirich, F.R. (1953). The Adsorption of Flexible Macromolecules. *J. Phys. Chem.*, **57**, 584.

118. Silberberg, A. (1962). The Adsorption of Flexible Macromolecules. Part 1. The Isolated Macromolecule at a Plane Interface. *J. Phy. Chem.*, **66**, 1872.

119. Hoeve, C.A.J., Di Marzio, E.A. and Peyser, P., (1965). Adsorption of Polymer Molecules at low Surface Coverage. *J. Chem. Phys.*, **42**, 2558.

120. Silberberg, A. (1968). Adsorption of Flexible Macromolecules. IV. Effect of Solvent-Solute Interaction, Solute Concentration, and Molecular Weight. *J. Chem Phys.* , **48**, 2835.

121. Hoeve, C.A.J., (1970). On the General Theory of Polymer Absorption at a Surface. *J. Polym. Sci.*, **30**, 361.

122. Roe, R.J., (1974). Multilayer Theory of Adsorption from Polymer Solution. *J. Chem. Phys.* **60**, 4192.

123. Scheutjens, J.M.H.M., Fleer, G.J., (1979). Statistical Theory of the Adsorption of Interacting Chain Molecules. 1. Partition Function, Segment Density Distribution, and Adsorption Isotherms. *J. Phys. Chem.*, **83**, 1619.

124. Scheutjens, J.M.H.M., Fleer, G.J., (1980). Statistical Theory of the Adsorption of Interacting Chain Molecules. 2. Train, Loop, and Tail Size Distribution. *J. Phys. Chem.*, **84**, 174.

125. Fleer, G.J., Scheutjens, J.M.H.M. (1982). Adsorption of interacting Oligomers and Polymers at an Interface. *Adv. Colloid Interface Sci.*, **16**, 341.

126. Schultz, G.E. and Schimer, R.H., (1979). "Principles of Protein Structure". Springer-Verlag, New York.

127. Bonekamp, B.C., van der Schee H.A., Lyklema, J. (1983). Adsorption of oligo-and polypeptides as model of polyelectrolytes. *Croat. Chem. Acta.*, **56(4)**, 695-704.

128. Brooks, D.E. and Greig, R.G. (1981). Protein Adsorption. *J. Colloid Interface Sci.*, **83**, 661.

129. **(a).** Felter, R.E., Moyer, E.S., and Ray, L.N. (1969). Gel Permeation Chromatography applied to Polymer Adsorption Studies. **B 7**, 529.
(b). Felter, R.E. and Ray, L.N. (1970).Polymer Adsorption Studies at the Solid-Liquid Interface using Gel Permeation Chromatography. 1. Molecular Weight Distribution Along the Adsorption Isotherm. *J. Colloid Interface Sci.*, **32**, 349.
(c). Howard, G.J. and Woods, S.J. (1972). Adsorption of Polymer at the solution-solid Interface. VIII. Competitive Effects in the Adsorption of Polystyrene on Silica. *J. Polymer Sci.*, **A-2**, **10**, 1023.

130. Cohen Stuart, M.A., Scheutjens, J.M.H.M., and Fleer, G.J. (1980). Polydispersity Effects and the Interpretation of Polymer Adsorption Isotherms. *J. Polym. Sci. Polym. Phy. Ed.* , **18**, 559.

131. Weathersby, P.K., Horbett, T.A., and Hoffman, A.S., (1976). A new method for analysis of the adsorbed plasma protein layer on biomaterial surfaces. *Trans. Am. Soc. Artif. Int. Organs.* **22**, 242.

132. Benacerraf, B. and Unanue, E.R. (1979). *Texbook of Immunology.* p.48. (Williams & Wilkins).

133. Stanworth, D.R. and Turner, M.W. (1978). Immunochemical analysis. In:*"Handbook of Experimental Immunology"*. Ed. Weir, D.M. p. 6.25. (Blackwell, Oxford).

134. Bell, G.I. (1974). Model for the binding of multivalent antigen to cells. *Nature (London).* **248**, 430.

135. Bell, G.I. and De Lisi, C. (1974). Antigen Binding to Receptors on Immunocompetent Cells. *Cell Immunol.* **10**, 415.

136. De Lisi, C. and Perelson, A. (1976). Kinetics of aggregation Phenomena. I. Minimal Models for Patch Formation on Lymphocyte Membranes. *J. Theor. Biol.* **62**, 159.

137. Dembo, M. and Goldstein, B. (1978). Theory of Equilbrium Binding of symmetric Bivalent Haptens to cell surface antibody: Application to Histamine release from Basophils. *J. Immunol.* **121**, 345.

138. Shoup, D., and Szabo, A. (1982). Role of Diffusion in Ligand Binding to Macromolecules and Cell-Bound Receptors. *J. Biophy. Soc.* **40**, 33-39.

139. Dower, S.K., Titus, J.A. and Segal, D.M. (1984). The Binding of Multivalent Ligands to Cell Surface Receptors. In:*"Cell Surface Dynamics"*. Eds. Perelson, A.S. De Lisi C., and Wiegel, F.W. (New York, Dekker). 277-328.

140. Tamm, L.K. and Bartoldus, I. (1988). Antibody Binding to Lipid Model Membranes. The Large-Ligand Effect. *Biochemistry*, **27**, 7453-7458.

141. Berg, H.C. and Purcell, E.M. (1977). Physics of Chemoreception. *Biophy. J.* **20**, 193-219.

142. Chang, E.L. and Waite, B.A. (1987). Analysis of Vesicle Immunolysis Assays: The Direct Binding Model. *J. Immunol. Meth*ods. **102**, 33.

143. Tandford, C. (1961). *Physical Chemistry of Macromolecules.* (New York: Wiley). 526.

144. Cohen, R.J. and Benedek, G. (1982). Equilibrium and Kinetic Theory of Polymerization and Sol-Gel Transition. *J. Phys. Chem.*, **86**, 3696-3714.

145. Cohen Stuart, M.A., Cosgrove, T., and Vincent, B. (1986). Experimental Aspects of Polymer Adsorption at Solid/Liquid Interfaces. *Adv. Colloid Interface Sci.*, **24**, 143-239.

146. Robb, I.D. and Day, J.C. (1980). Conformation of adsorbed poly(vinyl pyrrolidinone) studied by infra-red spectrometry. *Polymer*, **21**, 408-412.

147. Cosgrove, T., Vincent, B., Barnett, K.G, Cohen stuart, M.A. and Sissons, D.S. (1981). Measurement of the Polymer-bound Fraction at the Solid-Liquid Interface by Pulsed Nuclear Magnetic Resonance. *Macromolecules*, **14**, 1018-1020.

148. Cohen Stuart, M.A. Bijsterbosch, B.J. and Fleer, G.J. (1982). Adsorption of poly(vinyl pyrrolidinone) on Silica. II. The fraction of bound segments, measured by a variety of Techniques. *J. Colloid Interface Sci.*, **90**, 321-334.

149. Kawaguchi, M. and Takahashi, A. (1980). Adsorption of Polystyrene at the θ temperature. *Macromolecules*, **13**, 884.

150. Cohen Stuart, M.A., Waajen, F.H.W.H., Cosgrove, T., Crowley, T.L., and Vincent, B. (1984). Hydrodynamic Thickness of Adsorbed Polymer layers. *Macromolecules*, **17**, 1825-1830.

151. Priel, Z., and Silberberg, A. (1978). The thickness of Adsorbed Polymer Layers at a Liquid-Solid Interface as a Function of Bulk Concentration. *J. Polm. Sci. Polm. Phy. Ed.*, **16**, 1917-1925.

152. Baenett, K.G., Burgess, A.N., Cosgrove, T., Crowley, T.L., King, T., Turner, J.D., Tadros, Th. F., and Vincent, B. (1981). Neutron Scattering, Nuclear Magnetic Resonance, and Photon Correlation Studies of Polymers adsorbed at the solid-solution Interface. *Polymer*, **22**, 283.

153. Foster, J.F. (1960). Plasma Proteins . In: "*The Plasma Proteins*", Vol.1. pp. 179-233, Ed. Putman, F.W. Academic Press, New York.

154. Franglen, G. and Swaniker, G.R.E. (1968). Preparation and analysis of peptide fragments produced by pepsin hydrolysis of human plasma albumin and their relationship to its structure. *Biochem. J.*, **109**, 107-120.

155. Brown, J.R. (1977). Serum Albumin: Amino Acid Sequence. In: "*Albumin Structure, Function and Uses*". Eds. Rosenoer, V.M., Oratz, M., and Rotchschild, M.A. Pergamon Press.

156. Brown, J.R. (1975). Structure of Bovine Serum Albumin. *Fed. Proc. (Fed. Am. Soc. Exp. Bio.)*, **34**, 391.

157. Bloomfield, V. (1966). The structure of BSA at low pH. *Biochem.*, **5**, 684-689.

158. Behrens, P.O., Spiekermann, A.M. and Brown, J.R. (1975). Structure of Human Serum Albumin. *Fed. Proc. (Fed. Amer. Soc. Exp. Biol.)*, **34**, 591.

159. Brown, J.R. (1977). Structure and evolution of serum albumin. In:" *Proceedings of FEBS 11th Meeting, Copenhagen 1977*", Vol. **50**, pp. 1-10. Eds. Peters, T. and Sjöholm, (Pergamon Press).

160. Carter, D.C, He Xiao-Min, Munson, S.H., Twigg, P.G., Gernett, K.M., Broom, M.B., and Miller, T.Y. (1989). Three-Dimensional Structure of Human Serum Albumin. *Science*, **224**, 1195-1198.

161. Wright, A.K. and Thompson, M.R. (1975). Hydrodynamic Structure of Bovine Serum Albumin determined by Transient Electric Birefringence.. *Biophys. J.*, **15**, 137.

162. Aoki, K., and Foster, J.F. (1957). Electrophoretic behaviour of Bovine Plasma Albumin at low pH. *J. Am. Chem. Soc.*, **79**, 3385-3396.

163. (a). Sogami, M. and Foster, J.F. (1963). Microheterogeneity as the explanation for resolution of N and F forms of plasma albumin in electrophoresis and other experiments. *J. Biol. Chem.*, **238**, PC2245-PC2247.

(b). Sogami, M. and Foster, J.F. (1968). Isomerisation reaction of charcoal-defatted bovine plasma albumin. The N-F transition and acid expansion. *Biochem.*, **7**, 2172-2182.

(c). Sogami, M. Petersoon, H.A. and Foster, J.F. (1969). The microheterogeneity of plasma albumins. V. Permutations in disulfide pairings as a probable source of microheterogeneity in bovine albumin. *Biochem.*, **8**, 49-58.

164. (a). Wallevik, K. (1973).Reversible denaturation of human serum albumin by pH, temperature and guanidine hydrochloride followed by optical rotation. *J. Biol. Chem.*, **248**, 2650-2655.

(b). Hvidt, A. and Wallevik, K. (1972). Conformational changes in human serum albumin as revealed by hydrogen-deuterium exchange studies. *J. Biol. Chem.* **247**, 1530-1535.

165. Wallevik, K. (1973). Spontaneous denaturation as a possible initial step in the breakdown of serum albumin in vivo. *Clin. Sci. Mol. Med.*, **45**, 665-675.

166. Yutani, K. Ogasahara, K. Sugino, Y., and Matsusshiro, A. (1977). Effect of a single amino acid substitution on stability of conformation of a protein. *Nature (Lond.)*, **267**, 274-275.

167. Stroupe, S.D. and Foster, J.F. (1973). Further studies of the sulfhydryl-catalysed isomerisation of bovine mercaptalbumin. *Biochem.*, **12**, 384-3830.

168. Warner, R.C. and Levy, M. (1958). Denaturation of bovine plasma albumin. II. Isolation of intermediates and mechanism of the reaction at pH. 7. *J. Am. Chem. Soc.*, **80**, 5735-5744.

169. Finlayson, J.S. (1960). Effects of long term storage on human albumin. Chromatographical and Centrifugal aspects. *J. Clin. Invest.*, **39**, 1837-1840.

170. Frieldi, H. Kistler, P. (1970). Polymers in Preparation of Human Serum Albumin. *Vox Sang*, **18**, 542-546.

171. Janatova, J. Miles, O. and Sponar, J. (1968). Heterogeneity of Human Serum Albumin, preparation, isolation of components by gel filtration and ion exchange chromatography. *Chem. Comm.*, **33**, 788-800.

172. Luck, J.M., Balou, G.A., Basset, D., Boyer, P.D., Lum, F.G. and Rice, R. (1944). The stabilisation of standard human serum albumin with sodium mandelate and sodium phenylacetate. *Blood Substitute Report*, **15**, NRC.

173. Pappas, P., O'Donnel, T., Pennel, R.B., Clowes, G.H.A., Jr., and Pyle, H.M. (1972). Aged Human Serum Albumin: Properties and Clinical acceptability. *Transfusion*, **12**, 259-266.

174. Woolf, I.I., Pappas, P., Pennel, R.B., and Babior, B.M. (1972). Rate of disappearance of infuged aged albumin in human subjects. *Tranfusion*, **12**, 123-125.

175. King, T.P. (1961). On the sulphydryl group of human plasma albumin. *J. Biol. Chem.*, **236**, PC5.

176. Tanford, C. (1970). Protein denaturation. Theoretical models for the mechanism of denaturation. *Adv. Protein Chem.*, **24**, 1-95.

177. Hartley, R., Sober, H. and Peterson, E. (1962). The Relation of Free Sulphydryl Groups to chromatographic Heterogeneity and Polymerization of Bovine Plasma Albumin. *Biochemisty*, **1**, 60.

178. Anderson, Lars-Olov. (1966). The heterogeneity of BSA. *Biochim. Biophys. Acta*. **117**, 115-133.

179. Markwell, M.A.K. (1982). A New Solid-State Reagent to Iodinate Proteins. I. Conditions for the Efficient Labelling of Antiserum. *Anal. Biochem.*, **125**, 427-432.

180. Lee, D.S.C. and Griffiths, B.W. (1984). Competitive Studies of Iodo-Bead and Chloramine-T Methods for the Radioiodination of Human Alpha-Fetoprotein. *J. Immunol. Method*,**74**, 181-189.

181. (a) Tanford, C., Buzzel, J.G., Rands D.G., Swanson, S.A. (1955). The Reversible Expansion of Bovine Serum Albumin in Acid Solutions. *J. Am. Chem. Soc.*, **77**, 6421-6428.

(b). Spahr, P.F. and Edsall, J.T. (1964). Amino Acid Composition of Human and Bovine Serum Mercaptalbumins. *J. Biol. Chem.*, **239**, 850.

182. Vander Linden, C. and Van Leemput, R. (1978). Adsorption Studies of Polystyrene on Silica. II. Polydisperse Adsrbate. *J. Colloid Interface Sci.*, **67**, 63.

183. Zsom, R.L.J. (1986). Dependence of Preferential Bovine Serum Albumin Oligomer Adsorption on the surface Properties of Monodisperse Polystyrene Latices. *J. Colloid Interface Sci.*, **111**, 434.

184. Lensen, H.G.W., Bargeman, D., Bergveld, P., Smolders, C.A., and Feijen, J. (1984). High-Performance Liquid Chromatography as a Technique to Measure the Competitive Adsorption of Plasma Proteins onto Latices. *J. Colloid Interface Sci.*, **99**, 1-8.

185. Thies, C. (1976). The Adsorption of Polystyrene-Poly(methyl methacrylate) Mixtures at a solid-Liquid Interface. *J. Phys. Chem.*, **70**, 3783.

186. Furusawa, F. Yamashita, K. and Kono, K. (1982). Adsorption of Monodisperse Polystyrene latex onto Porous glass. I. Reference Adsorption and Displacement of High-Molecular-Weight Species. *J. Colloid Interface Sci.*, **86**, 35.

187. Weber, K. and Osborn, M. (1969). The reliability of Molecular weight determination by dodecyl sulphate-polyacrylamide gel electrophoresis. *J. Biol. Chem.*, **224**, 4406.

188. Fairnbanks, G., Theodore, L.S. and Wallach, D.F.H. (1971). Electrophoretic Analysis of the Major Polypetides of the Human Erythocyte Membrane. *Biochem.*, **10**, 2602.

189. Walton, A.G. and Maenpa, F.C. (1979). Application of Fluorescence Spectroscopy to the Study of Proteins at Interfaces. *J. Colloid Interface Sci.* **72**, 265-278.

190. Hlady, V., Reinecke, D.R. and Andrade, J.D. (1986). Fluorescence of Adsorbed Protein Layers. I. Quantitation of Total Internal Reflection Fluorescence. *J. Colloid Interface Sci.* **111**, 555-569.

191. Hlady, V. and Andrade, J.D. (1988). Fluorescence Emission from Adsorbed Bovine Serum Albumin and Albumin-bound 1-Anilinonaphthalene-8-Sulfonate studied by TIRF. *Colloids and Surfaces* **32**, 359-369.

192. **(a)** Goldberg, R.J. (1952). A Theory of Antibody-Antigen Reactions. I. Theory of Reactions of Multivalent Antigen with Bivalent and Univalent Antibody. *J. Am. Chem. Soc.*, **74**, 5715-5725.

(b) Steensgaard, J., Jacobsen, C., Lowe, J., Hardie, D., Ling, N.R., and Jefferies, R. (1980). The Development of Difference Turbidimetric Analysis for Monoclonal Antibodies to Human IgG. *Mol. Immunol.*, **17**, 1315.

193. Steward, M.W. and Steensgaard, J. (1983). *Antibody Affinity: Thermodynamic Aspects and Biological Significance.* CRC Press, Inc.

194. Dixon, M. and Webb, E.C., (1958). *Enzymes*, Longmans, Green & Co., London.

195. Langmuir, I. (1916). The Constitution and Fundamental Properties of Solids and Liquids. *J.Am. Chem. Soc.* **38**, 2221.

196. **(a)** Nimmo, I.A., Atkins, G.L., Strange, R.C., and Percy-Robb, I.W., (1977). An Evaluation of Ways of Using Equilibtrium Dialysis to Quantify the Binding of Ligand to Macromolecule. *Biochem. J.*, **165**, 107.

(b) Fazekas de St. Groth, S. (1979). The Quality of Antibodies and Cellular Receptors. *Immunological Methods.* Eds. Ivan Lefkovits and Benvenuto Pernis. Academic Press, (NY), p. 1-42.

197. Klotz, I.M. and Huntston, D.L., (1979). Protein Affinities for Small Molecules: Conceptions and Misconceptions. *Arch. Biochem. and Biophys.*, 314-328.

198. Steinhardt, J. & Reynolds, J.A. (1969). *Multiple Equilibria in Proteins,* Academic Press, New York.

199. Reynolds, J.A. (1979). Interaction of Divalent Antibody with Cell Surface antigens. *Biochem.* 264-269.

200. Herbert, W.J. (1973). Mineral-Oil Adjuvants and the Immunization of Laboratory Animals. *In*: "Handbook of Experimental Immunology". Ed. Weir, D.M., Vol. 3 pp. A2.1-2.14, Blackwell, Oxford.

201. "*Antibodies. A Practical Approach*" Ed. Catty D., Vol. 1, IRL Press, Oxford, England.

202. Bagchi, P. and Birnbaum, S.M. (1981). Effect of pH on the Adsorption of Immunoglobulin G on Anionic Poly(vinyltoluene) Model Latex Particles. *J. Colloid Interface Sci.* **83**, 460-478.

203. Day, E.D. (1972). "*Advanced Immunochemistry*". Williams & Wilkins, Baltimore, p. 181.

204. Bell, S.H. and Crowl, V.T. (1973). *Dispersions of Powder in Liquids.* 2nd. Edn., p. 267.

205. Ottewill, R.H. and Parriera, H.C. (1958). Photometer for light scattering and kinetic measurments at constant temperatures. *J. Phys. Chem.* **62**, 912-916.

206. Fleer, G.J. (1971). Ph. D. Thesis, Wageningnen, The Netherlands.

207. Van Wazer, J.R., Lyons, J.W., Kim, K.Y., and Colwell, R.E. (1963). In: *Viscosity and Flow Measurement.* A Laboratory Handbook of Rheology. Whiley-Interscience Publishers, New York.

208. Berne, B., J. and Pecora, R. (1975). In: *Dynamic Light Scattering.* Wiley-Interscience Publishers, New York.

209. Oster G. (1947). Light Scattering from polymerizing and coagulating systems. *J. Colloid Sci.* **2**, 291.

210. Kerker, M. (1969). In: *The Scattering of Light and Other Electromagnetic Radiation.* Academic Press, New York, NY.

211. Inagaki, T. Arakawa, E.T. , Hamm, R.N., and Williams, M. W. (1977). Optical properties of polystyrene from the near-infrared to the x-ray region and convergence of the optical sum rules. *Phys. Rev.*, **B15**, 3243-3253.

212. (see Berne, B., J. and Pocora, R. **[208]** or Kerker, M. **[210]**).

213. Lichtenbelt, J.W.T, Pathmamanoharan, C., and Wiersema, P.H. (1974). Rapid Coagulation of Polystyrene Latex in a Stopped-Flow Spectrophotometer. *J. Colloids Interface Sci.*, **49**, 281-285.

214. Reynolds, P.A. and Goodwin, J.W. (1987). The Aggregation of Large Polystyrene Latex Particles. *Colloids and Surfaces*, **23**, 273-299.

215. Force, C.G. and Matijevic E. (1968). Colloid Properties of Rubber Latex. II. Electrolytic Coagulation. *Kolloid Z Z Polymer*, **224**, 51.

216. Dickinson, E., Robson, E.W. and Stainsby, G. (1983). Colloid Stablity of Casein-coated Polystyrene Particles. *J. Chem. Soc., Faraday Trans. I,* **79**, 2937-2952.

217. Buscall, R., Goodwin, J.W., Hawkins, M.W., and Ottewill, R.H. (1983). Viscoelastic Properties of Concentrated Latices. Part I. Methods of Examination. *J. Chem. Soc. Far. Trans.* **I**, **78**, 2873.

218. van der Ven, T.G.M.. (1989). In: *Colloidal Hydrodynamics.* Colloid Science. A series of Monographs. Academic Press, London.

219. Shoemaker D.P., Garland C.W., and Steinfeld J.I., (1974). In :*Experiment in Physical Chemistry*. McGraw-Hill Book Company, New York.